



National Library
of Canada

Bibliothèque nationale
du Canada

Acquisitions and
Bibliographic Services Branch

Direction des acquisitions et
des services bibliographiques

395 Wellington Street
Ottawa, Ontario
K1A 0N4

395, rue Wellington
Ottawa (Ontario)
K1A 0N4

Your file Votre référence

Our file Notre référence

NOTICE

AVIS

The quality of this microform is heavily dependent upon the quality of the original thesis submitted for microfilming. Every effort has been made to ensure the highest quality of reproduction possible.

La qualité de cette microforme dépend grandement de la qualité de la thèse soumise au microfilmage. Nous avons tout fait pour assurer une qualité supérieure de reproduction.

If pages are missing, contact the university which granted the degree.

S'il manque des pages, veuillez communiquer avec l'université qui a conféré le grade.

Some pages may have indistinct print especially if the original pages were typed with a poor typewriter ribbon or if the university sent us an inferior photocopy.

La qualité d'impression de certaines pages peut laisser à désirer, surtout si les pages originales ont été dactylographiées à l'aide d'un ruban usé ou si l'université nous a fait parvenir une photocopie de qualité inférieure.

Reproduction in full or in part of this microform is governed by the Canadian Copyright Act, R.S.C. 1970, c. C-30, and subsequent amendments.

La reproduction, même partielle, de cette microforme est soumise à la Loi canadienne sur le droit d'auteur, SRC 1970, c. C-30, et ses amendements subséquents.

Canada

**The Photochemical Nucleophile-Olefin Combination,
Aromatic Substitution Reaction:
Methanol-Monoterpenes, 1,4-Dicyanobenzene**

by
Xinyao Du
B.Sc., Shandong

Submitted in partial fulfilment of the requirements
for the degree of Doctor of Philosophy
at
Dalhousie University
Halifax, Nova Scotia
July, 1992

© Copyright by Xinyao Du, 1992



National Library
of Canada

Acquisitions and
Bibliographic Services Branch

395 Wellington Street
Ottawa, Ontario
K1A 0N4

Bibliothèque nationale
du Canada

Direction des acquisitions et
des services bibliographiques

395, rue Wellington
Ottawa (Ontario)
K1A 0N4

Your file *Votre référence*

Our file *Notre référence*

The author has granted an irrevocable non-exclusive licence allowing the National Library of Canada to reproduce, loan, distribute or sell copies of his/her thesis by any means and in any form or format, making this thesis available to interested persons.

L'auteur a accordé une licence irrévocable et non exclusive permettant à la Bibliothèque nationale du Canada de reproduire, prêter, distribuer ou vendre des copies de sa thèse de quelque manière et sous quelque forme que ce soit pour mettre des exemplaires de cette thèse à la disposition des personnes intéressées.

The author retains ownership of the copyright in his/her thesis. Neither the thesis nor substantial extracts from it may be printed or otherwise reproduced without his/her permission.

L'auteur conserve la propriété du droit d'auteur qui protège sa thèse. Ni la thèse ni des extraits substantiels de celle-ci ne doivent être imprimés ou autrement reproduits sans son autorisation.

ISBN 0-315-80235-9

Canada

Name Xinyao Du

Dissertation Abstracts International is arranged by broad, general subject categories. Please select the one subject which most nearly describes the content of your dissertation. Enter the corresponding four-digit code in the spaces provided.

Organic Chemistry

0490

U·M·I

SUBJECT TERM

SUBJECT CODE

Subject Categories

THE HUMANITIES AND SOCIAL SCIENCES

COMMUNICATIONS AND THE ARTS

- Architecture 0729
- Art History 0377
- Cinema 0900
- Dance 0378
- Fine Arts 0357
- Information Science 0723
- Journalism 0391
- Library Science 0399
- Mass Communications 0708
- Music 0413
- Speech Communication 0459
- Theater 0465

EDUCATION

- General 0515
- Administration 0514
- Adult and Continuing 0516
- Agricultural 0517
- Art 0273
- Bilingual and Multicultural 0282
- Business 0688
- Community College 0275
- Curriculum and Instruction 0727
- Early Childhood 0518
- Elementary 0524
- Finance 0277
- Guidance and Counseling 0519
- Health 0680
- Higher 0745
- History of 0520
- Home Economics 0278
- Industrial 0521
- Language and Literature 0279
- Mathematics 0280
- Music 0522
- Philosophy of 0998
- Physical 0523

Psychology 0525

- Reading 0535
- Religious 0527
- Sciences 0714
- Secondary 0533
- Social Sciences 0534
- Sociology of 0340
- Special 0529
- Teacher Training 0530
- Technology 0710
- Tests and Measurements 0288
- Vocational 0747

LANGUAGE, LITERATURE AND LINGUISTICS

- Language 0679
 - General 0289
 - Ancient 0290
 - Linguistics 0291
 - Modern
- Literature
 - General 0401
 - Classical 0294
 - Comparative 0295
 - Medieval 0297
 - Modern 0298
 - African 0316
 - American 0591
 - Asian 0305
 - Canadian (English) 0352
 - Canadian (French) 0355
 - English 0593
 - Germanic 0311
 - Latin American 0312
 - Middle Eastern 0315
 - Romance 0313
 - Slavic and East European 0314

PHILOSOPHY, RELIGION AND THEOLOGY

- Philosophy 0422
- Religion
 - General 0318
 - Biblical Studies 0321
 - Clergy 0319
 - History of 0320
 - Philosophy of 0322
 - Theology 0469

SOCIAL SCIENCES

- American Studies 0323
- Anthropology
 - Archaeology 0324
 - Cultural 0326
 - Physical 0327
- Business Administration
 - General 0310
 - Accounting 0272
 - Banking 0770
 - Management 0454
 - Marketing 0338
 - Canadian Studies 0385
 - Economics
 - General 0501
 - Agricultural 0503
 - Commerce Business 0505
 - Finance 0508
 - History 0509
 - Labor 0510
 - Theory 0511
 - Folklore 0358
 - Geography 0366
 - Gerontology 0351
 - History
 - General 0578

- Ancient 0579
- Medieval 0581
- Modern 0582
- Black 0328
- African 0331
- Asia, Australia and Oceania 0332
- Canadian 03.4
- European 0335
- Latin American 0336
- Middle Eastern 0333
- United States 0337
- History of Science 0585
- Law 0398
- Political Science
 - General 0615
 - International Law and Relations 0616
 - Public Administration 0617
- Recreation 0814
- Social Work 0452
- Sociology
 - General 0626
 - Criminology and Penology 0627
 - Demography 0938
 - Ethnic and Racial Studies 0631
 - Individual and Family Studies 0628
 - Industrial and Labor Relations 0629
 - Public and Social Welfare 0630
 - Social Structure and Development 0700
 - Theory and Methods 0344
- Transportation 0709
- Urban and Regional Planning 0999
- Women's Studies 0453

THE SCIENCES AND ENGINEERING

BIOLOGICAL SCIENCES

- Agriculture
 - General 0473
 - Agronomy 0285
 - Animal Culture and Nutrition 0475
 - Animal Pathology 0476
 - Food Science and Technology 0359
 - Forestry and Wildlife 0478
 - Plant Culture 0479
 - Plant Pathology 0480
 - Plant Physiology 0817
 - Range Management 0777
 - Wood Technology 0746
- Biology
 - General 0306
 - Anatomy 0287
 - Biostatistics 0308
 - Botany 0309
 - Cell 0379
 - Ecology 0329
 - Entomology 0353
 - Genetics 0369
 - Limnology 0793
 - Microbiology 0410
 - Molecular 0307
 - Neuroscience 0317
 - Oceanography 0416
 - Physiology 0433
 - Radiation 0821
 - Veterinary Science 0778
 - Zoology 0472
- Biophysics
 - General 0786
 - Medical 0760

- Geodesy 0370
- Geology 0372
- Geophysics 0373
- Hydrology 0388
- Mineralogy 0411
- Paleobotany 0345
- Paleoecology 0426
- Paleontology 0418
- Paleozoology 0985
- Palyology 0427
- Physical Geography 0368
- Physical Oceanography 0415

HEALTH AND ENVIRONMENTAL SCIENCES

- Environmental Sciences 0768
- Health Sciences
 - General 0566
 - Audiology 0300
 - Chemotherapy 0992
 - Dentistry 0567
 - Education 0350
 - Hospital Management 0769
 - Human Development 0758
 - Immunology 0982
 - Medicine and Surgery 0564
 - Mental Health 0347
 - Nursing 0569
 - Nutrition 0570
 - Obstetrics and Gynecology 0380
 - Occupational Health and Therapy 0354
 - Ophthalmology 0381
 - Pathology 0571
 - Pharmacology 0419
 - Pharmacy 0572
 - Physical Therapy 0382
 - Public Health 0573
 - Radiology 0574
 - Recreation 0575

- Speech Pathology 0460
- Toxicology 0383
- Home Economics 0386

PHYSICAL SCIENCES

- Pure Sciences
 - Chemistry
 - General 0485
 - Agricultural 0749
 - Analytical 0486
 - Biochemistry 0487
 - Inorganic 0488
 - Nuclear 0738
 - Organic 0490
 - Pharmaceutical 0491
 - Physical 0494
 - Polymer 0495
 - Radiation 0754
 - Mathematics 0405
 - Physics
 - General 0605
 - Acoustics 0986
 - Astronomy and Astrophysics 0606
 - Atmospheric Science 0608
 - Atomic 0748
 - Electronics and Electricity 0607
 - Elementary Particles and High Energy 0798
 - Fluid and Plasma 0759
 - Molecular 0609
 - Nuclear 0610
 - Optics 0752
 - Radiation 0756
 - Solid State 0611
 - Statistics 0463
- Applied Sciences
 - Applied Mechanics 0346
 - Computer Science 0984

- Engineering
 - General 0537
 - Aerospace 0538
 - Agricultural 0539
 - Automotive 0540
 - Biomedical 0541
 - Chemical 0542
 - Civil 0543
 - Electronics and Electrical 0544
 - Heat and Thermodynamics 0348
 - Hydraulic 0545
 - Industrial 0546
 - Marine 0547
 - Materials Science 0794
 - Mechanical 0548
 - Metallurgy 0743
 - Mining 0551
 - Nuclear 0552
 - Packaging 0549
 - Petroleum 0765
 - Sanitary and Municipal System Science 0554
 - 0790
 - Geotechnology 0428
 - Operations Research 0796
 - Plastics Technology 0795
 - Textile Technology 0994

PSYCHOLOGY

- General 0621
- Behavioral 0384
- Clinical 0622
- Developmental 0620
- Experimental 0623
- Industrial 0624
- Personality 0625
- Physiological 0989
- Psychobiology 0349
- Psychometrics 0632
- Social 0451



To my parents

CONTENTS

Certificate of Examination	ii	
Copyright Agreement	iii	
Dedication	iv	
Contents	v	
List of Tables	vii	
List of Figures	viii	
Abstract	x	
List of Abbreviations	xi	
Acknowledgements	xiii	
Chapter 1	Photoinduced Electron Transfer in Organic Chemistry	1
Chapter 2	The Photochemical Nucleophile-Olefin Combination, Aromatic Substitution Reaction (Photo-NOCAS)	23
Chapter 3	The Photo-NOCAS Reaction: Methanol - Pinene (α - and β -), 1,4-Dicyanobenzene	36
Chapter 4	The Photo-NOCAS Reaction: Methanol - Tricyclene, 1,4-Dicyanobenzene	71
Chapter 5	<i>Ab Initio</i> Studies on the Interaction between the Allyl and Alkyl Radical and Carbocation Moieties, and on the Cleavage of the Radical Cations of Alkenes: 1-Butene and 4,4-Dimethyl-1-pentene	88
Chapter 6	The Photo-NOCAS Reaction: Methanol - Nopol and 2-(1-Cyclohexenyl)-1-Ethanol, 1,4-Dicyanobenzene	111
Chapter 7	The Photo-NOCAS Reaction: Methanol - 2-Carene, 1,4-Dicyanobenzene	124
Appendix 1	The Archive Entries of the <i>Ab Initio</i> Molecular Orbital Calculations	145

Appendix 2 X-Ray Data	169
References	177

List of Tables

3.1	The calculated free energy change for the electron transfer process with the singlet excited state of 1,4-dicyanobenzene (1) or 9,10-dicyanoanthracene as acceptor	37
3.2	The specific rotations of α - and β - pinene after different conversions of 1	40
3.3	The photo-NOCAS reaction: methanol-olefin, 1,4-dicyanobenzene	42
3.4	The charge and spin distributions calculated for the radical cation of α -pinene (Structure 25 in Figure 3.2)	49
3.5	The charge and spin distributions calculated for the distonic radical cation formed upon ring-opening of the radical cation of α -pinene (Structure 26 in Figure 3.4)	50
3.6	The charge and spin distributions calculated for the distonic radical cation formed upon ring-opening of the radical cation of α -pinene (Structure 27 in Figure 3.5)	51
3.7	The charge and spin distributions calculated for the distonic radical cation formed upon ring-opening of the radical cation of α -pinene (Structure 28 in Figure 3.6)	52
3.8	The calculated (STO-3G) total energies (a.u.), for the radical cation of α -pinene, and for the distonic radical cations formed upon ring-opening of the radical cation of α -pinene	53
4.1	The calculated charge and spin distributions for the radical cation of tricyclene (Structure 45)	83
5.1	The calculated (<i>ab initio</i>) total energies for the neutral alkenes 46 and 47, for several alternative structures of the alkene radical cations, and for the fragment alkyl and allyl radicals and cations	92
7.1	The calculated charge and spin distributions for the radical cation of 2-carene (Structure 69)	132
7.2	The specific rotations of 2-carene before and after irradiation	137
7.3	The calculated (STO-3G) total energies (a.u.) for the neutral alkenes and for the alkene radical cations	140

List of Figures

3.1	Structure 24: the fully optimized structure (minimum) for the molecule of α -pinene (14)	44
3.2	Structure 25: the fully optimized structure (minimum) for the radical cation of α -pinene (14)	45
3.3	Possible conformations of the distonic radical cation formed upon ring opening of the radical cation of α -pinene	46
3.4	Structure 26: the fully optimized structure (minimum) for the distonic radical cation formed upon ring opening of the radical cation of α -pinene	46
3.5	Structure 27: the fully optimized structure (transition state) for the distonic radical cation formed upon ring opening of the radical cation of α -pinene	47
3.6	Structure 28: the fully optimized structure (minimum) for the distonic radical cation formed upon ring opening of the radical cation of α -pinene	48
4.1	Structure 45: the fully optimized structure for the radical cation of tricyclene ($33^{+\bullet}$)	82
5.1	The four possible conformers of 1-butene resulting from rotation around the C2-C3 carbon-carbon single bond	91
5.2	The global minimum structure for the radical cation of 1-butene ($46^{+\bullet a}$); above: the optimized (UHF/6-31G*) structure; below: the spin and charge densities	94
5.3	Possible metastable intermediates/transition states preceding the complete separation of the allyl and alkyl fragments from the radical cation of alkenes	95
5.4	A transition state for the radical cation of 1-butene ($46^{+\bullet b}$); above: the optimized (UHF/6-31G*) structure; below: the spin and charge densities	96
5.5	The global minimum structure for the radical cation of 4,4-dimethyl-1-pentene ($47^{+\bullet a}$); above: the optimized (UHF/6-31G*) structure; below: the spin and charge densities	98
5.6	A transition state for the radical cation of 4,4-dimethyl-1-pentene ($47^{+\bullet b}$); above: the optimized (UHF/STO-3G*) structure; below: the spin and charge densities	100

5.7	The radical cation 46⁺b : (a) The highest filled molecular orbital (HOMO); (b) The singly occupied molecular orbital (SOMO); (c) the lowest unoccupied molecular orbital (LUMO)	102
5.8	Orbital correlation diagram for the cleavage of the radical cation 46⁺b . Cleavage of the radical cation to the allyl radical and methyl cation is orbital symmetry allowed	103
5.9	Thermochemical cycles for the cleavage of the radical cations 46⁺a . (a) Experimental results. (b) Differences in calculated (MP2/6-31G**//UHF/6-31G*) total energies. (c) Differences in calculated (UHF/6-31G*) total energies	105
5.10	Thermochemical cycles for the cleavage of the radical cations 47⁺a . (a) Experimental results. (b) Differences in calculated (UHF/STO-3G) total energies	106
5.11	The calculated (UHF/STO-3G) spin and densities on the alkyl fragment of the radical cation (a) 46⁺a and (b) 47⁺a as a function of allylic bond length	108
7.1	Structure 69 : the fully optimized structure for the radical cation of 2-carene (64⁺)	127
7.2	Structure 70 : the fully optimized structure for 2-carene (64) (RHF/STO-3G)	128
7.3a	The fully optimized structure for the radical cation of 2,2-dimethyl-1-vinyl)cyclopropane (71⁺)	129
7.3b	The spin and charge densities on the radical cation 71⁺	130
7.4a	The fully optimized structure for 2,2-dimethyl-1-(2,2-dimethylvinyl)cyclopropane (72⁺) (UHF/STO-3G)	130
7.4b	The spin and charge densities on the radical cation 72⁺	131
7.5	The fully optimized structure for 2,2-dimethyl-1-vinylcyclopropane (71) (RHF/STO-3G)	131
A2.1	X-ray crystal structure of 55	175
A2.2	X-ray crystal structure of 56	176

Abstract

The photo-induced electron transfer reaction between 1,4-dicyanobenzene (1) and 2,3-dimethyl-2-butene (7) in acetonitrile-methanol solution leads to the 1:1:1 adduct 8.

This type of reaction, the photo-NOCAS reaction, has been extended to other acceptor/donor systems. For unsymmetric olefins, the formation of *anti*-Markovnikov products is favored.

As part of a program to define the scope of the photo-NOCAS reaction, the dicyanobenzene/vinylcyclobutane (14, 15) and dicyanobenzene/vinylcyclopropane (64) systems have been examined in this study. The four-membered rings of the initially formed radical cations from both α -pinene (14) and β -pinene (15) cleave to give the distonic radical cations having the tertiary cation - allylic radical structure (29, 31). These radical cations either react with methanol, finally leading to photo-NOCAS products, or are trapped by acetonitrile, giving rise to the cyclic imines (19, 23). On the other hand, the initially formed radical cation from 2-carene (64) rapidly reacts with methanol before the three-membered ring cleaves completely.

The possible connection between $14^{+\bullet}$ and the radical cation of tricyclene (33) has also been investigated. The radical cation of tricyclene is relatively stable; the nucleophilic opening of the three-membered ring has been observed. No evidence was found for the ring-opening of $33^{+\bullet}$ to give the distonic radical cation 29.

By the study of the photo-NOCAS reactions with nopol (52) and 2-(1-cyclohexenyl)ethanol (57), a comparison was made between the ring-opening and the intramolecular and intermolecular nucleophilic reaction of the radical cation(s).

Ab initio calculations at the STO-3G level were performed on most of the radical cations involved in this study and the calculations were compared with the experimental results. Moreover, a detailed *ab initio* study at higher levels on the two model systems, 1-butene (46) and 4,4-dimethyl-1-pentene (47), shows the profound effects of the two geminal methyl groups on the energetics for the cleavage process of the radical cations involved. The calculations were also carried out on the interaction between the allyl and alkyl radical and carbocation moieties.

List of Abbreviations

AM1	Austin Model One
Chrom W	chromasorb white
CIDNP	chemically induced dynamic nuclear polarization
CV	cyclic voltammetry
d	doublet (NMR spectral)
δ	chemical shift in NMR
ESR	electron spin resonance
eV	electronvolt
G	Gibbs free energy
GC/MS	gas chromatography/mass spectrometry
GC/FID	gas chromatography/flame ionization detector
HOMO	highest occupied molecular orbital
<i>ipso</i>	position of substitution
LUMO	lowest unoccupied molecular orbital
<i>m/z</i>	mass-to-charge ratio in MS.
MP2	Second order Møller-Plesset perturbation theory
MPLC	medium pressure liquid chromatography
n	nano (10^{-1})
q	quartet in NMR
RHF	restricted Hartree-Fock
s	singlet in NMR

SCE	saturated calomel electrode
SE-30	100% methylsilicone gum
t	triplet in NMR
<i>tert</i>	tertiary
UHF	unrestricted Hartree-Fock
V	volt
WCOT	wall coated open tubular

All other abbreviations are standard.

Acknowledgements

Many people generously provided their help during my stay at Dalhousie; this was a memorable time of my life. I would like to take this opportunity to express my sincere thanks to my supervisor, Dr. D. R. Arnold, for his constant encouragement and guidance, and for sharing his enthusiasm, knowledge and expertise. My especial thanks are also extended to other members of my committee, Drs. R. J. Boyd, D. L. Hooper, and J. A. Pincock; their comments on my preliminary report and this thesis were appreciated.

I would reiterate my gratitude to the members of the Arnold group: Kim McManus, Allyson Perrott, Dennis Connor and Jing Chen, and also to the former members: Kevin McMahon, Miles Snow, for their friendship and help. I would also like to thank Xianqi Kong for our discussions on various topics.

The author is indebted to Dr. Hooper and Gang Wu (ARMRC, Dalhousie) for recording the NMR spectra; to Dr. Boyd for the use of his facilities to carry out calculations and to print out this thesis; to Dr. Cameron for X-ray structure determination; to the Department of Chemistry and Dalhousie University for financial support; to Dalhousie University Computing and Information Services for generous allocation of computer time; to IMB (NRC, Halifax) for the use of the polarimeter.

Lastly, many thanks are due to my wife for her invaluable assistance at various stages of the thesis's preparation.

Chapter 1

Photoinduced Electron Transfer in Organic Chemistry

The development in modern spectroscopic methods over the last decade has greatly increased our understanding of *photoinduced electron transfer* (PET).^{1,2,3,4,5} More and more reactions in photochemistry have been identified as PET reactions. To this day, the PET reaction has become of wide scope and versatility—playing an important role in various disciplines of chemistry and offering many possibilities for creative synthetic design. There are several good reviews on photoinduced electron transfer reactions.⁶ Here we will focus on a few general concepts related to PET in organic chemistry, and review some typical PET reactions of organic substrates in homogeneous solution.

1.1 The Nature of Light

Light, or more properly, electromagnetic radiation, can be described in terms of frequency (ν) or wavelength (λ). The two parameters are related to each other by the velocity of light (c) in the equation $c = \lambda\nu$. On the other hand, in the quantum model a beam of light is regarded as a stream of photons. A photon has no mass but it has a specific energy (E), related to the frequency of the light (ν) by the Planck relation: $E = h\nu$. Intensity of light is directly proportional to the amount of photons. The following schematic diagram (Scheme 1.1) shows the relation between E and ν (or λ).

The interaction of light with molecular systems is generally considered as an interaction between one molecule and one photon. After the photon is absorbed by the molecule, the photon ceases to exist and its energy is transferred to the molecule whose electronic structure then changes. The interaction process can be presented in the following form



where A denotes the ground-state molecule, $h\nu$ the absorbed photon, and A^* the molecule A in the excited state with the extra energy $h\nu$.

1.3 Excited States

Once we have an excited state molecule (A^*), the next concern is whether or not this light absorption will bring about a chemical reaction. This depends on the rate constant for the initial photochemical step involving the excited state. The rate constant must be high (typically in the range of 10^6 - 10^9 s⁻¹) for the initial photochemical step to occur, because the excited state is short-lived—decaying to the ground state very rapidly by various mechanisms. The decay processes may be radiative or non-radiative.

1.4 Electron Transfer - Contact and Solvent Separated Radical Ion Pairs

The phenomenon that a substance accelerates the decay of another molecule in an electronically excited state, back to the ground state or to a lower electronically

excited state, is often observed. This phenomenon is called quenching and the substance is described as a quencher.

The quenching process is of such generality that it occurs by many different mechanisms and it is induced by many different substances. For example, it is commonly observed that an increase in the concentration of a solute (e.g., pyrene⁷) is accompanied by a decrease in the intensity (quantum yield) of its fluorescence and by the appearance of a new emission at longer wavelengths, the intensity of which increases with concentration. These phenomena have been explained by the formation and subsequent fluorescence of an excited state pyrene dimer (*excimer*).

Similar phenomena are observed in solutions of mixed solutes (e.g., a solution of anthracene and diethylaniline in toluene⁸), which could be ascribed to the formation of an excited state of a complex (*exciplex*). Exciplexes are polar entities.⁹ Large electronic coupling exists in exciplexes (the distance between the two ions is relatively short, ca. 3 Å), and the consequence is that emission can be observed from these species.

It is important to point out that exciplex formation is not restricted to aromatic systems and that there is no requirement that exciplexes should necessarily luminesce. If the sum of the rate constants of radiationless processes involving the exciplexes is sufficiently high, the lifetime of the exciplexes will be so short that emission may be undetectable. In organic photochemistry, many reactions have been recognized as proceeding via exciplexes.¹⁰

The emission from an exciplex of an aromatic hydrocarbon with an amine in solvents of increasing polarity is observed not only to shift to the longer wavelengths

but also to diminish in intensity, finally becoming zero in solvents with a high dielectric constant, such as acetonitrile.⁸ Flash photolysis experiments carried out in acetonitrile solution indicate the transient formation of the hydrocarbon radical anion and the amine radical cation. This implies that the exciplex dissociates into solvated radical ions, or that the electron transfer process occurs in an encounter complex between the excited acceptor and the donor, giving rise to *solvent separated radical ion pair* (SSRIP) (the distance between the two ions is relatively long, ca. 7 Å).

If the acceptor and the donor in their ground states form a *charge-transfer (CT) complex*, irradiation of the complex will lead to the *excited charge-transfer complex*.¹¹ Sometimes the exciplex and excited CT complex are called *contact radical-ion pair* (CRIP).¹²

It is not necessary that either a CRIP or an exciplex is the primary product from PET. Detailed studies of the photoreduction of benzophenone by aromatic amines in acetonitrile leads to the conclusion that electron transfer occurs over a distance greater than the van der Waals radii, giving rise to the SSRIP as primary product that subsequently collapses to the more stable CRIP.¹³ Studies of the same system in ethanol show that the CRIP forms prior to the SSRIP.¹⁴

1.4 The Rehm-Weller Equation

Exciplexes or CRIP, SSRIP and excited CT complexes are all primary intermediates in photoinduced bimolecular electron transfer processes. Both classical¹⁵ and nonclassical (nonadiabatic)¹⁶ theories have been developed to analyze PET rates. In

practice, there is an empirical way to estimate the feasibility of formation of the radical ion pair, i.e., the Rehm-Weller relationship.¹⁷

The Rehm-Weller equation used in organic photochemistry has the following form:

$$\Delta G = 96.48(E_{1/2}^{\text{ox}} - E_{1/2}^{\text{red}} - e_0/a\epsilon) - E_{0,0}$$

where ΔG (kJ/mol) is the free-energy change for an electron transfer process from a ground state donor (e.g., an olefin) to the first excited singlet state of an acceptor (e.g., dicyanobenzene). $E_{1/2}^{\text{ox}}$ (V) is the oxidation potential of the donor, $E_{1/2}^{\text{red}}$ (V) is the reduction potential of the acceptor, $e_0/a\epsilon$ is the Coulombic interaction energy associated with bringing the two radical ions to the encounter distance a in the solvent of dielectric constant ϵ , and $E_{0,0}$ (kJ/mol) is the electronic excited state energy of the acceptor. Based on the calculated values of ΔG by this equation, we can estimate the rate constant for ET to form the radical ions. Figure 1.1 shows schematically the variations in the logarithm of the observed rate constant for quenching of the fluorescence of the acceptor with ΔG . When ΔG is more exothermic than 20-40 kJ mol⁻¹ (5-10 kcal mol⁻¹), the rate constant would be nearly diffusion-controlled. The rate constant falls as ΔG becomes less exothermic, and finally the logarithm of the rate constant has a linear relationship with ΔG .

When ΔG for radical ion pair formation, calculated by using the Rehm-Weller equation, is endergonic, it is still possible that exciplex formation can occur. In such cases, cycloaddition products are often observed. We shall give an illustrative example in Chapter 2.

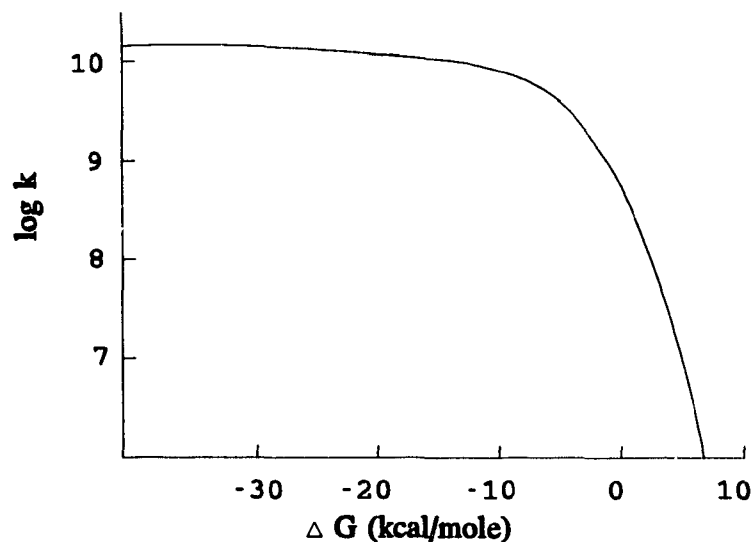


Figure 1.1. Plot of $\log k$ versus ΔG

Energy transfer, one of the major decay mechanisms for the excited state, is often in competition with electron transfer. In the literature there are many examples of competition between energy and electron transfer.¹⁸

1.6 Back Electron Transfer

Low quantum yields in PET reactions are often encountered. The reason for this is that back electron transfer can be very fast, so that the subsequent chemical reactions leading to the products cannot compete. This inefficiency has prevented PET reactions from becoming widely used in organic synthesis.

Polar solvents are often used in PET reactions, because in polar solvents formation of the solvent separated or free radical ions is often so fast that secondary chemical reactions can be observed. Generally, the chance for back electron transfer between the free radical ions is extremely small considering the low concentrations of

the radical ions and fast subsequent chemical reactions. But still, back electron transfer is commonly the major energy wasting step, even in polar solvents.

To increase quantum yields and product yield in PET reactions, a reasonable understanding of the main factors influencing the back electron transfer process is important. Gould, Farid and coworkers have published several papers, reporting their studies on back electron transfer within geminate radical ion pairs (CRIP and SSRIP) of aromatic systems. They observed the Marcus inverted region for back ET in both the SSRIP and CRIP.¹⁹ Reports from other research groups have also observed this phenomenal fact.²⁰ Marcus theory predicts that electron transfer rates increase with increasing driving force to a maximum and then decrease upon further increases in the driving force.^{15,21} The region where rates decrease upon increasing exothermally is referred to as the Marcus inverted region.

Back electron transfer in exciplexes and excited CT complexes may occur via both non-radiative or radiative process. The fluorescence of exciplexes has been recognized as a back ET process and the energy and width of the exciplex fluorescence spectrum are directly related to the ET reorganization parameters.²²

Gould, Farid and coworkers have also found that in some systems (e.g., cationic acceptor/olefinic donor systems) efficient photoinduced electron transfer leading to the formation of a neutral radical/radical cation pair could be achieved in solvents of medium and low polarity.²³ In less polar solvents, the reorganization energy associated with reorientation of the solvent is small. As a result, the rate constant for back electron transfer decreases.

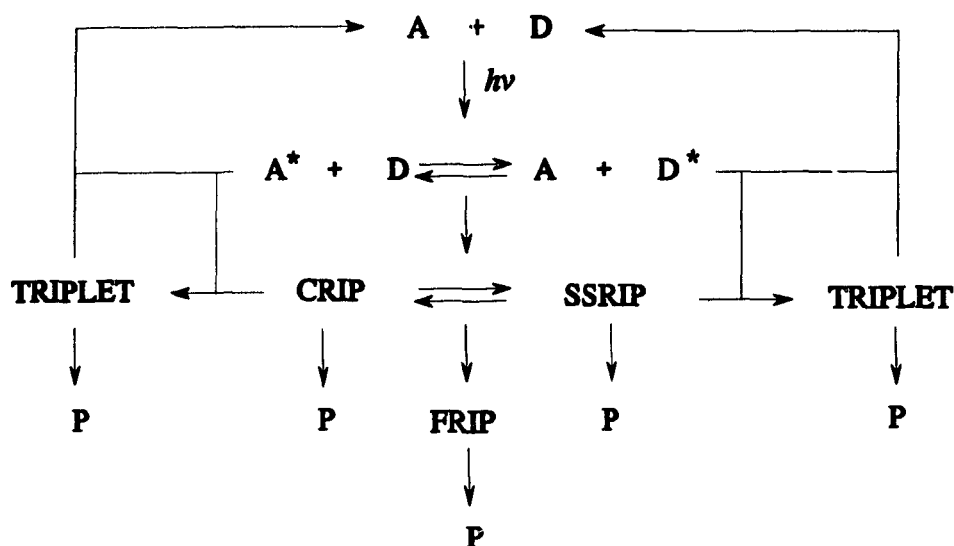
In a homogeneous solution, the rate of a bimolecular chemical reaction is often limited by the rate at which the reactant or the intermediate can diffuse through the solution. The diffusion-controlled rate constant depends on solvent viscosity and generally is on the order of 10^9 to $10^{10} \text{ M}^{-1} \text{ s}^{-1}$ for typical solvents at ambient temperature. The rate of back ET is also often diffusion controlled. Consequently the chance for a secondary chemical process to compete successfully with back ET is limited. Therefore, extensive efforts have been directed in recent years towards the development of organized photochemical assemblies that are capable of stabilizing the primary intermediates from ET against back electron transfer. The approaches include the design of microheterogeneous organized microenvironments where vectorial ET reactions proceed. The general topic of photosensitized electron transfer reactions in microheterogeneous media has been extensively reviewed.²⁴

The chemistry of triplets formed upon back ET has been observed. Triplet formation is favoured by back ET when the energy of the radical ion pair is higher than the triplet energy of one of the starting compounds. Some examples can be found in reference 25.

1.7 Chemistry of the Radical Ions

The intermediates generated by PET, including exciplexes or CRIP, SSRIP and excited CT complexes, are generally very chemically reactive. Many photoinduced electron transfer reactions with excellent yield have been reported, thus demonstrating potential synthetic utility. From a practical view, it is convenient to classify these reactions by the products (as shown in Scheme 1.2), rather than by the detailed

Scheme 1.2



P stands for "product(s)". They may be the same or different and can be classified as following:

Fragmentation
Dimerization
Electrophilic addition
Nucleophilic addition

mechanisms. This is because singlet and triplet contact and solvent separated radical ion pairs, and free radical ions (FRI) might all be reactive intermediates, and often all display different chemistry. This explains why a small modification of the structure of substrates or of reaction conditions often leads to completely different results.

However, it is not trivial to distinguish among these reactive intermediates in all cases.

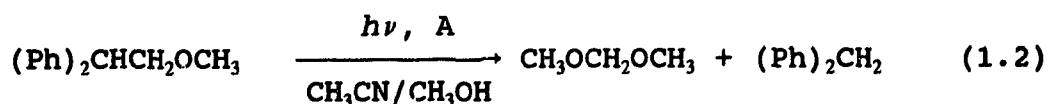
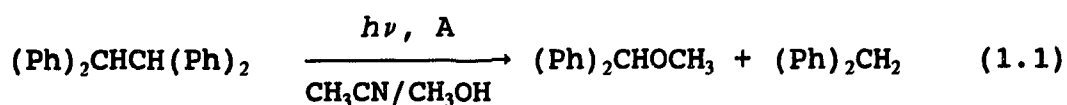
Scheme 1.2 summarizes the general situation encountered when a solution of A (the acceptor) and D (the donor) is irradiated. In actual cases, some equilibrium constants are small enough to be neglected, and so the situations in actual cases may be much simpler than that represented in Scheme 1.2. The final product(s) depend on

the individual case, or in other words, depend on the competition between possible pathways. In the following discussion we give only a few selected examples to illustrate the wide scope and potential synthetic utility of the PET reaction in the homogeneous solution.

Bond cleavage

Both radical anions and radical cations can undergo bond cleavage reactions. Bond cleavage can be induced both by intermolecular and intramolecular electron transfer, and it can occur either in a step-wise fashion through an intermediate such as radical ion or in a concerted pathway.

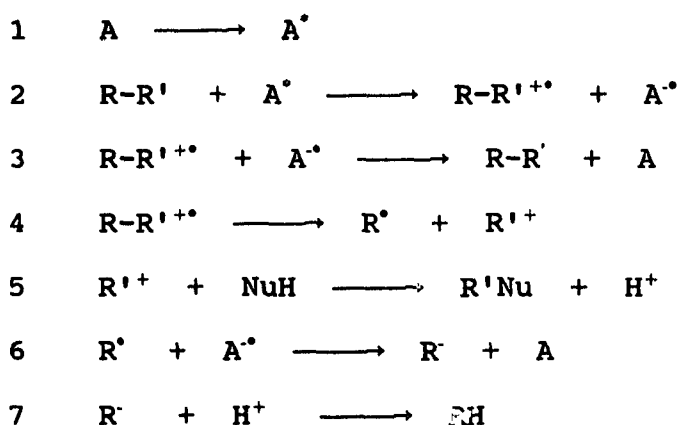
The cleavage of C-H and C-C bonds is often observed in the radical cations of olefin, arene, or bibenzyl compound. Work in this area has been pioneered by Arnold.^{26,27} In 1976, Arnold and Maroulis reported that the radical cations of 1,1,2,2-tetraphenylethane and methyl 2,2-diphenylethyl ether undergo C-C bond cleavage when irradiated in the presence of 1,4-dicyanobenzene (Equation 1.1 and 1.2).



A = 1,4-dicyanobenzene (1)

The proposed mechanism is shown in Scheme 1.3. Key steps in the proposed mechanism (Scheme 1.3) involve PET from the substrate to the sensitizer, and C-C bond cleavage of the resulting radical cation. The cleavage of the radical cation of methyl 2,2-diphenylethyl ether is regiospecific, i.e., no methyl diphenylmethyl ether was detected.

Scheme 1.3.

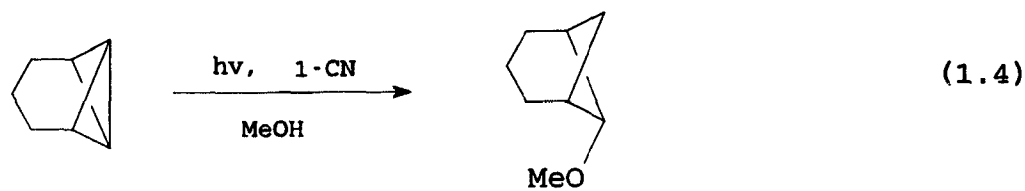
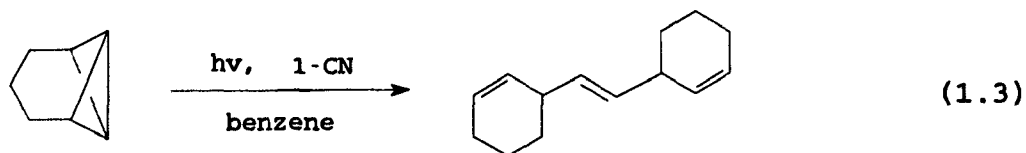


Subsequent studies both in Arnold's laboratory²⁸ and in other laboratories²⁹ provide more examples of this type of C-C bond cleavage reaction. The cleavage step must compete with other reaction pathways available to the radical cations, such as back electron transfer, deprotonation and reaction with nucleophiles. Several factors involved have been clarified. It has been shown that cleavage occurs only if the stability of the fragment radical and carbocation being formed is comparable to that of the parent radical cation.²⁸ In other words, the cleavage will occur only when the difference in energy between the radical cation and the fragment radical and

carbocation is about 60 kJ mol^{-1} . Substitution of the phenyl ring of methyl 2,2-diphenylethyl ether by the electron donating methoxy group either in *meta*- or *para*-position will make the radical cation much more stable, but will have a relatively minimal effect on the stability of the fragment radical and carbocation. This results in a greater energy difference between the radical cation and the fragment radical and carbocation (100 kJ mol^{-1}), hence no cleavage products were observed.³⁰

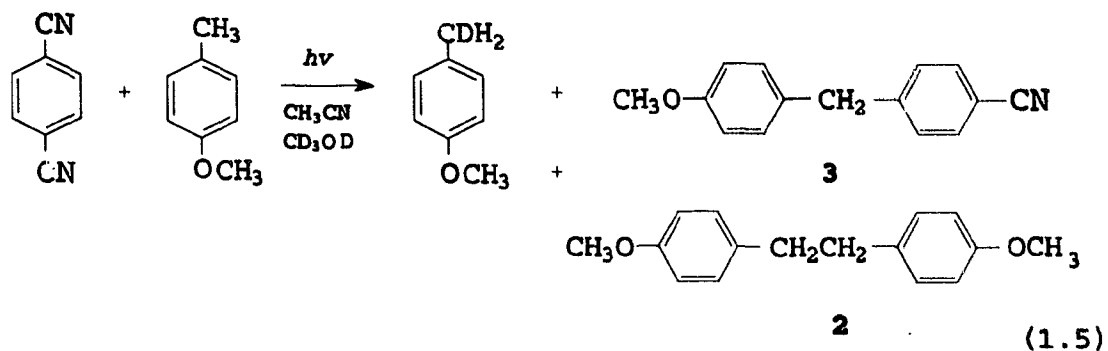
The regioselectivity of the cleavage reaction is controlled by the relative oxidation potentials of the two fragment radicals; cleavage selectively gives the more stable radical and cation pair.³¹ Also, the conformation of the substrate has been identified as having an influence on the feasibility of the cleavage step.³²

Besides the compounds discussed above, strained hydrocarbons have been investigated; these compounds have relative low oxidation potentials and can be conveniently oxidized by PET. As expected, the resulting radical cations undergo C-C bond cleavage to release the strain. For example, when a solution of tricyclo[4.1.0.0^{4,7}]heptane and 1-cyanonaphthalene (1-CN) in benzene is irradiated, a dimer is produced in 90-95% yield as an inseparable mixture of diastereomers (Equation 1.3). Changing the solvent from benzene to methanol results in the complete disappearance of dimer formation, and a solvent addition product is formed in quantitative yield (Equation 1.4).³³ A great deal of work on PET reactions has also been done with tricyclo[4.1.0.0^{4,7}]heptane system³⁴ and other strained systems such as bicyclo[1.1.0]butane.³⁵

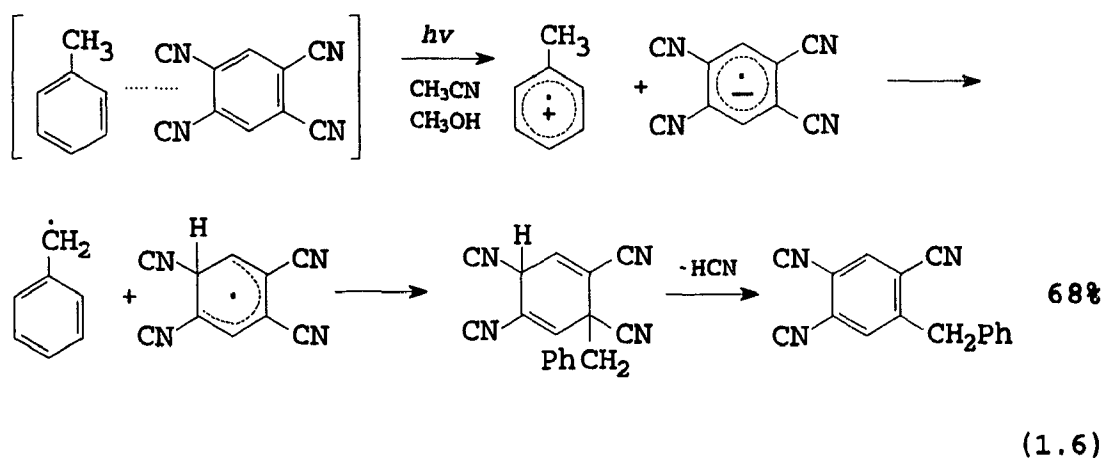


When the C-C bond cleavage is slow for some reason, deprotonation of radical cations might become the major competing reaction. Loss of a single electron greatly enhances the acidity of a neutral molecule.³⁶ For example, while the pK_a for toluene is over 50 in acetonitrile,³⁷ the radical cation of toluene is an extremely strong acid in acetonitrile solution with a pK_a between -9 and -13.³⁸

As a result of deprotonation of radical cations, radicals are formed. The resulting radicals may then undergo various processes. One of the most often observed processes is the reduction of the resulting radical by the radical anion, followed by protonation. For example, deuterium incorporation, along with the formation of two minor side products, was observed when CH_3OD was used as solvent (Equation 1.5).³⁰ The two products are indicative of the formation of the intermediate 4-methoxybenzyl radical. Coupling of this radical with another radical of the same kind gives 1,2-di(4-methoxyphenyl)ethane (2), and attack of this radical at the *ipso*-position of the 1,4-dicyanobenzene radical anion ($1^{\cdot-}$), followed by loss of



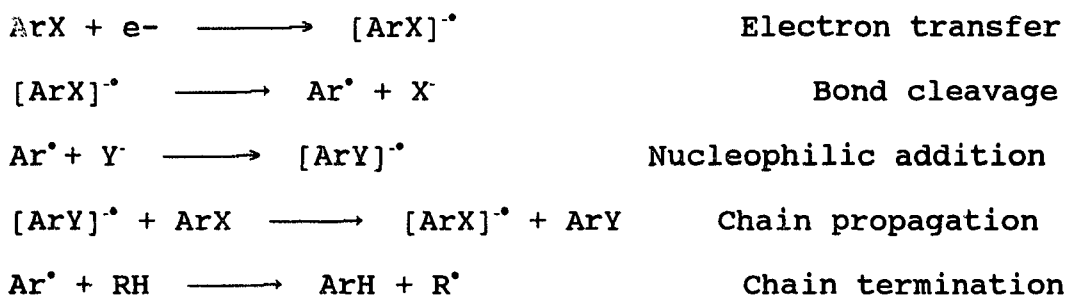
cyanide ion, leads to 4-cyano-4'-methoxy-diphenylmethane (3). Equation 1.6 shows another example of radical cation deprotonation.³⁹ The radical cations of aryl and aliphatic amines also undergo carbon-carbon bond cleavage and deprotonation.⁴⁰



PET induced bond cleavage of radical cations is not limited to the C-C bond and deprotonation. Other types of bond cleavage have been observed as well. Certain organoborane, organotin and organosilane compounds can undergo B-C, C-Sn or C-Si bond cleavage after PET. These areas were reviewed by Saeva.⁴¹

The radical anion, the counterpart of the radical cation, is also known to undergo bond cleavage. The best known PET bond cleavage of radical anions involves the substitution of aryl halides by the $S_{RN}1$ mechanism. This mechanism was first recognized by Bunnett and Rossi 1970.^{42,43,44} The $S_{RN}1$ mechanism requires one-electron reduction of an aryl halide to initiate the substitution reaction. Although a variety of ways can be used for the initiation, it is convenient to initiate the reaction photochemically. The general mechanism is shown in Scheme 1.4. The reactions have been found to be fairly general for aromatic compounds that are easily reduced.

Scheme 1.4

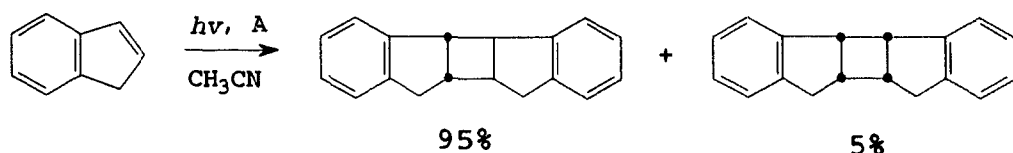


No special substituents are required on the aromatic ring; in fact, simple aryl halides undergo reaction, as do aryl halides substituted with alkyl, aryl, and alkoxy groups. All of the halides as well as $-SPh$, $+N(CH_3)_3$, and $-OP(OCH_2CH_3)_2$ have been used as leaving groups. A wide variety of groups have been employed as nucleophiles.⁴⁴ Polar solvents, such as liquid ammonia, acetonitrile, DMSO, and DMFO, are preferred. Some alkyl and benzyl halides also undergo aliphatic nucleophilic

substitution reactions via $S_{RN}1$ mechanism.⁴⁵ This area was first explored by Kornblum and by Russell in 1966.⁴⁶

Dimerization

Photoinduced electron transfer dimerization has been observed for indene and 1,1-dimethylindene. Electron-transfer sensitized irradiation of indene in acetonitrile solution using a cyanoaromatic sensitizer system^{47,48} or excitation of the charge transfer complexes of indenenes with anhydrides⁴⁹ results in formation of the anti head-to-head dimer as the major product (Equation 1.7).



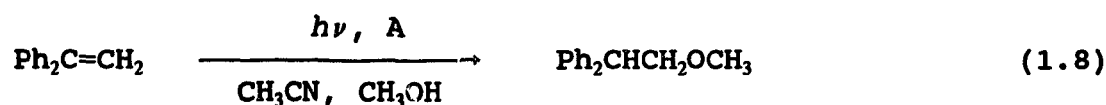
A = 1-cyanonaphthalene

(1.7)

Kinetic data for the reactions of several olefin radical cations with neutral olefin are reported in the literature. The reaction rate constants for terminal alkenes and alkynes are near the rate of diffusion in acetonitrile solution.^{50,51} The slower rates for 1,3-cyclohexadiene⁵² and dimethylindene⁵³ and the apparent failure of most acyclic internal olefins to undergo radical cation dimerization or polymerization reactions suggests that the reaction rate is sensitive to steric effects.

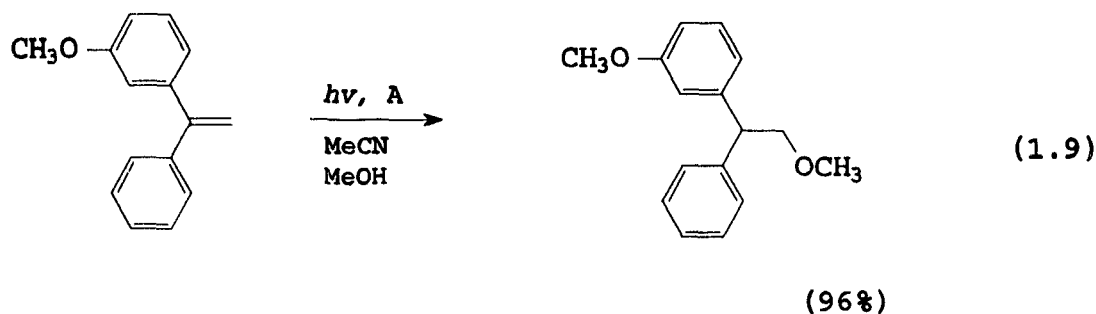
Addition of nucleophiles to the radical cations (1:1 adducts)

A very early example of this type of reaction was reported by Neunteufel and Arnold in 1973.⁵⁴ The first step in the proposed mechanism involves the excitation of 1,4-dicyanobenzene (1), followed by electron transfer from 1,1-diphenylethene to the excited 1. The rapid attack of methanol on the resulting radical cation leads to a radical, to which back electron transfer from the radical anion of 1 and subsequent protonation gives the *anti*-Markovnikov addition product in good yield (Equation 1.8). The meta- and para-methoxy derivatives of the arylalkene subject to the same reaction conditions as above show very interesting chemistry.³⁰ While the meta-methoxy



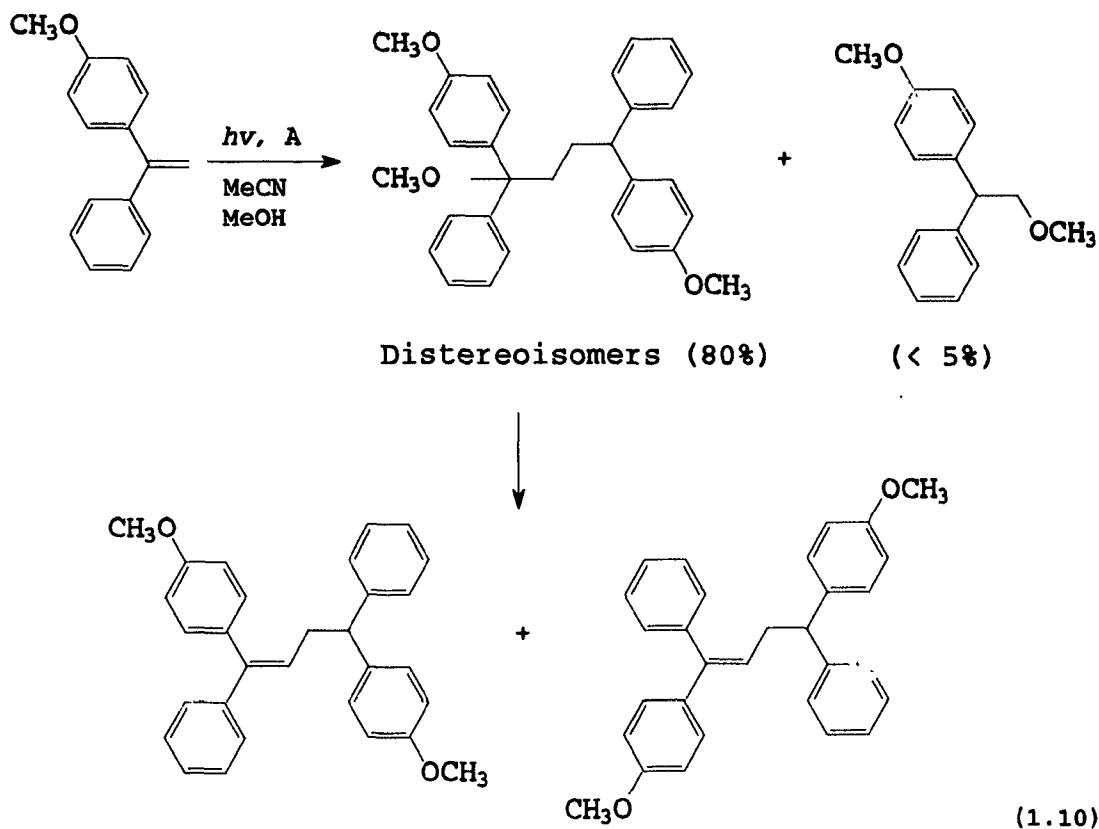
A = 1,4-dicyanobenzene (1)

derivative affords the *anti*-Markovnikov addition product in excellent yield (Equation 1.9), the para-isomer undergoes the other major reaction leading to a mixture of the



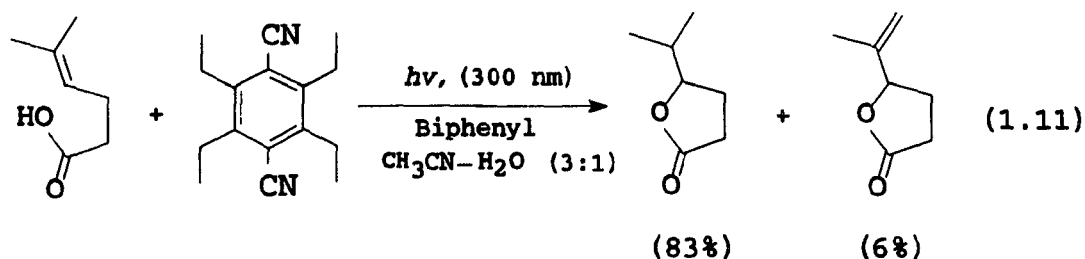
stereoisomeric two-to-one (alkene-methanol) adducts, which decompose slowly,

eliminating methanol, at room temperature to give a mixture of E- and Z-alkene (Equation 1.10).

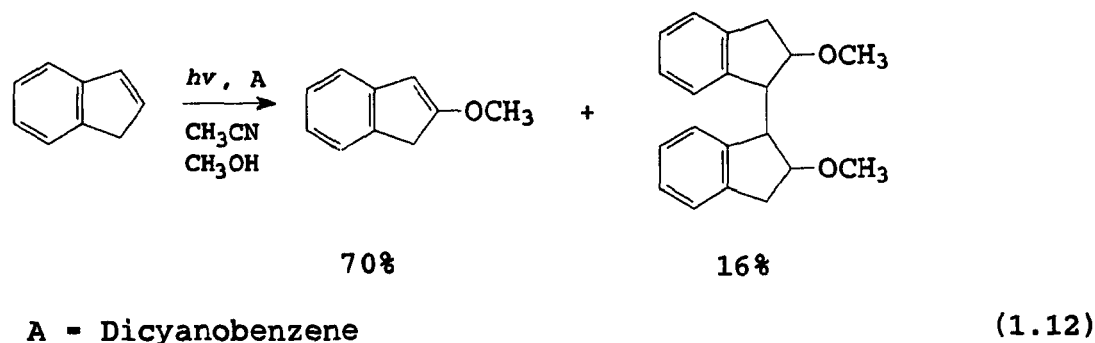


Recently, Gassman and coworkers have developed several sterically hindered sensitizers to increase the efficiency of PET reactions. For example, when 1,4-dicyanobenzene is used as the sensitizer instead of 1,4-dicyano-2,3,5,6-tetraethylbenzene in the reaction as depicted in Equation 1.11, the combined yield is only 36% (Equation 1.11).⁵⁵

The reaction of indene with the electron acceptor dicyanobenzene in methanol is interesting where both monomeric and dimeric ethers are formed (Equation



1.12).^{47,48} Radical dimerization and reduction apparently occur at comparable rates.

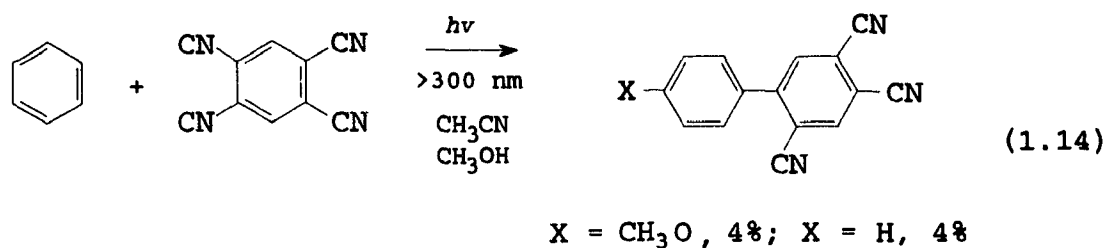
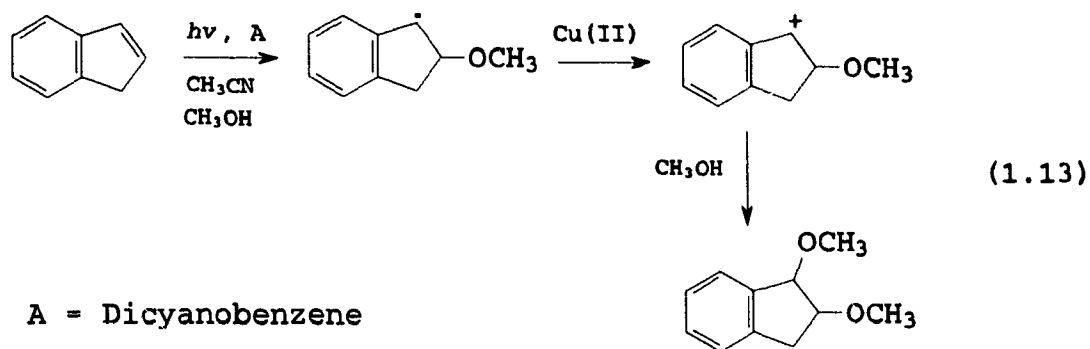


More interestingly, irradiation of indene or styrene with DCA and $\text{Cu}(\text{BF}_4)_2$ in acetonitrile-methanol (3:1) solution yields the 1,2-dialkoxy adducts in good to excellent yield, (Equation 1.13).⁵⁶ In this case the radical formed upon attack of methanol on the radical cation is further oxidized by the Cu (II) ion.

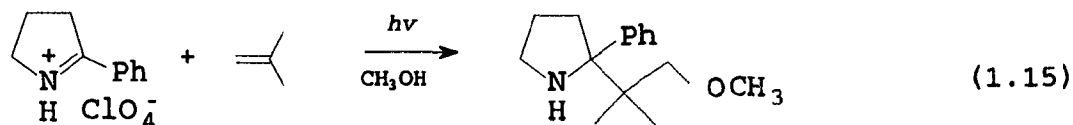
Formation of 1:1:1 adducts

Reactions affording 1:1:1 products usually involve formation of an aryl-aryl or aryl-heterocycle bond. One example is illustrated in equation 1.14.⁵⁷

Similar reactions are observed in the dicyanobenzene-furan-methanol system.^{48,58}

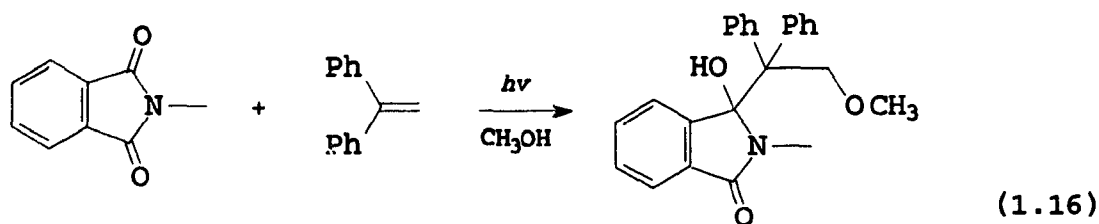


The iminium salt-olefin systems are also found to undergo reactions in which 1:1:1 adducts are formed (Equation 1.15).⁵⁹

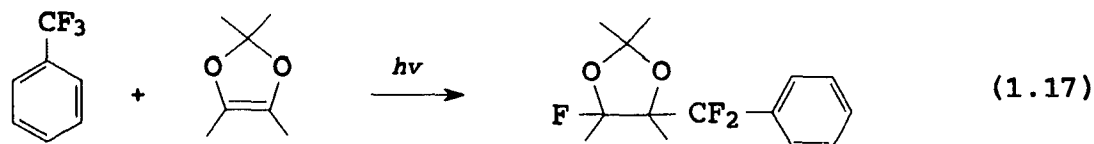


Singlet excited 2-phenyl-1-pyrrolium perchlorate is often used as an electron acceptor ($E_{1/2}^{ox} = -1.0 \text{ V}$ and $E_{0,0} = 3.9 \text{ V}$) in this type of reaction.

The formation of 1:1:1 adducts upon irradiation of phthalimides with alkenes and aryl alkenes in methanol solution has been extensively investigated.⁶⁰ One example is shown as in Equation 1.16.



Equation 1.17 gives another type of 1:1:1 adduct formation. The nucleophilic addition of fluoride ion to the olefin cation radical is proposed to occur in this reaction.⁶¹

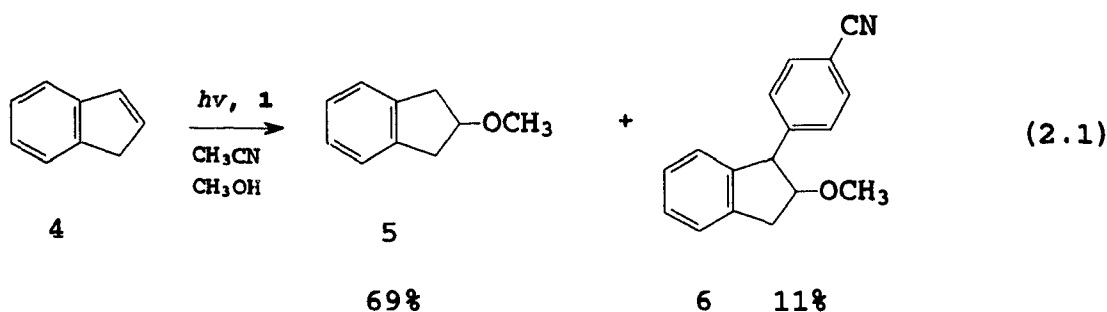


In 1984, Arnold and coworkers reported that irradiation of a solution of dicyanobenzene and an olefin in acetonitrile-methanol affords 1:1:1 adducts.⁶² The reaction was found to be fairly general with respect to olefins. Since then, a programme has been initiated to define the scope and limitations of the reaction. The details of this study will be reviewed in Chapter 2.

Chapter 2.

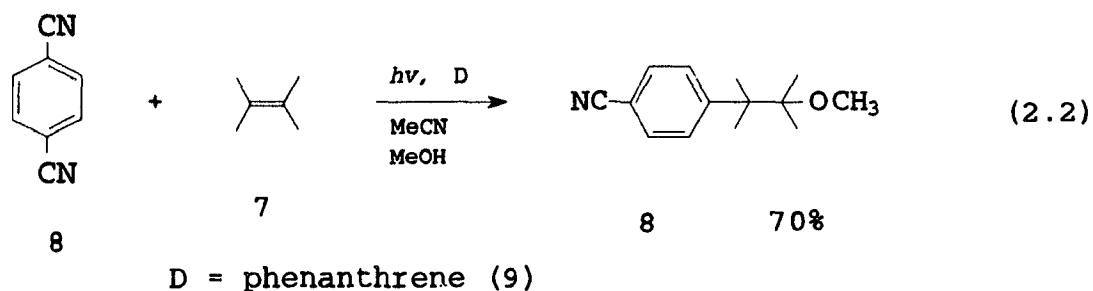
The Photochemical Nucleophile-Olefin Combination, Aromatic Substitution (Photo-NOCAS) Reaction

In Chapter 1, we have seen that when a solution of 1,4-dicyanobenzene (**1**) and 1,1-diphenylethene in acetonitrile-methanol (3:1) was irradiated, an *anti*-Markovnikov addition product was formed (Equation 1.8). However, when indene (**4**) was subjected to similar conditions, not only the *anti*-Markovnikov addition product (**5**) but also a 1:1:1 adduct (**6**) was obtained (Equation 2.1).⁴⁸ More interestingly, when 2,3-



dimethyl-2-butene (**7**) was used as a donor, the 1:1:1 adduct became the major product (**8**). The latter reaction proceeds much better in the presence of phenanthrene (**9**) (Equation 2.2).⁶²

The generality of this type of reaction with respect to the alkene (the donor) was first recognized in the Arnold laboratory. The reaction is termed the *photochemical nucleophile-olefin combination, aromatic substitution reaction* (photo-NOCAS).⁶² Since then, Arnold and co-workers have initiated an extensive study of

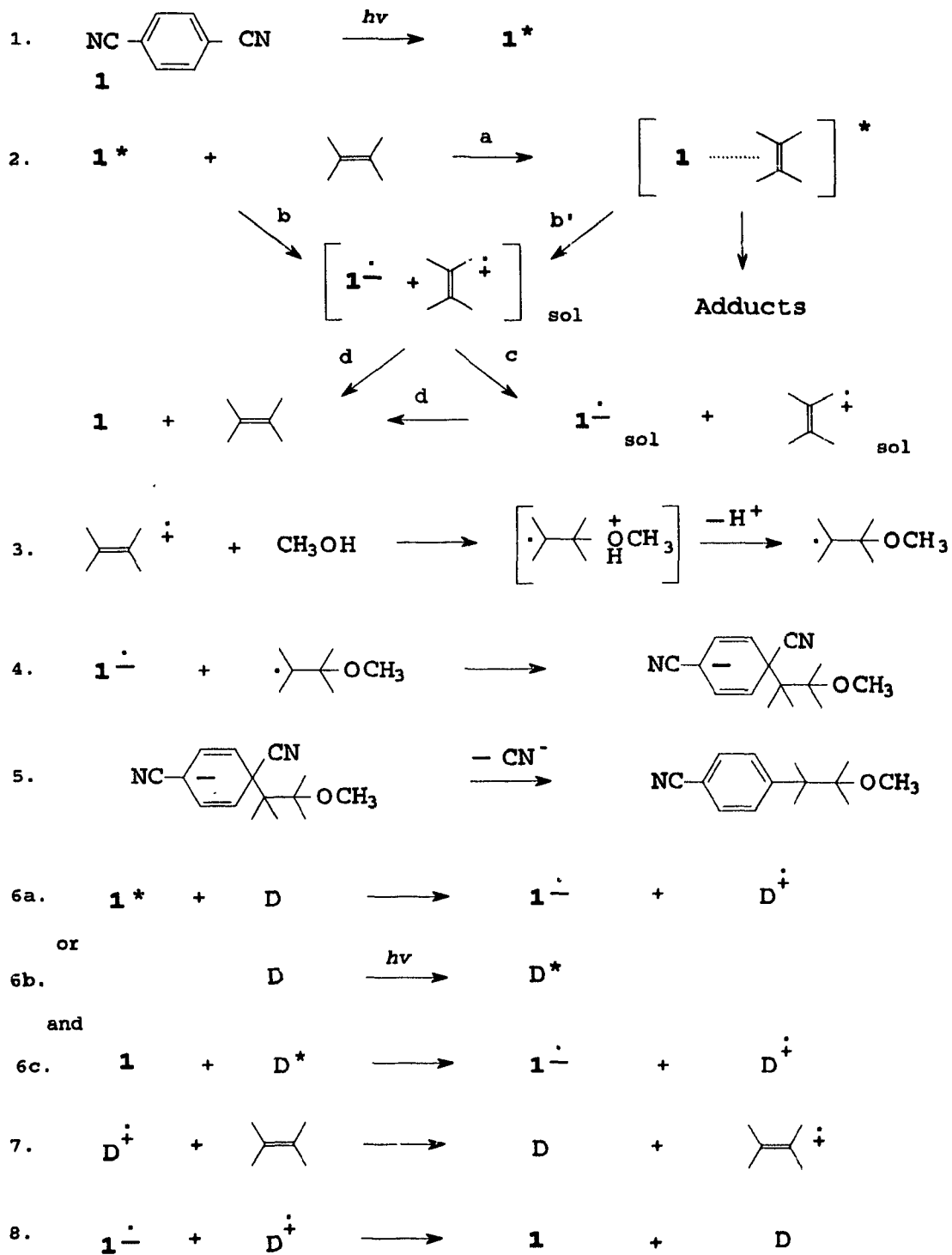


the reaction. A variety of acyclic and cyclic monoalkenes as well as conjugated and nonconjugated dienes have been studied, or are under investigation, in order to define the scope and limitations of the reaction.⁶³ Recently, the study has been extended to other aromatic electron acceptors. For example, a series of *para*-substituted benzonitriles has been examined, and the results are very encouraging.⁶⁴

In this chapter, we will give a general description of the photo-NOCAS reaction. We begin our discussion by providing the general mechanism of the photo-NOCAS reaction in Section 2.1. The remaining sections of the chapter will be devoted to more detailed discussion of the main steps in the reaction mechanism. The main purpose of this work is given at the end of the chapter.

2.1 The General Mechanism of the Reaction

Scheme 2.1 outlines a reasonable mechanism for the photo-NOCAS reaction. Steps 1 through 5 indicate what will occur upon direct irradiation, whereas steps 6 and 7 occur instead of step 2 when the reaction is sensitized by a co-sensitizer or mediated

Scheme 2.1

D = biphenyl or phenanthrene

by a co-donor[1]. Competing with product formation is deactivation by back electron transfer from the radical anion to the radical cation (steps 2d and 8). Step 3 is oversimplified since it does not specify any possibility of the association either between the radical ions or between the radical cation and the added co-sensitizer (or co-donor).

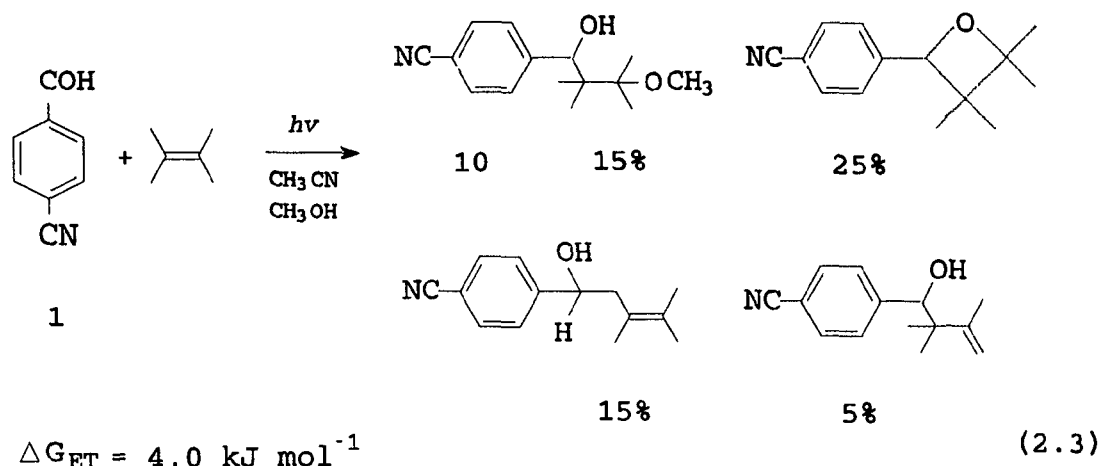
Addition of a co-donor or co-sensitizer to the reaction mixture generally increases the efficiency of the photo-NOCAS reaction. We shall discuss the functions of the added co-donor and co-sensitizer later.

2.2 Photoinduced Electron Transfer

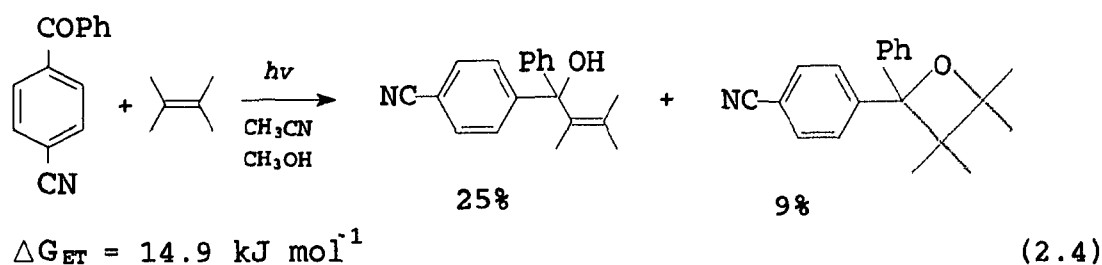
Irradiation of the reaction mixture is usually carried out through a Pyrex filter. Photons with energy higher than ca. 400 kJ/mol are absorbed by the Pyrex. In the reaction system, the light absorbing species is 1,4-dicyanobenzene (1) (or phenanthrene if it is used as a co-sensitizer). Fluorescence lifetime measurements and Stern-Volmer studies indicated a diffusion controlled quenching of the singlet excited state of 1 by the olefin donors.⁶² Calculations using the Rehm-Weller equation predict that the donor/acceptor systems studied should undergo a diffusion controlled electron transfer. Other evidence for electron transfer is the observation that irradiation of some donor/acceptor systems in non-polar solvents gave no photo-NOCAS products or gave typical exciplex products.

[1] If the added aromatic compound absorbs light under the reaction conditions, it is called a co-sensitizer; otherwise, it is called a co-donor.

When the calculated ΔG is less exergonic than -17 kJ/mol (-4 kcal/mol), ET is expected to occur at a rate that is slower than the diffusion controlled rate and other competing processes could dominate the reaction. This competition is illustrated by Equations 2.3 and 2.4 where 4-cyanobenzaldehyde and 4-cyanobenzophenone are used



as light-absorbing species, respectively. While the presence of product **10** (also see Equation 2.6), implies that a radical ion pair might be involved, the formation of other products apparently complicates the situation.⁶⁴



According to the Rehm-Weller equation, a good electron acceptor should have a relatively higher singlet excitation energy and a relatively lower (less negative) reduction potential. But these attributes are not enough; in addition, the life-time of

the excited state should be compatible with the rate constant for the electron transfer step.

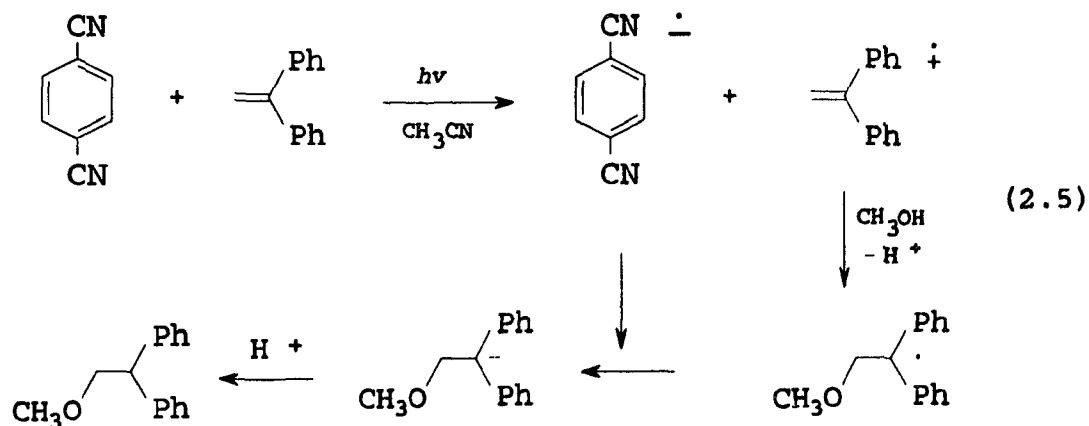
2.3 Nucleophilic Addition to Radical Cations of the Donors

Once an acceptor is chosen, the nature of the radical cations and the nucleophiles becomes the major consideration in designing the photo-NOCAS reaction. The nucleophilic addition to the radical cation must be fast enough to compete with other possible reaction pathways, for example, fragmentation, deprotonation, radical reaction, etc., as we have seen in Chapter 1.

Addition of the nucleophile to the radical cation generally favours formation of anti-Markovnikov products, i.e., the nucleophile attacks the less hindered end of the double bond. For example, addition of methanol to the radical cation of 1,1-diphenylethylene leads to a resonance stabilized radical.⁵⁴ Also, the previously reported photo-NOCAS reaction of methanol combining with 2-methylpropene and then substituting on 1,4-cyanobenzene suggests the involvement of the more stable radical intermediate.⁶² However, an argument based upon steric factors also could explain these results. Complications could arise in this regioselectivity of nucleophilic addition because other factors also might come into play—for example, the extent of separation of the radical ion pair formed upon direct irradiation, and the nature of the radical cation complex formed between the donor and the radical cation of co-donor in the mediated reactions. In a polar solvent, direct irradiation gives rise to the solvent separated radical ion pairs that will generally separate into free radical ions. The rate of diffusive separation has been determined to be ca. $5 \times 10^8 \text{ s}^{-1}$ for

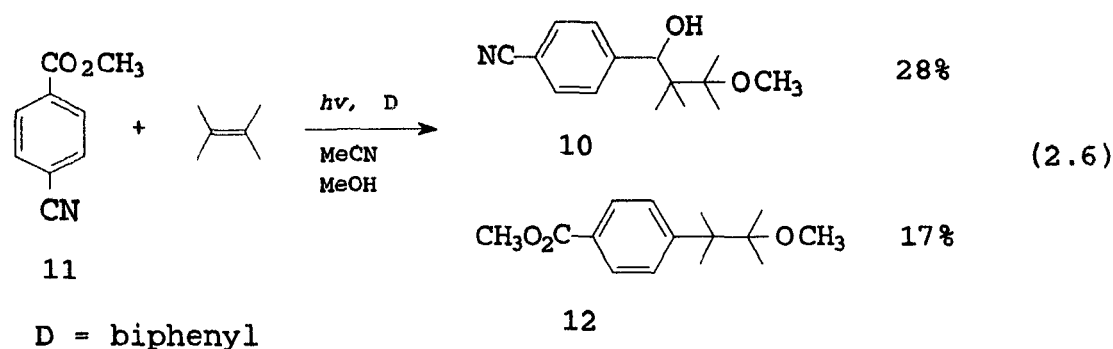
acceptor/donor systems such as 9,10-dicyanoanthracene (or 2,6,9,10-tetracyanoanthracene) /aromatic-donor⁶⁵ and pyrene/dimethylaniline⁶⁶ in acetonitrile at room temperature. The rate of addition of methanol to the olefin radical cation has been measured to be $1.6 \times 10^9 \text{ s}^{-1}$ for diphenylethylene.^{65c} More stable and sterically hindered radical cations, like 1,1-dianisylethylene radical cation and 1,1-dimethylindene radical cation, react more slowly with methanol.⁶⁷ Therefore, methanol might react with the contact or solvent separated radical ion pair, or the freely solvated radical cation, depending on the individual cases. The details of this addition are still uncertain. So far, only a few examples have been found where the added co-donor or co-sensitizer shows a significant effect on the regioselectivity of nucleophilic addition.^{63a}

Addition of methanol to the donor radical cation leads to the β -methoxy alkyl radical. If the reduction potential of the β -methoxy alkyl radical is less negative than that of the radical anion, the radical can acquire one electron from the radical anion, such as in the case of 1,1-diphenylethylene (Equation 2.5).⁵⁴ As a result, the *anti*-



Markovnikov addition product is the final product, not the photo-NOCAS product. On the other hand, if the β -methoxy alkyl radical couples with the radical anion, followed by loss of cyanide, the photo-NOCAS product will be formed (Equation 2.2). Saveant has recently measured the reduction potentials of alkyl radicals. Potentials were found to follow the order: *t*-butyl, -1.60; *sec*-butyl, -1.5; *n*-butyl, -1.4 (vs. SCE).⁶⁸ The reduction potential of **1** (-1.66 V) is comparable to that of the *tert*-butyl radical, so electron transfer will be in equilibrium between the radical anion of **1** and the *tert*-butyl radical; coupling can occur.

When methyl 4-cyanobenzoate (**11**) ($E_{1/2}^{red}$ -1.76 V)²⁶ is used as the acceptor, the reduction pathway becomes more important than in the case of **1**. This is demonstrated in Equation 2.6. In addition to the photo-NOCAS product (**12**), a



product formed upon reduction of the CO double bond of **11** was found. The reduction product (**10**) results from nucleophilic addition of the β -methoxy alkyl anion which is formed from ET to the β -methoxy alkyl radical from the radical anion of **11**.

2.5 Coupling and Substitution

The nature of the radical anion of the acceptor that is formed in the ET step plays an important role in determining the resulting chemistry. In order to get the photo-NOCAS products, the radical anion must be relatively stable on the time scale of the reaction sequence. Especially when a co-donor is used, the β -methoxy alkyl radical is formed away from the radical anion. Considering the very low concentration of both of these species and the fact that they are reactive (e.g., coupling and disproportionation of the radical), the encounter of these two species seems unlikely. However the high yield of the photo-NOCAS products may result from the buildup of the relatively stable radical anion. Thus, this coupling step (step 4) is controlled by "internal suppression of fast modes".⁶⁹

The evidence for the stability of the radical anion comes from electrochemical studies and ESR spectroscopy. Reversible reduction of **1** was observed in an acetonitrile solution by a cyclic voltammetry experiment. This indicates that the radical anion of **1** is relatively stable. Recently methyl 4-cyanobenzoate (**11**) was examined as an alternative electron acceptor in the photo-NOCAS reaction. The reversible reduction of this compound was also observed.⁶⁴

Step 4 is regioselective; the final product(s) indicates that substitution occurs at the *ipso*-position. The results support the hypothesis that coupling occurs at the position of greatest spin density. This is also the position that minimizes the localization energy in the resulting anion.^{62,70} Step 5 is the rearomatization of the phenyl ring.

2.6 The Effects of Co-donors and Co-sensitizers

Aromatic compounds such as biphenyl and phenanthrene are well known to increase the efficiency of the photo-NOCAS reaction. The degree of efficiency enhancement varies depending on whether the oxidation potential of the donor is lower or higher than that of the added aromatic compound. If the aromatic compound has a higher oxidation potential, complete hole transfer from the co-donor to the olefin occurs giving the discrete radical cation of the olefin. Accordingly, maximum efficiency of enhancement will be observed. In cases where the oxidation potential of the aromatic compound is lower than that of the donor, it has been suggested that a key mechanistic pathway for the reaction is the formation of a complex between the olefin and the radical cation of the co-donor.^{63a,71} Nucleophiles attack only on the olefin side of the complex where a partial positive charge develops. It is the complexes, which are stabilized by charge resonance, that make the photo-NOCAS reaction proceed more efficiently.

The requirements for an ideal co-donor can be listed:

1. stability in the ground state, and in the oxidized form under the reaction conditions.
2. suitable oxidation potential.
3. slow back ET step.
4. high efficiency of the redox process with the donor.

For an ideal co-sensitizer, additional requirements may be needed:

1. stability in the excited states and high efficiency of population of the excited state that is responsible for electron transfer;

2. absorption of light in a suitable spectral region;
3. suitable ground and excited state redox potentials;
4. long excited state lifetime.

Biphenyl is well known as a good co-donor. It increases the efficiency of the photo-NOCAS reaction in most cases.

Biphenyl has been extensively studied by both experimental and theoretical chemists. Its molecular structure is mainly characterized by the twist angle ϕ between the phenyl rings. The twist angle displays a unique dependence on the state of aggregation, this being a consequence of relatively low barriers of rotation around the bond (1.4-1.6 kcal/mol⁷²).

In the gaseous phase, ϕ was experimentally determined for biphenyl in the minimum energy conformation as $44.3^\circ \pm 1.3^\circ$.⁷² This angle becomes smaller in going from gas phase to condensed phases.⁷³ Various levels of molecular orbital calculations have also been carried out to estimate the twist angle of biphenyl.⁷⁴

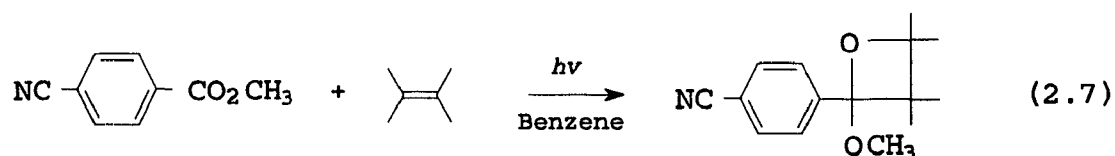
Ab initio calculations, with full geometry optimization at the STO-3G level, on the radical cation of biphenyl indicate that the radical cation of biphenyl has a coplanar conformation, i.e., the twist angle being zero (for the calculated result, see Appendix 1). An ESR study also shows that the biphenyl radical cation has a planar structure.⁷⁵

The effects of these findings on the electron transfer and back electron transfer processes between **1** and biphenyl (step 8 in Scheme 2.1) are not clear at this stage and require further elaboration. Nevertheless, if step 6 in Scheme 2.1 is considered

irreversible (back ET is slow), this step could play an important role in the efficiency enhancement of the photo-NOCAS reaction.

2.6 Solvent Effects

So far, most of the photo-NOCAS reactions described were carried out in an acetonitrile-methanol (3:1) solvent system. Using less polar solvents, sometimes only the oxetane was observed. Irradiation of a benzene solution of methyl 4-cyanobenzoate and 2,3-dimethyl-2-butene gives an oxetane as the major product (Equation 2.7).⁶⁴ In the less polar solvents, full ET will be less likely to occur or be



much slower than in acetonitrile. The products probably come from the exciplexes rather than from radical ions.

2.7 Salt Effects

Another important aspect of radical ion chemistry is the effect of added salt. Salts can affect PET reactions in various ways. For example, magnesium salts are known to have a profound effect on electron transfer mediated photoreactions.⁷⁶ They are known to extend the lifetime of the radical cation. For instance, magnesium ions form a complex with the radical anion which slows down the rate of back electron transfer from the radical anion to the radical cation.⁷⁷ Also, salts were found to have an effect on the regioselectivity of the photo-NOCAS reaction. Previous results have shown

that when magnesium perchlorate has been added, only *anti*-Markovnikov products are formed.^{63a}

2.8 The Focus of This Study

The above discussion has summarized the salient features of the photo-NOCAS reaction and has shown that some important aspects need further clarification. For example, a better understanding of the sequence of events occurring during the addition of methanol to the olefin may lead to greater control of the regio- and stereochemistry. This could be achieved by product analysis as long as we carefully select the starting materials (donors).

In this study, we have chosen several monoterpenes: α -pinene, β -pinene, nopol, tricyclene, 2-carene and others, so that the chirality and structural characteristics of these olefins and the photo-NOCAS products will lead to further insight into the mechanism of the photo-NOCAS reaction. The experimental results will be discussed in Chapters 3, 4, 6 and 7.

The rapid development in computer science and *ab initio* molecular orbital methods make it possible for experimental chemists to use *ab initio* molecular orbital methods for their own particular applications. Undoubtedly, we can gain insights into the nature of the radical ions and in turn into what is occurring at the molecular level during the course of reaction. Therefore, we have carried out a series of *ab initio* calculations on the radical cations involved in this work. Moreover, we have chosen two model systems, 1-butene and 4,4-dimethyl-1-pentene, for a detailed study on the cleavage process of the radical cation that will be presented in Chapter 5.

controlled rate because the free-energy change for the electron transfer process is exergonic (see Table 3.1). Indeed, the two pinenes quench the fluorescence of 9,10-dicyanoanthracene, which has a smaller excitation energy ($2.89 \text{ eV} = 278.8 \text{ kJ mol}^{-1}$; $E_{1/2}^{\text{red}} = -0.89 \text{ eV (SCE)}$) than that of **1** ($408.4 \text{ kJ mol}^{-1}$; $E_{1/2}^{\text{red}} = -1.66 \text{ V}$),⁶² at the diffusion-controlled rate ($k_q = 1.13 \times 10^{10} \text{ M}^{-1} \text{ s}^{-1}$ for α -pinene and $k_q = 0.67 \times 10^{10} \text{ M}^{-1} \text{ s}^{-1}$ for β -pinene).⁸¹

Table 3.1 The calculated free energy change for the electron transfer process with the singlet excited state of 1,4-dicyanobenzene (**1**) or 9,10-dicyanoanthracene as the acceptor

Donor	$E_{1/2}^{\text{ox}}$ (V) ^a	ΔG (kJ/mol) ^b
α -pinene	1.75	-84.8 -29.5 ^c
β -pinene	2.20	-41.4 13.9 ^c
limonene	2.15	-
1-methylcyclohexene	1.92 ^d	-
methylenecyclohexane	> 2.80	-
biphenyl	1.85	-75.1 -19.8 ^c

^aOxidation potentials measured at a platinum electrode relative to the saturated calomel electrode (SCE) using tetraethylammonium perchlorate (0.1 M TEAP) as the electrolyte in acetonitrile.

^bBased on the Rehm-Weller equation; $E_{0,0}$ (**1**) = $408.4 \text{ kJ mol}^{-1}$, $E_{1/2}^{\text{ox}}$ (**1**) = -1.66 V . The Coulombic attraction term was taken to be 5.40 kJ mol^{-1} .⁶²

^cThe acceptor is 9,10-dicyanoanthracene: $E_{0,0} = 278.8 \text{ kJ mol}^{-1}$; $E_{1/2}^{\text{red}} = -0.89 \text{ eV (SCE)}$.⁸³

⁴Shono, T.; Ikeda, A.; Hayashi, J.; Hakoza, S. *J. Am. Chem. Soc.* **1978**, *97*, 4261. Lithium perchlorate (0.1 M) was used as the electrolyte in this determination.

Based on the general mechanism for the photo-NOCAS reaction, after the radical cation forms attack of methanol on the double bond of the radical cation will lead to the β -methoxy alkyl radical. In the radical chemistry of the pinenes, opening of the four-membered ring is often observed.⁸² Thus one would expect that the β -methoxy alkyl radical might undergo opening of the four-membered ring. In contrast, a different reaction sequence was observed in this study, displaying the unique nature of the radical cations of the pinenes.

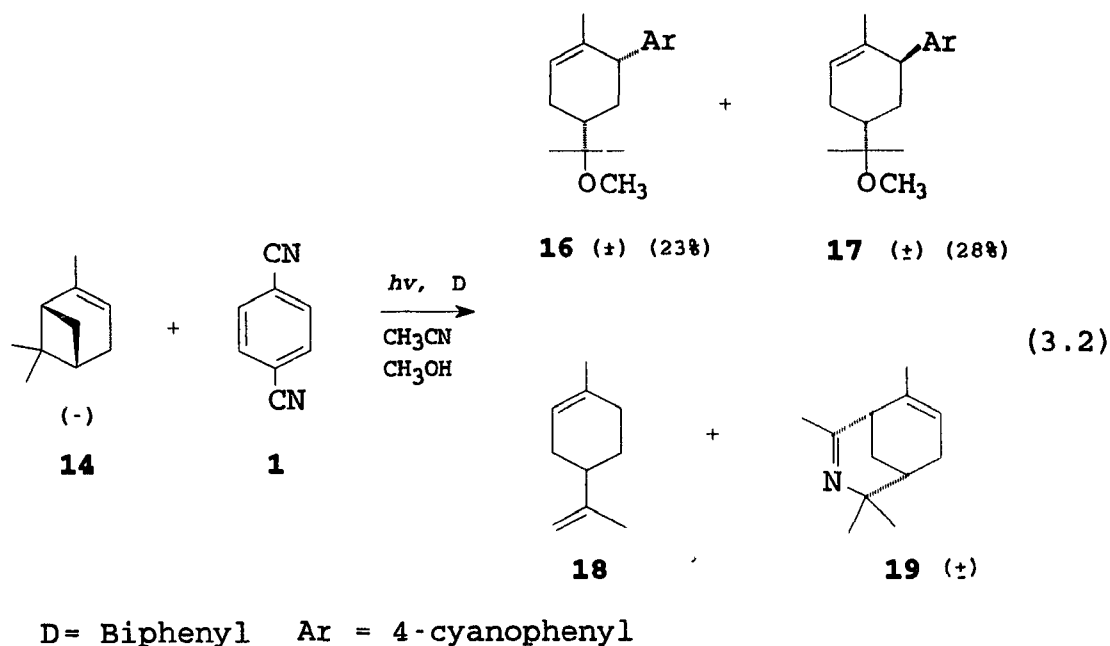
Experimental Results[1]

A solution of 1,4-dicyanobenzene (**1**) (0.05 M), biphenyl (**13**) (0.015M), and α -pinene (**14**) or β -pinene (**15**) in acetonitrile-methanol (3:1) was irradiated at 10 °C through a Pyrex filter with a medium-pressure mercury vapour lamp. After > 95% consumption of **1**, the photo-NOCAS products were isolated by medium pressure liquid chromatography on silica gel. The results are outlined in Equations 3.2 and 3.3. In Equation 3.2, the area ratios (determined by GC/FID) of the four major products (**16**, **17**, **18**, **19**) are 0.5:0.6:0.9:1.0 and in Equation 3.3, the ratios for **20**:**21**:**22**:**23** are 0.1:0.3:0.3:1.0.

The results show that both **16**, **17** and **19** are formed as racemic mixtures and

[1] A preliminary account of the work has been published as a communication (Reference 63b).

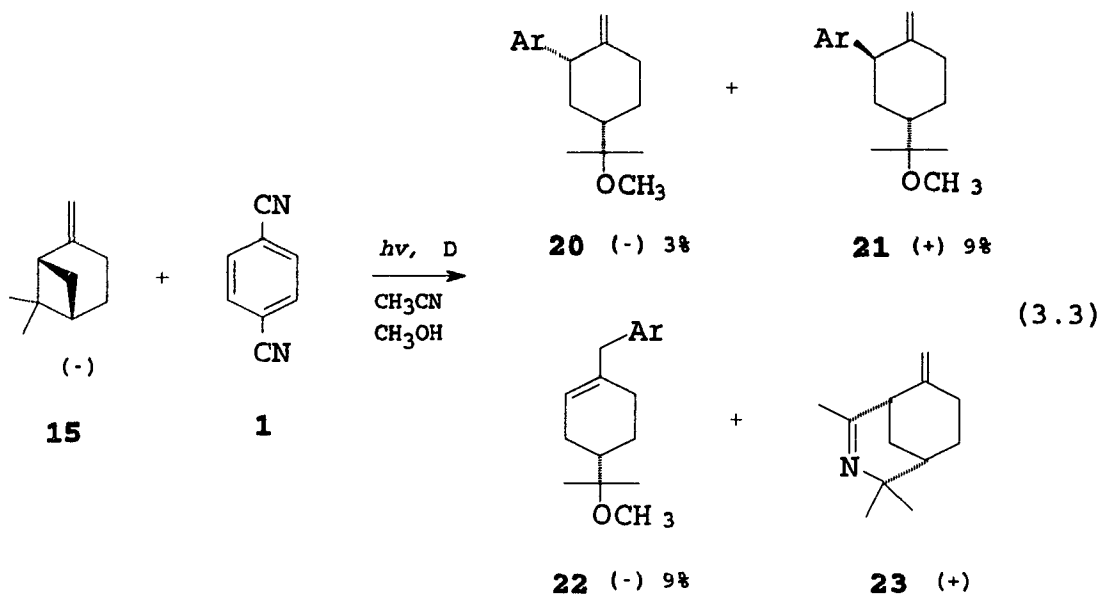
that **20**, **21**, **22** and **23** are chiral. Limonene (**18**) was detected (GC/MS and GC/FID) but was not isolated; the chirality of this product is not clear. The observed (minimum) specific rotations ($[\alpha]_D^{20^\circ\text{C}}$ (CHCl_3)) of **20**, **21**, **22** and **23** were -51.9,



+6.7 and -138.6 and +769.4, respectively. Formation of the *trans*- adducts **17** and **21** is only slightly favoured over that of the *cis*- isomers **16** and **20**.

The results of the photo-NOCAS reactions with α - and β - pinenes under different reaction conditions are summarized in Table 3.3.

Recovered from the three reaction mixtures after 45%, 69%, and 95% conversions of **1** respectively, the specific rotation of the unreacted α -pinene was essentially the same as before irradiation (see Table 3.2).



D = Biphenyl Ar = 4-cyanophenyl

Table 3.2 The specific rotations of α - and β - pinene after different conversions of 1 ($[\alpha]_D^{20^\circ\text{C}}$ in CHCl_3)

conversion of 1	0%	46%	69%	>95%
$[\alpha]$ of α -pinene	-56.7	-56.6	-60.2	-54.4
$[\alpha]$ of β -pinene	-15.5	-	-	-15.9 ^a

^aThe conversion of 1 is 88%.

In the absence of 13, both reactions shown in Equations 3.2 and 3.3 were less efficient (Table 3.3, reactions [3] and [4]). Although the yield of the photo-NOCAS reaction slightly improved by increasing the concentration of 13, the ratio of the photo-NOCAS products was essentially independent of the concentration of 13 (Table

3.3, reactions [1], [2], [5], [6] and [7]).

The polarity of the solvent has an effect on the yield of the photo-NOCAS reaction but no effect on the ratio of the products (Table 3.3, reaction [8]). In benzene-methanol (3:1 by volume), a less polar solvent system than acetonitrile-methanol (3:1) system, the yield of the photo-NOCAS products (**16** and **17**) decreased and the efficiency of the competing reactions increased.

In addition to the photo-NOCAS products, two other major products were formed from competing reactions as shown in Equation 3.2. One of them was produced from the isomerization of **14**. The isomerization product has been identified as limonene (**18**), by comparison of spectral data (GC/MS, retention time and fragment pattern) with those of an authentic sample.

The imine (**19**) resulted from addition of acetonitrile to the olefin. Irradiation of β -pinene under the same conditions did not lead to any isomerization products, but it did give an addition product (**23**) of acetonitrile to the olefin, which has the same molecular weight (but different retention time in the GC\FID and GC\MS spectra) as that of **19**. When propanenitrile was used as the solvent instead of acetonitrile, a similar product resulting from the addition of propanenitrile to the olefin was found. However, no addition product was observed when trimethylacetonitrile was employed as the solvent. These two imines (**19**, **23**) have previously been reported.⁸⁴ The spectral data of the imines are essentially identical with those reported.

In the case of **14**, there were small amounts of two additional isomerization products that have been tentatively identified as *cis*- and *trans*- β -ocimenes by comparison of mass spectra with those reported in the literature.¹²⁰ These two

compounds are known to result from triplet α -pinene as shown in Equation 3.1.

The ethers, resulting from addition of methanol to the olefin, are generally among the side products in photo-NOCAS reactions.^{63a} However, this type of ether was barely detected (GC/MS) in all the reactions studied here. Therefore, they were not isolated and characterized.

Table 3.3 The photo-NOCAS reaction: methanol-olefin, 1,4-dicyanobenzene^a

Reaction	Olefin	Products (yield) ^b
[1] ^c	α -pinene	<i>cis</i> -6-(4-cyanophenyl)-4-(1-methoxy-1-methylethyl)-1-methylcyclohexene (16) (23%); <i>trans</i> -6-(4-cyanophenyl)-4-(1-methoxy-1-methylethyl)-1-methylcyclohexene (17) (28%)
[2] ^c	β -pinene	1-(4-cyanophenylmethyl)-4-(1-methoxy-1-methylethyl)cyclohexene (20) (6.4%); <i>cis</i> -2-(4-cyanophenyl)-4-(1-methoxy-1-methylethyl)-methylenecyclohexane (21) (2.1%); <i>trans</i> -2-(4-cyanophenyl)-4-(1-methoxy-1-methylethyl)-methylenecyclohexane (22)(6.4%)
[3] ^d	α -pinene	16 (7.6%); 17 (9.4%)
[4] ^d	β -pinene	traces of 20 , 21 and 22
[5] ^e	α -pinene	16 (24%); 17 (30%)
[6] ^f	α -pinene	16 (27%); 17 (33%)
[7] ^f	β -pinene	20 (9%); 21 (3%); 22 (9%)
[8] ^g	α -pinene	16 (14%) and 17 (17%)
[9] ^h	limonene	traces of photo-NOCAS products

^aAll irradiations were carried out in acetonitrile-methanol (3:1) solution unless otherwise indicated.

^bThe yields are based on consumed **1** (**1** is taken as the limiting reagent) and on the isolated photo-NOCAS products.

^cBiphenyl was added (the mole ratio of **1** to **13** was 0.3). The conversion of **1** was > 90% in the case of α -pinene and 82% in the case of β -pinene.

^dDirect irradiation. The conversion of **1** was 71% in the case of α -pinene. In the case of β -pinene, **1** remained essentially unchanged.

^eBiphenyl was added (the mole ratio of **1** to **13** was 1) The conversion of **1** in reaction **5** was 100%.

^fBiphenyl was added (the mole ratio of **1** to **13** was 2). The conversion of **1** was 100% in the case of α -pinene, and 88% in the case of β -pinene.

^gIrradiation was carried out in benzene-methanol(3:1). The ratio of **16** and **17** was essentially the same as in reaction **1**.

^hThe irradiation time was similar to that needed for the photo-NOCAS reaction with **14**. Biphenyl was added (0.015 M⁻¹). The retention times for the products (GC/FID and GC/MS) are different from those for products **16** and **17**.

Since limonene, formed as a product in the reaction of α -pinene, might react to give rise to photo-NOCAS products with the same molecular weight as those that have been identified (**16**, **17**), a control reaction was carried out (see Table 3.3, reaction [9]). As expected, the photo-NOCAS reaction with limonene was slow and gave rise to different photo-NOCAS products from **16** and **17**.

Computational Details

The *ab initio* molecular orbital calculations were carried out with the GAUSSIAN86⁸⁵ or GAUSSIAN90⁸⁶ series of programs. Open-shell species were treated in the

unrestricted Hartree-Fock (UHF) formalism. The charge and spin distributions are calculated by Mulliken population analysis.⁸⁷ The limitations of this method have been discussed.⁸⁸

The calculations on α -pinene and the radical cation of α -pinene were carried out at the STO-3G level with full optimization of geometry. The optimized structures are verified to be minima by frequency calculation and are shown in Figure 3.1 (24) and 3.2 (25). The charge and spin distributions for structure 25 are listed in Table 3.4.

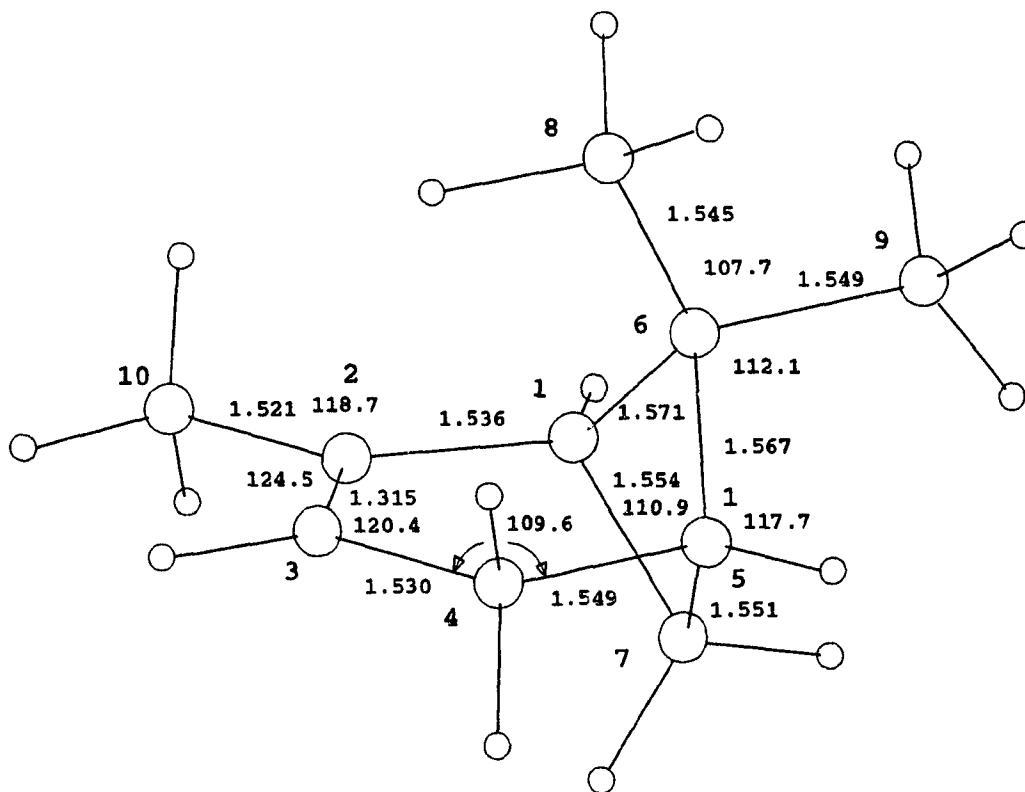


Figure 3.1 Structure 24: the fully optimized structure (minimum) for the molecule of α -pinene (14).

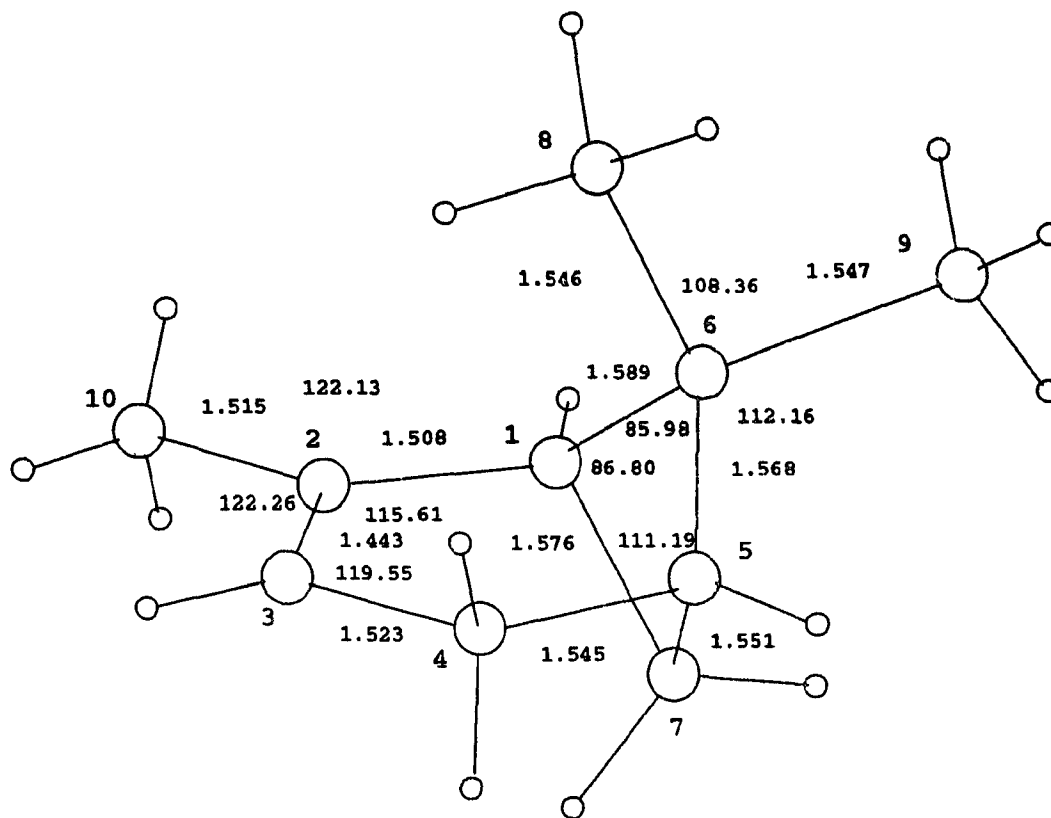


Figure 3.2 Structure 25: the fully optimized structure (minimum) for the radical cation of α -pinene (14^+).

The ring-opened structure of the radical cation of α -pinene could exist in at least three possible conformations as shown in Figure 3.3.a, b and c. In conformers a and b, the alkyl moiety and the allyl moiety are perpendicular, while in conformer c the two moieties are parallel. The calculation on conformer a or b started with a C_s symmetry constraint. Having identified a stationary point, full optimization was performed. Figures 3.4 (26) and 3.5 (27) display the fully-optimized structures for conformers a and b, and Tables 3.5 and 3.6 list the distributions of spin and charge.

A convenient starting point for the calculation on conformer c is to use the

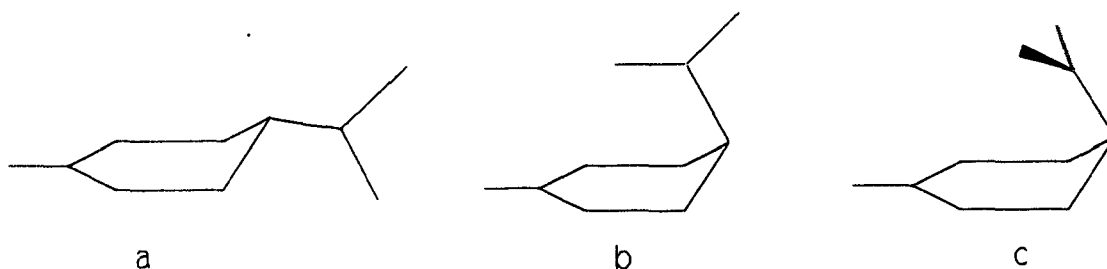


Figure 3.3 Possible conformations of the distonic radical cation formed upon ring opening of the radical cation of α -pinene

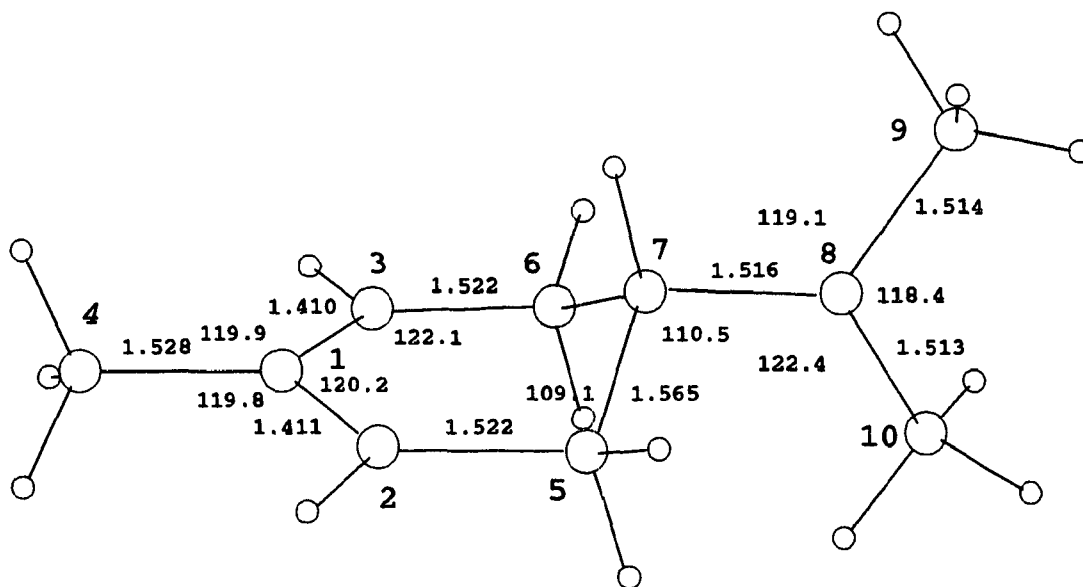


Figure 3.4 Structure 26: the fully optimized structure (minimum) for the distonic radical cation formed upon ring opening of the radical cation of α -pinene

fully-optimized structure for conformer b with a small revision; this can be achieved by rotating C7-C8 bond (Figure 3.5) until the alkyl moiety and the allyl moiety are parallel. The fully-optimized structure is shown in Figure 3.6 (28) and the spin and charge distributions are listed in Table 3.7.

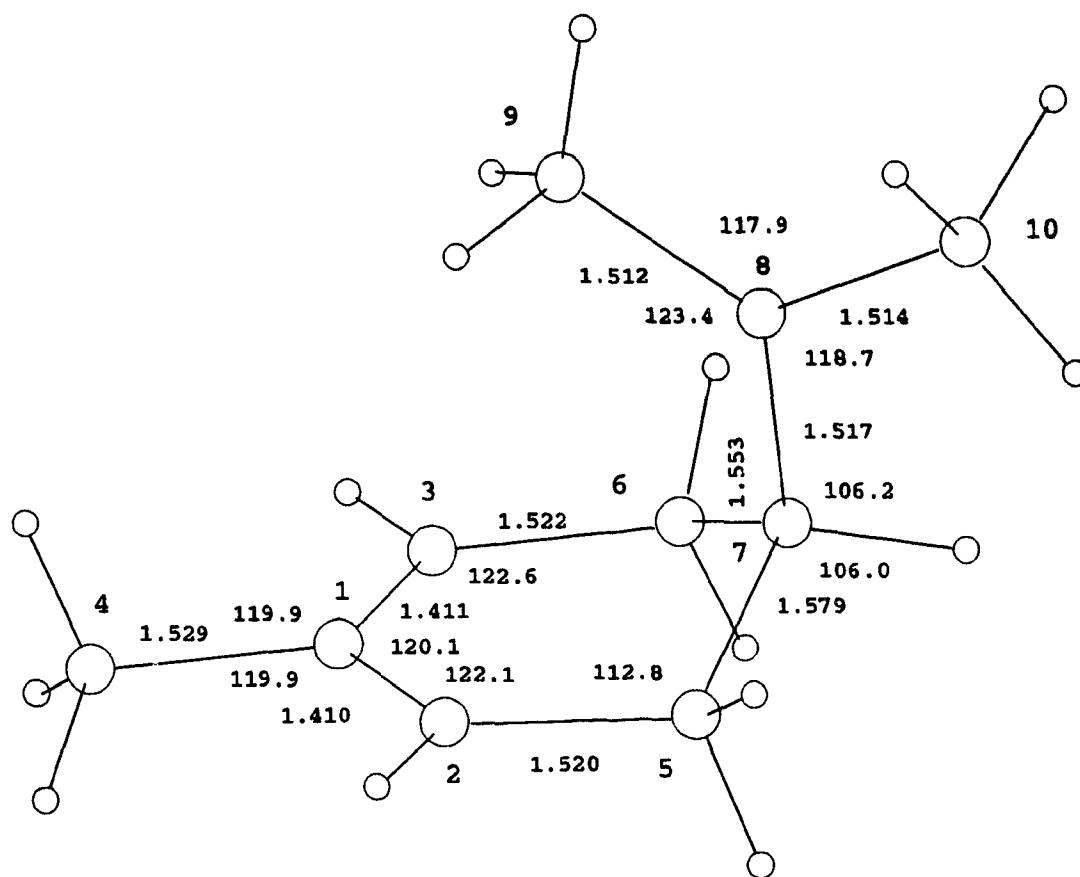


Figure 3.5 Structure **27**: the fully optimized structure (transition state) for the distonic radical cation formed upon ring opening of the radical cation of α -pinene

Further calculations verified that **26** and **28** shown in Figures 3.4, and 3.6 indeed correspond to local minima. Further characterization of the stationary point, **27** shown in Figure 3.5, showed one imaginary frequency on diagonalization of the force constant matrix; therefore, structure **27** does not correspond to an intermediate. Nevertheless, structure **27** is very similar to **28**; **27** is only 0.26 kJ/mol less stable than **28**. Structure **27** is probably the transition structure of a conformational change upon C1-C4 rotation.

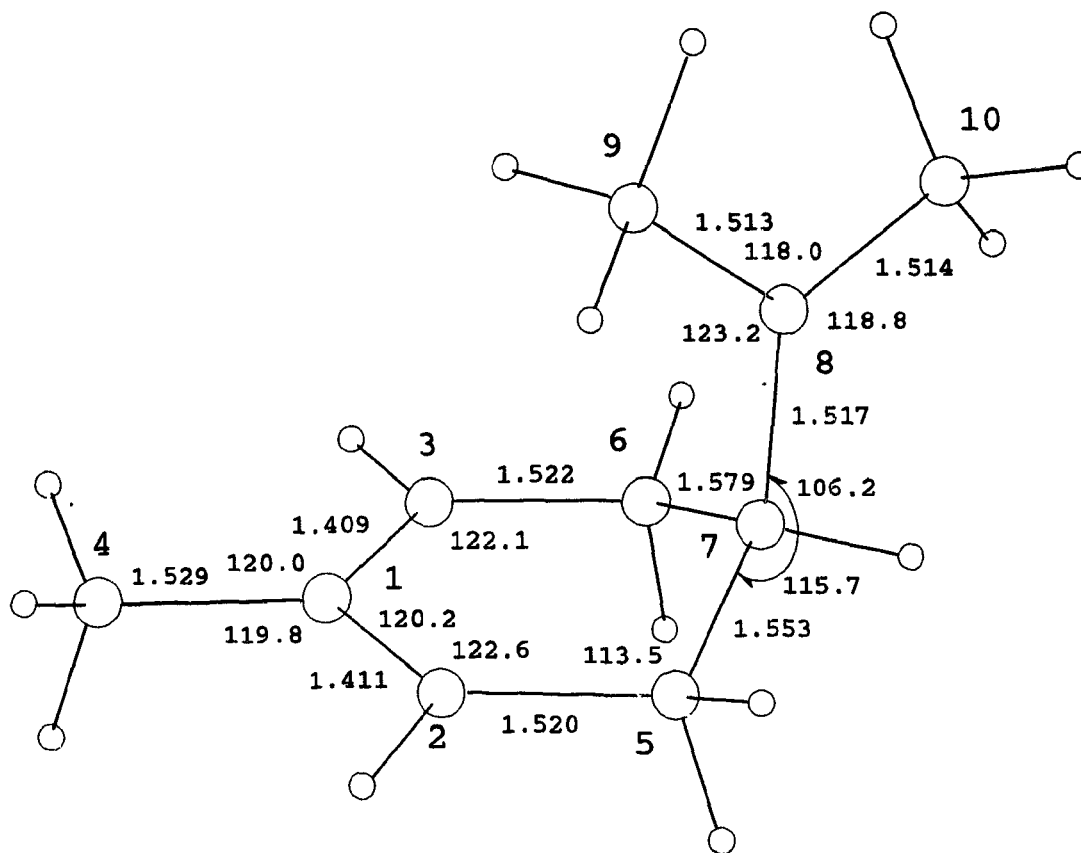


Figure 3.6 Structure 28: the fully optimized structure (minimum) for the distonic radical cation formed upon ring opening of the radical cation of α -pinene

The plane of C8, C9 and C10 in both 27 and 28 is neither perpendicular (as in conformer b) or parallel (as in conformer c) to the plane of the allylic moiety (the plane of C1, C2 and C3); the angle between the two planes is about 33° .

Table 3.4 The charge and spin distributions calculated for the radical cation of α -pinene (Structure 25 in Figure 3.2)

No. ^a	Group	Atomic Charges	Spins			
			Carbon	Hydrogen(s)		
1	CH	0.027	-0.037	0.001		
2	C	0.207	0.302			
3	CH	0.201	0.777			
4	CH ₂	0.110	-0.092	0.026	0.028	
5	CH	0.061	0.001			
6	C	0.058	0.031			
7	CH ₂	0.074	0.029	0.002	0.003	
8	CH ₃	0.025	0.006	0.000	0.000	-0.003
9	CH ₃	0.056	-0.002	0.000	0.000	0.002
10	CH ₃	0.181	-0.039	0.015	0.002	0.016

^aNumbering of carbon atoms in Figure 3.2.

Table 3.5 The charge and spin distributions calculated for the distonic radical cation formed upon ring-opening of the radical cation of α -pinene (Structure 26 in Figure 3.4)

No. ^a	Group	Atomic Charges	Spins				
			Carbon	Hydrogen(s)			
1	C	0.008	-0.850				
2	CH	0.039	1.033	-0.078			
3	CH	0.039	1.032	-0.078			
4	CH ₃	0.048	0.097	-0.028	-0.013	-0.012	
5	CH ₂	0.055	-0.123	0.017	0.036		
6	CH ₂	0.055	-0.123	0.017	0.036		
7	CH	0.043	0.035	-0.003			
8	C	0.302	-0.005				
9	CH ₃	0.205	-0.001	0.000	0.000	0.000	0.000
10	CH ₃	0.206	0.000	0.000	0.000	0.000	0.000

^aNumbering of carbon atoms in Figure 3.4.

Table 3.6 The charge and spin distributions calculated for the distonic radical cation formed upon ring-opening of the radical cation of α -pinene (Structure 27 in Figure 3.5)

No. ^a	Group	Atomic Charges	Spins			
			Carbon	Hydrogen(s)		
1	C	0.012	-0.846			
2	CH	0.022	1.024	-0.077		
3	CH	0.024	1.030	-0.077		
4	CH ₃	0.048	0.097	-0.028	-0.012	-0.013
5	CH ₂	0.080	-0.122	0.016	0.036	
6	CH ₂	0.064	-0.124	0.019	0.038	
7	CH	0.052	0.032	-0.004		
8	C	0.299	0.011			
9	CH ₃	0.208	0.001	-0.001	0.000	0.000
10	CH ₃	0.203	-0.001	0.001	0.000	0.000

^aNumbering of carbon atoms in Figure 3.5.

Table 3.7 The charge and spin distributions calculated for the distonic radical cation formed upon ring-opening of the radical cation of α -pinene (Structure 28 in Figure 3.6)

No. ^a	Group	Atomic Charges	Spins			
			Carbon	Hydrogen(s)		
1	C	0.000	-0.845			
2	CH	0.024	1.032	-0.078		
3	CH	0.022	1.022	-0.077		
4	CH ₃	0.048	0.097	-0.028	-0.014	-0.011
5	CH ₂	0.064	-0.124	0.019	0.038	
6	CH ₂	0.080	-0.122	0.016	0.036	
7	CH	0.052	0.032	-0.004		
8	C	0.299	0.011			
9	CH ₃	0.207	0.001	-0.001	0.000	0.001
10	CH ₃	0.203	-0.001	0.001	0.000	0.000

^aNumbering of carbon atoms in Figure 3.6.

Table 3.8 The calculated (STO-3G) total energies (a.u.) for α -pinene, for the radical cation of α -pinene, and for the distonic radical cation formed upon ring-opening of the radical cation of α -pinene

Structure 24 (α -pinene)	-383.38502
Structure 25 (ring-closed)	-383.18284
Structure 26 (ring-opened)	-383.16633
Structure 27 (ring-opened)	-383.16521
Structure 28 (ring-opened)	-383.16531

Discussion

Since the ultraviolet absorption spectrum of biphenyl (**13**) does not extend much beyond 290 nm, 1,4-dicyanobenzene (**1**) is still the major light-absorbing species under the reaction conditions. According to the Rehm-Weller equation, electron transfer from **13** to the excited singlet state of **1** is spontaneous ($-75.1 \text{ kJ mol}^{-1}$, see Table 3.1). Because it has been reported that quenching of the excited state of 9,10-dicyanoanthracene by **13** is almost diffusion-controlled ($k_q = 3.5 \times 10^9 \text{ M}^{-1} \text{ s}^{-1}$, ΔG for this process = $-19.8 \text{ kJ mol}^{-1}$)⁸⁹, it is reasonable to consider quenching of the fluorescence of **1** by **13** to be diffusion-controlled.

Therefore, irradiation of the reaction mixture causes two primary electron transfer processes, both of which are exergonic. One is between the singlet excited state of **1** and the olefin, and the other is between the singlet excited state of **1** and **13** (steps 2 and 6a in Scheme 2.1).

In polar solvents, exciplexes are not involved as reactive intermediates in photo-NOCAS reactions.^{63(a)} Thus, the electron transfer processes are likely to afford solvent-separated radical ion pairs (SSRIP), $[1^{\cdot-} + \text{Olefin}^{\cdot+}]$ and $[1^{\cdot-} + 13^{\cdot+}]$ (step 2b in Scheme 2.1), followed by solvent separation of the two pairs (step 2c).

Because back ET is very fast in SSRIP, the quantum yields for the photo-NOCAS reaction are generally low. Fortunately, secondary electron transfer occurs efficiently between the neutral olefin and the radical cation of biphenyl (step 7 in scheme 2.1). Because the oxidation potential of α -pinene is lower than that of biphenyl (see Table 3.1), the secondary ET is thermodynamically favourable. It is this electron relay that separates the radical cation of the olefin away from the radical anion, so the efficiency increases.

In the case of β -pinene, the oxidation potential of β -pinene is somewhat higher than that of biphenyl. Nevertheless, electron relay still occurs. This has been explained by assuming that there is formation of a bimolecular radical cation complex involving the olefin and the added co-donor.^{63(a),71} Even though such a complex might have most of the charge and spin density on the component with the lower oxidation potential, the olefin component could still be reactive toward methanol. If the attack were on the side of biphenyl, the olefin would depart as a "leaving group" and this would lead to loss of aromaticity of 13. On the other hand, the attack of methanol on the side of the olefin is favourable since 13 is a much better "leaving group".

Based on the structures of the identified products (16, 17, 18, 19, 20, 21, 22, 23), ring-opening of $14^{\cdot+}$ and $15^{\cdot+}$, leading to the distonic radical cations (29 and 31,

Scheme 3.1), occurs before reaction of the radical cation with methanol or with the radical anion of **1**. If the radical cation of the olefin coupled first with the radical anion before ring cleavage, the product (**17**) would be predominant and show optical activity. If methanol reacted with the ring-closed radical cations of the pinenes before ring cleavage, the methoxy group would be bonded to the ring rather than to the tertiary carbon.

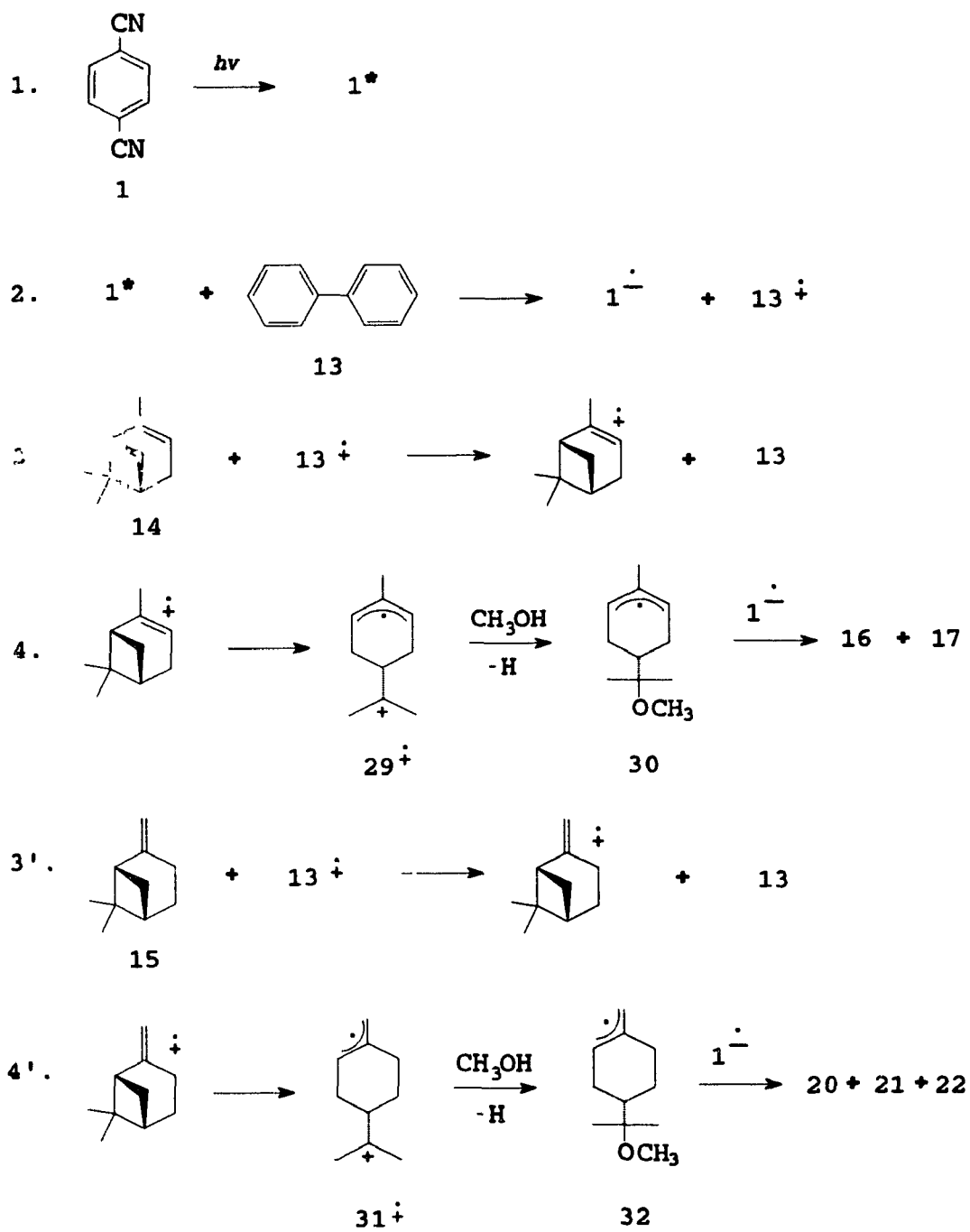
The rate constants for reaction of olefin radical cations with methanol vary with the structure of the olefin. With 1,1-diphenylethylene the rate constant is $1.6 \times 10^9 \text{ M}^{-1} \text{ s}^{-1}$;^{50,67,83} more stable and sterically hindered radical cations react more slowly. The approach of methanol to the radical cation of α -pinene is sterically hindered, so attack of methanol to the radical cations does not compete efficiently with cleavage of the radical cations.

There is little possibility that cleavage of the four-membered ring and attack of methanol on the tertiary carbon occur simultaneously since the approach of methanol from the back side of a tertiary carbon is sterically quite hindered. However, the presence of methanol will help the ring-opening process since methanol rapidly traps the tertiary cation.

In the case of β -pinene, since the oxidation potential is higher than that of **13**, secondary electron transfer between the $13^{+\bullet}$ and the olefin will be endergonic. Thus, a complex with the radical cation of biphenyl might be formed first, and then the partly charged olefin undergoes allylic cleavage prior to attack of methanol.

The radical **30** couples with 1^{\bullet} at both ambident ends (leading to racemic

Scheme 3.1.



products **16** and **17**) and from both sides of the ring. Coupling in the *pseudo*-axial side, *trans*- to the side chain, should be favoured and would account for the slight preference for formation of **17** and **21**. If coupling of the radical cation and the radical anion occurred before ring opening, or while the radical ion pair was still oriented, there would be a strong preference for coupling to occur from the side opposite to the *gem*-dimethyl group; **17** would be formed with retention of configuration at the chiral centre, and **16** and **20** would not be among the products.

The difference in the oxidation potential between α -pinene and 1-methylcyclohexene is about 0.2 V (see Table 3.1). This fairly large difference may be taken as an indication of the facile cleavage of the four-membered ring of the radical cation. In the case of β -pinene, when the measurement of oxidation potential was taken at 100 mV/s, the current i increased sharply all the way until the limit (2.7 V), but at 200 mV/s, a peak was observed ($E_{1/2}^{\text{ox}}$ 2.20 V). This suggests that the radical cation of **15** is not stable and is likely to undergo ring-opening to give the distonic radical cation in which the allylic radical can be further oxidized.

Ab initio calculations may provide us with further insight into the allylic cleavage of the radical cation of the pinenes. The calculated structure (**25**) for the radical cation of α -pinene is 43.36 kJ/mol lower in energy than the calculated ring-opened structure (**26**). If solvent effects were included in calculations, the energy difference between the ring-closed and the ring-opened structures (**25** and **26**) would have to be much smaller than this number. The ring-opened radical cation (**26**) might be, in fact, lower in energy than the ring-closed structure (**25**). The reason is that the

charge in the distonic radical cation (26) is more localized, which results in greater stabilization by solvation.

From the above analysis, we see that the ring-closed structure of $14^{+\bullet}$ must rapidly undergo ring-opening under the reaction conditions. Moreover, this ring-opening process occurs before any other competing processes, such as attack of methanol on the ring-closed structure of $14^{+\bullet}$ and coupling between 1^\bullet and the ring-closed structure.

Both reactions shown in Equation 3.2 and 3.3 are regioselective; cleavage of the four-membered ring of the radical cation ($14^{+\bullet}$ or $15^{+\bullet}$) affords a distonic radical cation (29 or 31) with spin density on the allylic moiety and positive charge density on the tertiary moiety. This is consistent with the general rule that cleavage of radical cations occurs selectively to give the carbocation of the fragment radical with the lower oxidation potential.⁹⁰ The oxidation potential of the allylic radical is not known, but there is reason to believe that the oxidation potential of the tertiary radical is lower. The oxidation potential of the tertiary butyl radical is 0.09 V (SCE) and the oxidation potential of the benzylic radical is 0.73. Even the cumyl radical has an oxidation potential 0.16 V, which is still greater than that of the *t*-butyl radical.⁹¹

The observed regioselectivity is also in agreement with the calculated results (see Figure 3.4 and Table 3.5). The spin density is essentially localized on the allylic moiety and charge density mainly on the $C(CH_3)_2$ moiety.

Table 3.2 shows that the specific rotation of the unreacted α -pinene recovered after 95% conversion of 1 is essentially the same as before irradiation. This suggests

that the radical cation cleavage is irreversible and that no 1,3-sigmatropic migration occurs. This fact may put light on the question: "is there any evidence for a weak interaction between the radical and cation centres in the distonic radical cation (29)?" If there were, the unreacted α -pinene might become racemic and the predominant formation of 17 and 21 would be observed. Obviously, this is not the case; the product ratios do not agree with this expectation. The experimental observation is consistent with the model in which the two reactive centres do not interact.

The *ab initio* calculations also show that no interaction between the two moieties, cationic and allylic radical. The calculations show that the spin density is essentially localized on the allyl moiety and charge density mainly on the $C(CH_3)_2$ moiety in Structure 28 (Table 3.7). Furthermore, the distance between C1 and C8 (3.551 Å) is too great for any interaction.

The reduction potentials of the allylic radicals 30 and 32 (Scheme 3.1) must be more negative than that of 1 (-1.66 V); otherwise electron transfer will occur. The reduction potentials of allylic radicals of the type 30 and 32 are not known but the results seem reasonable. The unsubstituted allyl radical is reduced at -1.63 V (SCE). Alkyl substitution at the terminal position will make the reduction potential more negative by ca. 0.2 V.⁹²

Based on the mechanism discussed above, the configuration of 15 (5 S) will not be affected and should be retained in 20, 21, 22 and 23.

In addition to the photo-NOCAS products, two solvent incorporation products (19 and 23) were formed. This reaction is no doubt also mediated by PET. There are

several reasons that lead us to this conclusion. First, biphenyl increases the efficiency of this reaction as well as that for photo-NOCAS reaction. Second, the two solvent incorporated products were observed upon electrochemical oxidation of the two pinenes.⁸⁴

There are several examples where solvent (acetonitrile) incorporated products have been reported. For example, the photooxidation of norbornene by silver trifluoromethanesulfonate in acetonitrile solution yields the solvent adduct.⁹³ Solvent addition occurs via a free radical chain mechanism, which is initiated by photoinduced electron transfer to Ag(I) from norbornene, followed by hydrogen atom abstraction from solvent by the norbornene radical cation.

Irradiation of phenylacetylene in the presence of DCA in acetonitrile solution leads to the radical cation of phenylacetylene. Reaction of the radical cation with a neutral phenylacetylene occurs with a rate constant of ca. $5 \times 10^9 \text{ M}^{-1} \text{ s}^{-1}$ to yield a dimeric 1,4-radical cation that either cyclizes to 1-phenylnaphthalene or reacts with a nucleophilic solvent to yield solvent incorporated products.^{65a}

9,10-Dicyanoanthracene irradiated in aqueous acetonitrile in the presence of triethylamine yields 9-amino-10-cyanoanthracene. The amine serves as electron donor, but isotopic labelling shows that the amino group in the product originates from the acetonitrile solvent.⁹⁴

The formation of limonene cannot be explained by the intermolecular deprotonation-protonation mechanism, because the allylic radical is difficult to reduce with $1^{\cdot-}$. The triplet mechanism also cannot explain it, as we note that the triplet of α -

pinene leads to other two isomerization products, *cis*- and *trans*- β -ocimenes as the only products rather than limonene.⁷⁹ In the absence of biphenyl, product 16, 17, 19, become minor products, and the limonene and the other two isomers are the major products. The other two isomerization products have been tentatively identified as *cis*- and *trans*- β -ocimenes by comparison of mass spectra with those reported in the literature.

The possible explanation for formation of limonene is the intramolecular deprotonation-protonation mechanism that probably occurs before complete ring cleavage. One of the methyl hydrogens of the tertiary carbocation is close to, indeed, right on the top of, one end of the allylic radical (2.520 Å in the calculated ring-closed structure (25) and 2.673 Å in the calculated ring-opened structure (28)). If the limonene is formed before formation of the complete ring-opened intermediate, the configuration of 14 (5 *S*) should be retained.

Experimental

General methods

The ¹H and ¹³C NMR spectra were recorded on a Nicolet 360 NB NMR spectrometer, and are reported in parts per million to high frequency from TMS. Coupling constants are reported as absolute values and the signs of the couplings were not determined.

Infrared spectra (ir) were recorded on an air-purged Perkin-Elmer 180 grating infrared spectrometer and are reported in wavenumbers relative to the 1602 cm⁻¹ absorption of polystyrene. The optical activities of the starting materials and products

were determined with a Perkin-Elmer Model 141 polarimeter. Mass spectra (MS) were recorded on a Hewlett-Packard 5970 series mass selective detector and are reported as m/z (relative intensity). Elemental analyses were performed by Canadian Microanalytics Services Inc. and agreed to within ± 0.3 of the calculated values. Melting points were determined using a Cybron Corporation Thermolyne melting point apparatus linked to a digital thermocouple, and were corrected.

The reactions were followed by gas chromatography (GC) using either an HP 5890 GC, fitted with a 5% phenyl methyl silicone fused silica WCOT column (25×0.20 mm, $0.33\text{-}\mu\text{m}$ film thickness), coupled to an HP 5970 mass selective detector (MS), or an HP 5890 GC, fitted with a DB-1701 or DB-225 fused silica WCOT column ($30 \text{ m} \times 0.25$ mm, $0.25 \mu\text{m}$ film thickness), with a flame ionization detector (FID). The digital signal from the FID is transmitted to an HP 3392A integrator and the data are acquired by the software developed at the Department of Chemistry, Dalhousie University, using a Commodore PC-II computer.

The photo-NOCAS products were isolated by medium pressure liquid chromatography (MPLC) using a $2.5 \text{ cm} \times 1 \text{ m}$ column packed with TLC grade silica gel (Merck) at 15 psi (helium) ($1 \text{ psi} = 6.9 \text{ kPa}$). The chromatograms were developed with a hexane-methylene chloride or hexane-50% ethyl ester in hexane linear gradient and the eluent was monitored and collected by a UV spectrometer-fraction collector. Dry column flash chromatography (DCFC) was performed using TLC grade silica gel (Merck).⁹⁵

Materials

Solvents were fractionally distilled. Acetonitrile (Fisher ACS grade) was distilled successively from sodium hydride and phosphorus pentoxide, and was then passed through a column of basic alumina, refluxed over calcium hydride for 24 h under a nitrogen atmosphere, and fractionally distilled. The 1,4-dicyanobenzene (Aldrich) was purified by treatment with Norite in methylene chloride, followed by recrystallization from 95% ethanol. Biphenyl (Aldrich) was recrystallized from methanol. (1S)-(-)- α -pinene, $[\alpha]_D^{20^\circ\text{C}} -42^\circ$ (neat) or $[\alpha]_D^{20^\circ\text{C}} -50.7^\circ$ (neat), and (1S)-(-)- β -pinene, $[\alpha]_D^{20^\circ\text{C}} -21^\circ$ (neat), and (R)-(+)-limonene, $[\alpha]_D^{20^\circ\text{C}} +123^\circ$ (neat), were obtained from Aldrich. These olefins were used as received except in the measurement of the oxidation potentials in which the olefins used were purified by GC (40% SE-30).

Cyclic voltammetric measurements

Oxidation potentials were obtained by cyclic voltammetry using an apparatus similar to that previously described.⁹⁰ The working electrode was a platinum sphere (1 mm diameter), while the counter electrode was a platinum wire. The reference electrode was a saturated calomel electrode (SCE), which was connected to the solution by a Luggin capillary. The electrolyte was tetraethylammonium perchlorate (0.1 M TEAP) and the solvent was acetonitrile. Substrate concentrations were typically 0.005 M. Since the anodic wave was not reversible, the half-wave potential was taken as 0.028 V before the anodic peak potential.⁹⁶

Irradiations

Irradiations were carried out using a CGE 1-kW medium pressure mercury vapour lamp contained in a water cooled quartz immersion well. The temperature was maintained at 10 °C. The solvent was acetonitrile-methanol (3:1 by volume) or benzene-methanol (3:1) at a typical concentration of 1,4-dicyanobenzene of 0.05 M and olefin of 0.1 M.. The concentration of biphenyl varied over the range of 0.02-0.1 M. The solutions were placed in 2 cm i.d. Pyrex tubes or 5 mm Pyrex NMR tubes, flushed with dry nitrogen and sealed.

Formation of adducts from α -pinene

A solution of 3.05 g (22.4 mmol) α -pinene (14), 0.52 g (3.4 mmol) biphenyl (13), and 1.44 g (11.2 mmol) 1,4-dicyanobenzene (1) in 160 ml acetonitrile-methanol (3:1) was degassed with nitrogen for 5 min and irradiated through Pyrex for 72 h. The volatile components of the photolysate, removed by distillation, included most of 14 and some of the isomerization products of 14 (analyzed by GC/MS). The major isomerization product has an identical retention time (GC/FID) and mass spectrum with those of the authentic sample, limonene. The nonvolatile residue was separated by MPLC using the hexanes - methylene chloride gradient. The photo-NOCAS products eluted as an oil. In addition to the photo-NOCAS products and limonene, another major product was found to be very polar, requiring washing out of the column by ethyl acetate or methylene chloride - methanol gradient. The crude yield of this product ranges between 20-35 % (based on initial amount of 14). The crude

imine was further purified by preparative GC using a 3/8 in. \times 10 ft aluminum column packed with 40% SE-30 on Chromosorb W 60/80 NAW. It was identified as the imine **19**.

Fraction no. 240-250: 400 mg of *cis*-6-(4-cyanobenzene)-4-(1-methoxy-1-methylethyl)-1-methylcyclohexene (**16**); IR (liq. film, NaCl) ν : 3033 (w), 2970 (s), 2933 (s), 2827 (m), 2228 (s), 1607 (s), 1503 (s), 1453 (m), 1381 (s), 1365 (s), 1150 (s), 1076 (s), 840 (s); MS m/z : 269(0.10), 254(0.17), 237(3.4), 194(5.4), 154(3.8), 116(4.1), 93(3.9), 77(4.1), 74(3.8), 73(100); ^1H NMR (CDCl_3 , 360 MHz) δ : 7.58 (d, 2H, $J = 8.2$ Hz arom), 7.27 (d, 2H, $J = 8.2$ Hz arom), 5.69 (d, 1H $J = 4.32$ Hz =CH), 3.36 (m, 1H, $J = 9.3$ Hz benzylic proton), 3.18 (s, 3H, OCH_3), 2.10-1.84 (m, 3H CH_2 , CH), 1.38 (s, 3H =CCH₃), 1.31-1.20 (m, 2H, ArCCH_2), 1.11 (s, 1H), 1.09 (s, 1H); ^{13}C NMR (90.80 MHz, CDCl_3) δ : 151.69 (s, 1C, arom), 133.77 (q, 1C, $J = 5.2$ Hz =C), 132.20 (dd, 2C, 5.7 Hz, 164.2 Hz, arom), 128.89 (dd, 2C, 4.5 Hz, 164.8 Hz, arom), 125.35 (dd, 4 Hz, 154.1 Hz, =CH), 119.01 (d, 4.7 Hz, CN), 109.82 (t, 8.8 Hz, 1C, arom), 76.14 (s, 1C), 48.81 (q, 139.9 Hz, OCH_3), 42.45 (d, 126.4 Hz, 2CH), 35.41 (t, 128.5 Hz, CH_2), 27.15 (t, 127.5 Hz, CH_2), 22.28 (q, 125.3 Hz, CH_3), 21.52 (q, 127.9 Hz, CH_3), 21.48 (q, 125.5 Hz, CH_3).

Anal. Calcd. for $\text{C}_{18}\text{H}_{23}\text{NO}$: C, 80.25; H, 8.61; N, 5.20. Found: C, 79.94; H, 8.38; N, 5.38.

Fraction no. 251-259: 300 mg of the mixture of the two photo-NOCAS products.

Fraction no. 260-276: 830 mg of *trans*-6-(4-cyanophenyl)-4-(1-methoxy-1-

methylethyl)-1-methylcyclohexene (**17**); IR (KBr disk) ν : 3034 (w), 2972 (s), 2933 (s), 2827 (m), 2228 (s), 1607 (s), 1502 (s), 1452 (m), 1382 (s), 1364 (s), 1154 (s), 1074 (s), 900 (m), 840 (s) 806 (m); MS m/z : 237(3.9), 194(10.2), 154(3.7), 116(3.9), 91(3.0), 77(3.9), 74(3.9), 73(100); ^1H NMR δ : 7.59 (d, 8.2 Hz, 2H, arom), 7.31 (d, 8.4 Hz, 2H, arom), 5.78-5.77 (m, 1H, =CH), 3.41 (s, 1H, ArCH), 2.83 (s, 3H, OCH₃), 2.11-1.61 (m, 5H), 1.59 (d, 1.05 Hz, 3H, =CCH₃), 1.01 (s, 3H, CH₃), 0.97 (s, 3H, CH₃); ^{13}C NMR δ : 150.43 (s, arom), 132.52 (m, small coupling, arom), 131.93 (dd, 5.5, 163.9 Hz, arom), 129.28 (d, 159.7 Hz, arom), 125.55 (dd, 4.2 Hz, 153.5 Hz, =CH), 119.08 (s, CN), 109.74 (t, 8.8 Hz, arom), 75.95 (s, tertiary carbon), 48.29 (q, 140.4 Hz, OCH₃), 45.91 (d, 128.0 Hz, CH), 34.45 (d, 124.0 Hz, CH), 32.17 (t, 131 Hz, CH₂), 27.08 (t, 126.0 Hz, CH₂), 22.43 (q, 128.0 Hz, CH₃), 22.12 (q, 125.5 Hz, CH₃), 22.05 (q, 129.0 Hz, CH₃).

Product **17** was purified again by MPLC and then distilled (small scale). A crystal with melting point 57.5 °C was obtained.

Anal. Calcd. for C₁₈H₂₃NO: C, 80.25; H, 8.61; N, 5.20. Found: C, 80.38; H, 8.32; N, 5.34.

The imine (**19**): MS m/z : 177 (2), 136 (11), 121 (5), 94 (13), 93 (100), 92 (42), 91 (33), 80 (11), 79 (19), 77 (32), 65 (15); Infrared (PE-180) : 3035(w), 2964(s), 2935(s), 2915(s), 2870(m), 2838(m), 1667(s), 1455(s), 1382(m), 1330(m), 1295(m), 867(s), 782(m); ^1H NMR δ : 5.35 (m, 1H, $w_{1/2}$ =9.3 Hz, =CH), 2.51 (s, 1H, br. $w_{1/2}$ =7.4 Hz), 2.23 (dm, 1H, 19.1 Hz, AB pattern), 2.17 (dm, 1H, 19.1 Hz, AB pattern), 2.05 (s, 3H), 1.86 (m, 1H), 1.84 (m, 1H, 11.1 Hz), 1.82 (d, 3H, 1.58

Hz), 1.56 (m, 1H, 11.1), 1.21 (s, 3H), 1.15 (s, 3H); ^{13}C NMR δ : 167.15, 134.48, 122.23, 58.50, 40.30, 33.35, 31.72, 28.81, 28.22, 27.92, 25.46, 23.90.

Formation of adducts from β -pinene

This procedure was similar to the formation of adducts from α -pinene. In this case, only traces of isomerization products of **15** were detected by GC/MS, and the imine still formed as a major product. The irradiation mixture was partly separated by MPLC and then the mixture of photo-NOCAS products was separated again by MPLC. Three compounds were obtained colourless oils. At last, using ethyl acetate, the imine (**23**) was obtained in 30%, based on β -pinene. The crude imine was further purified by preparative GC using a 3/8 in. \times 10 ft aluminum column packed with 40% SE-30 on Chromosorb W 60/80 NAW. The isolated yields of the photo-NOCAS products are based on the consumed DCB.

Cis-2-(cyanophenyl)-4-(1-methoxy-1-methylethyl)methylene-cyclohexane (**20**, 3%); MS m/z : 237(1.8), 194(3.5), 140(3.1), 127(2.1) 116(3.1), 74(3.9), 73 (100); H NMR, δ : 7.60 (d, 8.2 Hz, 2H, arom), 7.23 (d, 8.2 Hz, 2H, arom), 4.72 (d, 1.5 Hz, 1H, vinyl proton), 3.88 (d, 1.5 Hz, 1H, vinyl proton), 3.29 (m, 1.7 Hz, 11.3 Hz, 1H, ArCH), 3.19 (s, 3H, OCH₃), 2.54 (m, 1H, 13.3 Hz), 2.20 (m, 1H), 2.03-1.92 (m, 2H), 1.86-1.78 (m, 1H), 1.50 (ddd, 1H, 12.3, 12.3, 12.2), 1.26 (dddd, 1H, 12.9, 12.9, 12.9, 4.0), 1.15 (s, 3H, CH₃), 1.12 (s, 3H, CH₃); ^{13}C NMR δ : 151.50 (d, 4.0 Hz, arom), 148.99 (d, 6.9 Hz, =C), 131.97 (dd, 4.7 Hz, 159.4 Hz, arom), 129.52 (d, 160.4 Hz, arom), 119.06 (s, CN), 110.11 (d, 2.8 Hz, arom), 108.57 (t,

145.8 Hz, =CH₂), 76.37 (s, tertiary carbon), 50.05 (q, 140.4 Hz, OCH₃), 48.79 (d, 125.1 Hz, ArCH), 46.31 (d, 127.2 Hz, CH), 36.21 (t, 126.7 Hz, CH₂), 34.59 (t, 131.1 Hz, CH₂), 28.21 (t, 125.3 Hz, CH₂), 22.43 (q, 125.5 Hz, CH₃), 21.95 (q, 124.6 Hz, CH₃).

Anal. Calcd. for C₁₈H₂₃NO: C, 80.25; H, 8.61; N, 5.20. Found: C, 80.10; H, 8.61; N, 5.53.

Trans-1-(4-cyanophenyl)-4-(1-methoxy-1-methyl-2-propyl)ethylene-cyclohexane (21, 9%): IR (liq. film, NaCl, Nicolet 205) ν : 3040 (w), 2973 (s), 2936 (s), 2899 (s), 2830 (m), 2228 (s), 1607 (m), 1505 (m), 1466 (w), 1382 (m), 1365 (m), 1144 (m), 1078 (s), 823 (w) MS m/z : 254(0.4), 237(2.4), 194(6.1), 116(3.1), 74(5.0), 73 (100); ¹H NMR δ : 7.61 (d, 8.4 Hz, 2H, arom), 7.45 (d, 8.1 Hz, 2H, arom), 5.00 (t, 2.0 Hz, 1H, =CH), 4.90 (t, 1.5 Hz, 1H, =CH), 3.77 (s, 1H, ArCH), 3.12 (s, 3H, OCH₃), 2.52 (m, 1H, =CCH), 2.35 (m, 1H, =CCH), 2.02 (m, 1H, O-CCH), 1.76 (m, 1H, CH), 1.68-1.57 (m, 2H, CH₂), 1.15 (m, 1H, CH), 1.10 (s, 3H, CH₃), 1.05 (s, 3H, CH₃); ¹³C NMR δ : 148.67 (s, arom), 148.33 (s, =C), 132.08 (dd, 5.4 Hz, 162.7 Hz, arom), 128.14 (d, 161.3 Hz, arom), 119.08 (s, CN), 111.98 (t, 153.1 Hz, =C), 109.52 (s, arom), 76.37 (s, tertiary carbon), 48.79 (q, 140.1 Hz, OCH₃), 46.70 (d, 132.1 Hz, ArCH), 39.93 (d, 124.1 Hz, CH), 31.96 (t, 133.2 Hz, CH₂), 31.34 (t, 130.4 Hz, CH₂), 29.07 (t, 130.4 Hz, CH₂), 27.32 (q, 124.7 Hz, CH₃), 21.83 (q, 125.5 Hz, CH₃).

Anal. Calcd. for C₁₈H₂₃NO: C, 80.25; H, 8.61; N, 5.20. Found: C, 80.34; H, 8.70; N, 5.36.

1-(4-cyanophenylmethyl)-4-(1-methoxy-1-methylethyl)cyclohexene (**22**, 9%);

IR (liq. film, NaCl, Nicolet 205) ν : 3041 (w), 2973 (s), 2936 (s), 2899 (s), 2830 (m), 2228 (s), 1607 (m), 1503 (m), 1467 (w), 1381 (m), 1364 (m), 1143 (m), 1079 (s), 822 (w); MS m/z : 254(1.0), 237(24.5), 121(16.9), 116(17.3), 79(7.0), 73 (100); ^1H NMR δ : 7.56 (d, 8.1 Hz, 2H, arom), 7.27 (d, 7.8 Hz, 2H, arom), 5.49 (d, 5.1 Hz, 1H, =CH), 3.30 (s, 2H, ArCH₂), 3.17 (s, 3H, OCH₃), 2.10 - 1.60 (m, 6H), 1.21 (m, 1H), 1.09 (s, 6H, 2CH₃); ^{13}C NMR (CDCl₃), δ : 146.08 (s, arom), 135.77 (d, 6.4 Hz, =C), 132.03 (dd, 4.7 Hz, 159.3 Hz, arom), 129.56 (dd, 4.7 Hz, 158.8 Hz, arom), 124.09 (d, 155.2 Hz, =CH), 119.09 (s, CN), 109.75 (s, arom), 76.46 (s, tertiary carbon), 48.76 (q, 140.2 Hz, OCH₃), 44.16 (t, 125.5 Hz, ArCH₂), 41.70 (d, 121.9 Hz, CH), 29.07 (t, 124.2 Hz, CH₂), 26.87 (t, 125.6 Hz, CH₂), 23.78 (t, 126.9 Hz, CH₂), 22.19 (q, 126.0 Hz, CH₃), 21.83 (q, 124.9 Hz, CH₃).

Anal. Calcd. for C₁₈H₂₃NO: C, 80.25; H, 8.61; N, 5.20. Found: C, 80.13; H, 8.45; N, 5.33.

The imine (**23**): MS m/z : 177 (1.6), 136 (26.8), 121 (7), 94 (14), 93 (100), 91 (19), 80 (14), 79 (25), 77 (21), 69 (18); Infrared (PE-180) : 3067(w), 2972(s), 2934(s), 2863(m), 1668(m), 1649(s), 1455(m), 1361(m), 1286(m), 1242(m), 869(ni); ^1H NMR δ : 4.76 (s, 1H, br. $w_{1/2}=3.8$, =CH), 4.12 (s, 1H, br. $w_{1/2}=4.7$, =CH), 2.82 (m, $w_{1/2}=7.4$, 1H, 3.0), 2.06 (dddd, 1H, 12.5, 2.6, 2.7, 3.5), 2.08-2.04 (2H), 2.00 (m, 1H, 15.0), 1.88 (s, 3H), 1.71 (m, 1H, wf=11.8, 3.3), 1.58 (ddd, 1H, 12.5, 3.3, 3.0), 1.51 (m, 1H), 1.31 (s, 3H), 1.20 (s, 3H); ^{13}C NMR δ : 166.13, 148.17, 108.54, 57.54, 46.07, 35.16, 31.37, 29.91, 29.46, 28.98, 27.23, 25.84.

Formation of adducts from α -pinene on the direct irradiation

A solution of 1,4-dicyanobenzene (1) (529 mg, 4 mmol), and α -pinene (14) (1.09 g, 8 mmol) in 80 ml of acetonitrile-methanol (3:1) was purged with nitrogen and irradiated for 144 h. The mixture, after evaporating the volatile components, was separated by conventional chromatography. 136 mg of photo-NOCAS products (the yield was 17% based on consumed 1,4-dicyanobenzene), and 165 mg of 1,4-dicyanobenzene (the conversion was 71%) were obtained.

Chapter 4

The photo-NOCAS reaction:

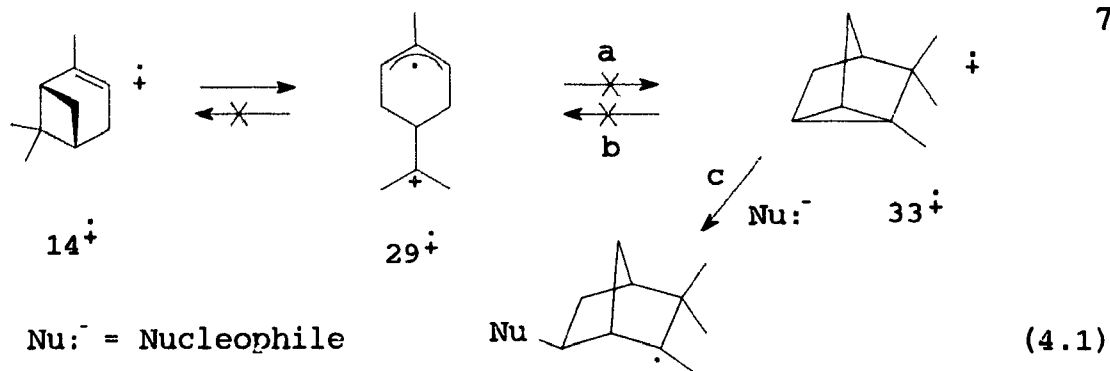
methanol - tricyclene, 1,4-dicyanobenzene

In the previous chapter, we have seen that when a solution of α -pinene (**14**), 1,4-dicyanobenzene (**1**) and biphenyl (**13**) in acetonitrile and methanol (3:1) was irradiated, two 1:1:1 adducts were obtained in the racemic form (Equation 3.2). The proposed mechanism for the reaction has been rationalized as in Scheme 3.1. The key step, preceded by the electron transfer step, is the four-membered ring opening of the initially formed radical cation from α -pinene. This leads to a distonic radical cation (**29** in scheme 3.1).

A strong interaction between the allylic and alkyl moieties in **29⁺** would lead to the initially formed radical cation from tricyclene (**33**) (Equation 4.1a). Product analysis and *ab initio* calculations in the previous chapter led to the conclusion that there is no evidence for such strong interaction.

The intermediate question is: will the radical cation of **33** undergo ring opening in such a way as to give the same radical cation as that (**29⁺**) which is formed upon ring-opening of the radical cation of α -pinene (Equation 4.1b)?

As indicated in Chapter 3, the ring-opened radical cation of α -pinene (**29⁺**) could be stable compared to the ring-closed radical cation (**14⁺**). This is because the charge and the spin in **29⁺** are both stabilized by formation of the tertiary alkyl cation and the allylic radical. Furthermore the structure of **29⁺** is less hindered, so close approach of the solvent molecules is possible and this results in more effective

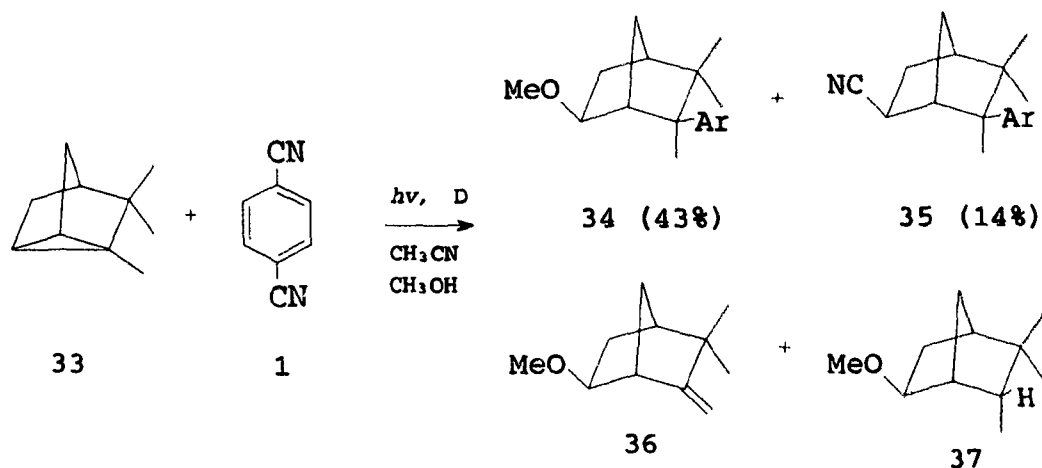


solvation. Therefore, with these considerations in mind, we have investigated the photo-NOCAS reaction with **33**. *Ab initio* calculations were also performed to compare the relative stability of the radical cations involved. Based on the experimental and the theoretical results, we have been able to establish the relationship between these radical cations.

Results and Discussion

Irradiation of a solution of 1,4-dicyanobenzene (**1**), biphenyl (**13**) and an excess of tricyclene (**33**) in acetonitrile-methanol (3:1) led to two 1:1:1 adducts (**34,35**), as well as two ethers (**36** and **37**) as depicted in Equation 4.2. The peak area ratio (GC/FID) for **34:35:36:37** is 1:0.3:0.75:1.23.

Clearly, there is no evidence that the radical cation of **33** undergoes cleavage to give $29^{+\dot{}}$. Nor does theory suggest this cleavage. *Ab initio* calculations show that the tricyclene radical cation ($33^{+\dot{}}$) is more stable than the distonic radical cation ($29^{+\dot{}}$) by 88.9 kJ mol^{-1} , and more stable than the radical cation of α -pinene ($14^{+\dot{}}$) by 45.5 kJ mol^{-1} . Therefore, the radical cations in Equation 4.1 do not interconvert under the conditions used.



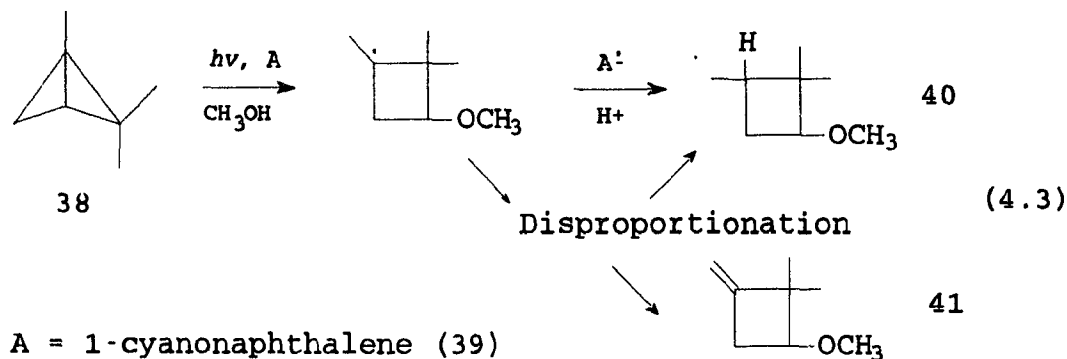
D = biphenyl Ar = 4-cyanophenyl (4.2)

Formation of the methanol adducts (36, and 37)

When the irradiation was carried out under the same conditions as described above but in MeCN-CD₃OD (3:1), it gave the same four products **34**, **35**, **36**, **37** as indicated by their retention times from the GC/MS. However the mass spectra indicate that incorporation of the deuterated methoxy group occurs in **34**, **36**, and **37**. For **34**, the base peak at $m/z = 186$ due to C₁₂H₁₂NO and the molecular ion peak at $m/z = 269$ due to C₁₈H₂₇NO moves to $m/z = 189$ (C₁₂H₉D₃NO) and 272 (C₁₈H₂₄D₃N). The only notable change in the spectrum of **36** is that the molecular ion peak at 166 is substituted by 169. In the mass spectrum of **37** the molecular ion peak at $m/z = 168$ and the peak at $m/z = 85$ are replaced by 171 and 88. These facts suggest that the formation of the two ethers mainly results from disproportionation of the γ -methoxy radical that formed upon reaction of the radical cation of **33** with methanol, followed by deprotonation. Apparently, as for the allylic radicals **30** and **32**, reduction of such γ -methoxy radical by the radical anion of **1** is slow.

The formation of **36** and **37** in large amounts is consistent with our knowledge of radical chemistry; disproportionation becomes more favourable relative to recombination in the series primary, secondary, tertiary, the ratios $k(\text{dis})/nk(\text{comb})$ being roughly 0.05, 0.2, and 0.8 in this series (n stands for the number of β hydrogens).⁹⁷ When tertiary radicals are stabilized by conjugation, disproportionation is slower relative to combination.⁹⁸

Some similar examples can be found in the literature. Equation 4.3 shows such a case where a tertiary radical is involved.⁹⁹ Irradiation of a solution of 1,2,2-trimethylbicyclo[1.1.0]butane (**38**) and 1-cyanonaphthalene (**39**) in methanol gives products **40** (major) and **41**. Product **40** is formed by two independent reaction pathways. One of these pathways, as in the case of **33**, is disproportionation of the tertiary radical. The other one, unlike the case of **33** where **1** is used as the acceptor,



is reduction of the tertiary radical by the radical anion of **39** followed by protonation is probably the major pathway for formation of **40**. This is because the reduction potential of **39** (-1.98) is more negative than that of **1** (-1.66 V). Similarly, irradiation

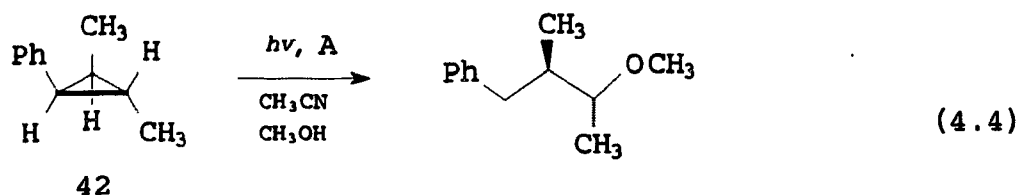
of 1,7-dimethyltricyclo[4.1.0.0^{2,7}]heptane with 1-cyanonaphthalene in the presence of methanol gives methanol adducts in the same way as discussed above.¹⁰⁰

Nucleophilic addition of methanol

The fact that only *exo*-products are formed suggests a nucleophilic ring-opening mechanism. This is distinguished from the mechanism suggested for the photo-NOCAS reactions of α -pinene and β -pinene. In those cases, the initially formed radical cation undergoes carbon-carbon bond cleavage to form the ring-opened radical cation before attack of methanol. If the ring-opened radical cation of **33** were an intermediate, the *endo*-products also should be observed although they might be minor products compared to *exo*-products.

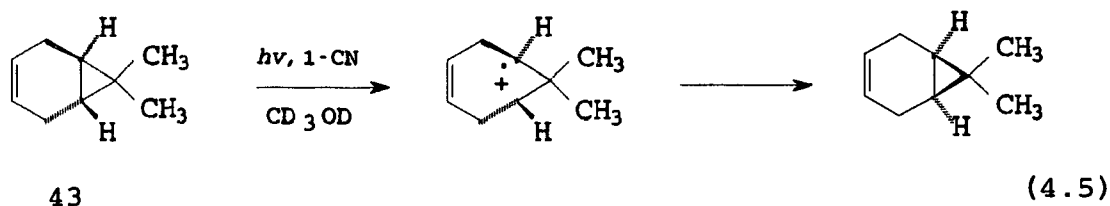
In the literature, several groups have reported that the many radical cations of cyclopropane derivatives may undergo ring-opening by nucleophilic assistance.¹⁰¹ Dinnocenzo *et al.* have studied a series of phenylcyclopropane derivatives and excluded the possibility that ring-opening of these radical cations occurs during or after electron transfer, followed by rapid nucleophilic capture.¹⁰² The stereochemical results they obtained are consistent with the nucleophilic ring-opening mechanism. One example of the reactions they studied is illustrated in Equation 4.4. They found the rate constant for reaction of methanol with the phenylcyclopropane radical cation ($9.5 \times 10^7 \text{ M}^{-1} \text{ s}^{-1}$) is comparable to that found for reaction of methanol with π radical cations.

Also, studies suggest that the cyclopropane radical cation is relatively stable due to the significant strength of the one electron two center bond. One example is



A = 1-cyanonaphthalene

the PET isomerization of 7,7-dimethyl-*trans*-bicyclo[4.1.0]hept-3-ene (**43**) in methanol (Equation 4.5).¹⁰³ The yield of the *cis*-isomer is 78%. This reaction suggests that the radical cation of **43** (*cis*- or *trans*-isomer) does not have a ring-opened structure (at



least the ring-opened structure is not the major intermediate), otherwise methanol would trap the ring-opened structure.

Formation of the 1:1:1 adduct **35** further supports the hypothesis that the cleavage process of the cyclopropane involves nucleophile-assistance. Product **35** was generated from attack by the cyanide ion. The only source of cyanide ion is the last step of the photo-NOCAS reaction—rearomatization. Therefore the concentration of cyanide ion must be low. It is well known that cyanide ion is a much better nucleophile than methanol. The competition of cyanide ion with methanol of much higher concentration (about 6 M) means that nucleophilicity plays an important role,

which is reminiscent of the importance of nucleophilicity in S_N2 reactions. If ring-opening occurred during or after electron transfer, nucleophilicity would play a much less important role in the reaction just as in the S_N1 reaction and the ring-opened structure of the radical cation of **33** would be predominantly trapped by the solvent (methanol), rather than cyanide ion. Furthermore, the ratio of products **34** to **35** monitored by GC/FID is constant as the reaction proceeds. This fact excludes the alternative explanation that the significant formation of **35** is because the concentration of cyanide ion could be built up as the reaction proceeds and so cyanide ion would capture the ring-opened radical cation of **33**. In summary, formation of the significant amount of **35** strongly suggests a nucleophilic ring-opening mechanism.

Further evidence for the nucleophilic ring-opening mechanism is provided by the *ab initio* calculation study.¹⁰⁴ Removing a single electron from a cyclopropane ring weakens one of the C-C bonds of the ring, but there is still significant barrier for cleavage. Calculations on the radical cation of **33** at the STO-3G level show that the energy minimum for the ring-closed structure (Figure 4.1) was easily found but for the ring-opened structure no minimum could be located. The details of these calculations will be described later in this chapter.

When methanol was omitted, photo-NOCAS product **34** and the two ethers (**36** and **37**) were not formed. Based on the general mechanism for the photo-NOCAS reaction, there is no source of the cyanide ion. However, the cyanide adduct **35** was still formed in a significant amount as shown by GC/MS. As we have indicated earlier, disproportionation of the γ -methoxy radical leads to the two ether (**36** and **37**). In contrast, 1:1 adduct between **33** and HCN was not observed. These facts

suggest that the concentration of the resulting radical is exceedingly low, so the probability that two radicals will encounter is low; on the other hand, the concentration of the radical anion of **1** is relatively high. That is the reason that **35** is formed rather than disproportionation products. The yield of **35** essentially remains the same, further supporting the idea that the formation of **35** is not due to the buildup of the cyanide ion, but due to the better nucleophilicity of this cyanide ion.

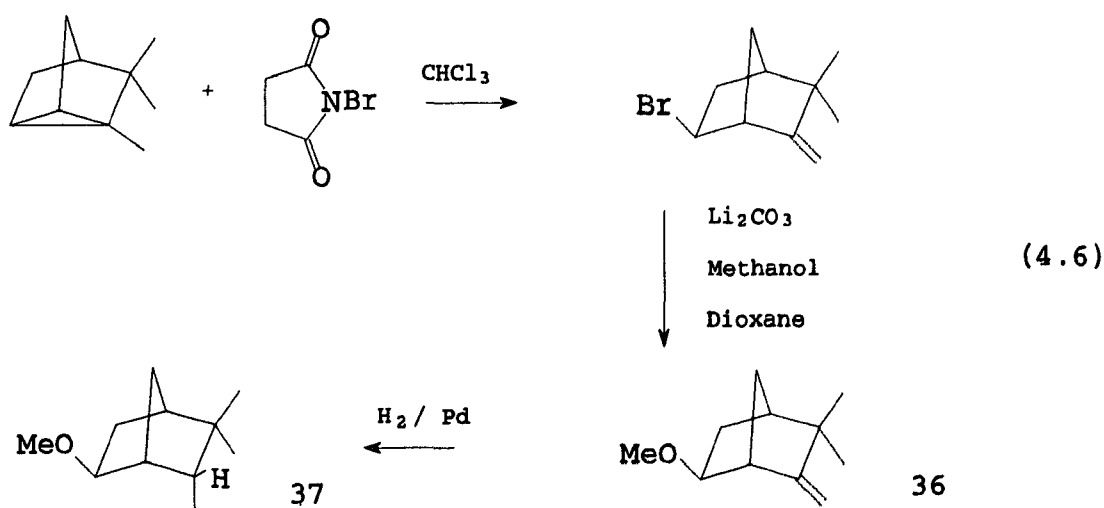
Addition of lithium perchlorate to the reaction mixture has an effect on the photo-NOCAS reaction: increasing the yield of the photo-NOCAS products incorporating methanol and reducing formation of the side product involving cyanide addition.^{63a} In this study, a similar effect was observed. In the presence of lithium perchlorate (0.3 M), the concentration of **35** was too low to be detected (GC/FID). However, a small amount of **35** (3%) was isolated, along with 54.7% **34**. More methanol addition products (**36** and **37**) were formed. Now the peak area ratio for **34:36:37** is 1.0:3.9:6.6. The explanation for the effect of lithium perchlorate is that the lithium cation may scavenge the cyanide anion.

It is not surprising that the radical cation of tricyclene (**33⁺**) undergoes cleavage at the more heavily substituted carbon-carbon bond if we notice that the radical cation of 1,1,2,2-tetramethylcyclopropane radical cation is stable in the ring-closed form at 77 K and undergoes cleavage at the more heavily substituted bond above 110 K in the $\text{CF}_2\text{ClCFCl}_2$.¹⁰⁵ Studies on other cyclopropane derivatives with no unsaturated group conjugated with the strained ring also led to the same conclusion—the most highly substituted bond is most likely to break.¹⁰⁶

When biphenyl (**13**) was not used, prolonged irradiation of the solution of **1** and **33** in acetonitrile-methanol did not lead to any product as shown by GC/FID. The oxidation potential of **33** is 2.31 (SCE) V and the reduction potential of **1** is -1.66. According to the Rehm-Weller equation,¹⁰⁷ the free energy for the electron transfer step is -30.7 kJ/mol (-7.34 kcal/mol) and hence the electron transfer process should be diffusion-controlled. However, back electron transfer proceeds even more rapidly than the other possible pathways. Hence, the observation that no product was formed in the absence of **13** is consistent.

Structural Assignments

The structures assigned to the four products were suggested by their NMR spectra. The coupling patterns were established from their coupled spectra. The resemblance of the four products in the coupling patterns suggests that the four products have the same carbon skeleton. Two of these assignments (i.e., **36** and **37**) were confirmed by synthesis as depicted in Equation 4.6.¹⁰⁸



A shift reagent experiment gives additional evidence that supports the structure suggested for **37**. Addition of $\text{Eu}(\text{fod})_3$ causes a downfield shift in the proton spectrum. The order of the magnitudes of the shift is $\text{exo-H3} > \text{H1} > \text{H}$ on the carbon of the methoxy group $> \text{H2}$. Shifts for the other protons are relatively small.

The assignments of stereostructures of **34** and **35** were based on the NOE effects and the coupling constants. Irradiation of H7s (the same side as the methyl groups, 1.80 ppm) in **34** causes a strong Overhauser effect only at 0.53 ppm (methyl group on C5). Also, irradiation of the methyl group on C6 (1.24 ppm) gives strong Overhauser effects at 3.81 ppm (*endo*-H2) and at aromatic region. Thus, the methyl group on C2 must be in the *endo* position and phenyl group in the *exo* position. The stereochemistry at C2 was established as that with the hydrogen in the *endo* position because the coupling between the *exo* hydrogen on C2 and the hydrogen on C1 (around 4.5 Hz) was not observed and $J_{\text{endo-endo}}$ (6.6 Hz), instead of $J_{\text{exo-exo}}$ (around 12 Hz), was observed. Furthermore, this assignment is consistent with the Overhauser effects.

In CDCl_3 , ^1H NMR spectrum for **34** shows that the two signals (1.82 and 1.80 ppm) for H1 and H7a overlap partially. However, in C_6D_6 , all signals move upfield and the signal associated with H1 moves more upfield than that associated with H7a (now a broad doublet corresponding to H7a clearly shows up).

Irradiation of methyl on C6 of **35** causes a definite Overhauser effect at 3.03 ppm (*endo*-H2). This leads to the assignment of *endo*-methyl group on C6.

Ab Initio Calculations on the Radical Cation of Tricyclene.

The STO-3G basis set and the open-shell, spin-unrestricted (UHF) procedure were used in this study.

First the geometry was fully optimized with a C_s symmetry on the bicyclic skeleton using AM1 for quick calculation and then using the STO-3G basis set. Further calculation (frequency) found there was one imaginary frequency, and therefore this symmetric stationary point (44) is a transition state. The total energy was found to be -383.190493 (e.u.) and the distances for C2-C6 and C1-C2 (or C1-C6) are 1.439 Å and 1.692 Å, respectively.

An attempt to find a minimum for the ring-opened structure of $33^{+\bullet}$ did not succeed. The distance between C1 and C2 was 2.457 Å, and that between C2 (or C1) and C6 was 1.5 Å in the initial structure. This initial structure did not have a three-membered ring. However, the finally optimized structure (45) does have a three-membered ring (see Figure 4.1) even though the C1-C2 bond length is quite long (1.879 Å). The energy for this fully optimized structure is lower than that for the structure with a symmetry plane (44) by 6.07 kcal/mol (25.2 kJ/mol). Further calculation on 45 showed that it is a minimum.

As expected for 45, the charge is delocalized over the whole radical cation, and the spin is mainly localized across the lengthened C1-C2 bond and the less heavily substituted carbon (C2) has the most spin.

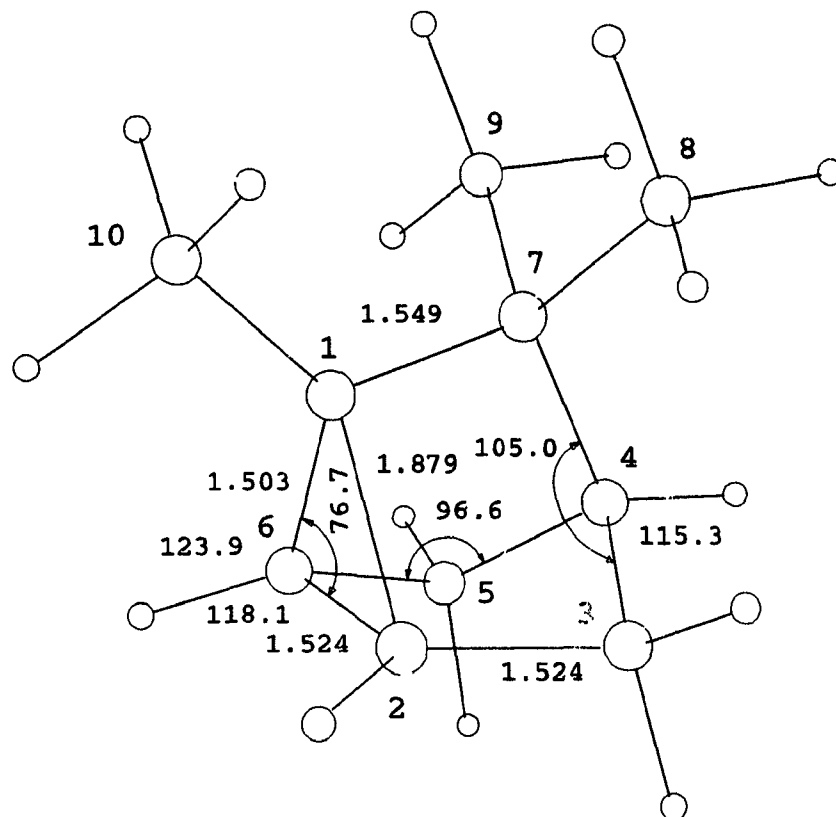


Figure 4.1 Structure 45: the fully optimized structure for the radical cation of tricyclene (33^{•+})

Table 4.1 The calculated charge and spin distributions for the radical cation of tricyclene (Structure 45)

No. ^a	Group	Atomic Charges	Spins			
			Carbon	Hydrogen(s)		
1	C	0.139	0.474			
2	CH	0.173	0.750	-0.055		
3	CH ₂	0.103	-0.085	0.015	0.031	
4	CH	0.071	0.011	-0.002		
5	CH ₂	0.100	0.039	-0.003	-0.002	
6	CH	0.094	-0.167	0.027		
7	C	0.038	-0.050			
9	CH ₃	0.072	0.026	-0.002	0.002	-0.002
8	CH ₃	0.058	0.012	-0.001	-0.001	-0.001
10	CH ₃	0.151	-0.059	0.017	0.003	0.024

^aNumbering of carbon atoms in Figure 4.1.

Experimental

For general methods, irradiations conditions and cyclic voltammetric measurements, see the experimental section in Chapter 3.

Materials

Tricyclene (99%) was obtained from Aldrich and used as received for reactions but was purified by GC for oxidation potential measurement. Tris(6,6,7,7,8,8,8-heptanfluoro-2,2-dimethyl-3,5-octanedionato)europium (Eu(fod)₃) was obtained from Norell Chemical Co., Inc.

Formation of adducts and ethers from tricyclene

A solution of 445 mg (3.3 mmol) tricyclene (**33**), 450 mg (2.9 mmol) biphenyl (**13**), and 340 mg (2.7 mmol) 1,4-dicyanobenzene (**1**) in 35 ml acetonitrile-methanol (3:1) was degassed with nitrogen for 5 min and irradiated through Pyrex for 7 days. The volatile components of the photolysate were removed by distillation, including most of **33** and some of the ethers (analyzed by GC/MS). The nonvolatile residue (1.28 g) was separated twice by DCFC. First, hexane-dichloromethane was used as eluting solvent. The solvent strength was gradually increased. Biphenyl was recovered in 98% yield. Unreacted DCB (152 mg) was isolated. The two adducts (**34**, **35**) were partly separated and came out as a colourless oil. The two ethers (**36**, **37**) came out as a mixture and were further separated by preparative GC (20% SE-30 150°C). Second, the mixture of the two adducts was separated by using hexane-ethyl acetate gradient. The photo-NOCAS product (**34**) weights 171 mg (43%) and the cyanide product (**35**)

55 mg (14%). Further purification of **34** and **35** gave crystals for both the products. The two products were purified prior to elemental analysis by recrystallization over methanol. The spectral data for these compounds are summarized as follows.

exo-6-(4-cyanophenyl)-5,5-dimethyl-exo-2-methoxy-endo-6-methylnorbornane (34)

IR (KBr disk, Nicolet 205) ν : 3040 (w), 2966 (s), 2937 (s), 2877 (m), 2227 (s), 1607 (s), 1506 (s), 1467 (s), 1453 (s), 1373 (m), 1214 (s), 1091 (s), 1069 (s), 1018 (s), 841 (s); ^1H NMR (360 MHz, CDCl_3) δ : 7.56 (d, 8.6 Hz, 2H, arom), 7.42 (d, 8.6 Hz, 2H, arom), 3.81 (dd, 6.6 Hz, 2.0 Hz, 1H, H2), 3.31 (s, 3H, methoxy), 2.70 (s, 1H, H1), 2.16 (ddd, 14.5 Hz, 6.6 Hz, 2.6 Hz, 1H, endo-H3), 1.82 (s, br, 1H, H4), 1.80 (dm, 8.9 Hz, 1H, H7s), 1.65 (d, 8.9 Hz, 1H, H7a), 1.34 (ddd, 14.5 Hz, 4.0 Hz, 2.0 Hz, 1H, H3), 1.24 (s, 3H, methyl), 1.07 (s, 3H, methyl), 0.53 (d, 3H, exo-5-methyl); ^{13}C NMR (360 MHz, CDCl_3) δ : 154.45 (s), 131.21 (d), 128.13 (d), 119.07 (s), 108.90 (s), 79.70 (d), 55.89 (q), 51.29 (d), 50.33 (d), 48.32 (s), 42.39 (s), 33.32 (q), 32.22 (t), 31.52 (t), 23.86 (q), 23.12 (q); MS, m/z : 269(0.3), 237(11), 211 (21), 196(17.3), 186(100), 168(26), 154(18), 116(13). C 80.25, H 8.61, N 5.17; found: C 80.25, H 8.55, N 5.25. m.p. 74.2 - 75.2°C.

exo-2-cyano-5,5-dimethyl-exo-6-(4-cyanophenyl)-endo-6-methylnorbornane (35)

IR (KBr disk, the infrared spectra were recorded on an air-purged Perkin-Elmer 180 grating infrared spectrometer and is relative to the 1601.4 cm^{-1} absorption of polystyrene), ν : 2970 (s), 2900 (m), 2800 (w), 2230 (s), 1610 (m), 1520 (m), 1470 (m), 820 (m), ^1H NMR (360 MHz, CDCl_3) δ : 7.54 (d, 8.5 Hz, 2H, arom.), 7.40 (d,

8.5 Hz, 2H, arom.), 3.30 (ddd, 9.0 Hz, 4.2 Hz, 1.9 Hz, 1H, H2), 2.97 (s, br. 1H, H1), 2.25 (ddd, 13.5 Hz, 9.0 Hz, 2.5 Hz, 1H, endo-H3), 2.11 (ddd, 11.1 Hz, 2.5 Hz, 1.9 Hz, 1H, H7s), 1.99 (dd, 3.8 Hz, 1.2 Hz, 1H, H4), 1.80 (m, 11.1 Hz, 1H, exo-H3), 1.79 (m, 13.5 Hz, 1H, H7a), 1.28 (s, 3H, methyl), 1.11 (s, 3H, methyl), 0.56 (s, 3H, methyl); ^{13}C NMR (360 MHz, CDCl_3) δ : 152.57 (s), 131.43 (d), 127.92 (d), 123.90 (s), 118.75 (s), 109.55 (s), 51.92 (d), 50.76 (d), 49.39 (s), 42.74 (s), 34.60 (t), 31.43 (q), 29.84 (t), 26.92 (d), 24.29 (q), 22.73 (q); MS, m/z : 264(48), 249(13), 221(21), 181(41), 154(39), 131(45.8), 116(24), 83(82), 55(100). C 81.78, H 7.63, N 10.60; found: C 81.66, H 7.46, N 10.64. m.p. 148.1 -- 148.7°C.

exo-6-methoxycamphene (36)

^1H NMR (360 MHz, CDCl_3) δ : 4.88 (dd, 1.5 Hz, 0.8 Hz, 1H), 4.66 (s, 1H), 3.31 (ddd, 6.9 Hz, 3.0 Hz, 3.0 Hz, 1H, H6), 3.30 (s, 3H, methoxy), 2.83 (s, br., 1H, H1), 2.12 (ddd, 13.5 Hz, 6.9 Hz, 2.8 Hz, 1H, endo-H5), 1.91 (ddd, 4.2 Hz, 1.3 Hz, 1.5 Hz, 1H, H4), 1.67 (dddd, 10.0 Hz, 3.0 Hz, 2.8 Hz, 1.5 Hz, 1H, H7s), 1.51 (ddd, 10.0 Hz, 1.3 Hz, 1.3 Hz, 1H, H7a), 1.23 (dddd, 13.5 Hz, 4.2 Hz, 3.0 Hz, 0.8 Hz, 1H, exo-H5), 1.05 (s, 3H, methyl), 0.99 (s, 3H, methyl); MS, m/z : 166(0.9), 134(52), 119(100), 93(47), 91(43), 79(20), 77(22).

5,5-dimethyl-exo-2-methoxy-endo-6-methylnorbornane (37)

^1H NMR (360 MHz, CDCl_3) δ : 3.52 (ddd, 6.9 Hz, 4.2 Hz, 0.7 Hz, 1H, H2), 3.24 (s, 3H, methoxy), 2.12 (dd, 3.7 Hz, 0.8 Hz, 1H, H1), 2.05 (ddd, 13.5 Hz, 6.9 Hz, 3.0 Hz, 1H, endo-H3), 1.76 (dd, 4.4 Hz, 0.8 Hz, 1H, H4), 1.58 (dd, 7.5 Hz, 3.7

Hz, 1H, H6), 1.52 (m, 9.8 Hz, 3.0 Hz, 1.5 Hz, 1H, H7s), 1.39 (ddd, 9.8 Hz, 1.6 Hz, 1.5 Hz, 1H, H7a), 1.14 (ddd, 13.5 Hz, 4.4 Hz, 4.2 Hz, 1H, *exo*-H3), 0.95 (s, 3H, methyl), 0.83 (d, 3H, 7.5 Hz, methyl), 0.74 (s, 3H, methyl). MS, m/z : 168(1.6), 136(26), 121(40), 95(100), 85(65), 67(40), 55(40).

The photosensitized (electron transfer) irradiation of tricyclene (3) in acetonitrile-deuterated methanol (CD₃OD)

When the irradiation of **33** was carried out as described above but in acetonitrile-methanol-d₄ (3:1) still led to the four products (**34**, **35**, **36**, and **37**) as shown by GC/MS. The mass spectra indicate that the incorporation of the deuterated methoxy group occurs in **34**, **36** and **37**. The base peak and the molecular ion peak in the mass spectrum of **34** become $m/z = 189$ (C₁₂H₉D₃NO) and 272, instead of 186, and 269. The only notable change in the mass spectrum of **36** is that the molecular ion peak becomes $m/z = 169$. In the mass spectrum of **37** the molecular ion peak at $m/z = 168$ and the peak at $m/z = 85$ are substituted by 171 and 88, respectively.

Chapter 5.

***Ab Initio* Studies on the Interaction between the Allyl and Alkyl Radical and Carbocation Moieties, and on the Cleavage of the Radical Cations of Alkenes: 1-Butene and 4,4-Dimethyl-1-pentene**

As shown in Chapter 3, the radical cations of α - and β -pinene undergo rapid allylic cleavage before attack of methanol (Equations 3.2, 3.3). Product analysis shows that the two moieties (the allylic radical and the alkyl cation) of the ring-opened radical cations ($29^{+\bullet}$, $31^{+\bullet}$) have no direct interaction that might sterically hinder the formation of the *cis* product (16). In other words, they are simply distonic radical cations with the allylic radical and the alkyl cation moieties.

More evidence against a strong interaction between the cationic center and the central carbon of the allylic radical in $29^{+\bullet}$ comes from the photo-NOCAS reaction of tricyclene. As we have discussed in Chapter 4, no connection between the photo-NOCAS reactions of α -pinene and tricyclene was observed.

Also, the above conclusion is supported by *ab initio* calculations on the radical cation of α -pinene (see Chapter 3), and on the tricyclene radical cation (Chapter 4). For example, in Figure 3.6 the distance between the allylic radical and the alkyl cation centers is too great for any interaction to occur. However, these calculations were not complete. α -Pinene and tricyclene are large molecules; any calculation on the radical cations of these molecules will be time consuming even though the smallest basis set (STO-3G) is used. Inevitably, it is not practical to study these

radical cations in detail by *ab initio* methods. Alternatively, suitable model systems are needed.

Moreover, many similar carbon-carbon bond cleavages^{31,109} and rearrangements¹¹⁰ of radical cations are known; however, little is known about the detailed course of these reactions. Direct observation of these processes is difficult because radical cations of this type are generally unstable transient species. Furthermore, when the radical cation is generated by photoinduced electron transfer, deactivation by back electron transfer is usually rapid. Back electron transfer from the radical anion to the radical cation within the radical ion pair has a rate constant of ca. 10^8 s^{-1} ^{19a}, so cleavage and rearrangement must be even more rapid in order to compete.

Ab initio molecular orbital calculations are particularly valuable for revealing the structure and relative energy of local minima, possible metastable intermediate(s) preceding the complete separation of the fragment radical and carbocation from the radical cation formed initially. Therefore, it is valuable to carry out a detailed study on the radical cations of small molecules by using *ab initio* molecular orbital methods. For this study we have selected the radical cations of 1-butene (46) and 4,4-dimethyl-1-pentene (47) as archetypical examples of alkene radical cations.

There is experimental evidence that illustrates the complexity of the problem even with these simple alkenes. The normal electron impact ionization mass spectra of the C_4H_8 isomers, 1-butene (46), *cis*- and *trans*-2-butene (48), and the cyclic isomers methylcyclopropane (49) and cyclobutane (50), are all very similar.¹¹¹ The molecular ions equilibrate to a common structure(s) before or during fragmentation. The

behaviour of the initially formed radical cations has been studied by neutralization-reionization mass spectrometry. Using this technique it was possible to show that although the initially formed radical cations readily undergo carbon-carbon bond cleavage, carbon-hydrogen bond cleavage and rearrangement, five distinct radical cations ($C_4H_8^+$) could still be characterized.^{111a}

Additional evidence for the structure and reactivity of the C_4H_8 radical cations comes from electron spin resonance (ESR) studies carried out on Freon matrices at low temperatures under conditions where the radical cations are somewhat stable.¹¹² Butene-1 (**46**), *cis*- and *trans*-2-butene (**48**), and 2-methylpropene (**51**) all give distinct ESR spectra attributed to their respective radical cations.^{112f} Analysis of the ESR proton hyperfine splitting of the radical cations of **46** and *cis*- and *trans*-**48** indicates that these radical cations maintain a structure similar to that of the original alkene, they are essentially planar.^{112f,113}

Computational

The computational methods used here have been described in Chapter 3. Here we shall describe the details of the calculations for the two alkene systems. Table 5.1 lists the calculated energies for the two neutral alkenes, for several alternative structures of the alkene radical cations, and for the fragment alkyl and allyl radicals and cations. The archive entries are given in Appendix 1 at the end of the thesis.

Calculations on the 1-butene (46) system

With 1-butene, four conformers can be distinguished by rotation around the C2-C3 single bond (Figure 5.1). The four possible conformers of 1-butene are: with the

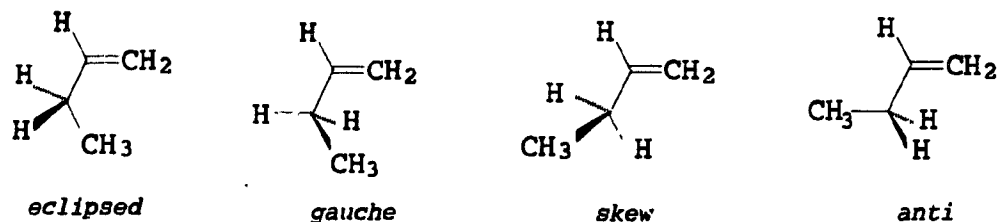


Figure 5.1 The four possible conformers of 1-butene resulting from rotation around the C2-C3 carbon-carbon single bond

methyl group and the vinyl group at an angle of ca. 0° (*eclipsed*), 60° (*gauche*), 120° (*skew*), and 180° (*anti*). It has been reported that a stationary point was found for each of four cases at the RHF 6-31G*/3-21G level.¹¹⁴ The *skew* conformer is the global minimum. For the sake of comparison, we carried out additional calculations on the *skew* conformer: a full geometry optimization at the RHF/6-31G* level and a single point calculation at the MP2/6-31G**/RHF/6-31G* level (46 *skew* in Table 5.1).

Table 5.1 The calculated (*ab initio*) total energies for the neutral alkenes **46** and **47**, for several alternative structures of the alkene radical cations, and for the fragment alkyl and allyl radicals and cations.

	STO-3G	6-31G ^a	MP/6-31G ^a
<i>C₄H₈ system (12)</i>			
46 gauche		-156.10162 ^a	
46 anti		-156.10238 ^a	
46 eclipsed		-156.10471 ^a	
46 skew		-156.10608 ^b	
		-156.10586 ^c	-156.62021
46⁺ b (Fig. 5.4)	-153.92624	-155.75745	-156.22480
46⁺ anti		-155.81037	
46⁺ eclipsed	-153.99062	-155.81122	
46⁺ skew (Fig. 5.2)	-153.99177	-155.81173	-156.28136
<i>C₄H₁₄ system</i>			
47 anti	-269.96601		
47 skew	-269.97122 ^c		
47⁺ b (Fig. 5.6)	-269.68224		
47⁺ eclipsed	-269.72788		
47⁺ anti	-269.73289		
47⁺ skew (Fig. 5.5)	-269.73564		
Allyl radical	-115.05429 ^d	-116.46810 ^d	-116.80964
Allyl cation	-114.80953 ^d	-116.19321 ^d	-116.54301
Methyl radical	-39.07701 ^d	-39.55899 ^d	-39.66867
Methyl cation	-38.77948 ^d	-39.23064 ^d	-39.32514
tert-Butyl radical	-154.83549		
tert-Butyl cation	-154.63766	-156.44241 ^c	

^aOptimized using RHF/6-31G^{*}//3-21G (ref. 114).

- ^bIP obtained from the energy of the HOMO is 9.7 eV (935.9 kJ/mol).
^cIP obtained from the energy of the HOMO is 8.45 eV (815.3 kJ/mol).
^dWhit~~z~~side, R. A.; Frisch, M. J.; Pople, J. A. *The Carnegie-Mellon Quantum Chemistry Archive*, 3rd. ed.; Carnegie-Mellon University: Pittsburgh, PA, 1983.
^eJorgensen, W. L. Buckner, J. K. *J. Am. Chem. Soc.* **1987**, *109*, 1891.

The geometry optimization of the radical cation of 1-butene was carried out at both the UHF/STO-3G and UHF/6-31G* levels. Minima were found for three of the four possible conformers around the C2-C3 carbon-carbon single bond. The conformer with the methyl group *skew* and a hydrogen on C3 *eclipsed* with the vinyl group is the global minimum (**46⁺a**, Figure 5.2). The conformation with the methyl group *gauche* and a hydrogen on C3 *anti* to the vinyl group is not a minimum; calculations starting with this initial structure converged to the global minimum. The conformer next in energy above the global minimum has C1, C2, C3, and C4 all in a plane, with the methyl group *eclipsed* with the vinyl group. The least stable conformer has the alternative planar structure with the methyl group *anti* to the vinyl group. This relative order of stability for the conformers is the same as that found from calculations on the neutral molecule 1-butene (**46**).¹¹⁴

In addition to the structure closely resembling the alkene (Figure 5.3a), a possible bridged structure for the radical cation would have the alkyl moiety interact with the allyl moiety, approaching in two nearly parallel planes (Figure 5.3b). This is a structure that also might result from cleavage of the radical cation of an alkylcyclopropane; or, as an intermediate or transition state in the suprafacial 1,3-sigmatropic rearrangement of an alkene radical cation.¹¹⁵ This structure has *C_s* symmetry. The calculations on this structure were carried out at both the

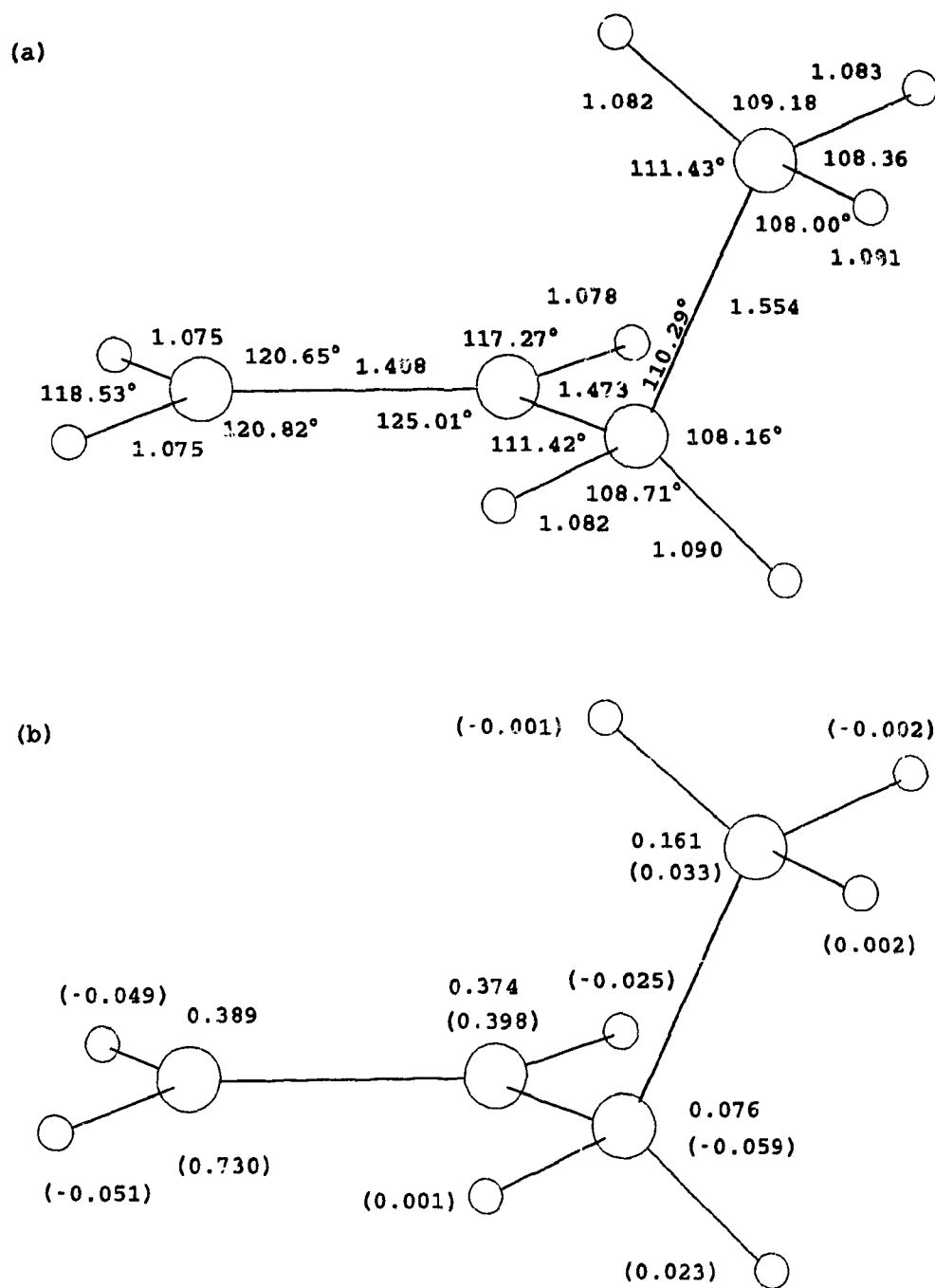


Figure 5.2 The global minimum structure for the radical cation of 1-butene (46^{+*a}); above: the optimized (UHF/6-31G^{*}) structure; below: the spin and charge densities

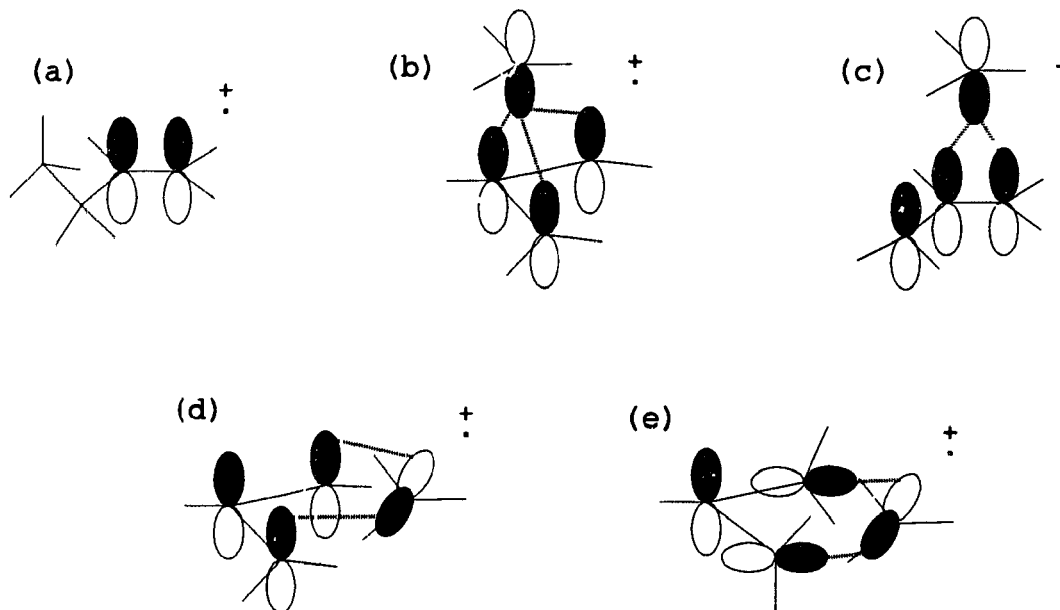


Figure 5.3 Possible metastable intermediates/transition states preceding the complete separation of the allyl and alkyl fragments from the radical cation of alkenes

UHF/STO-3G and the UHF/6-31G* levels. The initial search for a minimum imposed a C_s symmetry constraint and confined the allyl moiety to a plane. Having identified a stationary point, full geometry optimization was then carried out; the former stationary point did not change and the symmetry plane was maintained (46^{+*b} in Figure 5.4). Further characterization of the stationary point showed one imaginary frequency on diagonalization of the force constant matrix; therefore, while 46^{+*b} is more stable than the separated fragments, it is a transition state, not an intermediate.

Another possible structure would have the alkyl moiety interact with adjacent carbons of the allyl moiety (Figure 5.3c). A similar "nonclassical" structure has been proposed to explain the ESR spectrum of the radical cation of methylenecyclobutane

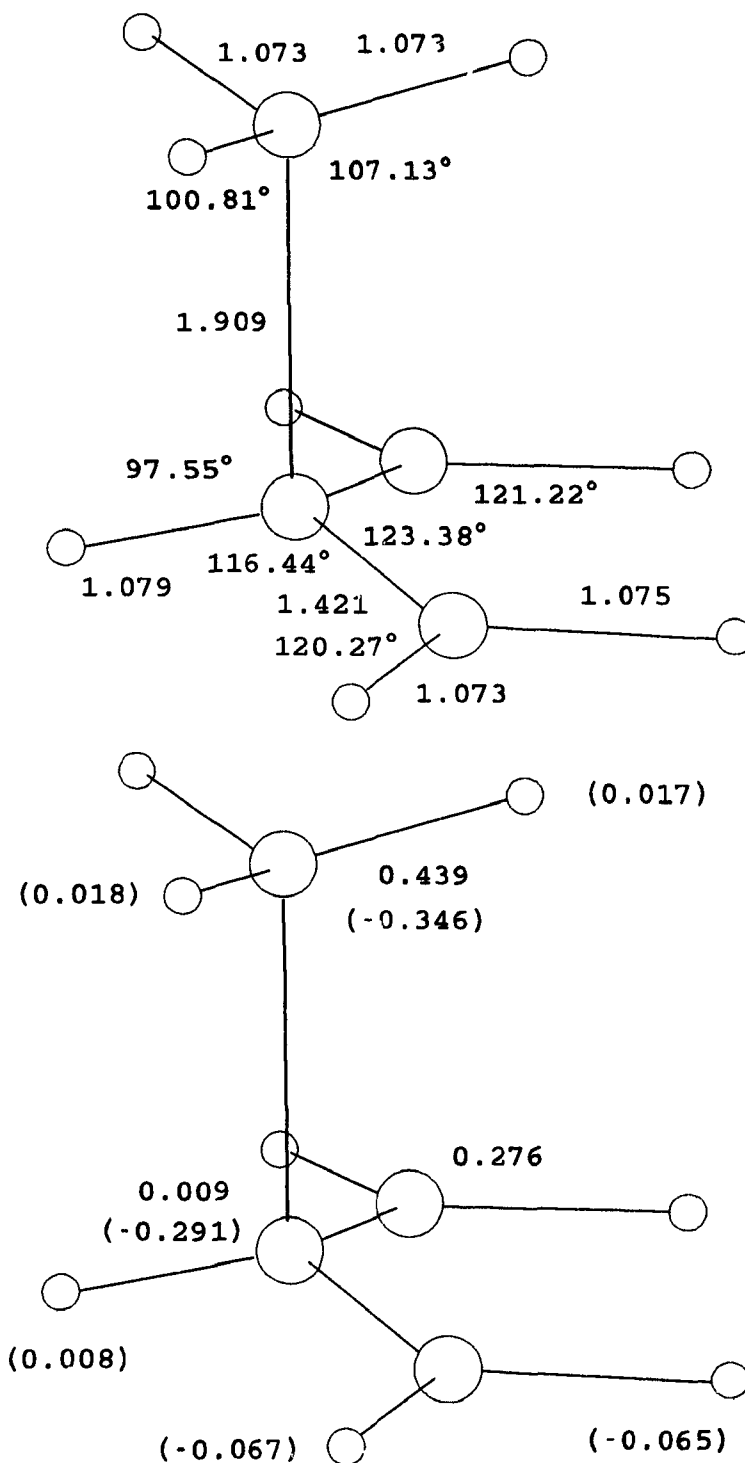


Figure 5.4 A transition state for the radical cation of 1-butene ($46^{**} \mathbf{b}$); above: the optimized (UHF/6-31G*) structure; below: the spin and charge densities

(51⁺).¹¹⁶ Calculations on the "nonclassical" structure of this kind were attempted only at the UHF/STO-3G level and were initially subject to constraint; the C4 carbon of the methyl moiety was confined to a plane perpendicular to the C1-C2 bond lying between the C1 and C2 atoms. Even with this constraint the calculation did not converge. When the constraints were removed the calculation converged to the global minimum structure 46⁺a *skew* (Table 5.1). Therefore, calculations at the UHF/STO-3G level do not find a stable structure analogous to Figure 5.3c for C₄H₈⁺ and this structure was not considered further.

Other possible structures for the radical cation were not given detailed consideration because of obvious unfavourable energetics or symmetry. Alternative arrangements having the allyl and alkyl moieties approach along two perpendicular planes (Figure 5.3d and 5.3e) are unlikely; either the orbital overlap is unsymmetric (Figure 5.3d) or overlap throughout the allyl system is lost (Figure 5.3e).

Single point calculations (MP2/6-31G**//UHF/6-31G*) were carried out on the radical cation in structures 46⁺a and 46⁺b; the results are summarized in Table 5.1.

Calculations on the 4,4-dimethyl-1-pentene (47) system

Similar considerations were used in the calculations for 4,4-dimethyl-1-pentene (47) system. The geometry optimization was carried out only at the UHF/STO-3G level. All four possible conformers were considered and three minima were identified. As in the case of the 1-butene radical cation (46⁺), the global minimum for 47⁺ has the *tert*-butyl group *skew* (ca. 120°) to the plane of the vinyl group (47⁺a, Figure 5.5). The conformers having the *tert*-butyl group *eclipsed* and *anti* to the vinyl group are

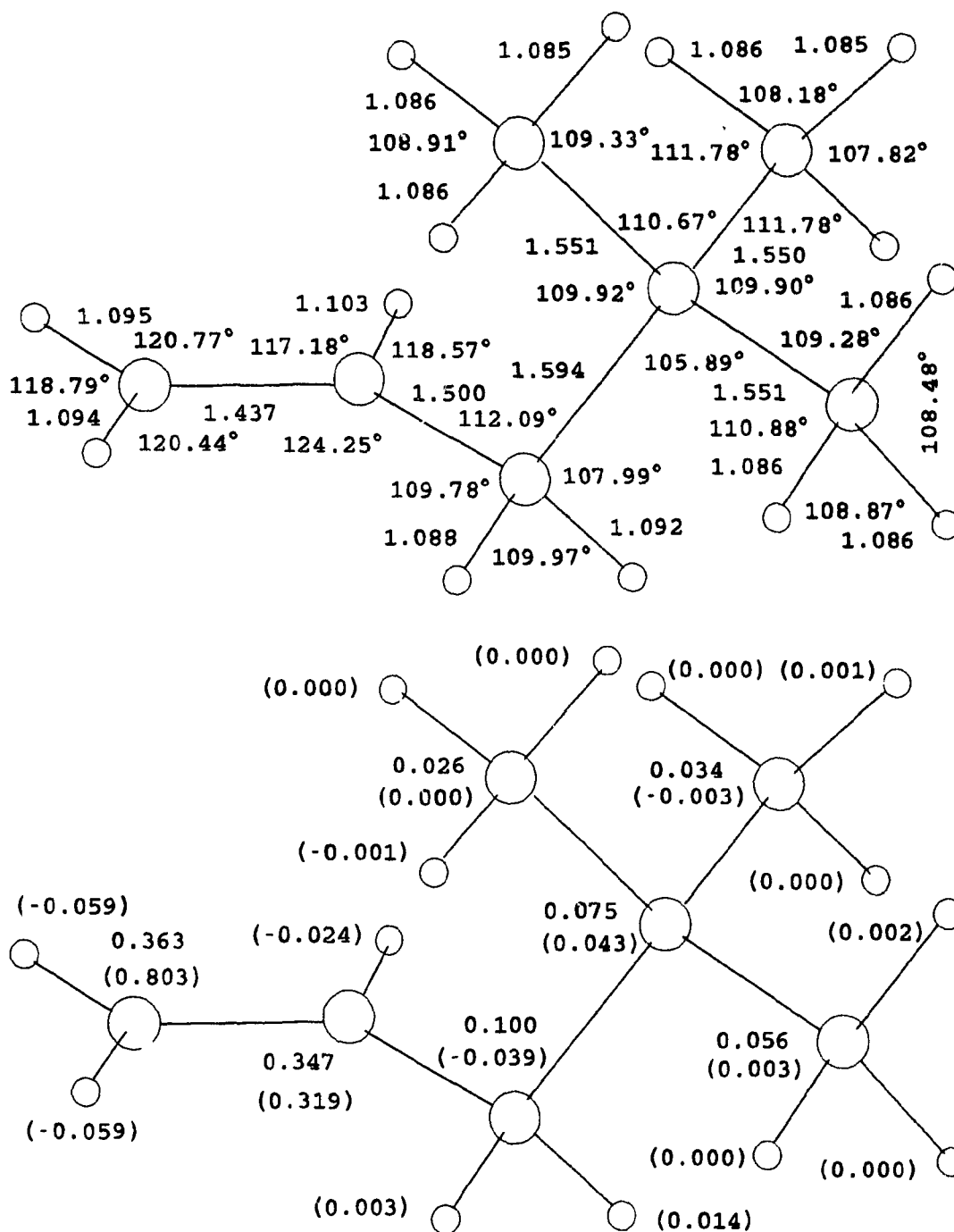


Figure 5.5 The global minimum structure for the radical cation of 4,4-dimethyl-1-pentene (47^{+a}); above: the optimized (UHF/6-31G*) structure; below: the spin and charge densities

energy minima but are considerably higher in energy. Calculations initiated with the radical cation in the conformation having the *tert*-butyl group *gauche* (ca. 60°) with the plane of the vinyl group converged to the global minimum. This order of stability for the conformers of the radical cation of 47 is the same as that observed for the parent molecule.¹¹⁷ Calculations on the bridged structure analogous to Figure 5.3b were also performed at the UHF/STO-3G level. Initially the structure was confined to C_s symmetry with the central carbon of the *tert*-butyl moiety in a plane perpendicular to the allyl moiety and through C2. The resulting stationary point was then fully optimized without these constraints; C_s symmetry was maintained ($47^{+\bullet b}$, Figure 5.6). This structure is less stable than the separated *tert*-butyl cation and allyl radical fragments, one imaginary frequency was found on diagonalization of the force constant matrix; therefore, $47^{+\bullet b}$ is not an intermediate.

Results and Discussion

The most stable of the structures considered for the radical cation of 1-butene ($46^{+\bullet}$) is very similar to that of the alkene (46^{+a} , Figure 5.2). The hydrogen on C3 and the three carbons, C1, C2, and C3, are all in the same plane. The allyl moiety is nearly planar, the terminal methylene group is only slightly ($< 1^\circ$) twisted out of the C1-C2-C3 plane. The methyl group is *skew* (119.8°) to the plane of the vinyl group and the C3-C4 bond length (1.558 Å) is normal. The singly occupied molecular orbital (SOMO) is largely associated with the π -bond between C1 and C2. There is little positive charge (0.161) or spin (0.032) density on the methyl moiety. This conformer is only 1.3 kJ mol⁻¹ more stable than the conformer having C1, C2, C3, and C4 all

essentially in the same plane, with the methyl group *eclipsed* with the vinyl group ($46^{+\bullet}$ *eclipsed*). The alternative planar arrangement, that with the methyl group *anti* to the vinyl group, is 3.5 kJ mol^{-1} above the global minimum.

Analysis of the ESR spectrum of the radical cation of 1-butene ($46^{+\bullet}$) in a Freon matrix at low temperature shows equivalent hyperfine coupling due to the hydrogens on C3. This has led to the assignment of the planar structure, that having the methyl group *eclipsed* with the vinyl group, for the radical cation.^{112f} The results of these calculations lead us to suggest that the *skew* conformer is in fact favoured; however, the two hydrogens on C3 appear equivalent in the ESR spectrum because the rotational barrier, which equilibrates the two hydrogens through the planar conformer, is small.

The bridged structure $46^{+\bullet}$ **b** (Figure 5.4) is an energy maximum, a possible transition state in the suprafacial 1,3-sigmatropic methyl migration of $46^{+\bullet}$. This structure is $148.5 \text{ kJ mol}^{-1}$ less stable than the global minimum $46^{+\bullet}$ **a** (Figure 5.2) and is only 34.4 kJ mol^{-1} more stable than the sum of the energy of the allyl cation and the methyl radical. The structure is similar to that found for the transition state for the 1,3-hydrogen migration in the propene homolog.¹¹⁵ The allyl moiety is almost planar, H2 is only 21° out of the plane of C1, C2, and C3, and the C2-C4 bond length is relatively long (1.909 \AA). The angle between H2-C2-C4 is 97.6° . Significant positive charge (0.439) and spin (-0.292) density is on the methyl moiety. This structure is related to the radical cation that could form upon cleavage of methylcyclopropane. However, when the radical cation of methylcyclopropane

cleaves, fragmentation to give the alternative radical cation with charge on the more heavily substituted carbon would be preferred.

An accurate description of the bonding involved in this structure is provided by an analysis of the individual molecular orbitals (Figure 5.7). In the highest filled

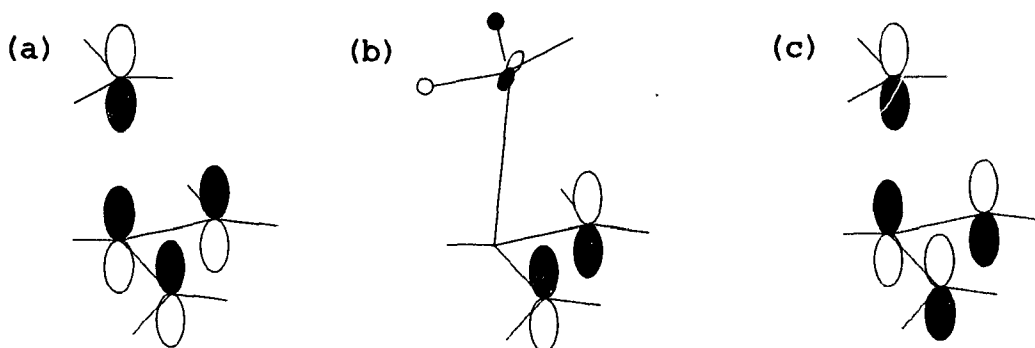


Figure 5.7 The radical cation $46^{+\bullet}b$: (a) The highest filled molecular orbital (HOMO); (b) The singly occupied molecular orbital (SOMO); (c) the lowest unoccupied molecular orbital (LUMO)

molecular orbital (Figure 5.7a) the contributions from the p_x orbitals on C1 and C3 are small; bonding involves both σ - and π -bonds. The major contributors to the singly occupied molecular orbital (SOMO) are the p_y atomic orbitals on C1 and C3 (Figure 5.7b). This species ($46^{+\bullet}b$) is best described as having the methyl moiety partially bonded to all of the carbons of the allyl moiety. The positive charge density is largely associated with the methyl moiety while the unpaired electron is largely distributed between the terminal carbons of the allyl moiety. These bonding orbitals correlate with the orbitals of the methyl cation and the allylic radical. Correlation with the methyl radical and allylic cation is symmetry forbidden (Figure 5.8).

The calculated results on the bridged radical cation (Figure 5.3b) at STO-3G basis level are qualitatively the same as those described above. In comparison with the

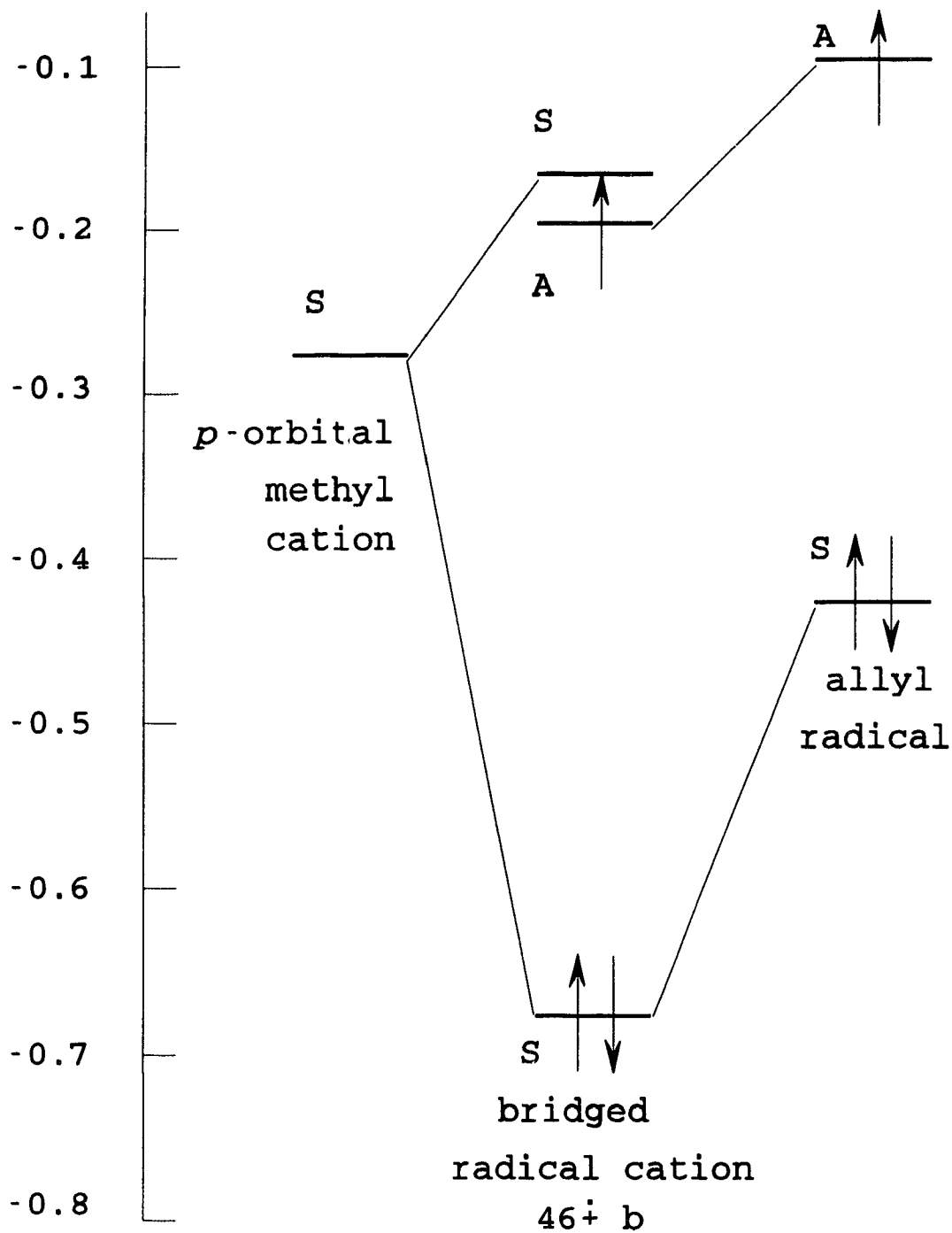


Figure 5.8 Orbital correlation diagram for the cleavage of the radical cation $46^{\cdot+}b$. Cleavage of the radical cation to the allyl radical and methyl cation is orbital symmetry allowed

results obtained from the 6-31G* calculations, the distance between C1 and C4 becomes shorter (1.726 Å), the allyl system deviates more from planarity (32.8° compared with 21°), and there is less charge (0.341 compared with 0.439) on the methyl group. These suggest that the interaction between the moieties is stronger at the STO-3G level.

Calculations on the radical cation of 4,4-dimethyl-1-pentene ($47^{+\bullet}$) were carried out only with the UHF/STO-3G basis set. Comparison of the results from the two basis sets calculations on $46^{+\bullet}$ indicates that the minimum structures for the radical cation are relatively more stable, compared to the energy of the separated fragments, with the lower level basis set (UHF/STO-3G). In the case of $47^{+\bullet}$ the minimum having the structure close to that of the alkene $47^{+\bullet}$ a (Figure 5.5) is closer in energy to the separated fragments; and, while the calculation of the radical cation having the bridged structure $47^{+\bullet}$ b (Figure 5.6) does converge, the calculated energy at the stationary point is higher than the sum of the energy of the separated fragments. The distance between C2-C4 is 2.00 Å. Bonding between the *tert*-butyl and allyl moieties in $47^{+\bullet}$ is weaker than bonding between the methyl and allyl moieties in $46^{+\bullet}$. The calculated stability of these bonded radical cation structures ($47^{+\bullet}$ a and $47^{+\bullet}$ b) would be even less if the higher level basis set (UHF/6-31G*) was used.

The cleavage process

These radical cations can undergo carbon-carbon bond cleavage in two modes: formation of the allyl radical and alkyl cation, or formation of the allyl cation and alkyl radical. The energy requirements for these alternatives can be estimated both

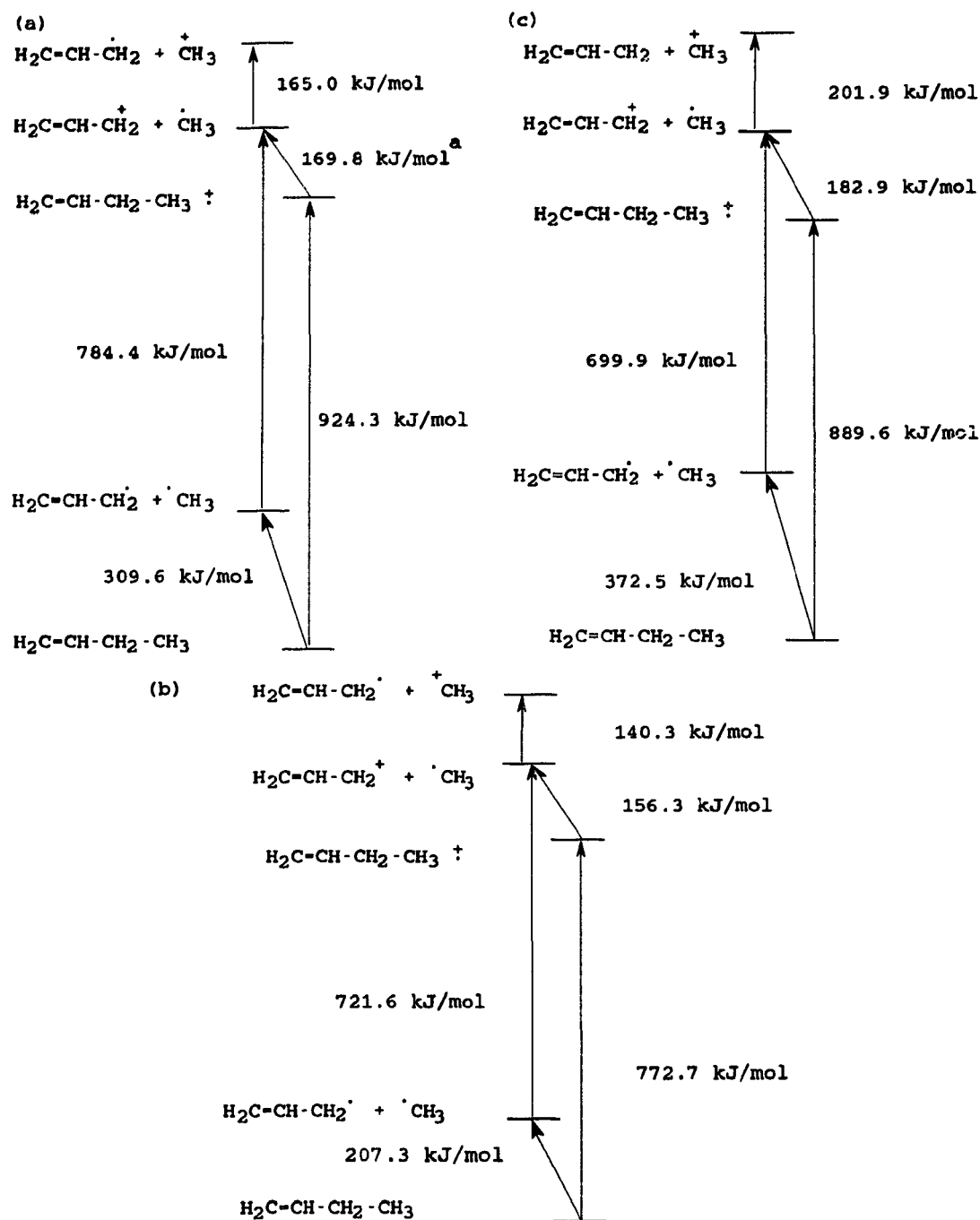


Figure 5.9 Thermochemical cycles for the cleavage of the radical cation 46+ (a) Experimental results.¹¹⁸ (b) Differences in calculated (MP2/6-31G*//UHF/6-31G*) total energies. (c) Differences in calculated (UHF/6-31G*) total energies. ^a Value calculated by completing the cycle.

from experimental thermochemical data (Figure 9a and 10a)¹¹⁸ and from the calculated values listed in Table 5.1 (Figure 9b and 10b). For the cleavage of the radical cation of 1-butene, there is good agreement between the experimental results and the calculated energy values when the larger basis set is used and when electron correlation is considered (MP2/6-31G*). The largest discrepancy caused by neglect of electron correlation involves the calculated homolytic C3-C4 bond dissociation energy. Bond dissociation energies calculated using Hartree-Fock theory are generally low.^{88,119} While formation of the alkyl radical and allyl cation is favoured in the case of 46⁺, cleavage to the alkyl cation and allyl radical is favoured in the case of 47⁺.

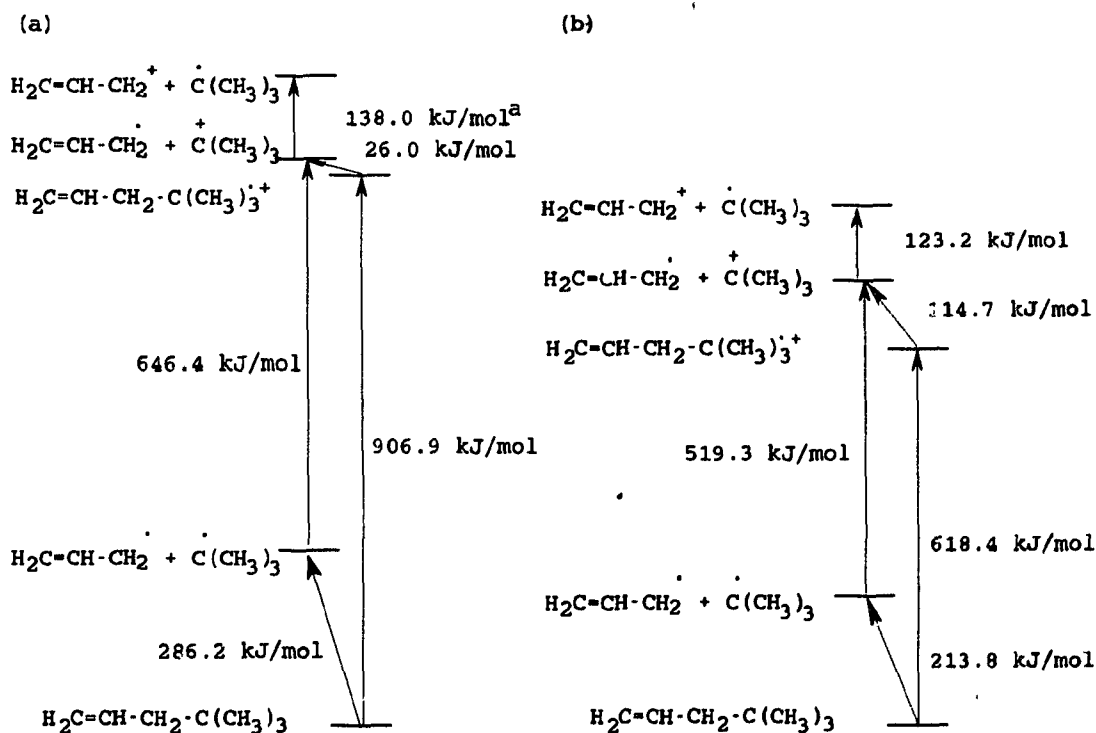


Figure 5.10 Thermochemical cycles for the cleavage of the radical cations 47⁺•. (a) Experimental results. (b) Differences in calculated (UHF/STO-3G) total energies

Figures 5.11a and b show the calculated (UHF/STO-3G) spin and charge density on the alkyl fragment as the allylic C3-C4 bond is progressively lengthened; the rest of the structure was optimized. The initial stages of bond lengthening increase both charge and spin density on both the methyl moiety and the *tert*-butyl moiety. The reason is that as the C3-C4 bond is progressively lengthened, the energy of the molecular orbital corresponding to the C3-C4 bond is becoming high and so mixing of this orbital with the SOMO is possible. However, as the bond lengthening increases beyond ca. 2 Å (after the transition state), spin density increases on the methyl moiety while charge density increases on the *tert*-butyl group, which is simply determined by the relative stabilities of the fragments. Therefore, when the radical cations **46^{•+}a** and **47^{•+}a** (Figures 5.2 and 5.5) cleave, there is no intrinsic barrier that favours cleavage in either mode. The singly occupied orbital of the product, alkyl or allyl radical, is determined on the basis of energetics.

There is experimental evidence indicative of these alternative modes of cleavage of **46^{•+}** and **47^{•+}**. The mass spectrum of 1-butene (**46**) shows the base peak at $m/z = 41$ (the allyl cation), and the peak at $m/z = 15$ (the methyl cation) has a relative abundance of only 6%; there is a significant (40%) peak due to the molecular ion ($m/z = 56$). The base peak in the mass spectrum of 4,4-dimethyl-1-pentene (**47**) is due to the *tert*-butyl cation ($m/z = 57$) and the peaks due to the allylic cation ($m/z = 41$, 53%) and the molecular ion ($C_7H_{14}^{•+}$, $m/z = 98$, <1%) are both relatively minor.¹²⁰

The interaction of an alkenyl radical cation with an alkene results in formation of an excited complex that fragments to yield new cations, radicals, and alkenes. This

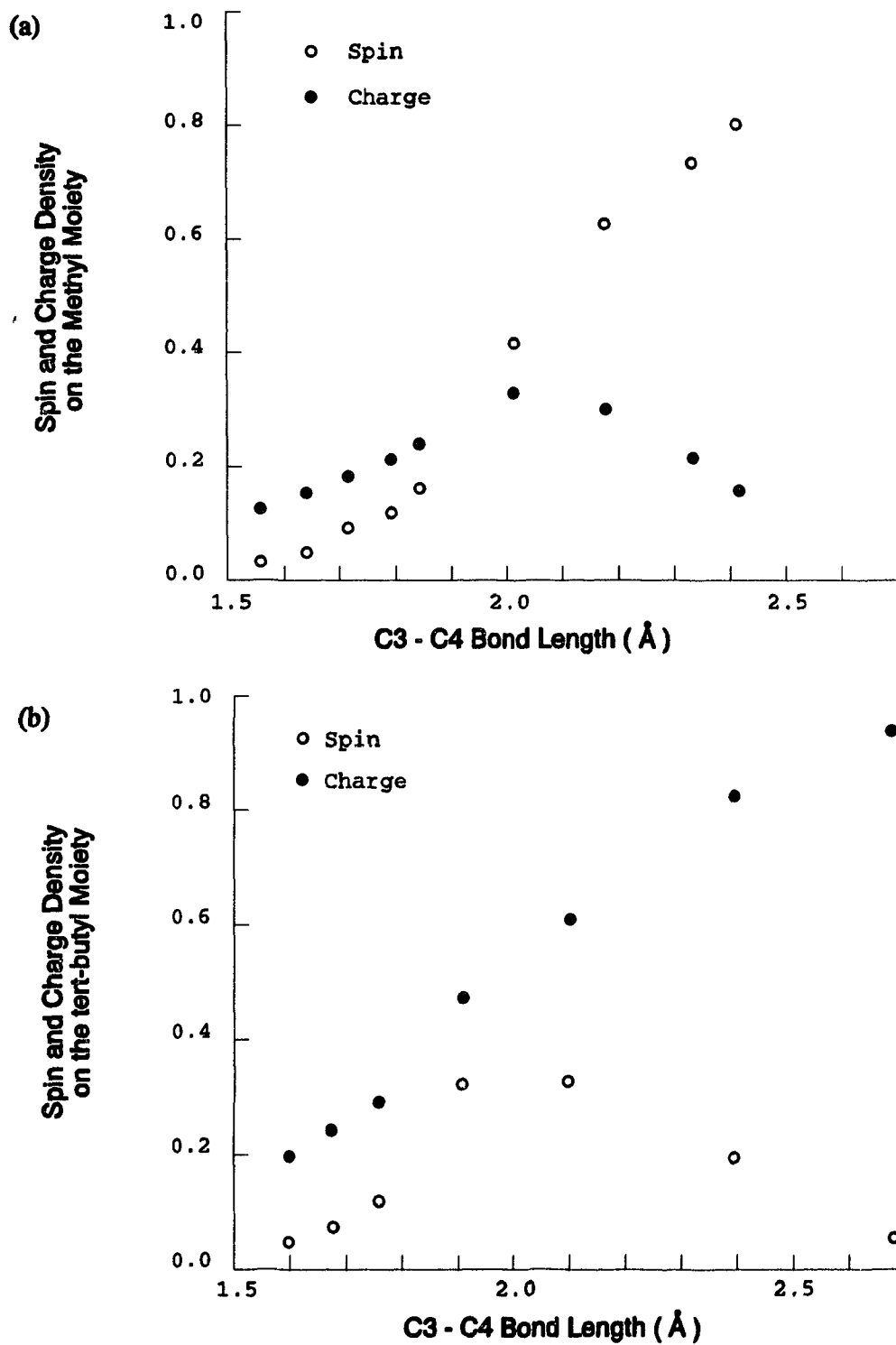


Figure 5.11. The calculated (STO-3G) spin and charge densities on the alkyl fragment of the radical cation (a) $46^{+\bullet}a$; (b) $47^{+\bullet}a$ as a function of allylic bond length

process has been studied by triple quadrupole mass spectrometry and the principal reaction between the ethenyl radical cation and ethylene yields a $C_4H_8^{+\bullet}$ complex that fragments exclusively to the allyl cation and the methyl radical. In marked contrast, reaction of radical cation of 2-methylpropene with 2-methylpropene gives a $C_7H_{14}^{+\bullet}$ complex that yields the 2-methylallyl radical and the t-butyl cation as the only products.¹²¹

In summary, removal of a single electron from 1-butene yields a relatively stable radical cation $46^{+\bullet a}$ with a structure closely resembling the original alkene. This intact radical cation is significantly more stable than the separated allyl and alkyl fragments. Fragmentation to the allyl cation and the methyl radical is energetically favoured over formation of the allyl cation and methyl radical. The alternative bridged structure for the radical cation, $46^{+\bullet b}$, formed by interaction of allyl and methyl fragments in which the unpaired electron resides mainly on the terminal carbons of the allyl moiety and nearly half the positive charge is distributed on the methyl moiety, is not an energy minimum.

Substitution of a *tert*-butyl group in place of the methyl group has a profound effect on the nature of the radical cation. Removal of a single electron from 4,4-dimethyl-1-pentene yields a radical cation, $47^{+\bullet a}$, which is only slightly more stable than the separated fragments. Cleavage of the $C_7H_{14}^{+\bullet}$ radical cation to the allyl radical and t-butyl cation is favoured over the alternative formation of the allyl cation and *tert*-butyl radical. These differences between $46^{+\bullet}$ and $47^{+\bullet}$ can be attributed to variation in the difference in the ionization potential of the two alternative fragments and to the variation in the stability of the alkyl cation: 1) Fragmentation of the radical

cation occurs in the direction that gives the carbocation of that fragment having the lower ionization potential. 2) If the carbocation is stable, cleavage of the radical cation is favoured and bonding interaction(s) between the fragments is minimized. These correlations have been recognized previously for cleavage of radical cations in solution of polar solvents.^{27b,31} Cleavage of radical cations in acetonitrile-methanol (3:1) solution occurs in such a direction that gives the carbocation of that fragment having the lower oxidation potential.

The results of these calculations are in good agreement with the observed behaviour of the radical cations of α -pinene (Equation 3.2) and tricyclene (Equation 4.2). The initial single electron transfer step (Equation 3.2) should give a weakly bonded radical cation ($14^{+\bullet}$). Cleavage of $14^{+\bullet}$ to $29^{+\bullet}$ will be assisted by relief of strain associated with the four-membered ring.¹²² Formation of the allylic radical and *tert*-carbocation should be favoured. The ionization potentials of alkyl-substituted allyl radicals will be lower than that of allyl radical,¹²³ for example, 7.90 eV for 2-methylallyl radical; 7.49 eV for 3-methylallyl radical; 7.07 eV for 3-penten-2-yl; these values are still greater than that of *tert*-butyl radical (IP = 6.70 eV^{118d}). Furthermore, the absence of a minimum for structure $47^{+\bullet b}$ makes it unlikely that there is significant bonding interaction between the allyl radical and carbocation centres in $29^{+\bullet}$. This is consistent with the observed stereochemistry; there is little preference of formation of the *trans*- products 17, and no rearrangement to the radical cation obtained from tricyclene ($33^{+\bullet}$).

Chapter 6

The Photo-NOCAS Reaction:

Methanol - Nopol and 2-(1-Cyclohexenyl)ethanol,

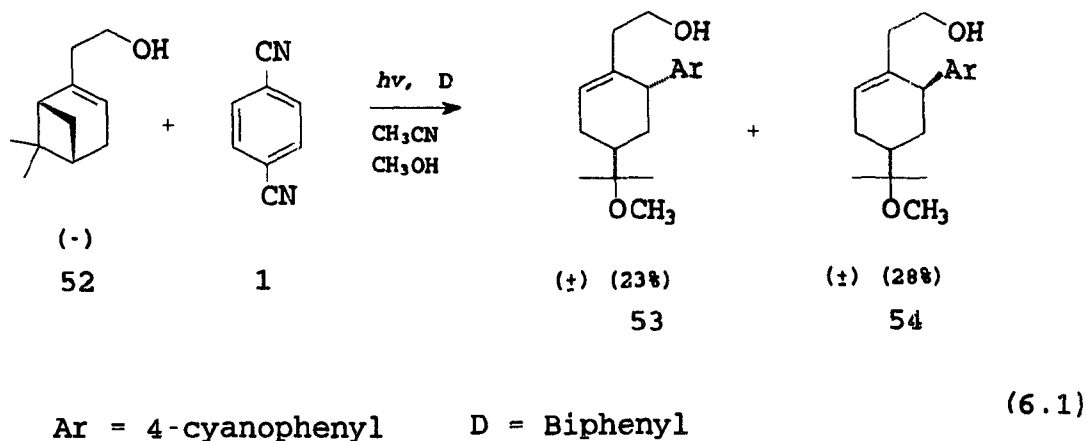
1,4-Dicyanobenzene

The radical cations of α - and β -pinene (14 and 15) in acetonitrile-methanol solution undergo rapid cleavage of the four-membered ring before attack of methanol on the unsaturated part of the radical cation (Equations 3.2 and 3.3). On the other hand, *ab initio* calculations at the STO-3G level show that the ring-closed radical cation of α -pinene (Structure 25) is more stable than the ring-opened intermediate (Structure 26) by 43.4 kJ/mol. This calculated value suggests a significant barrier for ring-cleavage of 14^{•+} (without considering solvent effects); therefore if nucleophilic attack is fast enough, photo-NOCAS products might be observed with the original four-membered ring intact. With this idea in mind, the photo-NOCAS reaction with nopol (52) was attempted. There is a hydroxy group in nopol; hence formation of a five-membered ring is expected, if the intramolecular nucleophilic addition to the double bond is fast relative to the opening of the four-membered ring of the radical cation of nopol.

Results and Discussions

A solution of 1,4-dicyanobenzene (1), biphenyl (2), and (-) nopol (52) in acetonitrile-methanol (3:1) was irradiated at 10°C through a Pyrex filter with a medium-pressure mercury vapour lamp. The photo-NOCAS products were isolated by dry column flash

chromatography on silica gel. Optical rotation measurements showed that the products were racemic. The results are outlined in Equations 6.1. The area ratio (determined



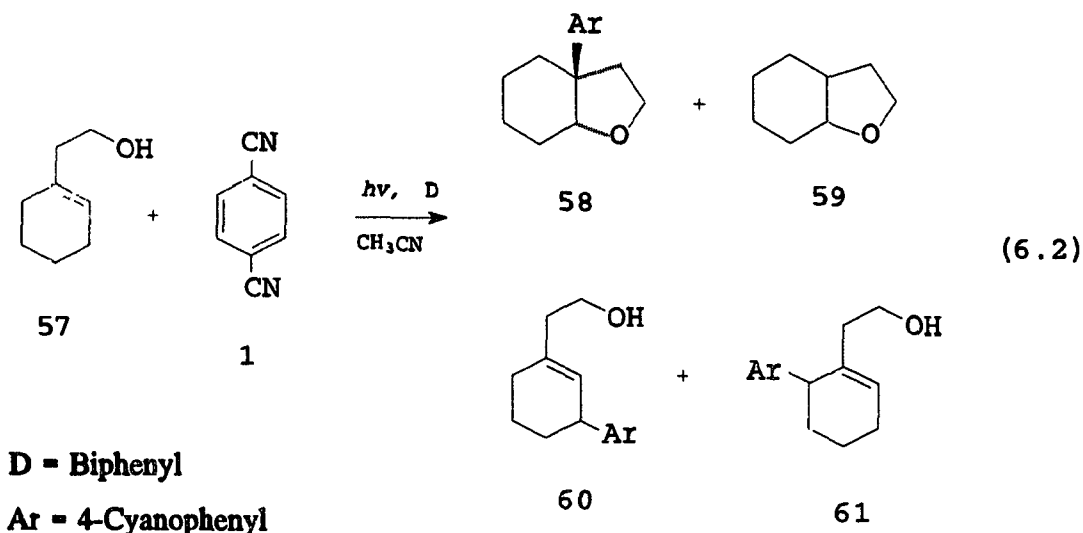
by GC/FID) of the two major products (**53**, **54**) was 0.9:1.0. No cyclized products were found by GC/MS analysis. Small amounts of imine and isomerization products, analogous to the imine (**19**) and limonene (**18**) were formed (analyzed by GC/MS), but these products were not isolated and further characterized.

If the above reaction was carried out in acetonitrile (without methanol), prolonged irradiation did not lead to any volatile products detectable by GC/MS. The starting material **52** was consumed and the reaction mixture simply turned dark yellow.

The NMR spectra of **53** and **54** are similar to those of **16** and **17** formed from the photo-NOCAS reaction with α -pinene as described in Chapter 3. Products **53** and **54** were further converted into 3,5-dinitrobenzoate derivatives (**55** and **56**), respectively. The structural assignments for **55** and **56**, based on the NMR spectra, were proven by X-ray crystallography (Appendix 2).

The oxidation potential of nopol is 1.74 V (SCE) which is similar to that of α -pinene. The discussion on the mechanism of the photo-NOCAS reaction in Chapter 3 can be applied to the present reaction (Equation 6.1). Ring opening of the radical cation of **52** is faster than any other process. The intramolecular nucleophilic addition to the double bond is slow relative to the ring opening. This conclusion raises the question about the relative rate of the intramolecular nucleophilic addition to that of intermolecular methanol addition.

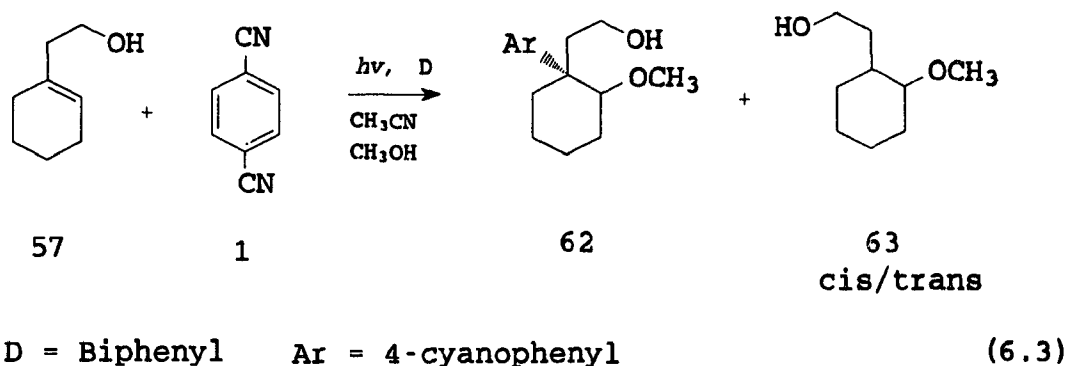
To answer this question, the photo-NOCAS reactions were performed with 2-(1-cyclohexenyl)ethanol (**57**). First, the reaction was carried out in acetonitrile solution (no methanol), and the results are depicted in Equation 6.2 where the area



ratio (GC/FID) for **58:59:60:61** is 0.7:0.3:1.0:1.0. The cyclized products (**58**, **59**) were formed along with two allylic radical substitution products (**60**, **61**). The cyclic ether **59** was tentatively assigned as the *cis* configuration by comparison with the reported mass spectra of both the *cis* and *trans* isomer.¹²⁴ Traces of the *trans* isomer

could be detected by GC/MS. The *cis* and *trans* isomers have been made previously in several different ways.¹²⁵

It seems clear that the rates for the cyclization and the deprotonation step are of the same order of magnitude, assuming that the subsequent steps are relatively fast. From the reaction of cyclohexene, the rate for formation of the allylic radical substitution product is known to be much slower than that for formation of the photo-NOCAS products.^{62,63a} Thus, the cyclization step is surprisingly slow and cannot compete with attack of methanol at the radical cation. Equation 6.3 shows the case.

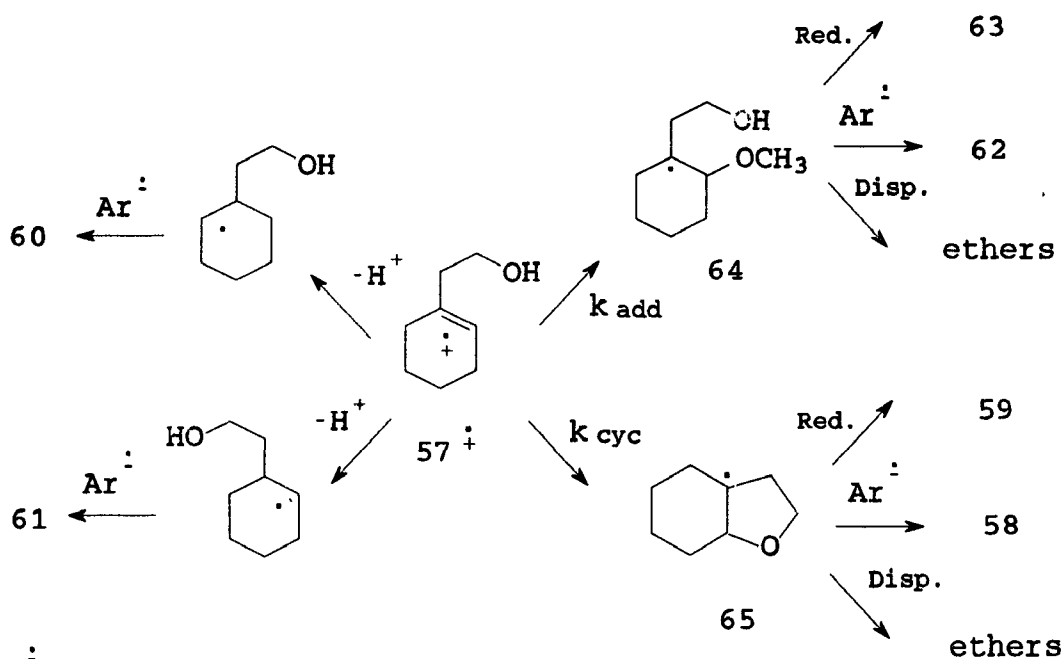


When the irradiation was carried out in the acetonitrile-methanol solution (3:1), only traces of the cyclized products (**58**, **59**) and the 1:1 adducts (**60**, **61**) were formed. Instead, a uncyclized photo-NOCAS product (**62**) and several uncyclized ethers, Markovnikov isomer, and *cis/trans anti*-Markovnikov isomers (**63**), were produced as the major products (Equation 6.3 where the ratio for **62**:(the ethers) is 1.0:0.6. Even when the concentration of methanol is low (e.g., about 0.5 M), the uncyclized products are still formed as the major products.

If we assume that the intermediates **64** and **65** are of equal reactivity in the subsequent reactions (i.e., coupling with the radical anion, reduction by the radical

anion and disproportionation, etc.), analysis of Scheme 6.1 leads to the conclusion that the mole ratio of **58** to **62** will have a linear relationship with the concentration of

Scheme 6.1



methanol; the slope of the line is the ratio of the rate constant for cyclization (k_{cyc}) to that for methanol addition (k_{add}). However, if the reactivity of the two intermediates is different, precise characterization of these two competing processes will not be straightforward and may need much more work.

In summary, the ring opening of the radical cations of type $14^{+\cdot}$, $15^{+\cdot}$ and $52^{+\cdot}$ is faster than nucleophilic attack of methanol at the initially formed radical cation. Cyclization of radical cations of type $57^{+\cdot}$ is much slower than attack of methanol on the radical cations under the reaction conditions.

Experimental

For general methods, irradiation conditions and cyclic voltammometric measurements, see Chapter 3. The ^1H and ^{13}C NMR spectra were recorded on a Bruker AMX 400 (WB) or a Bruker AC 250 spectrometer. 2-(1-Cyclohexenyl)ethanol (**57**) was prepared from 1-cyclohexenylacetonitrile (Aldrich, 92%) in two steps.¹³²

Formation of adducts (53 and 54) from nopol

A solution of 2.68 g (16.1 mmol) nopol (**52**), 1.14 g (7.4 mmol) biphenyl (**13**), and 1.33 g (10.4 mmol) 1,4-dicyanobenzene (**1**) in 160 ml acetonitrile-methanol (3:1) was degassed with nitrogen for 5 min and irradiated through Pyrex for 10 days. The volatile components of the photolysate were removed by distillation. The nonvolatile residue (6.8g) was loaded on Dry-Column (9.5 × 4.5 cm TLC grade silica gel) and the column was eluted with ethyl acetate-hexane gradient. The two photo-NOCAS products were partially separated Fr.13-43: **1** and nopol; Fr.53-57: **54** (0.57 g); Fr.58: a mixture of the two isomers (0.13 g); Fr.59-60: **53** (0.62 g); Fraction 13-43 was treated with hexane and 294 mg of **1** was recovered (78% conversion). The combined yields (based on consumed **1**) is 54% respectively. Optical rotation measurements showed that the products were racemic.

53 cis-: Infrared (PE-180) : 3420 (s), 3035 (w), 2970 (s), 2925 (s), 2225 (s), 1604 (s), 1500 (m), 1465 (m), 1380 (m), 1067 (s), 890 (s), 830 (s), 730 (s); ^1H NMR (361 MHz, CDCl_3 , Nicolet) δ : 7.58 (d, 2H, $J=7.9$ Hz), 7.28 (d, 2H, $J=7.9$ Hz), 5.81 (m, 1H, $J=5.2$), 3.46-3.55 (3H), 3.17 (s, 3H), 2.13-1.71 (7H), 1.26 (ddd, 1H, coupled to one of the protons at 3.46-3.55 ppm), 1.10 (s, 3H), 1.08 (s, 3H); ^{13}C NMR (90.78

MHz, CDCl₃, Nicolet) δ : 151.17 (s), 134.36 (d,), 132.14 (d), 128.76 (d), 126.97 (d), 118.75 (s), 109.70 (s), 75.96 (s), 60.24 (t), 48.64 (q), 46.88 (d), 42.11 (d), 37.77 (t), 35.32 (t), 27.00 (t), 21.99 (q), 21.30 (q); MS m/z : 267 (1.5), 206(7), 116(4), 91(5), 77 (5), 73(100), 55 (6).

54 trans-: Infrared (PE-180) : 3410 (s), 3030 (w), 2970 (s), 2925 (s), 2227 (s), 1604 (s), 1500 (m), 1465 (m), 1380 (m), 1067 (s), 890 (s), 832 (s), 735 (s); ¹H NMR (361 MHz, CDCl₃, Nicolet) δ : 7.59 (d, 2H, J=8.1 Hz), 7.33 (d, 2H, J=8.1 Hz), 5.88 (m, 1H, with small coupling constants), 3.61 (t, 2H, 6.54 Hz), 3.57 (s, br. 1H, $w_{1/2}$ = 14 Hz), 2.83 (s, 3H), 2.26-1.90 (5H), 1.80-1.57 (3H), 1.02 (s, 3H), 0.97 (s, 3H); ¹³C NMR (90.79 MHz, CDCl₃, Nicolet) δ : 150.11 (s), 133.15 (s), 131.80 (d), 129.18 (d), 127.11 (d), 118.83 (s), 109.62 (s), 75.84 (s), 60.41 (t), 48.13 (q), 43.73 (d), 38.50 (t), 34.34 (d), 31.92 (t), 26.84 (t), 21.97 (q), 21.87 (q); MS m/z : 267 (1.8), 206 (10), 116 (6), 91 (6), 77 (6), 73 (100), 55 (6).

The two compounds (**53**, **54**) were converted to 3,5-dinitrobenzoyl esters by the following procedure, respectively: 0.165 g (0.72 mmol) of 3,5-dinitrobenzoyl chloride and 0.210 g (0.72 mmol) of **53**, or **54** were dissolved into 1.5 ml pyridine. The solution was stirred at room temperature for 2 hours. The derivative was isolated by DCFC using dichloromethane-hexane gradient as eluent, and then recrystallized using ethanol-acetone system. Finally, recrystallization again using dichloromethane-hexane system gave yellowish crystal.

The spectral data for the derivatives were the following:

55 (from **53**):

^1H NMR (250 MHz, CDCl_3 , Bruker) δ : 9.19 (1H, m), 9.07 (2H, m), 7.60 (2H, d, 7.8 Hz), 7.30 (2H, d, 7.8 Hz), 5.83 (1H, m), 4.33 (2H, dd, 6.1, 7.9 Hz), 3.54 (1H, m, $w_{1/2}$ =24 Hz), 3.14 (s, 3H), 2.35 (dt, 1H, 14.6, 7.9 Hz), 2.18-1.92 (4H), 1.81 (m, 1H), 1.26 (ddd, 1H, 12.2, 11.9, 11.8, coupled to the proton at 3.54 ppm), 1.08 (s, 3H), 1.06 (s, 3H); ^{13}C NMR (62.9 MHz, CDCl_3 , Bruker) δ : 162.34, 150.809, 148.67, 133.89, 133.43, 132.65, 129.37, 129.90, 129.29, 122.41, 118.90, 110.43, 76.03, 64.78, 48.92, 47.13, 42.64, 35.54, 33.90, 27.25, 22.17, 21.36; m.p. 154.7-155.0 °C; For X-ray data, see Appendix 2.

56 (from **54**):

^1H NMR (250 MHz, CDCl_3 , Bruker) δ : 9.23 (m, 1H), 9.11 (m, 2H), 7.62 (d, 2H, 7.9 Hz), 7.36 (d, 2H, 7.9 Hz), 5.96 (m, 1H), 4.48 (m, 2H), 3.64 (m, $w_{1/2}$ =11.0 Hz), 2.84 (s, 3H), 2.50 (ddd, 1H, 15.3, 7.4, 7.2 Hz), 2.33-2.10 (2H), 1.98-1.69 (3H), 1.62 (m, 1H), 1.01 (s, 3H), 0.97 (s, 3H); ^{13}C NMR (62.9 MHz, CDCl_3 , Bruker) δ : 162.36 (C), 149.79 (C), 148.68 (C), 133.90 (C), 132.24 (CH), 132.15 (C), 129.37 (CH), 129.32 (CH), 128.35 (CH), 122.45 (CH), 118.94 (CN), 110.28 (C), 75.85 (C), 64.98 (CH_2), 48.45 (CH_3O), 44.17 (CH), 34.69 (CH), 34.65 (CH_2), 32.16 (CH_2), 27.10 (CH_2), 22.07 (2 CH_3); m.p. 149.2-150.5 °C. For the X-ray crystal structure, see Figure A2.2.

Irradiation of 2-(1-cyclohexenyl)ethanol (57) in acetonitrile solution

A solution of 0.492 g (3.9 mmol) **57**, 0.420 g (2.7 mmol) biphenyl (**13**), and 0.312 g (2.4 mmol) 1,4-dicyanobenzene (**1**) in 40 ml acetonitrile was degassed with nitrogen for 5 min and irradiated through Pyrex for 18 days until no **57** could be detected by GC. The volatile components of the photolysate were removed by distillation,

including most of **59** (analyzed by GC/MS). The nonvolatile residue (1.224 g) was treated with 40% ethyl acetate in hexane and 41 mg DCB was separated out. The rest was loaded on Dry-Column (TLC grade silica gel, 5 × 6 cm) by pre-adsorption and the column was eluted with ethyl acetate-hexane gradient. The photo-NOCAS product came out as an oil with **1**. Extraction of this mixture with hexane led to 110 g of **58**, which accounts for 27.5% of consumed **1**. 154 g of DCB (**1**) was left. The two isomers of 1:1 adducts (**60**, **61**) came out together (0.232 g; 58.1% based on consumed **1**). The cyclized ether (**58**) was further purified by preparative GC using a 3/8 in. x 10 ft aluminum column packed with 40% SE-30 on Chromosorb W 60/80 NAW.

58: IR (liq. film, NaCl, Nicolet 205) ν : 3040 (w), 2932 (s), 2870 (s), 2228 (s), 1608 (s), 1506 (m), 1459 (m), 1447 (s), 1050 (s), 1030 (s), 990 (s), 832 (s); ^1H NMR (250 MHz, CDCl_3 , Bruker) δ : 7.63 (d, 2H, 8.7 Hz), 7.45 (d, 2H, 8.7), 4.21 (dd, 1H, 3.1, 3.2 Hz), 4.07 (ddd, 1H, 8.2, 8.2, 8.1 Hz), 3.93 (ddd, 1H, 8.9, 8.2, 4.1 Hz), 2.18 (ddd, 1H, 12.2, 8.2, 4.1), 2.05-1.40 (8H), 1.22-1.01 (m, 1H); ^{13}C NMR (62.9 MHz, CDCl_3 , Bruker) δ : 151.13 (C), 132.09 (CH), 127.74 ($\text{C}^{\text{=O}}$), 118.92 (CN), 109.82 (C), 79.48 (CH), 64.91 (CH₂), 47.70 (C), 42.19 (CH₂), 33.36 (CH₂), 26.87 (CH₂), 21.93 (CH₂), 20.30 (CH₂). MS m/z : 227 (100), 226 (51.6), 183 (43.9), 168 (43.9), 154 (52.2), 143 (38.6), 142 (62.1), 140 (39.0), 116 (82.3), 115 (48.4).

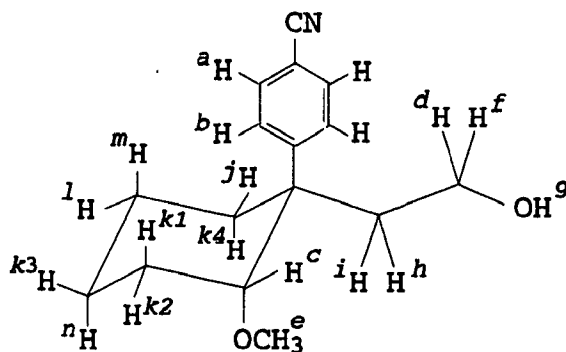
60 and **61**: Separation of **60** from **61** was not straightforward; hence the following structural assignments were based on analysis of the ^1H and ^{13}C NMR

(including HETCOR, COSY and NOSEY) spectral data collected from a mixture of **60** and **61**.

IR (PE-180), ν : 3380 (s, broad), 2925 (vs), 2785 (s), 2230 (s), 1606 (m), 1502 (m), 1445 (m), 1045 (m), 818 (m); ^1H NMR (400 MHz, CDCl_3 , Bruker) δ : 7.64-7.31 (8H, two AA'BB' systems, for each isomer), 5.90 (ddd, 1H, 3.29, 3.29, 1.07 Hz, isomer **61**), 5.53 (s, br., 1H, isomer **60**), 3.79 (dd, 2H, 6.41, 6.41 Hz, isomer **61**), 3.62 (dd, 2H, 5.45, 7.34 Hz, isomer **60**), 3.52 (m, 1H, benzyl proton of **60**), 3.48 (m, 1H, benzyl proton of **61**), 2.36 (ddd, 2H, 6.41, 6.41, coupled to the proton at 3.79 ppm and weakly coupled to the proton at 5.90 ppm, isomer **61**), 2.23-1.97 (7H), 1.84-1.46 (7H). ^{13}C NMR (250, CDCl_3 , Bruker) δ : 152.46 (s), 151.00 (s), 137.13 (s), 133.77 (s), 132.18 (d, two carbon, aromatic), 132.16 (d, two carbon, aromatic), 129.25 (d, two carbon, aromatic), 128.56 (d, two carbon, aromatic), 127.63 (d), 125.14 (d), 119.15 (s), 119.07 (s), 109.84 (s), 109.67 (s), 60.52 (t, two carbon), 44.03 (d, isomer **61**), 42.23 (d, isomer **60**), 41.00 (t, isomer **61**), 36.91 (t), 32.38 (t), 32.04 (t), 28.01 (t), 25.28 (t), 21.22 (t), 18.42 (t); MS m/z (15.45 min on GC/MS): 227 (25.0), 209 (50.0), 194 (30.4), 181 (52.2), 180 (31.1), 168 (53.4), 167 (100), 166 (61.4), 154 (80.5), 140 (29.4), 116 (53.4), 77 (24.5), 67 (26.1); MS m/z (16.01 min on GC/MS): 227 (4.7), 209 (100), 194 (14.1), 182 (45.3), 181 (28.5), 180 (53.3), 166 (28.1), 140 (21.7), 116 (45.3), 93 (16.2), 77 (18.6).

Irradiation of 2-(1-cyclohexenyl)ethanol (57) in acetonitrile-methanol solution

A solution of 0.517 g (4.1 mmol) of the ethanol (**57**), 0.324 g (2.1 mmol) biphenyl (**13**), and 0.413 g (3.2 mmol) 1,4-dicyanobenzene (**1**) in 40 ml acetonitrile was degassed with nitrogen for 5 min and irradiated through Pyrex for 10 days. GC analysis indicated that **57** was completely consumed. The volatile components of the photolysate were removed by distillation. The nonvolatile residue (1.415 g) was loaded on Dry-Column (TLC grade silica gel, 5 × 6 cm) by pre-adsorption and the column was eluted with hexane first (**13** was separated), and then dichloromethane (**1** (126 mg) was separated). Finally, the column was eluted with dichloromethane-acetone gradient. The photo-NOCAS product (**62**) came out as an oil (0.451 g; 71% based on consumed **1**). The combined yield for the ethers is 57% based on **57**. Also, 43 mg of **58**, **60**, and **61** was isolated.



62: Analysis of the ^1H and ^{13}C NMR, including HETCOR, COSY and NOSEY spectra, leads to the assignments as shown above. The NOSEY spectrum shows NOE effects both at $\delta = 3.52$ (corresponding to H^c) and at $\delta = 1.73\text{-}1.59$ (corresponding to one or more of the four protons marked with H^{k1} , H^{k2} , H^{k3} , H^{k4} , respectively) when the proton H^b is irradiated. If the aromatic ring were in the equatorial position, it

would be unlike to show the NOE effects at the same time for protons on the two side of the cyclohexane ring (marked with H^c and H^{k4}). On the contrary, if the aromatic ring is in the axial position, it is very likely that the protons, H^c and H^{k1}, at the same side of the cyclohexane ring show NOE effects.

IR (PE-180, neat film), ν : 3400 (s, broad), 2970 (vs), 2930 (m), 2220 (s), 1604 (m), 1502 (m), 1450 (m), 1085 (vs), 1040 (m), 875 (m), 805 (m), 715 (s); ¹H NMR (400 MHz, CDCl₃, Bruker) δ : a: 7.56 (d, 2H, 8.6 Hz), b: 7.41 (d, 2H, 8.6), c: 3.52 (dd, 1H, 5.8, 5.1 Hz), d: 3.27 (ddd, 1H, 12.0, 6.8, 6.6 Hz), e: 3.26 (s, 3H, OCH₃), f: 3.16 (ddd, 1H, 12.0, 6.7, 6.6 Hz), g: 2.74 (s, br., 1H, OH), h: 2.18 (ddd, 1H, 13.6, 6.8, 6.7 Hz), i: 1.85 (ddd, 13.6, 6.6, 6.6 Hz), j: 1.75 (ddd, 1H, 13.3, 7.1, 3.5), k: 1.73-1.59 (4H), l: 1.47 (m, 1H), m: 1.32 (m, 1H), n: 1.21 (m, 1H). (62.9 MHz, CDCl₃, Bruker) δ : 151.85 (s), 131.98 (d, two carbons), 127.75 (d, two carbons), 118.97 (s), 109.51 (s), 82.14 (d), 58.74 (t), 56.30 (q), 46.14 (s), 38.35 (t), 35.73 (t), 24.55 (t), 22.62 (t), 21.37 (t). MS *m/z*: 259 (12.7), 244 (2.5), 241 (1.3), 229 (25.4), 227 (11.9), 209 (33.7), 181 (76.7), 180 (38.3), 166 (26), 154 (40.9), 142 (24.9), 116.0 (50.8), 115 (25), 71 (100), 58 (25.4).

63-trans (*anti*-Markovnikov):

¹H NMR (250 MHz, CDCl₃, Bruker) δ : 3.70-3.49 (m, 2H, coupled to the protons at δ = ca. 1.7 and 1.5), 3.37 (s, 3H), 2.74 (ddd, 1H, 9.5, 9.5, 4.0 Hz, coupled to the protons at δ = 2.08, ca. 1.4 and 1.1), 2.50 (broad, 1H), 2.08 (m, 1H, 12.3 Hz, coupled to the protons at δ = 2.74, ca. 1.75 and 1.1), 1.79-0.95 (10H); ¹³C NMR (62.9 MHz, CDCl₃, Bruker) δ : 84.39 (CH), 61.73 (CH₂), 55.86 (OCH₃), 41.70

(CH), 37.73 (CH₂) 32.72 (CH₂), 30.29 (CH₂), 25.59 (CH₂), 24.52 (CH₂). MS *m/z*: 158 (0.4), 143 (13.0), 125 (23.8), 85 (23.8), 82 (24.1), 79 (20.7), 71 (100), 67 (40.9), 58 (24.1), 55 (26.0).

63-cis (*anti*-Markovnikov):

¹H NMR (400 MHz, CDCl₃, Bruker) δ : 3.78-3.58 (m, 2H, coupled to the protons at $\delta =$ ca. 1.7 and 1.5), 3.33 (s, 3H), 3.33 (m, 1H, coupled to the protons at $\delta =$ ca. 1.85 and 1.4), 3.11 (br., 1H), 1.82-1.0 (11H). MS *m/z*: 158 (0.4), 143 (13.0), 125 (23.8), 85 (23.8), 82 (24.1), 79 (20.7), 71 (100), 67 (40.9), 58 (24.1), 55 (26.0).

Chapter 7

The Photo-NOCAS Reaction:

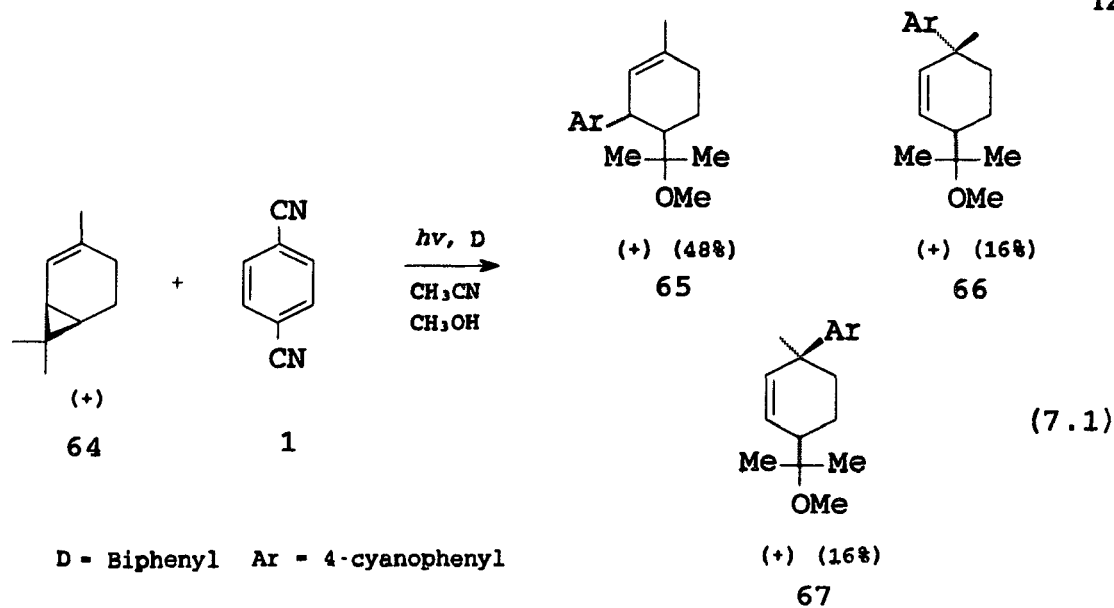
Methanol - 2-Carene, 1,4-Dicyanobenzene

The unique nature of the radical cations of vinylcyclobutane derivatives, α - and β -pinene (14, 15), has prompted us to extend our study of the photo-NOCAS reaction to the vinylcyclopropane system. The first vinylcyclopropane derivative we studied was 2-carene (64), one of the natural occurring chiral compounds that has been often used as a test for reaction mechanisms. Our investigation of the photo-NOCAS reaction with 64 will be presented in this chapter.

Results and Discussion

When a solution of 1,4-dicyanobenzene (1), biphenyl (13), and (+) 2-carene (64) in acetonitrile-methanol (3:1) was irradiated at 10 °C through a Pyrex filter with a medium-pressure mercury vapour lamp, the 1:1:1 (methanol:olefin:aromatic) adducts: *trans*-3-(4-cyanophenyl)-4-(1-methoxy-1-methylethyl)-1-methylcyclohexene (65), and *cis*- (66) and *trans*- (67) 3-(4-cyanophenyl)-6-(1-methoxy-1-methylethyl)-3-methylcyclohexene were isolated from the photolysate mixture (Equation 7.1). The product ratio for 65:66:67 is 2.9:1.0:1.0. The combined yield of the isolated products was over 80%.

The structural assignments for these three products were based on an analysis of the ^1H and ^{13}C NMR spectra. The spectra for the two *cis/trans* isomers are very similar. In the proton spectrum, the axial-H5 of the isomer assigned the *cis*



configuration (**66**) resonances at higher frequency (0.94 ppm) compared to the axial-H5 (1.58 ppm) of the other isomer, due to the shielding effect of the aromatic ring that is in the axial position of the cyclohexene. Therefore, the other isomer was assigned to the *trans* configuration (**67**). Analysis of the ^{13}C NMR spectra of the two isomers provides additional support for this assignment. In the ^{13}C NMR spectrum of the *cis* isomer, the half width of one of the lines of the quartet corresponding to the methyl group at $\delta = 30.31$ is narrow (8.2 Hz), which results from several small $^3J_{\text{C-H}}$ couplings. The ^{13}C NMR spectrum of the *trans* isomer displays a quartet at $\delta = 26.62$ with each line having a half width of 13.5 Hz, which suggests an axial-axial coupling of the methyl carbon to the axial-H4 (at ca. 1.68 ppm) plus several other small $^3J_{\text{C-H}}$ couplings.¹²⁶

Distribution of the charge and spin in the radical cation of 2-carene (64)

The oxidation potential of 2-carene is 1.39 V. Using the Rehm-Weller equation,¹⁷ the calculated free-energy change, for electron transfer to the excited singlet state of **1** from 2-carene is -118.4 kJ/mol (28.3 kcal/mole).

Considering that the ionization potentials of 2,3-dimethyl-2-butene and 1,1,2,3-tetramethylcyclopropane must be very close,[1] the charge and spin densities in the radical cation of **64** are expected to be delocalized. Experimental evidence pointing to this conclusion is found in the CIDNP studies on the radical cation of *cis*- and *trans*-diphenylcyclopropane (**68**). The CIDNP experiments indicated that $\text{68}^{+\bullet}$, generated by the reactions of excited-singlet¹²⁷ or excited-triplet¹²⁸ electron accepting photosensitizers with **68** in polar solvents, has a fully delocalized structure with positive spin densities not only in the *ortho* and *para* positions but also in the benzylic position. However, *ab initio* calculations at the STO-3G level on the radical cation of 2-carene gave a relatively localized structure (Structure **69** in Figure 7.1).

Table 7.1 and Figure 7.1 show the calculated charge and spin distributions and bond lengths for Structure **69**. Clearly, the charge and spin densities are mainly localized within the π system, and so the bond lengths of the cyclopropane ring do not change much, compared to those in the fully optimized structure (Structure **70** in Figure 7.2) for the neutral molecule of **64**. Also included for comparison are the analogous calculations on the 2,2-dimethyl-1-vinylcyclopropane (**71**) and 2,2-dimethyl-1-(2,2-dimethylvinyl)cyclopropane (**72**) systems. The calculated results are illustrated

[1] The ionization potentials of 2,3-dimethyl-2-butene and 1,1,2,3-trimethylcyclopropane are 8.68 and 8.90 eV respectively.

Rosenstock, H. M.; Draxl, K.; Steiner, B. W.; Herron, J. T. *J. Phys. Ref. Data* 1977, 6, Suppl. 1.

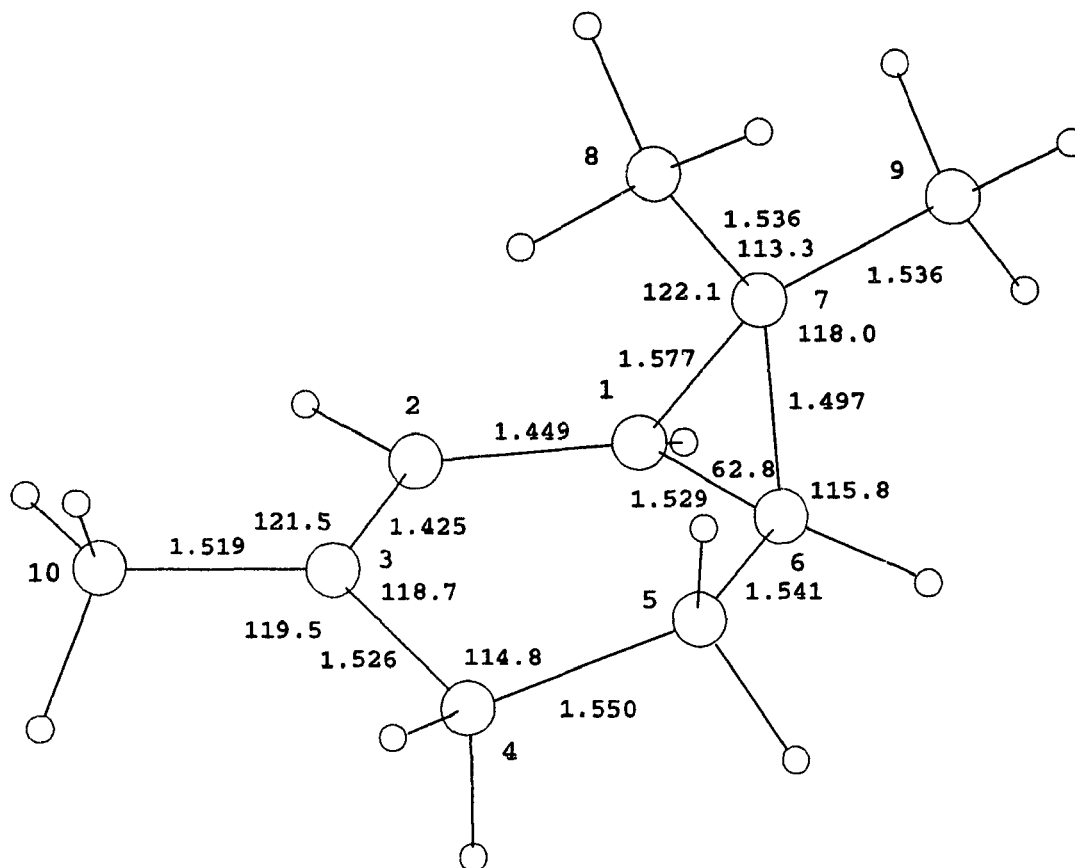


Figure 7.1 Structure **69**: the fully optimized structure for the radical cation of 2-carene ($64^{+\bullet}$).

in Figures 7.3, 7.4 and 7.5. In marked contrast to the calculated structure for the radical cation of 2-carene (Structure **69** in Figure 7.1), these two calculated radical cations have delocalized structures ($71^{+\bullet}$, $72^{+\bullet}$ in Figures 7.3a, 7.3b, 7.4a and 7.4b). The distance between C1 and C2 is quite long compared to the neutral molecule (**71**, in Figure 7.5).

Apparently, this difference can be ascribed principally to the relative position of the double bond to the cyclopropane ring. In the two simple vinylcyclopropane systems, the vinyl group can rotate freely to find the optimum position for interaction

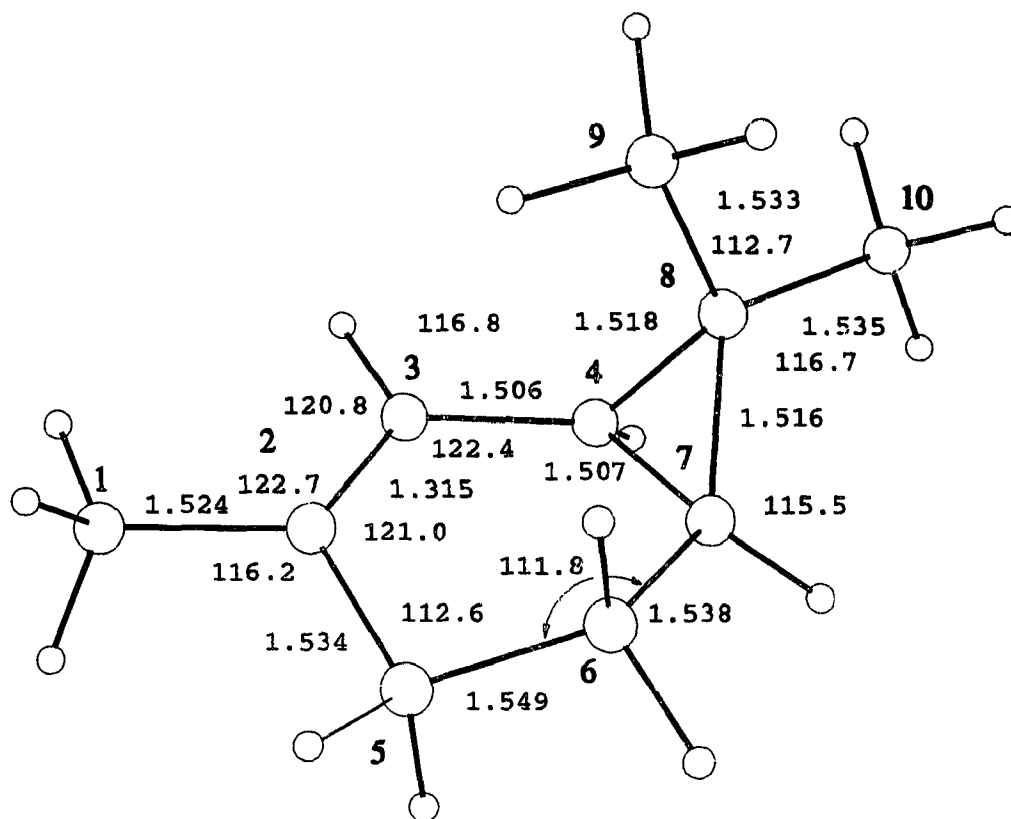


Figure 7.2. Structure 70: the fully optimized structure for 2-carene (64) (RHF/STO-3G)

with the cyclopropane ring. The dihedral angles of C5-C4-C1-C3 and C5-C4-C1-C2 in **71⁺** are about 180° and 125°, respectively; the same holds true with the case of **72⁺**. Since the Walsh model for the cyclopropane indicates that significant electron density is concentrated outside the triangle defined by the internuclear lines, the dihedral angle of C5-C4-C2-C1 (120°) is optimum for C1-C2 bond to overlap with the single occupied π orbital. On the other hand, in 2-carene, the vinyl group is locked in the bicyclic system in the unfavoured position; the dihedral angle of C3-C2-

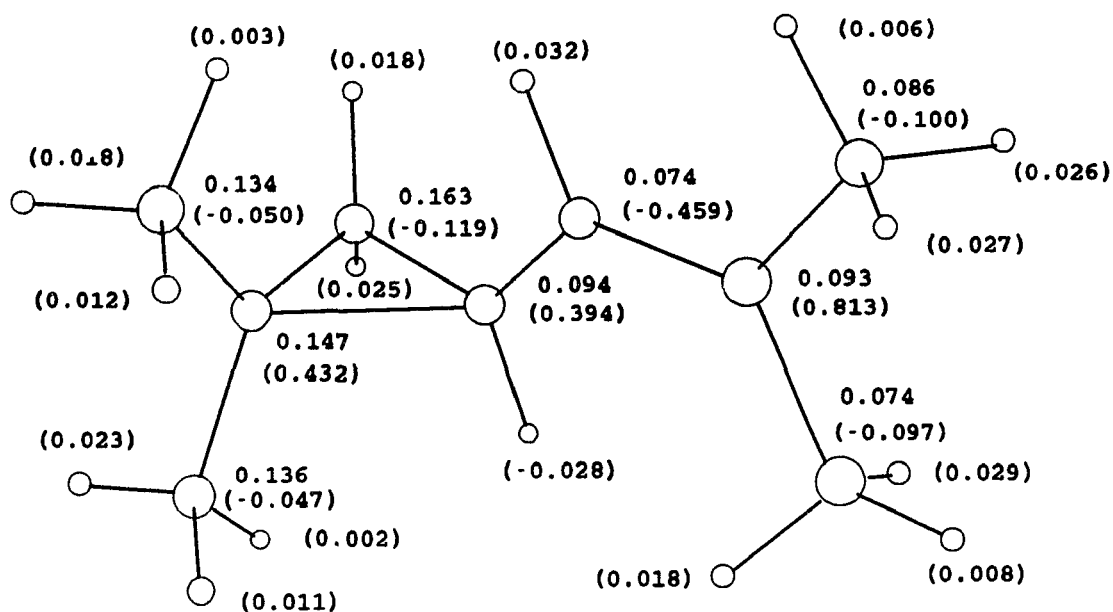


Figure 7.4b The spin and charge densities on the radical cation 72^{2+}

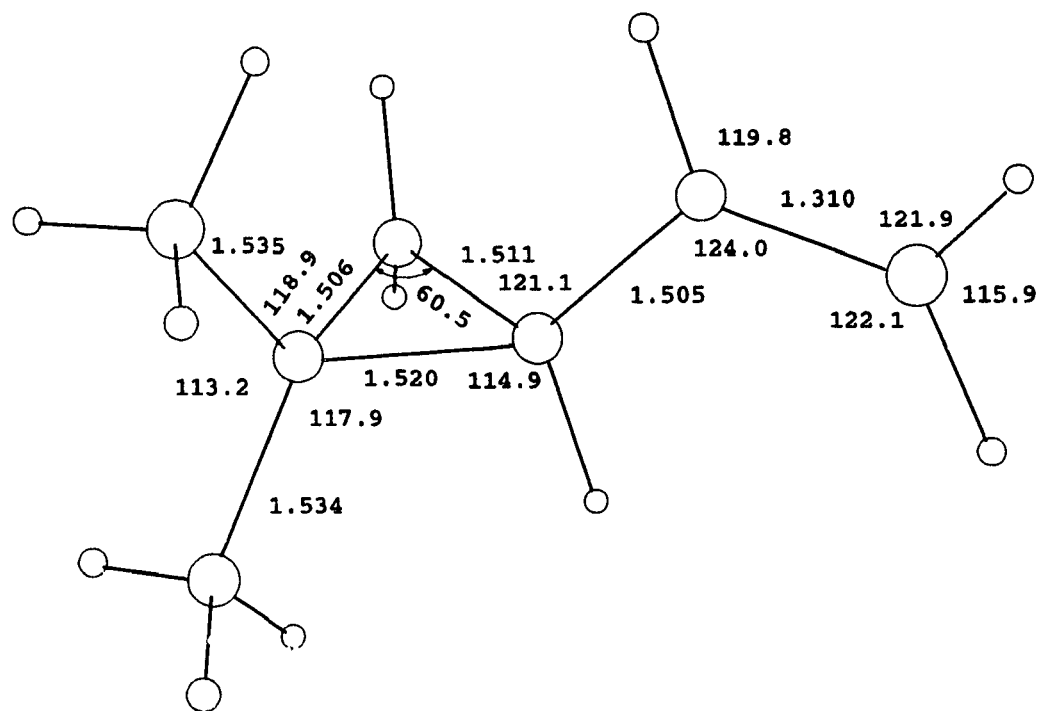


Figure 7.5. The fully optimized structure for 2,2-dimethyl-1-vinylcyclopropane (71) (RHF/STO-3G)

Table 7.1 The calculated charge and spin distributions for the radical cation of 2-carene (Structure 69)

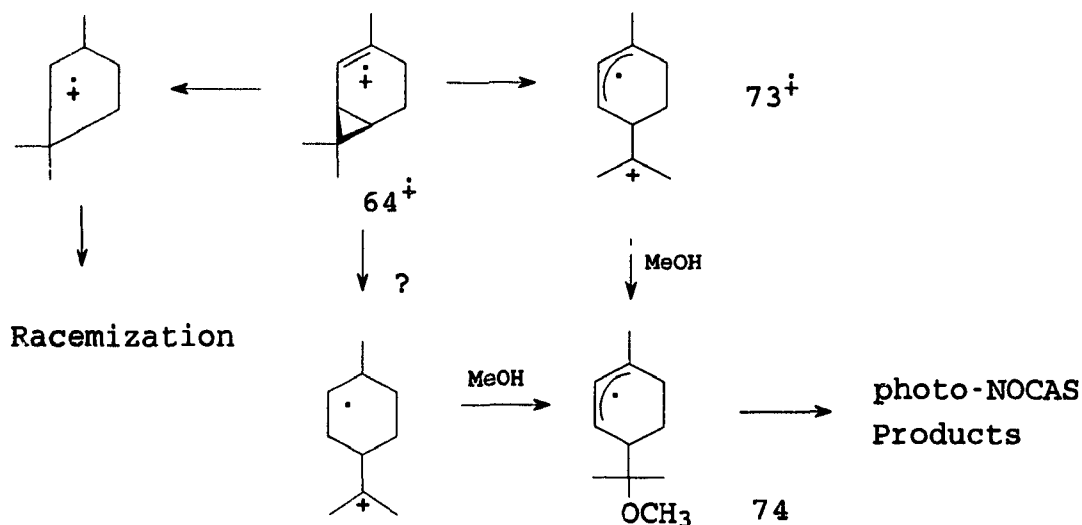
No. ^a	Group	Atomic Charges	Spins			
			Carbon	Hydrogen(s)		
1	CH	0.003	-0.042	0.011		
2	CH	0.229	0.402	-0.027		
3	C	0.158	0.564			
4	CH ₂	0.104	-0.066	0.025	0.010	
5	CH ₂	0.089	0.014	0.000	0.001	
6	CH	0.059	0.005	0.004		
7	C	0.067	0.126			
8	CH ₃	0.058	-0.006	0.003	0.002	-0.001
9	CH ₃	0.081	-0.010	0.006	0.001	0.001
10	CH ₃	0.151	-0.069	0.004	0.021	0.022

^aNumbering of carbon atoms in Figure 7.1.

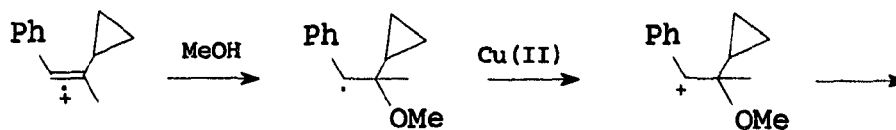
The cleavage process of the radical cation of 2-carene (64^{•+})

The specific rotation of the isolated unreacted 2-carene (**64**) did not change when the reaction was carried out in acetonitrile-methanol solution. Therefore, cleavage of C1-C7 bond of the radical cation of **64** must be faster than cleavage of C1-C6 bond which would result in racemization of the starting material (**64**). Indeed, cleavage of C1-C7 bond is a rapid process; there is no evidence for the formation of products as an result of methanol attack on the initially formed radical cation from **64**. Reaction of the resulting distonic radical cation (**73^{•+}**) with methanol would be rapid, leading to the allylic radical (**74**) (Scheme 7.1).

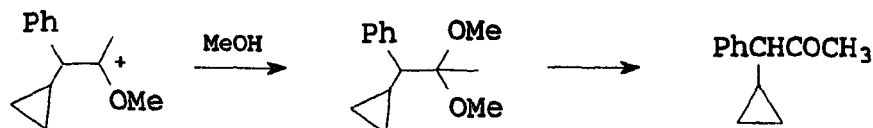
Scheme 7.1



The two geminal methyl groups are crucial to the opening of the cyclopropane ring. This can be exemplified by the PET reactions of the styrylcyclopropane derivatives without two geminal methyl groups in MeCN-MeOH solvent system.^{129,130} In all cases, the major products were derived from the attack of methanol on the double bond, and the cyclopropane ring remained intact. For example, irradiation of

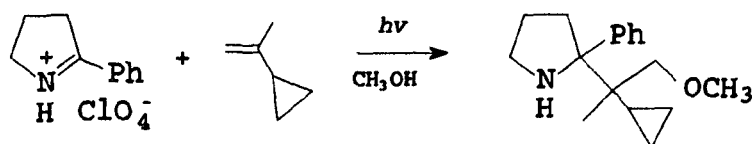


(7.2)



styrylcyclopropane in methanol solution using the 9,10-dicyanoanthracene, Cu(II) sensitizer system results in formation of a rearranged benzyl ketone as the major product (Equation 7.2).¹³⁰ The mechanism of this reaction is proposed to involve nucleophilic attack on the radical cation, followed by oxidation of the resulting radical, migration of a cyclopropyl group, and addition of methanol to the rearranged carbocation.

Another example is depicted in Equation 7.3 in that the radical cation of isopropenylcyclopropane does not undergo ring-opening. Singlet excited 2-phenyl-1-pyrrolinium perchlorate is a good electron acceptor ($E_{1/2}^{ox} = -1.0$ V and $E_{0,0} = 3.9$ V).⁵⁹

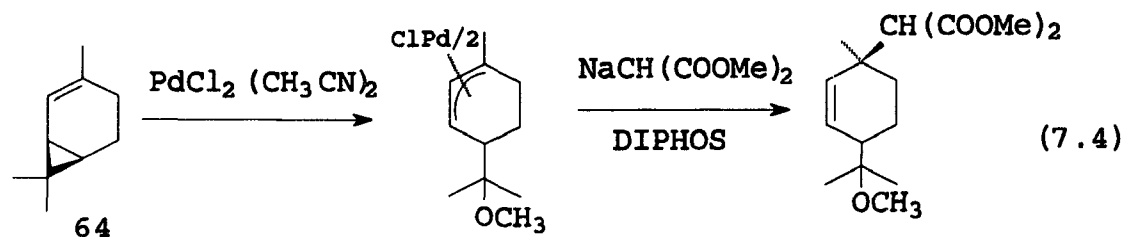


(7.3)

Cleavage of radical cations occurs selectively to give the carbocation of the fragment radical with the lower oxidation potential. As noted in Chapter 3, the

oxidation potential of an allylic radical of this kind is believed to be higher than the oxidation potential of the tertiary radical; this expectation is in agreement with the fact that the methoxy group is bonded to the tertiary carbon in all three photo-NOCAS products.

The allylic radical could couple with the radical anion of **1** at both ambident ends and from both sides of the ring, leading to four isomers. In fact, only three isomers were formed as major products, which indicates that the side of the ring *cis* to the side chain group is quite sterically hindered. A similar stereoselectivity was observed in the palladium-induced reaction of 2-carene (Equation 7.4).¹³¹



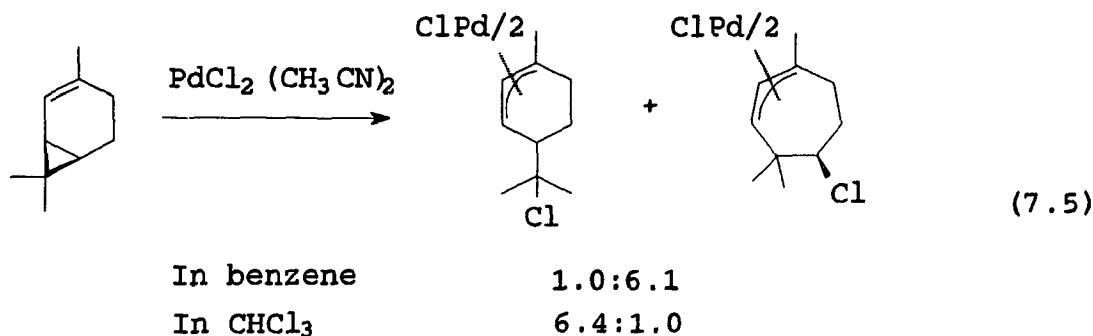
DIPHOS = 1,2-Bis(diphenylphosphino)ethane

As in the case of the pinene system, the reduction potential of the intermediate allylic radical (**74**) must be more negative than that of **1**, otherwise the radical anion of **1** would reduce the allylic radical **74** that would then be protonated. In the present case, the allylic radical **74** has a reduction potential even more negative than that of the allylic radical **30** derived from the α -pinene radical cation. The photo-NOCAS reaction with 2-carene is very clean (i.e., good material balance), and no methanol addition products were observed.

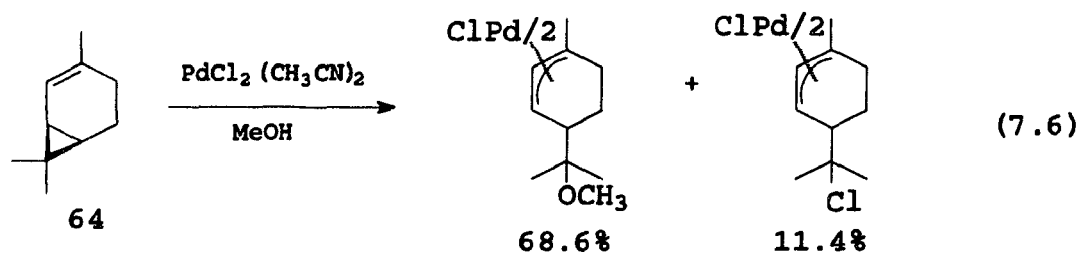
All three products are chiral. This is consistent with the mechanism discussed above. The configuration of C5 (*S*) in **64** should be intact.

So far, the mechanism for the reaction seems quite clear and consistent with that proposed for the case of the pinene system (Chapter 3). However, some differences are worth pointing out. In the case of the pinene system, the distonic radical cation leads to not only the photo-NOCAS products but the imines. In the case of 2-carene (**64**), even when methanol was omitted, the prolonged irradiation of a solution of **1**, **13** and **54** in acetonitrile led to no products as monitored by GC/FID and GC/MS. However, under these conditions the optical rotation of the isolated unreacted 2-carene decreased.

The partial racemization of the 2-carene suggests that the C1-C6 bond (the fused bond) of the radical cation of **64** is weakened; the seven-membered ring might be observed. Selective cleavage of C1-C6 and C1-C7 (outside) carbon-carbon bonds has been reported in the palladium(II)-induced ring opening of the cyclopropane in 2-carene (Equation 7.5).^{131a} In a nonpolar solvent, benzene, a secondary cationic center is developed, resulting in a seven-membered ring product. On the other hand, when



the reaction was carried out in chloroform, a more polar solvent, the six-membered ring product becomes predominant; moreover, no seven-membered ring product was detected when methanol was employed as solvent (Equation 7.6). This profound effect of methanol is consistent with our observation. When the reaction was carried out in



the presence of methanol, we did not find any evidence for the formation of the seven membered-ring product(s), and the optical rotation of the isolated unreacted **64** remained the same as before irradiation (Equation 7.1 and Table 7.2).

Table 7.2 The specific rotations of 2-carene before and after irradiation.

sample No	Sample 1	Sample 2	Sample 3
$[\alpha]_D^{20}$ (CHCl ₃)	97.1	97.7	48.9

sample 1. 2-carene obtained from Aldrich (97%).

sample 2. 2-carene isolated after irradiation under the photo-NOCAS reaction conditions (acetonitrile-methanol).

sample 3. 2-carene isolated after irradiation under the same condition as above but methanol was not used.

As discussed in Chapter 4, many studies have indicated that the radical cations of some cyclopropane derivatives have a relative stable ring-closed structure which undergoes nucleophilic ring-opening. Especially, the phenylcyclopropane system has been systematically examined (Equation 4.4).¹⁰⁹ Because the chiral center is crucial in the examination, substrates with the geminal dimethyl group on the three-membered ring, as in 2-carene, were not included in the previous study.

At this stage, whether the radical cation of **64** undergoes *complete* ring cleavage before attack of methanol is unknown. The photo-NOCAS products incorporating methanol are formed in high yield and no 1:1:1 adduct incorporating cyano group (analogous to **35** in the case of tricyclene (**33**)) was detected. These facts suggest a rapid ring-opening process, leading to the distonic radical cation (**73⁺**). However, the failure to locate a stationary point at the STO-3G level for the ring-opened structure of the radical cation (**71⁺**) (see the detailed description of the calculation later) and the lack of formation of the acetonitrile addition product (like in the case of the pinene system) suggest that C1-C7 bond in the radical cation of **64** might be still weakly associated when methanol attacks. This weak interaction might slow down the reaction to form the acetonitrile addition product, but not the attack of methanol. The fact that the fourth isomer formed upon coupling of the allylic radical (**74**) with the radical anion from the same side as the side chain group of **74** was not observed is also consistent with methanol addition occurs before the three-membered ring cleaves completely. It should be pointed out that locating a stationary point for the distonic radical cation (**73⁺**) could be achieved. In **71⁺** and **72⁺** the allylic moiety maintains the planar structure while at the same time interacting with the tertiary carbon (see Figures 7.3 and 7.4). On the other hand, it is unlikely that in the distonic radical cation **73⁺** the allylic moiety can maintain planar while at the same time interacting with the tertiary carbon, due to the geometrical restrictions as we have discussed earlier.

It is interesting to note the different behaviour of the radical cation of **64** from the tricyclene radical cation. The ring-opening of the tricyclene radical cation involves

nucleophilic assistance, hence significant amount of the cyano substituted compound (35) was also obtained (Equation 4.2). In the present case, the ring-opening of 64⁺ is driven by better solvation. The ring-opened structure of radical cation of 64 can acquire better solvation than its ring-closed structure and much more effective solvation than the ring-opened structure of the tricyclene radical cation. If the ring-opened structure of the radical cation of tricyclene could be formed, the bicyclic system and the two geminal methyl groups near the carbocation centre would create very large steric hindrance for solvation.

The effects of the co-donor, biphenyl

When the reaction was carried out in the absence of biphenyl, the reaction was much less efficient. While the ratio of the three identified photo-NOCAS products remains essentially the same, the amount of other minor products relatively increased.

Ab Initio Calculations

All calculations were carried out at the STO-3G level. Table 7.3 lists the calculated (STO-3G) total energies for the neutral alkenes 71 and 72 and for the alkene radical cations.

Calculation on the radical cation of 2-carene

To obtain the optimized structure, first, the π -system was constrained to a plane and the C-H bond distances and the CH₃ groups were not optimized. Optimization under these conditions converged (HF=-383.16528 a.u.). Following this, further

Table 7.3 The calculated (STO-3G) total energies (a.u.) for the neutral alkenes and for the alkene radical cations

Structure 69 (for the radical cation of 2-carene)	-383.16935
Structure 70 (for 2-carene)	-383.37277
2,2-Dimethyl-1-vinylcyclopropane (71)	-268.76981
71⁺	-268.56440
Radical cation of 2,2-Dimethyl-1-(2,2-dimethylvinyl)cyclopropane (72⁺)	-345.74148

optimization was carried out only with the π system fixed in a plan. Then, a full optimization was carried out based on the previous optimization result. Finally, the frequency calculation showed that the stationary point was a minimum (Structure **69**).

Calculation on the radical cation of 2,2-dimethyl-1-vinylcyclopropane

When the AM1 method was used, the ring-closed structure of the radical cation of 2,2-dimethyl-1-vinylcyclopropane could not be located (for this calculation, the fully optimized structure (**77**) for the neutral molecule obtained by AM1 was used as the initial input), instead, a ring-opened structure was obtained (**78⁺**). However, when this ring-opened structure (**78⁺**) was used as the initial input for the STO-3G calculation, the ring-closed structure (**71⁺**) was obtained. Another STO-3G calculation, starting with a initial structure (**77**) obtained from AM1 calculation for the neutral molecule, gave the same stationary point as **71⁺**. Therefore, using the

STO-3G method, only the ring-closed structure (**71**⁺) was found; on the other hand, the AM1 calculation gave a ring-opened structure only (**78**⁺).

Calculations on neutral molecule **71** were also performed (Figure 7.5).

Frequency calculations on the stationary points, **71** and **71**⁺ showed they are indeed minima.

Calculation on the radical cation of 2,2-dimethyl-1-(2,2-dimethylvinyl)cyclopropane

Based on the calculated result of 2,2-dimethyl-1-vinylcyclopropane system, the geometry optimization was straightforward; the stationary point was further characterized as a minimum by frequency calculation (Figure 7.4).

By comparing the two vinylcyclopropane systems (**71**, **72**), it can be seen that the two geminal methyl groups on C5 have limited effects. The charge and spin distributions on the unsaturated part increases slightly and the distance between C1 and C2 decrease slightly in going from **71**⁺ to **72**⁺.

Experimental

For general methods and Cyclic voltammetric measurements, see Chapter 3.

Formation of adducts (65, 66, and 67) from 2-carene

A solution of 2.18 g (16 mmol) 2-carene (**64**), 1.31 g (8.5 mmol) biphenyl (**13**), and 1.03 g (8 mmol) 1,4-dicyanobenzene (**1**) in 160 ml acetonitrile-methanol (3:1) was degassed with nitrogen for 5 min. and irradiated through Pyrex for 140 h. The volatile components of the photolysate was removed by distillation, including **64**.

Since DCB dissolves only slightly in 10% ethyl acetate in hexane, the nonvolatile residue was treated with 10% ethyl acetate in hexane and 100 mg DCB was separated out. The solution was loaded on Dry-Column (5 × 6 cm) and the column was eluted with ethyl acetate-hexane gradient. Most of 13 (91%) was recovered. The photo-NOCAS products came out as an oil (1.57 g), which accounts for 80% of consumed 1. The isomers of adducts were separated by MPLC using two different solvent systems, 6% ethyl acetate in toluene and 6% ethyl acetate in hexane.

trans-3-(4-cyanophenyl)-4-(1-methoxy-1-methylethyl)-1-methylcyclohexene (**65**); ¹H NMR (361 MHz, CDCl₃, Nicolet) δ: 7.54 (d, 2H, J=8.4 Hz), 7.29 (d, 2H, J=8.4 Hz), 5.13 (s, br, 1H, coupled to the proton at 3.46 ppm), 3.46 (m, 1H, w_{1/2}=16 Hz, coupled to the proton at 1.95 ppm), 2.82 (s, 3H), 2.12-2.07 (m, 1H), 2.03 (dd, 1H, J=4.8, 0.5 Hz), 1.95 (ddd, 1H, J=3.6, 7.7, 10.3 Hz), 1.83 (dddd, 1H, J=3.6, 4.9, 4.8, 13.3 Hz), 1.70 (s, br, 3H), 1.49 (dddd, 1H, J=5.2, 9.9, 10.3, 13.3 Hz), 1.11 (s, 3H), 1.01 (s, 3H); ¹³C NMR (90.79 MHz, CDCl₃) δ: 154.23 (s), 134.67 (s), 131.78 (d, 160.5), 129.17 (d, 158.5), 124.53 (d, 155.5), 119.26 (s), 109.03 (s), 76.88 (s), 48.29 (q, 141.7), 47.38 (d, 124.0), 44.30 (d, 127.2), 29.68 (t, 126.0), 23.58 (q, 125.7), 23.44 (q, 123.1), 23.34 (q, 127.6), 23.32 (t, 123.7); MS *m/z*: 254 (0.2), 237(14.5), 222(9.8), 209(7.2), 194(13.9), 169(7.0), 154(19.3), 73(100). Anal. calcd. for 4, C₁₈H₂₃NO: C 80.25, H 8.61, N 5.20; found: C 80.45, H 8.69, N 5.17. [α]_D = -240.0° (c 1%, CHCl₃).

3-cis-(4-cyanophenyl)-6-(1-methoxy-1-methylethyl)-3-methylcyclohexene (**66**); IR (liq. film, NaCl, Nicolet 205) ν : 3016 (w), 2979 (s), 2937 (s) 2827 (m), 2228 (s), 1606 (s), 1504 (m), 1381 (m), 1366 (m) 1148 (m), 1072 (s) 836 (m); ^1H NMR (361 MHz, CDCl_3) δ : 7.58 (d, 2H, $J=8.6$ Hz), 7.47 (d, 2H, $J=8.6$ Hz), 5.98 (ddd, 1H, $J=1.4, 2.2, 10.2$ Hz). 5.74 (ddd, 1H, $J=1.8, 2.5, 10.2$ Hz). 3.21 (s, 3H), 2.38 (dddd, 1H, $J=2.2, 2.5, 5.6, 11.1$ Hz), 2.01 (dddd, 1H, $J=1.4, 1.9, 3.2, 13.3$ Hz), 1.71 (ddd, 1H, $J=2.7, 13.0, 13.3$ Hz), 1.51 (dddd, 1H, $J=1.8, 1.9, 2.7, 5.6, 12.5$ Hz), 1.36 (s, 3H), 1.07 (s, 3H), 1.06 (s, 3H), 0.94 (dddd, 1H, $J=3.2, 11.1, 12.5, 13.0$ Hz); ^{13}C NMR (90.78 MHz, CDCl_3) δ : 154.89 (s), 134.49 (d, 155.3), 131.75 (d, 165.2), 129.54 (d, 150.5), 127.78 (d, 160.8), 119.13 (s), 109.41 (s), 76.82 (s), 48.86 (q, 140.3), 44.02 (d, 124.8), 40.16 (s), 38.71 (t, 129.1), 30.31 (q, 127.9, $w_{1/2}=8.2$ Hz), 22.31 (q, 125.0), 22.03 (q, 125.2), 20.93 (t, 127.4); MS m/z : 254 (0.2), 237(1.5), 222(1.9), 194(1.4), 140(.6), 73(100). Anal. calcd. for **5**, $\text{C}_{18}\text{H}_{23}\text{NO}$: C 80.25, H 8.61, N 5.20; found: C 80.59, H 8.73, N 5.10. $[\alpha]_D=-47.9^\circ$ (c 1%, CHCl_3).

trans-3-(4-cyanophenyl)-6-(1-methoxy-1-methylethyl)3-methylcyclohexene (**67**); ^1H NMR (361 MHz, CDCl_3) δ : 7.58 (d, 2H, $J=8.6$ Hz), 7.46 (d, 2H, $J=8.6$ Hz), 5.89 (ddd, 1H, $J=0.7, 2.2, 10.3$ ppm), 5.74 (ddd, 1H, $J=1.6, 2.7, 10.3$ Hz), 3.23 (s, 3H), 2.37 (dddd, 1H, $J=2.2, 5.7, 11.0$ Hz), 1.83 (m, 1H, 12.6, 4.4, 1.5 Hz), 1.64-1.72 (m, 2H, one of them is coupled to the proton at 2.37 ppm), 1.58 (m, 1H, coupled to the proton at 2.37 ppm), 1.41 (s, 3H), 1.16 (s, 3H), 1.15 (s, 3H); 3H), ^{13}C NMR (90.78 MHz, CDCl_3) δ : 156.12 (s), 135.27 (d, 159.6), 132.02 (d, 165.1), 128.29 (d, 151.3), 126.93 (d, 160.8), 119.13 (s), 109.44 (s), 76.87 (s), 48.92 (q,

140.2), 43.30 (d, 123.9), 39.99 (d, 127.2), 38.9 (t, 124.0), 26.62 (q, 125.6), 22.40 (q, 125.1), 22.09 (q, 125.0), 21.46 (t, 126.9). MS *m/z*: 254 (0.2), 237(3.8), 222(3.8), 194(2.7), 116(4.1), 79(4.8), 73(100). Anal. calcd. for **6**, C₁₈H₂₃NO: C 80.25, H 8.61, N 5.20; found: C 79.90, H 8.61, N 5.16. [α]_D = 89.1° (c 1%, CHCl₃).

Appendix 1

The Archive Entries of the *Ab Initio* Calculations

One of the aims of quantum molecular physics is to solve the time-independent Schrödinger equation. In the case of a molecule containing N nuclei and n electrons, the hamiltonian operator H associated with the total energy of the molecule can be written as

$$H = T_N + T_e + V_{Ne} + V_{ee} + V_{NN}$$

The Born-Oppenheimer approximation allows separation of electronic and nuclear motions. Therefore for a given nuclear configuration, we seek solutions only to the electronic Schrödinger equation

$$H_{\text{elect}} \Phi = E_{\text{elect}} \Phi$$

where $H_{\text{elect}} = T_e + V_{Ne} + V_{ee}$, and E_{elect} is the electronic energy which depends on the relative nuclear coordinates. This equation has an exact solution only when $n = 1$. In practice, Φ can be expressed in terms of Slater determinants. The individual molecular orbitals in the determinants may be expressed as linear combinations of a set of m prescribed one-electron functions known as basis functions. The individual basis functions can be, in turn, expressed in terms of contracted or uncontracted Gaussian type orbitals for rapid calculations. These lead to the Roothaan-Hall equation which has to be solved iteratively.

If only one Slater determinant is used in the above procedure, the solutions are at the Hartree-Fock level. The Hartree-Fock method is the procedure most used for numerical quantum chemical calculations. However, the calculation results suffer

from the limitations of independent-particle wave functions constructed as products of one-electron functions. Other Slater determinants (configuration interaction), or other technique, can be added to improve the accuracy of the results, but always at greater computational expense. Nevertheless, Hartree-Fock calculations can be carried out nonempirically to a high degree of accuracy if sufficient flexibility is allowed in the wave functions.

Dependent upon the flexibility allowed in different sets of basis functions, Hartree-Fock calculations have different levels such as STO-3G, STO-4G, 6-31G levels and so forth. In practice, which basis set should be chosen depends on several considerations such as, the size of the system to be studied and computer time that can be afforded. For example, a molecule, like α -pinene, tricyclene or 2-carene, contains ten carbon atoms and sixteen hydrogen atoms, and so they are considered "huge" systems. Thus, the lowest basis set level, STO-3G, has been chosen for this system and the like. Higher level basis sets can be used for smaller systems, so that the reliability of calculations could be improved; furthermore, we can study the problem in detail in a reasonably short period of time.

The optimized geometries used in this thesis are given in the following. The results of frequency calculations and like are not included.

The radical cation of biphenyl (13)

1\1\UNK-DAL\FOPT\UHF\STO-3G\C12H10(1+,2)\XYD\24-JUL-1992\1\#\N
 STO-3G OPT POP=REGULAR\the radical cation of
 biphenyl\1,2\X\X,1,1.\C,2,r1,1,90.\C,2,r1,1,90.,3,180.,0\C,3,r2,2,a1,1,b1,0\C,3,r3
 ,2,a2,5,b2,0\C,4,r4,2,a3,1,b3,0\C,4,r5,2,a4,7,b4,0\C,5,r6,3,a5,2,b5,0\C,8,r7,4,a6,2
 ,b6,0\C,6,r8,3,a7,2,b7,0\C,7,r9,4,a8,2,b8,0\C,11,r10,6,a9,3,b9,0\C,12,r11,7,a10,4,
 b10,0\H,5,r12,3,a11,2,b11,0\H,8,r13,4,a12,2,b12,0\H,6,r14,3,a13,2,b13,0\H,7,r15,4
 ,a14,2,b14,0\H,9,r16,5,a15,3,b15,0\H,10,r17,8,a16,4,b16,0\H,11,r18,6,a17,3,b17,0\
 H,12,r19,7,a18,4,b18,0\H,13,r20,11,a19,6,b19,0\H,14,r21,12,a20,7,b20,0\r1=0.71
 86\r2=1.4532\r3=1.4533\r4=1.4533\r5=1.4532\r6=1.396\r7=1.396\r8=1.3959\r9
 =1.3959\r10=1.4203\r11=1.4203\r12=1.0809\r13=1.0809\r14=1.0809\r15=1.080
 9\r16=1.0841\r17=1.0841\r18=1.0841\r19=1.0841\r20=1.0852\r21=1.0852\ a1=1
 21.4652\ a2=121.4677\ a3=121.4662\ a4=121.4666\ a5=121.0069\ a6=121.0067\ a7=
 121.0134\ a8=121.0136\ a9=120.5783\ a10=120.5781\ a11=119.935\ a12=119.9361\ a
 13=119.9324\ a14=119.9322\ a15=119.3004\ a16=119.3004\ a17=119.3078\ a18=119
 .3078\ a19=120.1181\ a20=120.1181\ b1=179.9025\ b2=180.\ b3=179.9326\ b4=180.\
 b5=180.0054\ b6=180.0054\ b7=180.0054\ b8=180.0054\ b9=-0.0109\ b10=-0.0109\
 b11=-0.0205\ b12=-0.0205\ b13=-0.0205\ b14=-0.0205\ b15=179.9867\ b16=179.986
 7\ b17=179.9867\ b18=179.9867\ b19=180.0055\ b20=180.0055\ \Version=VAX-VM
 S-G86RevC\HF=-454.4879303\S2=2.132\S2-1=0.\S2A=3.556\RMSD=0.922D-09\
 RMSF=0.322D-04\Dipole=-0.0000023,0.0000009,-0.0000098\PG=C01
 [X(C12H10)]\@

Structure 24 (α -pinene)

1\1\GINC-LINUS\FOPT\RHF\STO-3G\C10H16\XYD\13-Dec-1991\1\#\NSTO-3G
 OPT POP=REGULAR\pinene, from pmodel\0,1\C\C,1,r1\C,2,r2,1,a1\C,3,r3,2,
 a2,1,b1,0\C,1,r4,2,a3,3,b2,0\C,1,r5,2,a4,3,b3,0\C,4,r6,3,a5,2,b4,0\C,4,r7,3,a6,2,b5
 ,0\C,7,r8,4,a7,3,b6,0\C,7,r9,4,a8,3,b7,0\H,4,r10,3,a9,2,b8,0\H,8,r11,4,a10,3,b9,0\
 H,8,r12,4,a11,3,b10,0\H,5,r13,1,a12,2,b11,0\H,3,r14,2,a13,1,b12,0\H,3,r15,2,a14,1
 ,b13,0\H,2,r16,3,a15,1,b14,0\H,6,r17,1,a16,2,b15,0\H,6,r18,1,a17,2,b16,0\H,6,r19,
 1,a18,2,b17,0\H,9,r20,7,a19,4,b18,0\H,9,r21,7,a20,4,b19,0\H,9,r22,7,a21,4,b20,0\
 H,10,r23,7,a22,4,b21,0\H,10,r24,7,a23,4,b22,0\H,10,r25,7,a24,4,b23,0\r1=1.3149
 17\r2=1.529814\r3=1.548532\r4=1.536096\r5=1.521435\r6=1.567198\r7=1.5513
 15\r8=1.544602\r9=1.548758\r10=1.088857\r11=1.08599\r12=1.084238\r13=1.0
 87952\r14=1.090004\r15=1.090527\r16=1.082251\r17=1.085487\r18=1.088115\r1
 9=1.088094\r20=1.085953\r21=1.082317\r22=1.086053\r23=1.086068\r24=1.086
 146\r25=1.083242\ a1=120.449784\ a2=109.617172\ a3=116.78791\ a4=124.474955\
 a5=110.879268\ a6=107.957433\ a7=119.236006\ a8=112.096097\ a9=111.878275\ a1
 0=116.845065\ a11=113.147504\ a12=113.049641\ a13=110.239883\ a14=110.05659
 2\ a15=117.34596\ a16=110.996617\ a17=110.584309\ a18=110.651399\ a19=109.90
 9004\ a20=112.475367\ a21=109.910582\ a22=110.116755\ a23=110.04328\ a24=112

.421417\b1=-1.460453\b2=1.515378\b3=-179.208411\b4=48.043131\b5=-46.4744
 73\b6=39.972159\b7=167.101033\b8=-178.386916\b9=-34.382754\b10=-162.7248
 13\b11=178.270429\b12=120.508491\b13=-121.976725\b14=-179.199084\b15=0.0
 23407\b16=120.461828\b17=-120.463457\b18=-174.927234\b19=-54.422297\b20=
 66.384927\b21=166.771826\b22=-74.286403\b23=46.19896\\Version=Stellar-Stelli
 x-G90RevH\HF=-383.3850151\RMSD=1.235e-09\RMSF=1.661e-05\Dipole=0.004
 2824,0.0143615,-0.0555078\PG=C01 [X(C10H16)]\@

Structure 25 (the ring-closed structure for the radical cation of α -pinene)

1\1\GINC-LINUS\FOPT\UHF\STO-3G\C10H16(1+,2)\XYD\9-Sep-1991\1\1\#NSTO-
 3G OPT=READFC GEOM=CHECKPOINT GUESS=READ OPTCYC=300
 POP=REGULAR\\radical cation of α -pinene, ring closed structure\\1,2\X\C,1,r1\H,
 2,r2,1,a1\C,1,r3,2,a2,3,b1,0\C,1,r4,2,a3,3,b2,0\C,1,r5,2,a4,3,b3,0\H,4,r6,1,a5,2,b4
 ,0\C,1,r1,4,a6,7,b5,0\C,5,r7,1,a7,2,b6,0\H,6,r8,1,a8,2,b7,0\H,8,r9,1,a9,3,b8,0\H,8,
 r10,1,a10,3,b9,0\H,9,r11,5,a11,1,b10,0\H,9,r12,5,a12,13,b11,0\H,9,r13,5,a13,13,b1
 2,0\C,2,r14,1,a14,4,b13,0\C,2,r15,1,a15,4,b14,0\C,16,r16,2,a16,1,b15,0\C,16,r17,2
 ,a17,1,b16,0\H,18,r18,16,a18,2,b17,0\H,18,r19,16,a19,2,b18,0\H,18,r20,16,a20,2,b
 19,0\H,19,r21,16,a21,2,b20,0\H,19,r22,16,a22,23,b21,0\H,19,r23,16,a23,23,b22,0\
 H,17,r24,2,a24,1,b23,0\H,17,r25,2,a25,1,b24,0\\r1=0.773717\r2=1.087973\r3=1.9
 45171\r4=2.575041\r5=2.427248\r6=1.093258\r7=1.514721\r8=1.087276\r9=1.0
 91748\r10=1.092707\r11=1.0914\r12=1.085895\r13=1.091708\r14=1.56839\r15=
 1.551275\r16=1.546334\r17=1.547385\r18=1.085938\r19=1.08567\r20=1.084206\
 r21=1.085849\r22=1.083541\r23=1.086086\r24=1.084604\r25=1.087618\al=109.
 246755\aa2=129.084631\aa3=95.3683\aa4=60.432498\aa5=142.50103\aa6=46.766341\aa
 7=170.705754\aa8=169.650196\aa9=111.786442\aa10=109.603129\aa11=108.445747\
 aa12=112.067793\aa13=108.37635\aa14=112.90462\aa15=109.058531\aa16=119.86806
 8\aa17=112.262434\aa18=109.793927\aa19=109.279145\aa20=113.53576\aa21=110.04
 2272\aa22=112.350075\aa23=109.145606\aa24=113.440755\aa25=117.631454\b1=181
 .097283\b2=181.026923\b3=181.486054\b4=180.445383\b5=-0.74498\b6=181.521
 347\b7=6.864581\b8=59.123131\b9=-59.298366\b10=121.399284\b11=-121.85689
 9\b12=116.473205\b13=47.978112\b14=-48.198739\b15=36.186798\b16=165.052
 66\b17=-172.321541\b18=69.399554\b19=-51.160221\b20=166.486029\b21=-121.
 079984\b22=118.740605\b23=-160.774924\b24=-31.477475\\Version=Stellar-Stelli
 x-G90RevH\HF=-383.1828449\S2=0.757\S2-1=0.\S2A=0.75\RMSD=1.500e-09\R
 MSF=2.459e-06\Dipole=-0.9380314,0.5910278,-1.3479534\PG=C01
 [X(C10H16)]\@

Structure 26 (the ring-opened structure for the radical cation of α -pinene)

1\1\GINC-LINUS\FOPT\UHF\STO-3G\C10H16(1+,2)\XYD\3-Sep-1991\1\1\#NSTO-
 3G OPT=READFC GEOM=CHECKPOINT GUESS=READ OPTCYC=300 POP
 =REGULAR\\ring-opened radical cation of pinene, more stable conformation\\1,2\
 C\C,1,r1\C,1,r2,2,a1\C,1,r3,2,a2,3,b1,0\C,2,r4,1,a3,4,b2,0\C,3,r5,1,a4,4,b3,0\C,5,

r6,2,a5,1,b4,0\C,7,r7,5,a6,6,b5,0\C,8,r8,7,a7,6,b6,0\C,8,r9,7,a8,6,b7,0\H,3,r10,1,a
 9,4,b8,0\H,2,r11,1,a10,4,b9,0\H,4,r12,1,a11,2,b10,0\H,4,r13,1,a12,13,b11,0\H,4,r1
 4,1,a13,13,b12,0\H,5,r15,2,a14,1,b13,0\H,5,r16,2,a15,1,b14,0\H,6,r17,3,a16,1,b15,
 0\H,6,r18,3,a17,1,b16,0\H,9,r19,8,a18,10,b17,0\H,9,r20,8,a19,10,b18,0\H,9,r21,8,a
 20,10,b19,0\H,10,r22,8,a21,9,b20,0\H,10,r23,8,a22,9,b21,0\H,10,r24,8,a23,9,b22,0
 \H,7,r25,8,a24,9,b23,0\|r1=1.410587\r2=1.410399\r3=1.528638\r4=1.522427\r5=
 1.522449\r6=1.564933\r7=1.515823\r8=1.514231\r9=1.512561\r10=1.082611\r11
 =1.08262\r12=1.088346\r13=1.085733\r14=1.085659\r15=1.089539\r16=1.09084
 7\r17=1.089541\r18=1.090848\r19=1.085875\r20=1.092925\r21=1.092928\r22=1
 .093072\r23=1.093072\r24=1.084524\r25=1.089177\|a1=120.247529\|a2=119.8443
 61\|a3=122.076012\|a4=122.076567\|a5=109.118018\|a6=110.460493\|a7=119.14994\
 a8=122.439627\|a9=121.098341\|a10=121.094014\|a11=110.511538\|a12=110.69050
 1\|a13=110.696606\|a14=110.169711\|a15=110.477133\|a16=110.169412\|a17=110.4
 77674\|a18=112.426159\|a19=107.881334\|a20=107.876527\|a21=107.671985\|a22=1
 07.670388\|a23=113.014439\|a24=107.899091\|b1=181.54818\|b2=180.732141\|b3=1
 79.270282\|b4=28.678866\|b5=-122.148922\|b6=119.046818\|b7=-60.949514\|b8=-2.
 742607\|b9=2.743065\|b10=88.404863\|b11=-119.734505\|b12=119.758593\|b13=149
 .10237\|b14=-91.940629\|b15=-149.109355\|b16=91.932699\|b17=-0.012762\|b18=-1
 22.254191\|b19=122.223316\|b20=57.639667\|b21=-57.633988\|b22=180.003359\|b23
 =-0.01828\|Version=Stellar-Stellix-G90RevH\HF=-383.1663277\|S2=1.101\|S2-1=0
 .\|S2A=0.774\|RMSD=9.385e-10\|RMSF=2.771e-06\|Dipole=2.7759901,0.5559094,1
 .5946353\|PG=C01 [X(C10H16)]\|@

Structure 27 (the ring-opened structure for the radical cation of α -pinene)

1\|UNK-LINUS\FOPT\UHF\STO-3G\C10H16(1+,2)\XYD\27-MAY-90\1\#PSTO-
 3G OPT POP=REGULAR\|radical cation of α -pinene ring opened same conformation
 \|1,2\C,1,r1\C,1,r2,2,a1\C,1,r3,2,a2,3,b1,0\C,2,r4,1,a3,4,b2,0\C,3,r5,1,a4,4,b3,0
 \C,5,r6,2,a5,1,b4,0\C,7,r7,5,a6,6,b5,0\C,8,r8,7,a7,6,b6,0\C,8,r9,7,a8,6,b7,0\H,3,r1
 0,1,a9,4,b8,0\H,2,r11,1,a10,4,b9,0\H,4,r12,1,a11,2,b10,0\H,4,r13,1,a12,13,b11,0\H
 ,4,r14,1,a13,13,b12,0\H,5,r15,2,a14,1,b13,0\H,5,r16,2,a15,1,b14,0\H,6,r17,3,a16,1
 ,b15,0\H,6,r18,3,a17,1,b16,0\H,9,r19,8,a18,10,b17,0\H,9,r20,8,a19,10,b18,0\H,9,r2
 1,8,a20,10,b19,0\H,10,r22,8,a21,9,b20,0\H,10,r23,8,a22,9,b21,0\H,10,r24,8,a23,9,b
 22,0\H,7,r25,8,a24,9,b23,0\|r1=1.409754\r2=1.411068\r3=1.529088\r4=1.520164\
 r5=1.522077\r6=1.578794\r7=1.517307\r8=1.512444\r9=1.514275\r10=1.082663
 \r11=1.082632\r12=1.088478\r13=1.085628\r14=1.085716\r15=1.089752\r16=1.
 091789\r17=1.089468\r18=1.091391\r19=1.086905\r20=1.096213\r21=1.087082\r
 22=1.088599\r23=1.086642\r24=1.096501\r25=1.091018\|a1=120.144583\|a2=119
 .89307\|a3=122.125901\|a4=122.636297\|a5=112.752524\|a6=106.023987\|a7=123.35
 6546\|a8=118.723897\|a9=120.55735\|a10=120.942764\|a11=110.760437\|a12=110.6
 68443\|a13=110.566697\|a14=111.087365\|a15=110.284677\|a16=110.646899\|a17=1
 09.804716\|a18=111.511026\|a19=105.701323\|a20=110.975117\|a21=110.862982\|a2
 2=111.805445\|a23=105.418457\|a24=106.163548\|b1=181.908859\|b2=177.421863\
 b3=-180.119265\|b4=27.64785\|b5=126.163612\|b6=33.947425\|b7=-148.488893\|b8

=-3.809873\b9=3.070022\b10=90.744813\b11=-119.870769\b12=119.765034\b13
 =152.233633\b14=-89.515106\b15=-147.095787\b16=95.610771\b17=146.163529\
 b18=-96.689921\b19=21.11931\b20=33.430815\b21=158.736497\b22=-83.170554\
 b23=156.646588\\Version=Stellar-Stellix-G86RevC\HF=-383.1652073\S2=1.099\S
 2-1=0.\S2A=0.774\RMSD=5.374e-10\RMSF=7.502e-05\Dipole=1.584191,1.6973
 067,1.173837\PG=C01 [X(C10H16)]\@

Structure 28 (the ring-opened structure for the radical cation of α -pinene)

1\1\GINC-LINUS\FOPT\UHF\STO-3G\C10H16(1+,2)\XYD\11-Jan-1992\1\#\N
 STO-3G OPT=READFC GUESS=READ GEOM=CHECKPOINT\ring opened
 radical cation of pinene, same conformation\\1,2\C\C,1,r1\C,1,r2,2,a1\C,1,r3,2,a2,
 3,b1,0\C,2,r4,1,a3,4,b2,0\C,3,r5,1,a4,4,b3,0\C,5,r6,2,a5,1,b4,0\C,7,r7,5,a6,6,b5,0\
 C,8,r8,7,a7,6,b6,0\C,8,r9,7,a8,6,b7,0\H,3,r10,1,a9,4,b8,0\H,2,r11,1,a10,4,b9,0\H,4
 ,r12,1,a11,2,b10,0\H,4,r13,1,a12,13,b11,0\H,4,r14,1,a13,13,b12,0\H,5,r15,2,a14,1,
 b13,0\H,5,r16,2,a15,1,b14,0\H,6,r17,3,a16,1,b15,0\H,6,r18,3,a17,1,b16,0\H,9,r19,8
 ,a18,10,b17,0\H,9,r20,8,a19,10,b18,0\H,9,r21,8,a20,10,b19,0\H,10,r22,8,a21,9,b20,
 0\H,10,r23,8,a22,9,b21,0\H,10,r24,8,a23,9,b22,0\H,7,r25,8,a24,9,b23,0\\r1=1.4112
 63\r2=1.409347\r3=1.528937\r4=1.52192\r5=1.520279\r6=1.553149\r7=1.51742
 7\r8=1.512522\r9=1.514048\r10=1.082642\r11=1.082697\r12=1.085666\r13=1.0
 86023\r14=1.088167\r15=1.089444\r16=1.091389\r17=1.089743\r18=1.091806\r1
 9=1.09583\r20=1.087676\r21=1.08665\r22=1.096468\r23=1.086579\r24=1.08879
 \r25=1.091005\a1=120.18795\a2=119.828601\a3=122.573781\a4=122.1285\a5=1
 13.547238\a6=115.667161\a7=123.213927\a8=118.774103\a9=120.947635\a10=1
 20.547979\a11=110.873954\a12=110.869554\a13=110.253971\a14=110.687211\a1
 5=109.792965\a16=111.112429\a17=110.279157\a18=105.972674\a19=111.05998
 8\a20=111.194453\a21=105.411303\a22=111.886201\a23=110.778655\a24=106.1
 51303\b1=179.687167\b2=177.903992\b3=-175.412322\b4=23.279264\b5=120.65
 5203\b6=89.572247\b7=-88.210504\b8=-0.577457\b9=1.46014\b10=155.011367\b
 11=-120.836238\b12=119.634267\b13=147.325084\b14=-95.338954\b15=-152.077
 846\b16=89.687437\b17=101.590824\b18=-141.635841\b19=-16.89972\b20=81.63
 7251\b21=199.884384\b22=-34.834683\b23=203.716118\\Version=Stellar-Stellix-G
 90RevH\HF=-383.165312\S2=1.099\S2-1=0.\S2A=0.774\RMSD=1.362e-09\RMS
 F=4.532e-06\Dipole=1.7946506,1.6881073,0.7821066\PG=C01[X(C10H16)]\@

Structure 44 (the radical cation of tricyclene with a symmetry plane about the ring skeleton)

1\1\GINC-LINUS\FREQ\UHF\STO-3G\C10H16(1+,2)\XYD\13-Aug-1991\0\#\NSTO-
 3G FREQ\radical cation of tricyclene, symmetric\\1,2\C\C,1,1.56734\C,2,1.543974,
 1,96.896\C,3,1.516851,2,126.904,1,180.0\C,1,1.552099,2,103.901,3,-52.332,0\C,1,
 1.552099,2,103.901,3,52.332,0\C,3,1.691749,2,106.483,1,-26.328,0\C,3,1.691749,2
 ,106.483,1,26.328,0\C,2,1.553732,3,111.73,4,-60.733,0\C,2,1.553732,3,111.73,4,60

.733,0\H,1,1.086647,2,115.596,3,180.,0\H,4,1.086472,3,111.569,2,180.024,0\H,4,1.089524,3,109.354,2,-59.12,0\H,4,1.089527,3,109.385,2,59.168,0\H,5,1.084962,1,115.351,2,-62.609,0\H,6,1.084962,1,115.351,2,62.609,0\H,5,1.090498,1,112.211,2,171.632,0\H,6,1.090498,1,112.211,2,-171.632,0\H,7,1.090598,3,112.473,2,-143.85,0\H,8,1.090598,3,112.473,2,143.85,0\H,9,1.085791,2,109.102,1,-60.165,0\H,9,1.085252,2,109.893,1,181.343,0\H,9,1.083782,2,112.705,1,60.549,0\H,10,1.085798,2,109.106,1,60.082,0\H,10,1.085262,2,109.894,1,178.581,0\H,10,1.08377,2,112.699,1,-60.63,0\Version=Stellar-Stellix-G90RevH\HF=-383.1904929\S2=0.758\S2-1=0.\S2A=0.75\RMSD=7.233e-10\RMSF=1.944e-05\Dipole=1.1986003,-0.0000256,-0.2739496\DipoleDeriv=-0.0575047,-0.0000086,-0.0508134,0.0000116,0.0128747,0.0000152,-0.0686125,-0.0000022,

Structure 45 (the radical cation of tricyclene)

1\1\GINC-LINUS\FOPT\UHF\STO-3G\C10H16(1+,2)\XYD\7-Aug-1991\1\#\N
 STO-3G\OPT\OPTCYC=300POP=REGULAR\tricycleneradicalcation\1,2\H\C,1,r1\C,2,r2,1,a1\C,3,r3,2,a2,1,b1,0\H,4,r4,3,a3,2,b2,0\C,2,r5,3,a4,4,b3,0\C,4,r6,3,a5,2,b4,0\C,4,r7,3,a6,2,b5,0\C,2,r8,3,a7,4,b6,0\H,3,r9,2,a8,1,b7,0\H,3,r10,2,a9,1,b8,0\H,6,r11,2,a10,1,b9,0\H,7,r12,4,a11,5,b10,0\H,7,r13,4,a12,5,b11,0\C,9,r14,2,a13,1,b12,0\C,8,r15,4,a14,5,b13,0\C,8,r16,4,a15,5,b14,0\H,15,r17,9,a16,2,b15,0\H,15,r18,9,a17,2,b16,0\H,15,r19,9,a18,2,b17,0\H,16,r20,8,a19,4,b18,0\H,16,r21,8,a20,4,b19,0\H,16,r22,8,a21,4,b20,0\H,17,r23,8,a22,4,b21,0\H,17,r24,8,a23,4,b22,0\H,17,r25,8,a24,4,b23,0\r1=1.088145\r2=1.546714\r3=1.550786\r4=1.086688\r5=1.5235\r6=1.552966\r7=1.568399\r8=1.503398\r9=1.087352\r10=1.085255\r11=1.091204\r12=1.086002\r13=1.091529\r14=1.51752\r15=1.557719\r16=1.550388\r17=1.088083\r18=1.08631\r19=1.091172\r20=1.083915\r21=1.085908\r22=1.085525\r23=1.0852\r24=1.083957\r25=1.085633\ a1=123.859812\ a2=96.571424\ a3=116.141285\ a4=103.355901\ a5=100.591782\ a6=103.179661\ a7=105.664743\ a8=111.157627\ a9=112.163722\ a10=124.425488\ a11=115.521286\ a12=111.639233\ a13=124.831471\ a14=113.013602\ a15=114.896141\ a16=110.939396\ a17=111.451361\ a18=107.330234\ a19=112.682241\ a20=108.671444\ a21=109.984307\ a22=110.069058\ a23=112.603329\ a24=109.115328\ b1=180.983489\ b2=181.115537\ b3=-41.093499\ b4=55.992636\ b5=-52.312016\ b6=38.635591\ b7=-61.555055\ b8=61.003064\ b9=-22.246331\ b10=64.809517\ b11=-59.759364\ b12=18.740372\ b13=58.232558\ b14=-66.966656\ b15=134.685586\ b16=11.651051\ b17=252.599141\ b18=57.846266\ b19=-62.581216\ b20=179.01067\ b21=176.197292\ b22=-62.917178\ b23=57.656881\ \Version=Stellar-Stellix-G90RevH\HF=-383.2001708\S2=0.785\S2-1=0.\S2A=0.751\RMSD=7.649e-10\RMSF=5.885e-06\Dipole=-0.4629922,-0.5120418,-0.8669859\ PG=C01 [X(C10H16)]\@

46 skew (6-31G*)

1\1\DALHOUSIE-LINUS\FOPT\RHF\6-31G(D)\C4H8\XYD\21-DEC-90\1\#\N

HF/6-31G* OPT=CALCFPOP=REGULAR\\1-BUtene\\0,1\\C\\C,1,r1
 \\C,2,r2,1,a1\\C,3,r3,2,a2,1,b1,0\\H,1,r4,2,a3,3,b2,0\\H,1,r5,2,a4,3,b3,0\\H,2,r6,1,a5,6
 ,b4,0\\H,3,r7,2,a6,7,b5,0\\H,3,r8,2,a7,7,b6,0\\H,4,r9,3,a8,2,b7,0\\H,4,r10,3,a9,2,b8,0\\
 H,4,r11,3,a10,2,b9,0\\r1=1.318758\\r2=1.505038\\r3=1.532308\\r4=1.075671\\r5=1.
 077082\\r6=1.080016\\r7=1.085882\\r8=1.088413\\r9=1.085506\\r10=1.085174\\r11=
 1.086219\\a1=125.392351\\a2=112.484801\\a3=121.700826\\a4=121.835421\\a5=118.
 901614\\a6=109.580297\\a7=109.112924\\a8=110.951369\\a9=110.894568\\a10=111.
 146724\\b1=-119.849226\\b2=179.684966\\b3=-0.480805\\b4=180.039484\\b5=-177.8
 74101\\b6=-61.359584\\b7=181.390965\\b8=61.171092\\b9=-58.7265\\Version=Stella
 r-Stellix-G86RevC\\HF=-156.1060832\\RMSD=4.048e-10\\RMSF=4.520e-05\\Dipole
 =0.0401518,-0.0027182,0.1084843\\PG=C01 [X(C4H8)]\\@

46 skew (MP2/6-31G*)

1\\1\\DALHOUSIE-LINUS\\SP\\RMP2-FC\\6-31G(D)\\C4H8\\XYD\\27-FEB-91\\0\\#N
 MP2/6-31G*POP=REGULAR\\1-BUtene\\0,1\\C\\C,1,1.318758\\C,2,1.505038,1,125.
 392\\C,3,1.532308,2,112.485,1,-119.849,0\\H,1,1.075671,2,121.701,3,179.685,0\\H,1,
 1.077082,2,121.835,3,-0.481,0\\H,2,1.080016,1,118.902,6,180.039,0\\H,3,1.085882,2,
 109.58,7,-177.874,0\\H,3,1.088413,2,109.113,7,-61.36,0\\H,4,1.085506,3,110.951,2,
 181.391,0\\H,4,1.085174,3,110.895,2,61.171,0\\H,4,1.086219,3,111.147,2,-58.727,0\\
 \\Version=Stellar-Stellix-G86RevC\\HF=-156.1060832\\MP2=-156.6202141\\RMSD=
 7.379e-10\\PG=C01 [X(C4H8)]\\@

46** b (STO-3G)

1\\1\\UNK-DAL1\\POPT\\UHF\\STO-3G\\C4H81+,2\\XYD\\6-JAN-1990\\1\\#N STO-3G
 OPT POP=REGULAR \\bridged radical cation\\1,2\\H\\C,1,R1\\C,2,R2,1,A1\\
 C,2,R3,1,A2,3,B1,0\\C,2,R3,1,A2,3,-B1,0\\H,4,R4,2,A3,3,B2,0\\H5,R4,2,A3,3,-
 B2,0\\H,4,R5,2,A4,3,B3,0\\H,5,R5,2,A4,3,-B3,0\\H,3,R6,2,A5,1,B4,0\\H,3,R7,2,
 A6,1,B5,0\\H,3,R8,2,A7,1,B6,0\\R1=1.092979\\R2=1.726122\\R3=1.456298\\R4=1.
 090615\\R5=1.090242\\R6=1.09028\\R7=1.090877\\R8=1.090878\\A1=102.499799\\A
 2=114.869992\\A3=120.867074\\A4=119.671916\\A5=109.696834\\A6=104.899105\\
 A7=104.899095\\B1=106.422355\\B2=-84.079907\\B3=84.203357\\B4=179.999963\\
 B5=-58.821626\\B6=58.821426\\Version=VAX-VMS-G86RevC\\HF=-153.9262439
 \\S2=0.971\\S2-1=0.\\S2A=0.757\\RMSD=0.248D-09\\RMSF=0.350D-04\\Dipole=
 0.1876859,0.000032,0.0482233\\PG=C01 [X(C4H8)]\\@

46** b (6-31G*)

1\\1\\DALHOUSIE-LINUS\\FOPT\\UHF\\6-31G(D)\\C4H8(1+,2)\\XYD\\23-JAN-91\\1\\#
 N HF/6-31G* OPT=CALCF POP=REGULAR\\radical cation from methyl and
 allyl\\1,2\\H\\C,1,r1\\C,2,r2,1,a1\\C,2,r3,1,a2,3,b1,0\\C,2,r4,1,a3,3,b2,0\\H,4,r5,2,a4,3,
 b3,0\\H,5,r6,2,a5,3,b4,0\\H,4,r7,2,a6,3,b5,0\\H,5,r8,2,a7,3,b6,0\\H,3,r9,2,a8,1,b7,0\\H
 ,3,r10,2,a9,1,b8,0\\H,3,r11,2,a10,1,b9,0\\r1=1.079662\\r2=1.908327\\r3=1.420838\\r
 4=1.420838\\r5=1.074656\\r6=1.074655\\r7=1.073145\\r8=1.073145\\r9=1.073423\\r

10=1.073436\r11=1.073436\al=97.479451\la2=116.438903\la3=116.438759\la4=12
1.216675\la5=121.216718\la6=120.288252\la7=120.288218\la8=107.113384\la9=100.
844191\la10=100.844412\lb1=100.490175\lb2=-100.489875\lb3=-89.802567\lb4=89.8
02413\lb5=85.744816\lb6=-85.7456\lb7=180.000708\lb8=-58.876396\lb9=58.877662\
\Version=Stellar-Stellix-G86RevC\HF=-155.7574539\S2=1.009\S2-1=0.\S2A=0.75
8\RMSD=8.410e-10\RMSF=3.216e-07\Dipole=0.5399705,0.000026,-0.0367532\PG
=C01 [X(C4H8)]\@

46⁺ b (MP2/6-31G*)

1\1\DALHOUSIE-LINUS\SP\UMP2-FC\6-31G(D)\C4H8(1+,2)\XYD\27-FEB-91\0\
#N MP2/6-31G* POP=REGULAR\radical cation from methyl and allyl
mp2/6-31G*\1,2\H\C,1,1.079662\C,2,1.908327,1,97.479\C,2,1.420838,1,116.439,3
,100.49,0\C,2,1.420838,1,116.439,3,-100.49,0\H,4,1.074656,2,121.217,3,-89.803,0\
H,5,1.074655,2,121.217,3,89.802,0\H,4,1.073145,2,120.288,3,85.745,0\H,5,1.0731
45,2,120.288,3,-85.746,0\H,3,1.073423,2,107.113,1,180.001,0\H,3,1.073436,2,100.
844,1,-58.876,0\H,3,1.073436,2,100.844,1,58.878,0\Version=Stellar-Stellix-G86Re
vC\HF=-155.7574539\MP2=-156.2247983\S2=1.009\S2-1=0.942\S2A=0.758\RM
SD=5.375e-10\PG=C01 [X(C4H8)]\@

46⁺ anti (6-31G*)

1\1\UNK-LINUS\FOPT\UHF\6-31G(D)\C4H8(1+,2)\XYD\10-OCT-90\1\#N
HF/6-31G* OPT POP=REGULAR\1-BUtene radical
cation\1,2\C\1,1\C,2,r2,1,a1\C,3,r3,2,a2,1,b1,0\H,1,r4,2,a3,3,b2,0\H,1,r5,2,a4,
3,b3,0\H,2,r6,1,a5,6,b4,0\H,3,r7,2,a6,7,b5,0\H,3,r8,2,a7,7,b6,0\H,4,r9,3,a8,2,b7,0\
H,4,r10,3,a9,2,b8,0\H,4,r11,3,a10,2,b9,0\r1=1.408053\r2=1.480329\r3=1.528187
\r4=1.07457\r5=1.075579\r6=1.078687\r7=1.092348\r8=1.092348\r9=1.081643\r
10=1.083643\r11=1.083643\al=123.415816\la2=114.872709\la3=120.739584\la4=1
20.832726\la5=117.158779\la6=106.769472\la7=106.769472\la8=109.517888\la9=11
1.335304\la10=111.335304\lb1=180.\lb2=180.\lb3=0.\lb4=180.\lb5=124.41542\lb6=-
124.41542\lb7=180.\lb8=60.778603\lb9=-60.778603\Version=Stellar-Stellix-G86Rev
C\HF=-155.8103693\S2=0.755\S2-1=0.\S2A=0.75\RMSD=4.386e-10\RMSF=4.9
36e-05\Dipole=-0.6249259,0.,-1.4812527\PG=C01 [X(C4H8)]\@

46⁺ eclipsed (STO-3G)

1\1\UNK-LINUS\FOPT\UHF\STO-3G\C4H8(1+,2)\XYD\27-SEP-90\1\#NSTO-3G
OPT OPTCYC=60\1-BUtene radical cation\1,2\C\C,1,r1\C,2,r2,1,a1\C,3,r3,2,
a2,1,b1,0\H,1,r4,2,a3,3,b2,0\H,1,r5,2,a4,3,b3,0\H,2,r6,1,a5,6,b4,0\H,3,r7,2,a6,7,b
5,0\H,3,r8,2,a7,7,b6,0\H,4,r9,3,a8,2,b7,0\H,4,r10,3,a9,2,b8,0\H,4,r11,3,a10,2,b9,0
\r1=1.435626\r2=1.514107\r3=1.539122\r4=1.095638\r5=1.094517\r6=1.104538
\r7=1.097223\r8=1.097223\r9=1.085735\r10=1.086236\r11=1.086236\al=126.05
2182\la2=116.662181\la3=120.383514\la4=120.983776\la5=116.963086\la6=105.190

294\a7=105.19025\a8=108.353331\a9=111.148067\a10=111.148068\b1=0.000053\
 b2=179.999997\b3=0.000049\b4=179.999948\b5=-55.534367\b6=55.534331\b7=
 179.999999\b8=61.120524\b9=-61.120526\\Version=Stellar-Stellix-G86RevC\HF=-
 153.9906175\S2=0.756\S2-1=0.\S2A=0.75\RMSD=2.421e-10\RMSF=5.207e-05\
 ipole=-1.4288538,0.0000002,-0.5203792\PG=C01 [X(C4H8)]\@

46** eclipsed (6-31G*)

1\1\UNK-LINUS\FOPT\UHF\6-31G(D)\C4H8(1+,2)\XYD\05-OCT-90\1\#N
 HF/6-31G* OPT=CALCFC POP=REGULAR\1-BUtene radical cation\1,2\C
 \C,1,r1\C,2,r2,1,a1\C,3,r3,2,a2,1,b1,0\H,1,r4,2,a3,3,b2,0\H,1,r5,2,a4,3,b3,0\H,2,r6
 ,1,a5,6,b4,0\H,3,r7,2,a6,7,b5,0\H,3,r8,2,a7,7,b6,0\H,4,r9,3,a8,2,b7,0\H,4,r10,3,a9,
 2,b8,0\H,4,r11,3,a10,2,b9,0\r1=1.408792\r2=1.475773\r3=1.526637\r4=1.074544
 \r5=1.073749\r6=1.078186\r7=1.092922\r8=1.092922\r9=1.081595\r10=1.08402
 8\r11=1.084028\al=126.369\aa2=117.986\aa3=120.304\aa4=121.219\aa5=116.811\aa6
 =105.306\aa7=105.306\aa8=108.962\aa9=111.849\aa10=111.849\b1=0.\b2=180.\b3
 =0.\b4=180.\b5=-54.428\b6=54.428\b7=180.\b8=61.384\b9=-61.384\\Version=
 Stellar-Stellix-G86RevC\State=2-A\HF=-155.8112206\S2=0.755\S2-1=0.\S2A=0.
 75\RMSD=2.370e-10\RMSF=5.777e-05\Dipole=-1.2893978,0.,-0.5204624\Polar=3
 9.0179631,0.,26.1447293,4.721157,0.,51.8621836\HyperPolar=-63.8209291,0.,5.59
 25911,0.,-37.428148,0.,4.8907379,-16.4435122,0.,170.6496283\PG=CS
 [SG(C4H4),X(H4)]\@

46** sckew (STO-3G)

1\1\DALHOUSIE-LINUS\FOPT\UHF\STO-3G\C4H8(1+,2)\XYD\05-MAR-91\1
 \#N STO-3G OPT=READFC OPTCYC=90
 GEOM=CHECKPOINTGUESS=READ\nonclassical
 radicalcation\1,2\X\C,1,r1\H,2,r2,1,a1\H,2,r3,1,a2,3,b1,0\H,2,r4,1,a3,3,b2,0\C,1,r
 5,2,90.,3,b3,0\H,6,r6,1,a4,2,b4,0\H,6,r7,1,a5,2,b5,0\C,1,r8,2,90.,3,b6,0\H,9,r9,1,a
 6,2,b7,0\C,9,r10,10,a7,1,b8,0\H,11,r11,9,a8,1,b9,0\H,11,r12,9,a9,1,b10,0\r1=1.46
 2535\r2=1.086656\r3=1.086701\r4=1.086447\r5=0.543224\r6=1.088383\r7=1.09
 3937\r8=2.032443\r9=1.103947\r10=1.435831\r11=1.095476\r12=1.095607\al=1
 12.130802\aa2=88.630934\aa3=125.787532\aa4=56.011406\aa5=90.053689\aa6=122.11
 4994\aa7=117.531531\aa8=120.459986\aa9=120.769623\b1=109.803039\b2=-137.668
 06\b3=-269.313204\b4=224.287484\b5=-249.724193\b6=77.13503\b7=58.438649\
 b8=-184.453186\b9=-3.455084\b10=-183.207605\\Version=Stellar-Stellix-G86Rev
 C\HF=-153.9917635\S2=0.756\S2-1=0.\S2A=0.75\RMSD=9.637e-10\RMSF=1.6
 69e-04\Dipole=0.5165206,-1.2495556,-0.6580398\PG=C01 [X(C4H8)]\@

46** sckew (6-31G*) (Figure 5.2)

1\1\UNK-LINUS\FOPT\UHF\6-31G(D)\C4H8(1+,2)\XYD\06-OCT-90\1\#N
 HF/6-31G* OPT=CALCFC POP=REGULAR\1-BUtene radical cation\1,2

```

\C\C,1,r1\C,2,r2,1,a1\C,3,r3,2,a2,1,b1,0\H,1,r4,2,a3,3,b2,0\H,1,r5,2,a4,3,b3,0\H,2
,r6,1,a5,6,b4,0\H,3,r7,2,a6,7,b5,0\H,3,r8,2,a7,7,b6,0\H,4,r9,3,a8,2,b7,0\H,4,r10,3,
a9,2,b8,0\H,4,r11,3,a10,2,b9,0\|r1=1.408281\r2=1.473146\r3=1.553618\r4=1.074
598\r5=1.075093\r6=1.078439\r7=1.08176\r8=1.089612\r9=1.081322\r10=1.082
408\r11=1.082775\|a1=125.012814\|a2=110.314462\|a3=120.817462\|a4=120.650002
\|a5=117.27337\|a6=111.398983\|a7=106.816417\|a8=108.003303\|a9=111.439183\|a1
0=111.443489\|b1=-118.745611\|b2=180.070858\|b3=-0.103937\|b4=180.809457\|b5
=-175.579845\|b6=-57.014385\|b7=182.422707\|b8=63.578111\|b9=-58.663903\|Ver
sion=Stellar-Stellix-G86RevC\HF=-155.8117349\|S2=0.755\|S2-1=-0.\|S2A=0.75\|RM
SD=6.817e-10\|RMSF=7.389e-06\|Dipole=-0.7486543,0.4658025,-1.123755\|PG=C0
1 [X(C4H8)]\|@

```

46* sckew (MP2/6-31G*)

```

1\|DALHOUSIE-LINUS\SP\UMP2-FC\6-31G(D)\C4H8(1+,2)\XYD\26-FEB-91\0\
#N MP2/6-31G*\|1-Butene radical cation opt at 6-31G*\|1,2\C\C,1,1.4083\C,2,
1.4731,1,125.0128\C,3,1.5536,2,110.3145,1,-118.7456,0\H,1,1.0746,2,120.8175,3,1
80.0709,0\H,1,1.0751,2,120.65,3,-0.1039,0\H,2,1.0784,1,117.2734,6,180.8095,0\H,
3,1.0818,2,111.399,7,-175.5798,0\H,3,1.0896,2,106.8164,7,-57.0144,0\H,4,1.0813,
3,108.0033,2,182.4227,0\H,4,1.0824,3,111.4392,2,63.5781,0\H,4,1.0828,3,111.443
5,2,-58.6639,0\|Version=Stellar-Stellix-G86RevC\HF=-155.8117349\|MP2=-156.281
3576\|S2=0.755\|S2-1=0.75\|S2A=0.75\|RMSD=4.970e-10\|PG=C01 [X(C4H8)]\|@

```

47 anti (STO-3G)

```

1\|DALHOUSIE-LINUS\FOPT\RHF\STO-3G\C7H14\XYD\21-DEC-90\1\#N
STO-3GOPT\|4,4-dimethyl-1-pentene\|0,1\C\H,1,R1\H,1,R2,2,A1\C,1,R3,2,A2,3,B1
,0\H,4,R4,1,A3,3,B2,0\C,4,R5,1,A4,3,B3,0\H,6,R6,4,A5,1,B4,0\H,6,R7,4,A6,1,B5
,0\C,6,R8,4,A7,1,B6,0\C,9,R9,6,A8,4,B7,0\C,9,R10,6,A9,4,B8,0\C,9,R11,6,A10,4,
B9,0\H,10,R12,9,A11,6,B10,0\H,10,R13,9,A12,6,B11,0\H,10,R14,9,A13,6,B12,0\H
,11,R15,9,A14,6,B13,0\H,11,R16,9,A15,6,B14,0\H,11,R17,9,A16,6,B15,0\H,12,R1
8,9,A17,6,B16,0\H,12,R19,9,A18,6,B17,0\H,12,R20,9,A19,6,B18,0\|R1=1.08072\|R
2=1.081456\|R3=1.308882\|R4=1.081081\|R5=1.533498\|R6=1.088544\|R7=1.08856
9\|R8=1.577299\|R9=1.550708\|R10=1.552906\|R11=1.55285\|R12=1.08509\|R13=1.
085578\|R14=1.085005\|R15=1.085762\|R16=1.085647\|R17=1.085842\|R18=1.0857
7\|R19=1.085653\|R20=1.08583\|A1=115.646392\|A2=121.961497\|A3=119.070392\
|A4=123.062905\|A5=107.750087\|A6=107.629438\|A7=118.622206\|A8=114.03094
3\|A9=108.895974\|A10=108.891964\|A11=111.417183\|A12=109.365092\|A13=111.
431565\|A14=110.599416\|A15=110.70112\|A16=110.633935\|A17=110.593966\|A18
=110.699831\|A19=110.636555\|B1=179.984214\|B2=179.94859\|B3=-0.006248\|B4
=-56.957102\|B5=56.558114\|B6=179.755606\|B7=-0.683343\|B8=120.165866\|B9=-
121.512689\|B10=-60.680583\|B11=180.091219\|B12=60.882646\|B13=178.167199\|B
14=58.208862\|B15=-61.862618\|B16=182.172312\|B17=-57.875074\|B18=62.20041\

```

\Version=Stellar-Stellix-G86RevC\HF=-269.9660134\RMSD=2.923e-10\RMSF=1.258e-04\Dipole=-0.0756277,-0.0003405,-0.1030032\PG=C01 [X(C7H14)]\@

47 skew

1\1\DALHOUSIE-LINUS\FOPT\RHF\STO-3G\C7H14\XYD\23-DEC-90\1\#N
 STO-3G OPT\4,4-dimethyl-1-pentene\0,1\C\H,1,R1\H,1,R2,2,A1\C,1,R3,2,A2,3,
 B1,0\H,4,R4,1,A3,3,B2,0\C,4,R5,1,A4,3,B3,0\H,6,R6,4,A5,1,B4,0\H,6,R7,4,A6,1,
 B5,0\C,6,R8,4,A7,1,B6,0\C,9,R9,6,A8,4,B7,0\C,9,R10,6,A9,4,B8,0\C,9,R11,6,A10
 ,4,B9,0\H,10,R12,9,A11,6,B10,0\H,10,R13,9,A12,6,B11,0\H,10,R14,9,A13,6,B12,0
 \H,11,R15,9,A14,6,B13,0\H,11,R16,9,A15,6,B14,0\H,11,R17,9,A16,6,B15,0\H,12,
 R18,9,A17,6,B16,0\H,12,R19,9,A18,6,B17,0\H,12,R20,9,A19,6,B18,0\|R1=1.0810
 3\R2=1.081348\R3=1.308805\R4=1.084328\R5=1.524985\R6=1.086571\R7=1.08
 8885\R8=1.579541\R9=1.551459\R10=1.552057\R11=1.551908\R12=1.084895\R
 13=1.085657\R14=1.085164\R15=1.085786\R16=1.085716\R17=1.085808\R18=
 1.085797\R19=1.085736\R20=1.085832\A1=115.777746\A2=122.033353\A3=119
 .669027\A4=124.540531\A5=108.235475\A6=107.949775\A7=116.024287\A8=11
 2.57639\A9=108.972272\A10=109.348\A11=111.2212\A12=109.778646\A13=111
 .032625\A14=110.621849\A15=110.693494\A16=110.593432\A17=110.611251\A
 18=110.688467\A19=110.647218\B1=179.832224\B2=179.599813\B3=0.945385\
 B4=8.399004\B5=123.525235\B6=-114.342528\B7=0.027077\B8=120.348343\B9
 =-120.781652\B10=-63.097938\B11=177.414461\B12=57.786865\B13=178.48545
 3\B14=58.48754\B15=-61.554626\B16=181.058013\B17=-58.948163\B18=61.093
 337\Version=Stellar-Stellix-G86RevC\HF=-269.9712153\RMSD=3.527e-10\RMSF
 =3.179e-05\Dipole=-0.061822,0.0094523,-0.0820398\PG=C01 [X(C7H14)]\@

47* b

1\1\UNK-LINUS\FOPT\UHF\STO-3G\C7H14(1+,2)\XYD\08-OCT-90\1\#N
 STO-3G POP=REGULAR OPT\T-but-allyl\1,2\H\C,1,r1\C,2,r2,1,a1\C,2,r3,1,
 a2,3,b1,0\C,2,r4,1,a3,3,b2,0\H,4,r5,2,a4,3,b3,0\H,5,r6,2,a5,3,b4,0\H,4,r7,2,a6,3,b5
 ,0\H,5,r8,2,a7,3,b6,0\C,3,r9,2,a8,1,b7,0\C,3,r10,2,a9,1,b8,0\C,3,r11,2,a10,1,b9,0\
 H,10,r12,3,a11,2,b10,0\H,10,r13,3,a12,2,b11,0\H,10,r14,3,a13,2,b12,0\H,11,r15,3,
 a14,2,b13,0\H,12,r16,3,a15,2,b14,0\H,11,r17,3,a16,2,b15,0\H,12,r18,3,a17,2,b16,0\
 H,11,r19,3,a18,2,b17,0\H,12,r20,3,a19,2,b18,0\|r1=1.088878\r2=1.998988\r3=1.4
 39968\r4=1.439972\r5=1.085285\r6=1.085285\r7=1.08435\r8=1.084349\r9=1.55
 2735\r10=1.542422\r11=1.542419\r12=1.083728\r13=1.086705\r14=1.086705\r15
 =1.090712\r16=1.09072\r17=1.084458\r18=1.084426\r19=1.085755\r20=1.08578
 8\|a1=94.403815\|a2=115.642782\|a3=115.643544\|a4=120.988994\|a5=120.988921\|a
 6=120.578197\|a7=120.578158\|a8=107.494587\|a9=101.830816\|a10=101.828683\|a
 11=112.83642\|a12=108.982336\|a13=108.981921\|a14=105.374389\|a15=105.37524
 7\|a16=112.008236\|a17=112.036445\|a18=111.937673\|a19=111.909272\|b1=104.94
 2956\|b2=-104.945369\|b3=-91.131615\|b4=91.1315\|b5=83.496052\|b6=-83.496009\
 b7=179.999707\|b8=-58.424255\|b9=58.425786\|b10=0.000102\|b11=120.324266\|b1

2=-120.324757\b13=170.612838\b14=-170.62225\b15=-71.616101\b16=71.669965
 \b17=53.108712\b18=-53.054197\\Version=Stellar-Stellix-G86RevC\HF=-269.6822
 448\S2=1.146\S2-1=0.\S2A=0.771\RMSD=4.771e-10\RMSF=5.532e-05\Dipole=
 0.0210819,0.0000735,-0.021581\PG=C01 [X(C7H14)]\@

47⁺ eclipsed

1\1\UNK-LINUS\FOPT\UHF\STO-3G\C7H14(1+,2)\XYD\22-OCT-90\1\#N
 STO-3G OPT\T-BUTYLBUTENE radical cation\\1,2\C\H,1,R1\H,1,R2,2,A1
 \C,1,R3,2,A2,3,B1,0\H,4,R4,1,A3,3,B2,0\C,4,R5,1,A4,3,B3,0\H,6,R6,4,A5,1,B4,0\
 H,6,R7,4,A6,1,B5,0\C,6,R8,4,A7,1,B6,0\C,9,R9,6,A8,4,B7,0\C,9,R10,6,A9,4,B8,0\
 \C,9,R11,6,A10,4,B9,0\H,10,R12,9,A11,6,B10,0\H,10,R13,9,A12,6,B11,0\H,10,R1
 4,9,A13,6,B12,0\H,11,R15,9,A14,6,B13,0\H,11,R16,9,A15,6,B14,0\H,11,R17,9,A1
 6,6,B15,0\H,12,R18,9,A17,6,B16,0\H,12,R19,9,A18,6,B17,0\H,12,R20,9,A19,6,B1
 8,0\R1=1.095191\R2=1.091646\R3=1.437072\R4=1.104834\R5=1.514805\R6=1
 .097345\R7=1.097345\R8=1.561833\R9=1.55354\R10=1.551288\R11=1.551308\R
 12=1.085697\R13=1.084965\R14=1.08571\R15=1.084915\R16=1.085874\R17=1.
 084267\R18=1.084902\R19=1.085888\R20=1.08426\A1=118.374236\A2=119.505
 401\A3=115.140851\A4=130.281818\A5=103.60879\A6=103.608604\A7=122.119
 435\A8=105.577592\A9=111.201181\A10=111.22683\A11=110.831644\A12=109.
 661389\A13=110.824807\A14=109.370283\A15=110.623009\A16=112.517585\A1
 7=109.341933\A18=110.643402\A19=112.516173\B1=180.069905\B2=180.11674
 2\B3=0.124341\B4=125.473703\B5=-125.392345\B6=0.060494\B7=180.078617\B
 8=62.456637\B9=-62.316758\B10=-59.987332\B11=180.401502\B12=60.799354\
 B13=174.507105\B14=55.559721\B15=-65.8973\B16=186.706084\B17=-54.35960
 4\B18=67.147551\\Version=Stellar-Stellix-G86RevC\HF=-269.7278841\S2=0.756\
 S2-1=0.\S2A=0.75\RMSD=5.499e-10\RMSF=3.997e-05\Dipole=-0.6805987,0.005
 5489,2.9743145\PG=C01 [X(C7H14)]\@

47⁺ anti

1\1\UNK-LINUS\FOPT\UHF\STO-3G\C7H14(1+,2)\XYD\20-OCT-90\1\#N
 STO-3G OPT\T-BUTYLBUTENE radical cation\\1,2\C\H,1,R1\H,1,R2,2,A1\C,1,
 R3,2,A2,3,B1,0\H,4,R4,1,A3,3,B2,0\C,4,R5,1,A4,3,B3,0\H,6,R6,4,A5,1,B4,0\H,6,
 R7,4,A6,1,B5,0\C,6,R8,4,A7,1,B6,0\C,9,R9,6,A8,4,B7,0\C,9,R10,6,A9,4,B8,0\C,9
 ,R11,6,A10,4,B9,0\H,10,R12,9,A11,6,B10,0\H,10,R13,9,A12,6,B11,0\H,10,R14,9,
 A13,6,B12,0\H,11,R15,9,A14,6,B13,0\H,11,R16,9,A15,6,B14,0\H,11,R17,9,A16,6,
 B15,0\H,12,R18,9,A17,6,B16,0\H,12,R19,9,A18,6,B17,0\H,12,R20,9,A19,6,B18,0\
 R1=1.095021\R2=1.095015\R3=1.437035\R4=1.103117\R5=1.515287\R6=1.096
 249\R7=1.096352\R8=1.561462\R9=1.550935\R10=1.550478\R11=1.550536\R12
 =1.085806\R13=1.085041\R14=1.085799\R15=1.084823\R16=1.085946\R17=1.0
 85869\R18=1.084811\R19=1.085951\R20=1.085847\A1=118.713703\A2=120.770
 891\A3=117.063508\A4=122.709824\A5=105.914265\A6=105.837392\A7=116.06
 9012\A8=106.816351\A9=110.123878\A10=110.135589\A11=110.807229\A12=1

09.712018\A13=110.796837\A14=109.561796\A15=110.83218\A16=111.730815\
 A17=109.543223\A18=110.838099\A19=111.753161\B1=180.175996\B2=179.937
 811\B3=-0.010851\B4=-55.827416\B5=56.232021\B6=180.161925\B7=180.18711
 2\B8=61.28891\B9=-60.834252\B10=-60.217289\B11=180.161679\B12=60.5337
 57\B13=177.037527\B14=57.719904\B15=-63.614496\B16=183.370023\B17=-57.
 319104\B18=64.040208\Version=Stellar-Stellix-G86RevC\HF=-269.7328863\S2=0
 .756\S2-1=0.\S2A=0.75\RMSD=9.231e-10\RMSF=4.753e-05\Dipole=2.2383571,-
 0.0154965,2.5132811\PG=C01 [X(C7H14)]\@

47⁺ skew (Figure 5.5)

1\1\UNK-LINUS\FOPT\UHF\STO-3G\C7H14(1+,2)\XYD\13-OCT-90\1\#N
 STO-3G SCF OPT\T-BUTYLBUTENE radical cation\1,2\C\H,1,R1\H,1,R2,2,A1
 \C,1,R3,2,A2,3,B1,0\H,4,R4,1,A3,3,B2,0\C,4,R5,1,A4,3,B3,0\H,6,R6,4,A5,1,B4,0\
 H,6,R7,4,A6,1,B5,0\C,6,R8,4,A7,1,B6,0\C,9,R9,6,A8,4,B7,0\C,9,R10,6,A9,4,B8,0
 \C,9,R11,6,A10,4,B9,0\H,10,R12,9,A11,6,B10,0\H,10,R13,9,A12,6,B11,0\H,10,R1
 4,9,A13,6,B12,0\H,11,R15,9,A14,6,B13,0\H,11,R16,9,A15,6,B14,0\H,11,R17,9,A1
 6,6,B15,0\H,12,R18,9,A17,6,B16,0\H,12,R19,9,A18,6,B17,0\H,12,R20,9,A19,6,B1
 8,0\R1=1.094551\R2=1.094324\R3=1.436453\R4=1.102872\R5=1.500129\R6=1
 .091878\R7=1.087781\R8=1.594007\R9=1.550685\R10=1.550985\R11=1.550427\
 R12=1.085651\R13=1.085662\R14=1.085647\R15=1.085098\R16=1.085943\R17
 =1.08637\R18=1.085142\R19=1.08583\R20=1.085584\A1=118.782218\A2=120.7
 76361\A3=117.195218\A4=124.233863\A5=107.258177\A6=109.763915\A7=112.
 109718\A8=105.896815\A9=109.912244\A10=110.440465\A11=110.869393\A12
 =109.275902\A13=110.804657\A14=109.334585\A15=111.008462\A16=111.5285
 78\A17=109.10073\A18=110.946372\A19=111.775072\B1=179.806514\B2=181.0
 15798\B3=0.223607\B4=135.838439\B5=16.39117\B6=-105.768733\B7=180.2785
 55\B8=61.586019\B9=-60.785784\B10=-60.288642\B11=180.197962\B12=60.707
 595\B13=174.778925\B14=55.575907\B15=-66.060142\B16=186.511172\B17=-54
 .400715\B18=67.366303\Version=Stellar-Stellix-G86RevC\HF=-269.735636\S2=0
 .756\S2-1=0.\S2A=0.75\RMSD=4.600e-10\RMSF=3.912e-05\Dipole=0.9482121,-
 1.4945085,2.2857737\PG=C01 [X(C7H14)]\@

Allyl radical (6-31G*)

1\1\DALHOUSIE-LINUS\SP\UHF\6-31G(D)\C3H5(2)\XYD\29-JAN-91\0\#N
 6-31G* POP=REGULAR\allyl radical\0,2\C\H,1,1.07802\C,1,1.39048,2,
 117.72027\C,1,1.39048,2,117.72027,3,180.,0\H,3,1.07415,1,121.41143,2,0.,0\H,4,1
 .07415,1,121.41143,2,0.,0\H,3,1.0757,1,121.18332,2,180.,0\H,4,1.0757,1,121.1833
 2,2,180.,0\Version=Stellar-Stellix-G86RevC\State=2-A2\HF=-116.4680998\S2=0.
 973\S2-1=0.\S2A=0.758\RMSD=6.666e-10\Dipole=0.,0.,0.0163628\PG=C02V
 [C2(H1C1),SGV(C2H4)]\@

Allyl radical (MP2/6-31G*)

1\1\DALHOUSIE-LINUS\SP\UMP2-FC\6-31G(D)\C3H5(2)\XYD\26-FEB-91\0\#N
 MP2/6-31G* POP=REGULAR\allyl radical
 mp2/6-31G*\0,2\C\H,1,1.07802\C,1,1.39048,2,117.72027\C,1,1.39048,2,117.72027
 ,3,180.,0\H,3,1.07415,1,121.41143,2,0.,0\H,4,1.07415,1,121.41143,2,0.,0\H,3,1.07
 57,1,121.18332,2,180.,0\H,4,1.0757,1,121.18332,2,180.,0\Version=Stellar-Stellix-
 G86RevC\State=2-A2\HF=-116.4680998\MP2=-116.809641\S2=0.973\S2-1=0.905
 \S2A=0.758\RMSD=6.666e-10\PG=C02V [C2(H1C1),SGV(C2H4)]\@

Allyl cation (MP2/6-31G*)

1\1\DALHOUSIE-LINUS\SP\RMP2-FC\6-31G(D)\C3H5(1+)\XYD\26-FEB-91\0\#
 N MP2/6-31G*\allyl cation mp2/6-31G*\1,1\C\H,1,1.07338\C,1,1.37302,
 2,120.97356\C,1,1.37302,2,120.97356,3,180.,0\H,3,1.07573,1,121.53201,2,0.,0\H,3
 ,1.07593,1,121.56342,2,180.,0\H,4,1.07573,1,121.53201,2,0.,0\H,4,1.07593,1,121.
 56342,2,180.,0\Version=Stellar-Stellix-G86RevC\State=1-A1\HF=-116.1932129\M
 P2=-116.5430141\RMSD=8.194e-10\PG=C02V [C2(C1H1),SGV(C2H4)]\@

Methyl radical (MP2/6-31G*)

1\1\DALHOUSIE-LINUS\SP\UMP2-FC\6-31G(D)\C1H3(2)\XYD\26-FEB-91\0\#N
 MP2/6-31G* POP=REGULAR\methyl radical mp2/6-31G*\0,2\
 C\X,1,1.\H,1,1.07258,2,90.07587\H,1,1.07258,2,90.07587,3,120.,0\H,1,1.07258,2,
 90.07587,3,-120.,0\Version=Stellar-Stellix-G86RevC\HF=-39.558992\MP2=-39.66
 86691\S2=0.761\S2-1=0.753\S2A=0.75\RMSD=4.971e-10\PG=C03V
 [C3(C1),3SGV(H1)]\@

Methyl cation (MP2/6-31G*)

1\1\DALHOUSIE-LINUS\SP\RMP2-FC\6-31G(D)\C1H3(1+)\XYD\26-FEB-91\0\#
 N MP2/6-31G* POP=REGULAR\methyl cation\1,1\C\H,1,1.07837\H,1,1.07837,2,
 120.\H,1,1.07837,2,120.,3,180.,0\Version=Stellar-Stellix-G86RevC\HF=-39.23063
 99\MP2=-39.3251423\RMSD=8.483e-11\PG=D03H[O(C1),3C2(H1)]\@.

Tertiary butyl radical (STO-3G)

1\1\UNK-DAL1\FOPT\UHF\STO-3G\C4H9(2)\XYD\14-JAN-1990\1\#N STO-DG
 OPT POP=REGULAR OPTCYC=60\t-butyl radical\0,2\C\X,1,1.\C,1,r1,2, a1

```

\C,1,r1,2,a1,3,120.,0\C,1,r1,2,a1,3,-120.,0\H,3,r2,1,a2,2,180.,0
\H,3,r3,1,a3,2,b1,0\H,3,r3,1,a3,2,-b1,0\H,4,r2,1,a2,2,180.,0\H,4,r3,1,
a3,2,b1,0\H,4,r3,1,a3,2,-b1,0\H,5,r2,1,a2,2,180.,0
\H,5,r3,1,a3,2,b1,0\H,5,r3,1,a3,2,-b1,0\r1=1.523744\r2=1.089613\r3=
1.086319\A1=98.295009 \A2=111.238635\A3=110.842095\B1=60.159285\
Version=VAX-VMS-G86RevC\State=2-A1\HF=-154.8354893\S2=0.765\S2-
1=0.\S2A=0.75\RMSD=.758D-09\RMSF=0.332D-04\Dipole=0.,0,-0.067594
\PG=C03V [C3(C1),3SGV(C1H1),X(H6)]\@

```

Tertiary butyl cation (STO-3G)

```

1\1\UNK-DAL1\FOPT\RHF\STO-3G\C4H9(1+)\XYD\22-JAN-1990\1\#\P STO-DG
OPT POP=REGULAR OPTCYC=60\t-butyl cation\0,2\C\X,1,1.\C,1,r1,2, a1
\C,1,r1,2,a1,3,120.,0\C,1,r1,2,a1,3,-120.,0\H,3,r2,1,a2,2,180.,0\
H,3,r3,1,a3,2,b1,0\H,3,r3,1,a3,2,-b1,0\H,4,r2,1,a2,2,180.,0\
H,4,r3,1,a3,2,b1,0\H,4,r3,1,a3,2,-b1,0\H,5,r2,1,a2,2,180.,0\H,5,r3,1,
a3,2,b1,0\H,5,r3,1,a3,2,-b1,0\r1=1.51407\r2=1.097525\r3=1.087745\
A1=91.610452 \A2=105.550368\A3=111.231018\B1=62.557642\Version=VAX-
VMS-G86RevC\State=1-A1\HF=-154.6376569\RMSD=0.464D-09\RMSF=0.983D-
05\Dipole=0.,0,-0.1710198\PG=C03V [C3(C1),3SGV(C1H1),X(H6)]\@

```

The cleavage process of the 1-butene radical cation (46⁺)

```

1\1\DALHOUSIE-LINUS\FOPT\UHF\STO-3G\C4H8(1+,2)\XYD\28-JAN-91\1\#\N
STO-3G OPT POP=REGULAR\1-butene radical cation C3-C4 is
fixed\1,2\C\C,1,r1\C,1,r2,2,a1\C,3,1.6363,1,a2,2,b1,0\H,2,r3,1,a3,3,b2,0\H,2,r4,1,
a4,3,b3,0\H,1,r5,2,a5,6,b4,0\X,3,r6,1,a6,2,b5,0\H,3,r7,8,a7,1,b6,0\H,3,r8,8,a8,1,b
7,0\X,4,r9,3,a9,1,b8,0\H,4,r10,11,a10,3,b9,0\H,4,r11,11,a11,3,b10,0\H,4,r12,3,a12
,1,b11,0\r1=1.436232\r2=1.498721\r3=1.094843\r4=1.094946\r5=1.103765\r6=
1.\r7=1.091122\r8=1.088464\r9=1.\r10=1.086966\r11=1.086962\r12=1.087078\A
1=124.171491\A2=107.260479\A3=120.466667\A4=120.716025\A5=117.456157\A6
=128.450295\A7=54.224752\A8=56.837008\A9=127.174115\A10=55.448979\A11=5
5.012517\A12=106.509731\B1=100.268218\B2=1.200057\B3=180.857909\B4=-1.91
0565\B5=-83.615427\B6=86.904991\B7=-91.876405\B8=-0.775009\B9=90.24325\B
10=-89.652902\B11=178.877513\Version=Stellar-Stellix-G86RevC\HF=-153.9888
559\S2=0.756\S2-1=0.\S2A=0.75\RMSD=6.203e-10\RMSF=8.982e-03\Dipole=-0
.8687223,0.4980918,0.9238795\PG=C01 [X(C4H8)]\@

```

```

1\1\DALHOUSIE-LINUS\FOPT\UHF\STO-3G\C4H8(1+,2)\XYD\26-JAN-91\1\#\N
STO-3G OPT POP=REGULAR\1-butene radical cation C3-C4 is
fixed\1,2\C\C,1,r1\C,1,r2,2,a1\C,3,1.714,1,a2,2,b1,0\H,2,r3,1,a3,3,b2,0\H,2,r4,1,a
4,3,b3,0\H,1,r5,2,a5,6,b4,0\X,3,r6,1,a6,2,b5,0\H,3,r7,8,a7,1,b6,0\H,3,r8,8,a8,1,b7,

```

0\X,4,r9,3,a9,1,b8,0\H,4,r10,11,a10,3,b9,0\H,4,r11,11,a11,3,b10,0\H,4,r12,3,a12,1,b11,0\|r1=1.436449\r2=1.484814\r3=1.093932\r4=1.094027\r5=1.103232\r6=1.\r7=1.089762\r8=1.088203\r9=1.\r10=1.087359\r11=1.087435\r12=1.087738\|a1=124.005364\|a2=105.103083\|a3=120.468949\|a4=120.658905\|a5=117.47806\|a6=130.266354\|a7=55.72161\|a8=56.482337\|a9=126.628454\|a10=56.107809\|a11=55.302495\|a12=105.237845\|b1=95.883356\|b2=0.767768\|b3=180.151392\|b4=-3.176562\|b5=-86.388039\|b6=89.363274\|b7=-92.126905\|b8=-1.10478\|b9=89.926607\|b10=-89.168072\|b11=178.347682\|Version=Stellar-Stellix-G86RevC\HF=-153.9811825\|S2=0.757\|S2-1=0.\|S2A=0.75\|RMSD=6.035e-10\|RMSF=1.516e-02\|Dipole=-0.7943561,0.4322887,0.7713783\|PG=C01 [X(C4H8)]\|@

1\|DALHOUSIE-LINUS\FOPT\UHF\STO-3G\C4H8(1+,2)\XYD\26-JAN-91\|1\|#N STO-3G OPT POP=REGULAR\|1-butene radical cation C3-C4 is fixed\|1,2\C,1,r1\C,1,r2,2,a1\C,3,1.792,1,a2,2,b1,0\H,2,r3,1,a3,3,b2,0\H,2,r4,1,a4,3,b3,0\H,1,r5,2,a5,6,b4,0\X,3,r6,1,a6,2,b5,0\H,3,r7,8,a7,1,b6,0\H,3,r8,8,a8,1,b7,0\X,4,r9,3,a9,1,b8,0\H,4,r10,11,a10,3,b9,0\H,4,r11,11,a11,3,b10,0\H,4,r12,3,a12,1,b11,0\|r1=1.436049\r2=1.466897\r3=1.092712\r4=1.092785\r5=1.102249\r6=1.\r7=1.088792\r8=1.087868\r9=1.\r10=1.087953\r11=1.08806\r12=1.088689\|a1=123.919894\|a2=102.25822\|a3=120.464747\|a4=120.579629\|a5=117.51311\|a6=132.518179\|a7=56.826182\|a8=56.714774\|a9=126.114855\|a10=56.627008\|a11=55.775464\|a12=103.627819\|b1=93.566194\|b2=0.928267\|b3=179.996553\|b4=-3.766548\|b5=-87.917794\|b6=91.580369\|b7=-93.155307\|b8=-1.138447\|b9=89.548085\|b10=-88.801422\|b11=178.284208\|Version=Stellar-Stellix-G86RevC\HF=-153.9705244\|S2=0.761\|S2-1=0.\|S2A=0.75\|RMSD=3.478e-10\|RMSF=1.843e-02\|Dipole=-0.6623421,0.3227714,0.5869501\|PG=C01 [X(C4H8)]\|@

1\|DALHOUSIE-LINUS\FOPT\UHF\STO-3G\C4H8(1+,2)\XYD\27-JAN-91\|1\|#N STO-3G OPT POP=REGULAR\|1-butene radical cation C3-C4 is fixed\|1,2\C,1,r1\C,1,r2,2,a1\C,3,1.84,1,a2,2,b1,0\H,2,r3,1,a3,3,b2,0\H,2,r4,1,a4,3,b3,0\H,1,r5,2,a5,6,b4,0\X,3,r6,1,a6,2,b5,0\H,3,r7,8,a7,1,b6,0\H,3,r8,8,a8,1,b7,0\X,4,r9,3,a9,1,b8,0\H,4,r10,11,a10,3,b9,0\H,4,r11,11,a11,3,b10,0\H,4,r12,3,a12,1,b11,0\|r1=1.434909\r2=1.453345\r3=1.091712\r4=1.091788\r5=1.101161\r6=1.\r7=1.088367\r8=1.087769\r9=1.\r10=1.088392\r11=1.088564\r12=1.089492\|a1=123.828734\|a2=99.962176\|a3=120.536714\|a4=120.499422\|a5=117.585786\|a6=134.239\|a7=57.48368\|a8=57.082333\|a9=125.872889\|a10=57.006737\|a11=56.073039\|a12=102.308449\|b1=92.6873\|b2=0.81566\|b3=179.814507\|b4=-4.013199\|b5=-88.520704\|b6=93.170971\|b7=-94.224357\|b8=-1.234906\|b9=89.349106\|b10=-88.556759\|b11=178.149103\|Version=Stellar-Stellix-G86RevC\HF=-153.9633039\|S2=0.77\|S2-1=0.\|S2A=0.75\|RMSD=4.291e-10\|RMSF=1.888e-02\|Dipole=-0.5418149,0.2242449,0.4397771\|PG=C01 [X(C4H8)]\|@

1\|DALHOUSIE-LINUS\FOPT\UHF\STO-3G\C4H8(1+,2)\XYD\01-FEB-91\|1\|#N STO-3G OPT POP=REGULAR\|1-butene radical cation C3-C4 is fixed\|1,2\C,1,r1\C,1,r2,2,a1\C,3,2.02,1,a2,2,b1,0\H,2,r3,1,a3,3,b2,0\H,2,r4,1,a4,3,b3,0\H,1

,r5,2,a5,6,b4,0\X,3,r6,1,a6,2,b5,0\H,3,r7,8,a7,1,b6,0\H,3,r8,8,a8,1,b7,0\X,4,r9,3,a9,1,b8,0\H,4,r10,11,a10,3,b9,0\H,4,r11,11,a11,3,b10,0\H,4,r12,3,a12,1,b11,0\|r1=1.421091\r2=1.417056\r3=1.088453\r4=1.088374\r5=1.094519\r6=1.\r7=1.090107\r8=1.089964\r9=1.\r10=1.09022\r11=1.090423\r12=1.092096\|a1=123.29157\|a2=93.174303\|a3=120.884465\|a4=120.453812\|a5=118.409927\|a6=140.99805\|a7=59.176565\|a8=59.201808\|a9=123.66856\|a10=58.214508\|a11=57.319482\|a12=96.68704\|b1=93.327413\|b2=0.519215\|b3=178.993901\|b4=-2.930408\|b5=-88.25823\|b6=98.302794\|b7=-99.02469\|b8=-1.350948\|b9=88.970795\|b10=-88.199899\|b11=178.0472\|Version=Stellar-Stellix-G86RevC\HF=-153.9390928\|S2=0.89\|S2-1=0.\|S2A=0.753\|RMSD=5.474e-10\|RMSF=1.437e-02\|Dipole=-0.0157901,-0.1617668,-0.1229378\|PG=C01 [X(C4H8)]\|@

1\1\DALHOUSIE-LINUS\FOPT\UHF\STO-3G\C4H8(1+,2)\XYD\01-FEB-91\1\#\N
STO-3G OPT POP=REGULAR\|1-butene radical cation C3-C4 is
fixed\|1,2\C\C,1,r1\C,1,r2,2,a1\C,3,2.18,1,a2,2,b1,0\H,2,r3,1,a3,3,b2,0\H,2,r4,1,a4,3,b3,0\H,1,r5,2,a5,6,b4,0\X,3,r6,1,a6,2,b5,0\H,3,r7,8,a7,1,b6,0\H,3,r8,8,a8,1,b7,0\X,4,r9,3,a9,1,b8,0\H,4,r10,11,a10,3,b9,0\H,4,r11,11,a11,3,b10,0\H,4,r12,3,a12,1,b11,0\|r1=1.407653\r2=1.412542\r3=1.08849\r4=1.088394\r5=1.091248\r6=1.\r7=1.092902\r8=1.092843\r9=1.\r10=1.089732\r11=1.089891\r12=1.090915\|a1=122.58878\|a2=94.528207\|a3=121.181962\|a4=120.602681\|a5=119.098272\|a6=143.562897\|a7=59.801512\|a8=60.258241\|a9=121.654133\|a10=58.88226\|a11=57.998262\|a12=95.250345\|b1=94.436738\|b2=0.0536\|b3=178.74647\|b4=-1.729455\|b5=-87.794602\|b6=100.171404\|b7=-101.213667\|b8=-1.378617\|b9=87.620914\|b10=-86.80367\|b11=178.026358\|Version=Stellar-Stellix-G86RevC\HF=-153.9226824\|S2=0.992\|S2-1=0.\|S2A=0.757\|RMSD=9.847e-10\|RMSF=1.136e-02\|Dipole=0.1548231,-0.1240867,-0.2222019\|PG=C01 [X(C4H8)]\|@

1\1\DALHOUSIE-LINUS\FOPT\UHF\STO-3G\C4H8(1+,2)\XYD\28-JAN-91\1\#\N
STO-3G OPT POP=REGULAR\|1-butene radical cation C3-C4 is
fixed\|1,2\C\C,1,r1\C,1,r2,2,a1\C,3,2.3376,1,a2,2,b1,0\H,2,r3,1,a3,3,b2,0\H,2,r4,1,a4,3,b3,0\H,1,r5,2,a5,6,b4,0\X,3,r6,1,a6,2,b5,0\H,3,r7,8,a7,1,b6,0\H,3,r8,8,a8,1,b7,0\X,4,r9,3,a9,1,b8,0\H,4,r10,11,a10,3,b9,0\H,4,r11,11,a11,3,b10,0\H,4,r12,3,a12,1,b11,0\|r1=1.400241\r2=1.410027\r3=1.090211\r4=1.090231\r5=1.090322\r6=1.\r7=1.095141\r8=1.095125\r9=1.\r10=1.087008\r11=1.087127\r12=1.087738\|a1=121.865996\|a2=95.136431\|a3=121.352286\|a4=120.730669\|a5=119.549431\|a6=145.444282\|a7=60.496193\|a8=61.271441\|a9=121.556196\|a10=59.065486\|a11=58.379998\|a12=95.047272\|b1=95.040053\|b2=-0.671144\|b3=178.29193\|b4=-1.263616\|b5=-87.765233\|b6=101.838749\|b7=-103.176552\|b8=-1.154071\|b9=86.614197\|b10=-85.599308\|b11=178.290451\|Version=Stellar-Stellix-G86RevC\HF=-153.9103039\|S2=1.046\|S2-1=0.\|S2A=0.759\|RMSD=6.105e-10\|RMSF=8.079e-03\|Dipole=0.1043363,0.2464747,-0.0355212\|PG=C01 [X(C4H8)]\|@

The cleavage process of the radical cation of 4,4-dimethyl-1-pentene (47⁺)

1\1\DALHOUSIE-LINUS\POPT\UHF\STO-3G\C7H14(1+,2)\XYD\28-JAN-91\1\#\#
 N STO-3G OPT POP=REGULAR\T-BUTYLBUTENE radical cation C6-C9 is
 fixed\1,2\C\H,1,R1\H,1,R2,2,A1\C,1,R3,2,A2,3,B1,0\H,4,R4,1,A3,3,B2,0\C,4,R5,
 1,A4,3,B3,0\H,6,R6,4,A5,1,B4,0\H,6,R7,4,A6,1,B5,0\C,6,1.6737,4,A7,1,B6,0\C,9,
 R9,6,A8,4,B7,0\C,9,R10,6,A9,4,B8,0\C,9,R11,6,A10,4,B9,0\H,10,R12,9,A11,6,B1
 0,0\H,10,R13,9,A12,6,B11,0\H,10,R14,9,A13,6,B12,0\H,11,R15,9,A14,6,B13,0\H,
 11,R16,9,A15,6,B14,0\H,11,R17,9,A16,6,B15,0\H,12,R18,9,A17,6,B16,0\H,12,R19
 ,9,A18,6,B17,0\H,12,R20,9,A19,6,B18,0\|R1=1.093484\R2=1.093217\R3=1.43654
 3\R4=1.102266\R5=1.483429\R6=1.087393\R7=1.089727\R9=1.548937\R10=1.5
 48809\R11=1.548773\R12=1.085593\R13=1.086254\R14=1.085537\R15=1.08563
 5\R16=1.085872\R17=1.085958\R18=1.085715\R19=1.085775\R20=1.085531\A1
 =118.857363\A2=120.693401\A3=117.138093\A4=124.198029\A5=110.939889\A
 6=109.094817\A7=110.541622\A8=104.834446\A9=109.512764\A10=109.624255
 \A11=110.949053\A12=108.966455\A13=110.895705\A14=108.922598\A15=111.
 072322\A16=111.667833\A17=108.843137\A18=111
 .01532\A19=111.76277\B1=179.342188\B2=181.428273\B3=-0.177499\B4=20.46
 1271\B5=143.279132\B6=260.195938\B7=180.772404\B8=62.135777\B9=-60.441
 104\B10=-60.258028\B11=180.378258\B12=61.034605\B13=173.818206\B14=54.
 841866\B15=-67.176775\B16=187.304768\B17=-53.719094\B18=68.248277\|Versi
 on=Stellar-Stellix-G86RevC\HF=-269.733211\S2=0.757\S2-1=0.\S2A=0.75\RMS
 D=9.976e-10\RMSF=5.293e-03\Dipole=0.7372703,-1.438079,2.0884595\PG=C01
 [X(C7H14)]\@

1\1\DALHOUSIE-LINUS\POPT\UHF\STO-3G\C7H14(1+,2)\XYD\27-JAN-91\1\#\#
 N STO-3G OPT POP=REGULAR\T-BUTYLBUTENE radical cation C6-C9 is
 fixed\1,2\C\H,1,R1\H,1,R2,2,A1\C,1,R3,2,A2,3,B1,0\H,4,R4,1,A3,3,B2,0\C,4,R5,
 1,A4,3,B3,0\H,6,R6,4,A5,1,B4,0\H,6,R7,4,A6,1,B5,0\C,6,1.7534,4,A7,1,B6,0\C,9,
 R9,6,A8,4,B7,0\C,9,R10,6,A9,4,B8,0\C,9,R11,6,A10,4,B9,0\H,10,R12,9,A11,6,B1
 0,0\H,10,R13,9,A12,6,B11,0\H,10,R14,9,A13,6,B12,0\H,11,R15,9,A14,6,B13,0\H,
 11,R16,9,A15,6,B14,0\H,11,R17,9,A16,6,B15,0\H,12,R18,9,A17,6,B16,0\H,12,R19
 ,9,A18,6,B17,0\H,12,R20,9,A19,6,B18,0\|R1=1.091984\R2=1.091692\R3=1.43494
 5\R4=1.100872\R5=1.461346\R6=1.086821\R7=1.088224\R9=1.547413\R10=1.5
 46644\R11=1.546813\R12=1.085489\R13=1.087045\R14=1.08546\R15=1.086362\
 R16=1.085811\R17=1.085554\R18=1.086443\R19=1.08574\R20=1.085372\A1=1
 18.850152\A2=120.639093\A3=117.165528\A4=124.111299\A5=112.479954\A6=
 111.101457\A7=108.758685\A8=103.518948\A9=109.038064\A10=108.814719\A
 11=111.06799\A12=108.516278\A13=111.012329\A14=108.450472\A15=111.149
 331\A16=111.76902\A17=108.443123\A18=111.091238\A19=111.789845\B1=179
 .278151\B2=182.907188\B3=0.762601\B4=21.232013\B5=148.261779\B6=263.09
 1696\B7=180.610437\B8=62.068603\B9=-60.797441\B10=-60.288113\B11=180.5
 43809\B12=61.385902\B13=173.104926\B14=54.394866\B15=-68.039354\B16=18
 7.944527\B17=-53.296416\B18=69.010383\|Version=Stellar-Stellix-G86RevC\HF=
 -269.7274675\S2=0.763\S2-1=0.\S2A=0.75\RMSD=8.749e-10\RMSF=7.807e-03\

Dipole=0.5500181,-1.2697446,1.7942828\PG=C01 [X(C7H14)]\@G=C01
[X(C4H8)]\@

1\DALHOUSIE-LINUS\POPT\UHF\STO-3G\C7H14(1+,2)\XYD\27-JAN-91\
fixed\1,2\C\H,1,R1\H,1,R2,2,A1\C,1,R3,2,A2,3,B1,0\H,4,R4,1,A3,3,B2,0\C,4,R5,
1,A4,3,B3,0\H,6,R6,4,A5,1,B4,0\H,6,R7,4,A6,1,B5,0\C,6,1.9128,4,A7,1,B6,0\C,9,
R9,6,A8,4,B7,0\C,9,R10,6,A9,4,B8,0\C,9,R11,6,A10,4,B9,0\H,10,R12,9,A11,6,B1
0,0\H,10,R13,9,A12,6,B11,0\H,10,R14,9,A13,6,B12,0\H,11,R15,9,A14,6,B13,0\H,
11,R16,9,A15,6,B14,0\H,11,R17,9,A16,6,B15,0\H,12,R18,9,A17,6,B16,0\H,12,R19
,9,A18,6,B17,0\H,12,R20,9,A19,6,B18,0\|R1=1.087139\R2=1.086947\R3=1.41337
1\R4=1.091966\R5=1.419625\R6=1.087553\R7=1.087773\R9=1.543204\R10=1.5
40206\R11=1.540686\R12=1.085563\R13=1.089545\R14=1.085471\R15=1.08901
5\R16=1.085852\R17=1.084877\R18=1.089051\R19=1.085919\R20=1.085001\A1
=118.269733\A2=120.644118\A3=118.148556\A4=123.503385\A5=116.701094\A
6=116.107322\A7=105.754069\A8=99.806559\A9=106.754874\A10=106.359132\
A11=111.498109\A12=106.887478\A13=111.512075\A14=106.947919\A15=111.
418814\A16=111.83505\A17=107.029886\A18=111.416521\A19=111.793852\B1=
177.892911\B2=181.51372\B3=0.034629\B4=16.394578\B5=156.721158\B6=264.
778529\B7=181.950172\B8=63.56527\B9=-59.578136\B10=-61.0964\B11=180.51
9187\B12=62.117434\B13=171.221519\B14=53.219893\B15=-70.348603\B16=189
.723834\B17=-52.161126\B18=71.259816\|Version=Stellar-Stellix-G86RevC\HF=-
269.7164959\S2=0.9\S2-1=0.\S2A=0.753\RMSD=1.407e-10\RMSF=4.354e-03\Di
pole=0.1479595,-0.5414856,0.5462699\PG=C01 [X(C7H14)]\@

1\DALHOUSIE-LINUS\POPT\UHF\STO-3G\C7H14(1+,2)\XYD\02-FEB-91\1\#\#
N STO-3G OPT POP=REGULAR\T-BUTYLBUTENE radical cation C6-C9 is
fixed\1,2\C\H,1,R1\H,1,R2,2,A1\C,1,R3,2,A2,3,B1,0\H,4,R4,1,A3,3,B2,0\C,4,R5,
1,A4,3,B3,0\H,6,R6,4,A5,1,B4,0\H,6,R7,4,A6,1,B5,0\C,6,2.1,4,A7,1,B6,0\C,9,R9,
6,A8,4,B7,0\C,9,R10,6,A9,4,B8,0\C,9,R11,6,A10,4,B9,0\H,10,R12,9,A11,6,B10,0\
H,10,R13,9,A12,6,B11,0\H,10,R14,9,A13,6,B12,0\H,11,R15,9,A14,6,B13,0\H,11,R
16,9,A15,6,B14,0\H,11,R17,9,A16,6,B15,0\H,12,R18,9,A17,6,B16,0\H,12,R19,9,A
18,6,B17,0\H,12,R20,9,A19,6,B18,0\|R1=1.08492\R2=1.085037\R3=1.401017\R4
=1.087394\R5=1.419547\R6=1.087905\R7=1.087685\R9=1.535903\R10=1.53349
4\R11=1.534252\R12=1.085737\R13=1.09142\R14=1.085681\R15=1.091313\R16
=1.086027\R17=1.085104\R18=1.091289\R19=1.08617\R20=1.085149\A1=117.8
29939\A2=120.814167\A3=118.806127\A4=123.185005\A5=118.336327\A6=118.
113083\A7=105.332447\A8=97.814783\A9=103.229608\A10=103.250859\A11=1
11.659333\A12=106.183387\A13=111.654896\A14=106.17677\A15=111.548161\
A16=111.769459\A17=106.241724\A18=111.529805\A19=111.76174\B1=177.979
446\B2=179.785048\B3=-0.819938\B4=12.771536\B5=160.541885\B6=264.96528
9\B7=183.428558\B8=64.548691\B9=-57.571902\B10=-60.455214\B11=181.6159
21\B12=63.591451\B13=173.710513\B14=55.990749\B15=-68.191601\B16=188.7
89995\B17=-53.519782\B18=70.576466\|Version=Stellar-Stellix-G86RevC\HF=-26
9.7081658\S2=1.001\S2-1=0.\S2A=0.759\RMSD=6.184e-10\RMSF=4.312e-03\Di

pole=-0.0579958,0.0138576,-0.1347551\PG=C01 [X(C7H14)]\#@

1\DALHOUSIE-LINUS\POPT\UHF\STO-3G\C7H14(1+,2)\XYD\31-JAN-91\1\#
 N STO-3G OPT POP=REGULAR\T-BUTYLBUTENE radical cation C6-C9 is
 fixed\1,2\C\H,1,R1\H,1,R2,2,A1\C,1,R3,2,A2,3,B1,0\H,4,R4,1,A3,3,B2,0\C,4,R5,
 1,A4,3,B3,0\H,6,R6,4,A5,1,B4,0\H,6,R7,4,A6,1,B5,0\C,6,2.391,4,A7,1,B6,0\C,9,R
 9,6,A8,4,B7,0\C,9,R10,6,A9,4,B8,0\C,9,R11,6,A10,4,B9,0\H,10,R12,9,A11,6,B10,
 0\H,10,R13,9,A12,6,B11,0\H,10,R14,9,A13,6,B12,0\H,11,R15,9,A14,6,B13,0\H,11
 ,R16,9,A15,6,B14,0\H,11,R17,9,A16,6,B15,0\H,12,R18,9,A17,6,B16,0\H,12,R19,9,
 A18,6,B17,0\H,12,R20,9,A19,6,B18,0\R1=1.082902\R2=1.083277\R3=1.401358\
 R4=1.085417\R5=1.415045\R6=1.08463\R7=1.084188\R9=1.52609\R10=1.5244
 09\R11=1.525231\R12=1.086313\R13=1.094527\R14=1.08618\R15=1.094596\R1
 6=1.08651\R17=1.085884\R18=1.094608\R19=1.086615\R20=1.085813\A1=117.
 592305\A2=121.057659\A3=118.536404\A4=123.607942\A5=119.51665\A6=119.
 625928\A7=104.311408\A8=94.569009\A9=98.840815\A10=98.631361\A11=111.
 650882\A12=105.261622\A13=111.712068\A14=105.245531\A15=111.544658\A1
 6=111.702883\A17=105.268425\A18=111.549888\A19=111.725874\B1=178.9948
 89\B2=179.724623\B3=-0.992858\B4=10.569683\B5=165.900343\B6=266.600426
 \B7=i8i.053769\B8=61.643443\B9=-59.462603\B10=-61.659579\B11=180.92774
 3\B12=63.369318\B13=175.561643\B14=58.264088\B15=-66.745946\B16=185.88
 7824\B17=-56.87427\B18=68.166129\Version=Stellar-Stellix-G86RevC\HF=-269.
 6975001\S2=1.056\S2-1=0.\S2A=0.765\RMSD=3.918e-10\RMSF=2.025e-03\Dipole
 le=-0.2840483,1.0541115,-0.7770542\PG=C01 [X(C7H14)]\#@

1\DALHOUSIE-LINUS\POPT\UHF\STO-3G\C7H14(1+,2)\XYD\31-JAN-91\1\#
 N STO-3G OPT POP=REGULAR\T-BUTYLBUTENE radical cation C6-C9 is fixed
 \1,2\C\H,1,R1\H,1,R2,2,A1\C,1,R3,2,A2,3,B1,0\H,4,R4,1,A3,3,B2,0\C,4,R5,1,A4
 ,3,B3,0\H,6,R6,4,A5,1,B4,0\H,6,R7,4,A6,1,B5,0\C,6,2.6856,4,A7,1,B6,0\C,9,R9,6
 ,A8,4,B7,0\C,9,R10,6,A9,4,B8,0\C,9,R11,6,A10,4,B9,0\H,10,R12,9,A11,6,B10,0\H
 ,10,R13,9,A12,6,B11,0\H,10,R14,9,A13,6,B12,0\H,11,R15,9,A14,6,B13,0\H,11,R1
 6,9,A15,6,B14,0\H,11,R17,9,A16,6,B15,0\H,12,R18,9,A17,6,B16,0\H,12,R19,9,A1
 8,6,B17,0\H,12,R20,9,A19,6,B18,0\R1=1.081939\R2=1.082494\R3=1.40409\R4=
 1.084902\R5=1.409256\R6=1.082528\R7=1.082052\R9=1.518842\R10=1.518115\
 R11=1.518838\R12=1.087425\R13=1.096495\R14=1.086515\R15=1.096375\R16
 =1.086469\R17=1.087575\R18=1.096349\R19=1.087664\R20=1.086308\A1=117.
 500016\A2=121.174938\A3=118.185057\A4=123.862848\A5=120.488971\A6=12
 0.627388\A7=102.667213\A8=92.293488\A9=94.93756\A10=95.723834\A11=111
 .247222\A12=105.04777\A13=111.775983\A14=105.158581\A15=111.730678\A1
 6=111.052084\A17=105.152829\A18=111.099568\A19=111.749765\B1=177.8032
 89\B2=178.647609\B3=-2.099138\B4=7.682302\B5=171.137501\B6=268.00676\B
 7=187.43493\B8=67.615451\B9=-52.782113\B10=-57.040477\B11=186.156071\B
 12=68.277287\B13=185.049935\B14=66.990624\B15=-58.13182\B16=188.827661
 \B17=-54.462433\B18=70.707399\Version=Stellar-Stellix-C86RevC\HF=-269.694
 8364\S2=1.085\S2-1=0.\S2A=0.769\RMSD=3.616e-10\RMSF=1.360e-04\Dipole

=-0.4192906,1.8098199,-1.0934541\PG=C01 [X(C7H14)]\@

Structure 69 (the radical cation of 2-carene)

1\1\GINC-LINUS\FOPT\UHF\STO-3G\C10H16(1+,2)\XYD\21-Aug-1991\1\#N
 STO-3G OPT=READFC GEOM=CHECKPOINT GUESS=READ OPTCYC=300
 SCFCYC=150\radical cation of 2-carene\1,2\C\C,1,r1\C,2,r2,1,a1\C,3,r3,2,a2,1,
 b1,0\C,4,r4,3,a3,2,b2,0\C,5,r5,4,a4,3,b3,0\C,5,r6,4,a5,3,b4,0\C,7,r7,5,a6,4,b5,0\C,
 7,r8,5,a7,4,b6,0\C,2,r9,3,a8,1,b7,0\H,1,r10,2,a9,3,b8,0\H,3,r11,2,a10,1,b9,0\H,3,r
 12,2,a11,1,b10,0\H,4,r13,3,a12,2,b11,0\H,4,r14,3,a13,2,b12,0\H,5,r15,4,a14,3,b13,
 0\H,6,r16,5,a15,4,b14,0\H,10,r17,2,a16,3,b15,0\H,10,r18,2,a17,3,b16,0\H,10,r19,2,
 a18,3,b17,0\H,8,r20,7,a19,5,b18,0\H,8,r21,7,a20,5,b19,0\H,8,r22,7,a21,5,b20,0\H,
 9,r23,7,a22,5,b21,0\H,9,r24,7,a23,5,b22,0\H,9,r25,7,a24,5,b23,0\|r1=1.425093\r2
 =1.52625\r3=1.550116\r4=1.540778\r5=1.52862\r6=1.497013\r7=1.535334\r8=1
 .536069\r9=1.518753\r10=1.095608\r11=1.094562\r12=1.088436\r13=1.087463\r
 14=1.087322\r15=1.084608\r16=1.082567\r17=1.085687\r18=1.08966\r19=1.090
 871\r20=1.086925\r21=1.086574\r22=1.083893\r23=1.08731\r24=1.085214\r25=
 1.086686\|a1=118.660965\|a2=114.834314\|a3=114.457156\|a4=119.122039\|a5=120.
 842151\|a6=122.052966\|a7=117.954579\|a8=119.479669\|a9=118.105491\|a10=104.
 987796\|a11=109.261441\|a12=109.070361\|a13=107.612861\|a14=114.579463\|a15=
 120.238817\|a16=111.729797\|a17=109.311887\|a18=108.662347\|a19=108.873862\|a
 20=109.978349\|a21=112.827659\|a22=109.019389\|a23=111.170568\|a24=110.4607
 16\|b1=36.404397\|b2=-37.243159\|b3=18.549196\|b4=92.511855\|b5=-1.19466\|b6=
 148.115058\|b7=173.624764\|b8=161.848991\|b9=-84.201075\|b10=161.28931\|b11=
 86.058192\|b12=-158.224369\|b13=-121.402206\|b14=-147.247469\|b15=190.109048\
 b16=-48.010485\|b17=69.297152\|b18=87.91075\|b19=-153.841765\|b20=-32.361633
 \b21=-92.30983\|b22=27.486167\|b23=148.664728\|Version=Stellar-Stellix-G90Rev
 H\HF=-383.1693524\|S2=0.759\|S2-1=0.\|S2A=0.75\|RMSD=1.323e-09\|RMSF=7.1
 29e-05\|Dipole=-0.9950807,-0.8790369,0.5531641\PG=C01 [X(C10H16)]\@

Structure 70 (2-carene)

1\1\GINC-LINUS\FOPT\RHF\STO-3G\C10H16\XYD\10-Jun-1992\1\#N STO-3G
 OPT POP=REGULAR\carene-cis, from pmodel\0,1\C\C,1,r1\C,2,r2,1,a1\C,3,r
 3,2,a2,1,b1,0\C,2,r4,3,a3,1,b2,0\C,5,r5,2,a4,3,b3,0\C,6,r6,5,a5,2,b4,0\C,7,r7,6,a6,
 5,b5,0\C,8,r8,7,a7,6,b6,0\C,8,r9,7,a8,6,b7,0\H,5,r10,2,a9,3,b8,0\H,5,r11,2,a10,3,b
 9,0\H,6,r12,5,a11,2,b10,0\H,6,r13,5,a12,2,b11,0\H,7,r14,6,a13,5,b12,0\H,4,r15,3,a
 14,2,b13,0\H,3,r16,2,a15,1,b14,0\H,1,r17,2,a16,3,b15,0\H,1,r18,2,a17,3,b16,0\H,1,
 r19,2,a18,3,b17,0\H,9,r20,8,a19,7,b18,0\H,9,r21,8,a20,7,b19,0\H,9,r22,8,a21,7,b20
 ,0\H,10,r23,8,a22,7,b21,0\H,10,r24,8,a23,7,b22,0\H,10,r25,8,a24,7,b23,0\|r1=1.52
 4426\r2=1.3148\r3=1.50609\r4=1.534262\r5=1.548794\r6=1.537695\r7=1.51605
 7\r8=1.533123\r9=1.535395\r10=1.088148\r11=1.09058\r12=1.08758\r13=1.086
 994\r14=1.082166\r15=1.083858\r16=1.083156\r17=1.085236\r18=1.088014\r19

=1.088074\r20=1.086856\r21=1.086488\r22=1.083882\r23=1.086872\r24=1.086993\r25=1.085383\|a1=122.733197\|a2=122.430069\|a3=121.048216\|a4=112.556063\|a5=111.778712\|a6=122.354466\|a7=120.962531\|a8=116.739205\|a9=109.674099\|a10=108.86635\|a11=109.185764\|a12=108.982245\|a13=114.045572\|a14=114.301197\|a15=120.756531\|a16=111.068996\|a17=110.530422\|a18=110.687348\|a19=110.565896\|a20=109.854525\|a21=111.730054\|a22=110.588242\|a23=110.524426\|a24=110.974393\|b1=-178.60397\|b2=178.441729\|b3=33.400793\|b4=-46.677772\|b5=101.534445\|b6=3.014786\|b7=146.826933\|b8=155.362401\|b9=-88.065714\|b10=-167.806335\|b11=75.784568\|b12=-111.18057\|b13=125.007169\|b14=0.520155\|b15=1.232076\|b16=121.675287\|b17=-119.319974\|b18=78.622397\|b19=-162.263641\|b20=-42.374624\|b21=153.250294\|b22=-87.114794\|b23=33.045947\|Version=Stellar-Stellix-G90RevH\|HF=-383.372767\|RMSD=2.581e-09\|RMSF=6.416e-06\|Dipole=-0.0984385,0.0288779,-0.0355627\|PG=C01 [X(C10H16)]\|@

2,2-Dimethyl-1-vinylcyclopropane (71)

1\|GINC-LINUS\FOPT\UHF\STO-3G\C7H12\XYD\17-Jun-1992\1\|#p OPT
STO-3G\|dimethyl vinylcyclopropane\|0,1\|X\X,1,1.\|C,2,0.9978,1,90.\|C,3,1.5053,2,115.5968,1,45.3848,0\|C,4,1.3103,3,123.9594,2,160.3249,0\|C,2,0.6822,3,128.6581,4,-115.6466,0\|C,2,1.047,3,95.2785,4,109.1117,0\|C,6,1.5339,2,107.9452,1,-31.9116,0\|C,6,1.5346,2,138.7183,1,153.5107,0\|H,7,1.0807,2,111.4251,1,-20.6282,0\|H,7,1.0807,2,133.8611,1,171.2914,0\|H,3,1.0826,2,129.7754,1,209.642,0\|H,4,1.0838,3,116.1924,12,172.8098,0\|H,5,1.0808,4,121.9378,3,179.6082,0\|H,5,1.0811,4,122.1472,3,-0.2855,0\|H,8,1.0843,6,111.6229,2,9.3603,0\|H,8,1.0867,6,109.9653,2,129.3194,0\|H,8,1.0868,6,110.5693,2,248.605,0\|H,9,1.0869,6,110.4767,2,-125.8762,0\|H,9,1.0854,6,110.9394,2,-5.7305,0\|H,9,1.0868,6,110.5218,2,114.4963,0\|Version=Stellar-Stellix-G90RevH\|HF=-268.7698121\|RMSD=3.943e-10\|Dipole=-0.1423409,-0.0158309,0.0581692\|PG=C01 [X(C7H12)]\|@

The radical cation of 2,2-dimethyl-1-vinylcyclopropane (71⁺)

1\|GINC-LINUS\FOPT\UHF\STO-3G\C7H12(1+,2)\XYD\13-Jun-1991\1\|#N OPT
STO-3G\|dimethyl vinyl cyclopropane radical cation\|1,2\|X\X,1,1.\|C,2,1.2315,1,90.\|C,3,1.4167,2,123.1246,1,17.6268,0\|C,4,1.3982,3,122.0992,2,183.3121,0\|C,2,1.4067,3,91.7988,4,-95.9479,0\|C,2,0.3072,3,168.2907,4,111.1099,0\|C,6,1.5266,2,121.5698,1,1.0431,0\|C,6,1.5269,2,120.8116,1,186.8853,0\|H,7,1.0871,2,113.3958,1,-3.5715,0\|H,7,1.0879,2,120.0861,1,137.0023,0\|H,3,1.0875,2,117.8708,1,202.3866,0\|H,4,1.086,3,118.7123,12,177.3665,0\|H,5,1.0845,4,120.7412,3,177.7025,0\|H,5,1.0847,4,121.3167,3,-1.0334,0\|H,8,1.0847,6,112.0932,2,2.7511,0\|H,8,1.0911,6,106.4055,2,121.5533,0\|H,8,1.0879,6,110.9223,2,238.8523,0\|H,9,1.0912,6,106.8086,2,-120.5092,0\|H,9,1.0855,6,111.8004,2,-1.4788,0\|H,9,1.088,6,110.765,2,121.977,0\|Version=Stellar-Stellix-G90RevH\|HF=-268.5644006\|S2=1.043\|S2-1=0.\|S2A=0.772\|RMSD=9.364e-10\|Dipole=-0.29456,0.0252116,0.2114175\|PG=C01 [X(C7H12)]\|@

The radical cation of 2,2-dimethyl-1-(2,2-dimethyl)vinylcyclopane (72⁺)

```
1\1\GINC-LINUS\FOPT\UHF\STO-3G\C9H16(1+,2)\XYD\6-Sep-1991\1\1\#NOPT
STO-3G\radical cation of 1,1-dimethyl-2-(2,2-dimethylvinyl)-cyclopropane\
1,2\X\X,1,1.\C,2,1.2939,1,90.\C,3,1.4077,2,123.4797,1,9.1314,0\C,4,1.4029,3,124.
5254,2,187.6003,0\C,2,1.4483,3,83.5691,4,-97.7363,0\C,2,0.2369,1,90.9526,6,94.5
432,0\C,6,1.5285,2,122.6805,1,7.1122,0\C,6,1.5287,2,120.4405,1,184.8898,0\H,7,1
.0863,2,113.789,1,6.4904,0\H,7,1.087,2,112.9943,1,139.5331,0\H,3,1.0851,2,116.4
554,1,199.6424,0\H,4,1.0859,3,117.7571,12,175.7874,0\C,5,1.5236,4,119.8639,3,17
6.5373,0\C,5,1.5268,4,122.6503,3,-1.236,0\H,8,1.0845,6,112.072,2,-3.1119,0\H,8,1
.09,6,106.8317,2,115.7707,0\H,8,1.0874,6,110.9399,2,233.3635,0\H,9,1.0903,6,107
.2634,2,-114.2746,0\H,9,1.0854,6,111.725,2,4.8713,0\H,9,1.0876,6,110.7593,2,127
.9031,0\H,14,1.0851,5,111.6119,4,-0.0735,0\H,14,1.0886,5,109.7,4,120.8878,0\H,1
4,1.0886,5,109.6807,4,-120.9645,0\H,15,1.089,5,110.24,4,74.2288,0\H,15,1.0863,5
,111.5805,4,-46.2886,0\H,15,1.085,5,109.9189,4,193.3381,0\Version=Stellar-Stelli
x-G90RevH\HF=-345.7414788\S2=0.943\S2-1=0.\S2A=0.76\RMSD=5.399e-10\D
ipole=-0.8869789,0.1779867,0.3927426\PG=C01 [X(C9H16)]\@
```

Appendix 2 X-ray data

A white needle crystal of $C_{26}H_{27}N_3O_7$ (**55**) having approximate dimensions of $0.35 \times 0.25 \times 0.20$ mm was mounted on a glass fiber. All measurements were made on a *Rigaku AFC5R* diffractometer with graphite-monochromated MoK_{α} radiation and a 2.4 kW sealed tube generator. The structure was solved by direct methods.¹³³ All calculations were performed by using *TEXSAN* crystallographic software package of Molecular Structure Corporation.¹³⁴

Table A2.1 Intramolecular Distances (Å) for **55**

O1	C23	1.437(6)
O1	C26	1.392(6)
O2	N1	1.210(6)
O3	N1	1.227(6)
O4	N2	1.223(6)
O5	N2	1.214(6)
O6	C7	1.194(6)
O7	C7	1.327(5)
O7	C8	1.458(5)
N1	C5	1.486(6)
N2	C3	1.478(6)
N3	C20	1.136(7)
C1	C2	1.408(5)
C1	C6	1.389(6)
C1	C7	1.487(6)
C2	C3	1.382(6)
C3	C4	1.374(7)
C4	C5	1.386(6)
C5	C6	1.381(6)
C8	C9	1.499(6)
C9	C10	1.511(6)
C10	C11	1.329(6)
C10	C15	1.514(6)
C11	C12	1.500(7)
C12	C13	1.529(7)
C13	C14	1.525(6)
C13	C23	1.550(6)
C14	C15	1.530(6)
C15	C16	1.530(6)
C16	C17	1.390(6)
C16	C22	1.375(6)
C17	C18	1.375(7)
C18	C19	1.367(6)
C19	C20	1.463(7)
C19	C21	1.394(7)
C21	C22	1.383(6)
C23	C24	1.513(7)
C23	C25	1.535(6)

Table A2.2 Intramolecular Bond Angles (degree) for **55**

C23	O1	C26	118.1(3)
C7	O7	C8	119.0(3)
O2	N1	O3	125.4(4)
O2	N1	C5	117.6(4)
O3	N1	C5	117.0(4)
O4	N2	O5	124.2(4)
O4	N2	C3	118.5(4)
O5	N2	C3	117.3(4)
C2	C1	C6	119.9(4)
C2	C1	C7	118.8(4)
C6	C1	C7	121.3(3)
C1	C2	C3	118.4(4)
N2	C3	C2	119.3(4)
N2	C3	C4	117.3(4)
C2	C3	C4	123.4(4)
C3	C4	C5	116.3(4)
N1	C5	C4	117.9(4)
N1	C5	C6	118.7(4)
C4	C5	C6	123.5(4)
C1	C6	C5	118.5(3)
C12	C13	C14	108.9(4)
C12	C13	C23	113.8(4)
C14	C13	C23	113.6(3)
O6	C7	O7	124.3(4)
O6	C7	C1	125.1(4)
O7	C7	C1	110.6(4)
O7	C8	C9	105.9(3)
C8	C9	C10	113.0(4)
C9	C10	C11	120.3(4)
C9	C10	C15	118.1(4)
C11	C10	C15	121.5(4)
C10	C11	C12	125.1(4)
C11	C12	C13	112.2(4)
C18	C19	C20	120.4(4)
C18	C19	C21	120.2(4)
C20	C19	C21	119.4(4)
N3	C20	C19	177.6(5)
C13	C14	C15	111.4(3)
C10	C15	C14	111.5(4)
C10	C15	C16	111.6(4)

Table A2.2 Intramolecular Bond Angles (degree) for 55 (Continued)

C14	C15	C16	111.2(3)
C15	C16	C17	120.2(3)
C15	C16	C22	120.8(4)
C17	C16	C22	119.1(4)
C16	C17	C18	120.9(4)
C17	C18	C19	119.8(4)
C19	C21	C22	119.6(4)
C16	C22	C21	120.4(4)
O1	C23	C13	110.2(3)
O1	C23	C24	110.7(4)
O1	C23	C25	102.3(3)
C13	C23	C24	111.6(3)
C13	C23	C25	112.1(3)
C24	C23	C25	109.6(4)

Table A2.3 Torsion or conformation Angles (degrees) for **55**

O1	C23	C13	C12	-179.4(3)
O1	C23	C13	C14	55.2(4)
O2	N1	C5	C4	-162.3(4)
O2	N1	C5	C6	17.5(6)
O3	N1	C5	C4	16.1(6)
O3	N1	C5	C6	-164.1(4)
O4	N2	C3	C2	-175.6(4)
O4	N2	C3	C4	4.9(7)
O5	N2	C3	C2	6.4(7)
O5	N2	C3	C4	-173.1(5)
O6	C7	O7	C8	8.9(7)
O6	C7	C1	C2	13.1(7)
O6	C7	C1	C6	-167.0(4)
O7	C7	C1	C2	-167.4(4)
O7	C7	C1	C6	12.5(6)
O7	C8	C9	C10	-55.7(5)
N1	C5	C4	C3	179.0(4)
N1	C5	C6	C1	-179.3(4)
N2	C3	C2	C1	-179.6(4)
N2	C3	C4	C5	-179.9(4)
N3	C20	C19	C18	-70(14)
N3	C20	C19	C21	109(13)
C1	C2	C3	C4	-0.1(7)
C1	C6	C5	C4	0.5(7)
C1	C7	O7	C8	-170.6(3)
C2	C1	C6	C5	0.1(6)
C14	C13	C23	C25	-58.1(5)
C14	C15	C16	C17	-120.8(4)
C14	C15	C16	C22	60.6(5)
C15	C14	C13	C23	-169.1(3)
C15	C16	C17	C18	-177.7(4)
C15	C16	C22	C21	178.8(4)
C2	C3	C4	C5	0.7(7)
C3	C2	C1	C6	-0.2(6)
C3	C2	C1	C7	179.6(4)
C3	C4	C5	C6	-0.9(7)
C5	C6	C1	C7	-179.8(4)
C7	O7	C8	C9	165.3(4)
C8	C9	C10	C11	113.3(4)
C8	C9	C10	C15	-63.2(5)

Table A2.3 Torsion or conformation Angles (degrees) for **55** (Continued)

C9	C10	C11	C12	-174.6(4)
C9	C10	C15	C14	-168.6(3)
C9	C10	C15	C16	-43.5(4)
C10	C11	C12	C13	13.8(6)
C10	C15	C14	C13	-47.3(4)
C10	C15	C16	C17	114.0(4)
C10	C15	C16	C22	-64.6(5)
C11	C10	C15	C14	15.0(5)
C11	C10	C15	C16	140.0(4)
C11	C12	C13	C14	-44.6(4)
C11	C12	C13	C23	-172.6(3)
C12	C11	C10	C15	1.7(6)
C12	C13	C14	C15	62.9(4)
C12	C13	C23	C24	-56.0(4)
C12	C13	C23	C25	67.4(5)
C13	C14	C15	C16	-172.5(3)
C13	C23	O1	C26	64.5(5)
C14	C13	C23	C24	178.6(4)
C16	C17	C18	C19	-0.8(7)
C16	C22	C21	C19	-1.4(7)
C17	C16	C22	C21	0.2(7)
C17	C18	C19	C20	178.0(4)
C17	C18	C19	C21	-0.4(7)
C18	C17	C16	C22	0.9(7)
C18	C19	C21	C22	1.5(7)
C20	C19	C21	C22	-176.9(4)
C24	C23	O1	C26	-59.4(5)
C25	C23	O1	C26	-176.1(4)

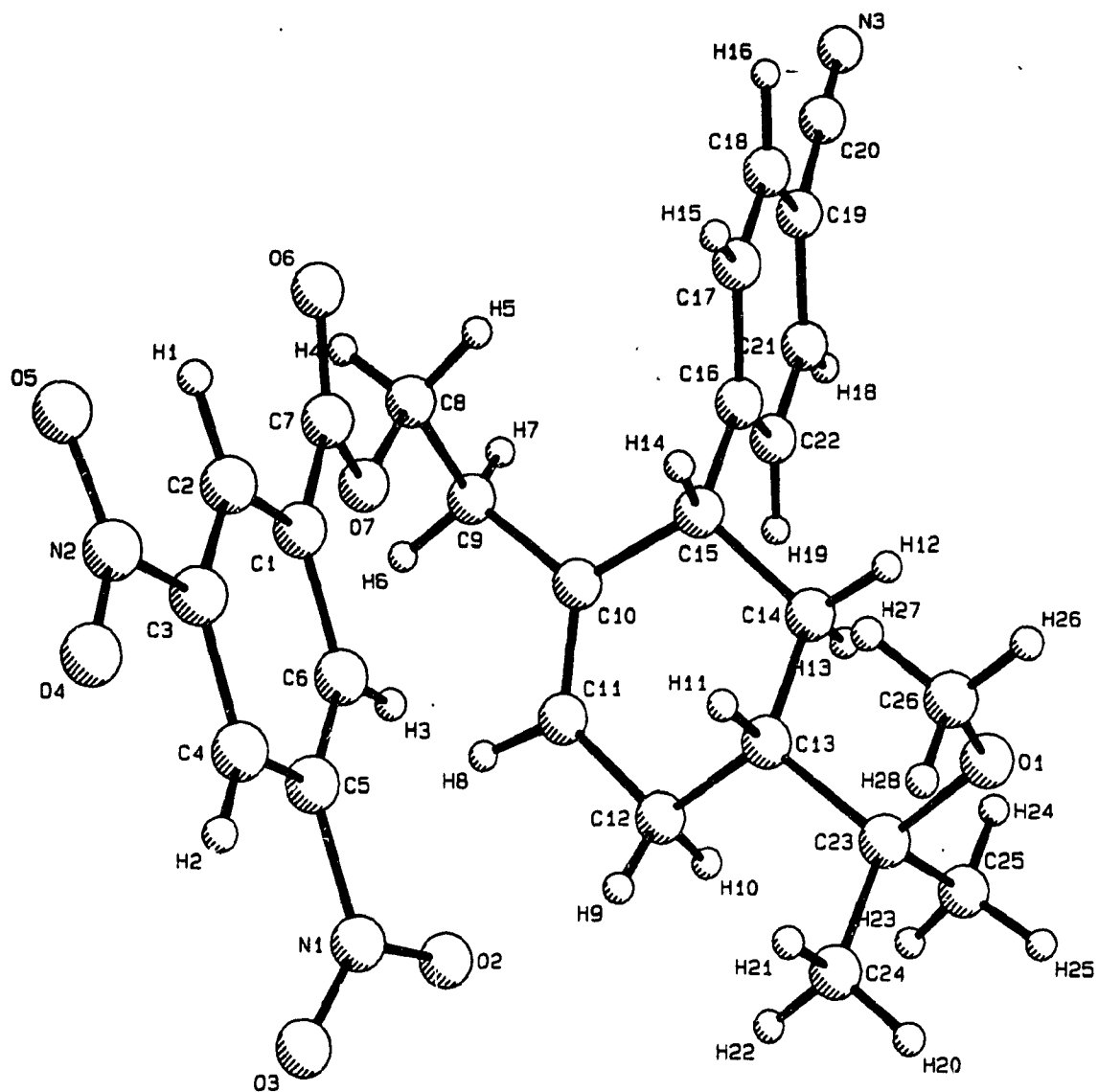


Figure A2.1 X-ray crystal structure of 55

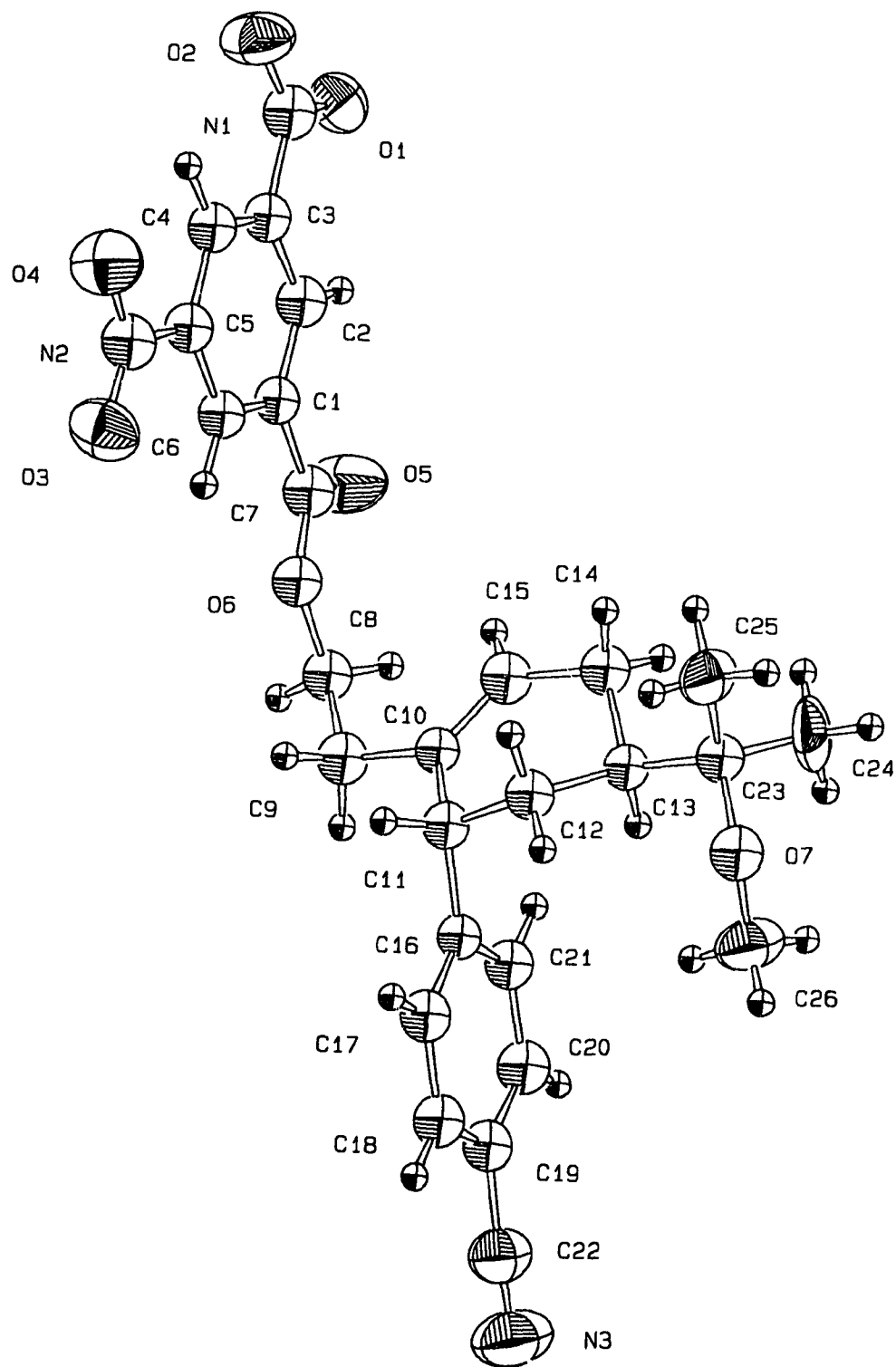


Figure A2.2 X-ray crystal structure of 56

References

1. For laser spectroscopy with nanosecond resolution, see: (a) Novak, J. R. Windsor, R. W. *J. Chem. Phys.* **1967**, *47*, 3075. (b) Porter, G. Topp, M. R. *Nature (London)* **1968**, *220*, 1228. (c) Rentzepis, P. M. *Photochem. Photobiol.* **1968**, *8*, 579.
2. For time resolved Raman spectroscopy, see: Spiro, T.G. *Accounts Chem. Res.* **1974**, *7*, 339.
3. For time resolved electron spin resonance spectroscopy (TR-ESR), see: McLaughlan K.A.; Steven D.G. *Accounts Chem. Res.* **1987**, *21*, 54.
4. For steady-state, see: Roth, H. D. Lamola, A. A. *J. Am. Chem. Soc.* **1972**, *94*, 1013.
5. For time resolved chemically induced dynamic nuclear polarization (CIDNP), see: Closs, G. L.; Miller, R. L.; Redwine, O. D. *Accounts Chem. Res.* **1985**, *18*, 196.
6. Most of the following references are concerned with PET reactions of organic substrates. (a) Mattay, J.; Vondenhof, M. *Topics in Current Chemistry* **1991**, *159*, 219. (b) Mattay, J. *Synthesis* **1989**, 233. (c) *Photoinduced Electron Transfer, Part C. Photoinduced Electron Transfer Reactions: Organic Substrates: Organic Substrates*; Fox, M. A, Chanon, M., Eds; Elsevier: Amsterdam, 1988. (d) Ebersson, L. In *Electron Transfer Reactions in Organic Chemistry*; Hafmer, K., Ed.; Springer-Verlag: Berlin Heidelberg, 1987. (e) Mattay, J. *Photochem.* **1987**, *37*, 167. (f) Mattay, J. *Angew. Chem. Int. Ed.* **1987**, *26*, 825. (g) Mattay, J. *Angew. Chem.* **1987**, *99*, 849. (h) Kavarnos, G. J.; Turro, N. J. *Chem. Rev.* **1986**, *86*, 401. (i) Mattay, J. *Tetrahedron* **1985**, *41*, 2393, 2405. (j) Mattes, S. L.; Farid, S. *Science* **1984**, *226*, 917. (k) Hammerich, O.; Parker, V. D. *Adv. Phy. Org. Chem.* **1984**, *20*, 55-189. (l) Mattes, S. L.; Farid, S. In *Organic Photochemistry*; Padwa, A., Ed: Marcel Dekker: New York, 1983; Vol. 6, p233. (m) Davidson, R. S. In *Advances in Physical Organic Chemistry*; Gold, V., Bethell, D., Eds.; Academic Press: London, 1983; Vol. 19, p 130. (n) Davidson, R. S. In *Molecular Association*; Forster, R., Ed.; Academic Press: London, 1975; Vol. 1, p215. (o) Cohen, S. G.; Parson, Jr., G. H. *Chem. Rev.* **1973**, *73*, 141.
7. (a) Förster, T. H.; Kasper, K. *Z. Phys. Chem. N.F.* **1954**, *1*, 275. (b) Z. *Electrochem.* **1955**, *59*, 976.
8. Weller, A. *Pure Appl. Chem.* **1968**, *16*, 115.

9. Beens, H.; Knibbe, H.; Weller, A. *J. Chem. Phys.* **1967**, *47*, 1183.
10. (a) Volman, D. H.; Gollnick, K.; Hammond, G. S. *Adv. Photochem.* **1986**, *13*, 165. (b) *Acc. Chem. Res.* **1986**, *19*, 401. (c) Crimmins, M. T. *Chem. Rev.* **1988**, *88*, 1453. (d) Ossclton, E. M.; Dijk-Knepper, J. J. van; Cornelisse, J. J. *Chem. Soc., Perkin Trans* **1988**, *11*, 1021. (e) Barltrop, J. A.; Carless, H. A. J. *J. Am. Chem. Soc.* **1972**, *94*, 1951. (f) Caldwell, R. A.; Smith, L. *J. Am. Chem. Soc.* **1974**, *96*, 2994.
11. (a) Förster, R. *Organic Charge-Transfer Complexes*, Academic, New York, 1969. (b) "Photoinduced Electron Transfer, Part A. Conceptual Basis", p245. Fox, M. A, Chanon, M., Eds; Elsevier: Amsterdam, 1988.
12. Weller, A. *Z. Phys. Chem. Neue Folge.* **1982**, *133*, 93.
13. Simon, J.D. Peters, K. S. *J. Am. Chem. Soc.* **1981**, *103*, 6403.
14. Simon, J.D. Peters, K. S. *J. Am. Chem. Soc.* **1982**, *104*, 6542.
15. (a) Marcus, R. A. *Annu. Rev. Phys. Chem.* **1964**, *15*, 155. (b) Balzani, V.; Bolletta, F.; Gandolfi, M. T.; Maestri, M. *Top. Curr. Chem.* **1978**, *75*, 1. (c) Ebersson, L. *Adv. Phys. Org. Chem.* **1982**, *18*, 79.
16. Beratan, D. N. Onuchic, J. N. *J. Chem. Phys.* **1988**, *89*, 6195.
17. Rehm, D.; Weller, A. *Isr. J. Chem.* **1970**, *8*, 259.
18. Wikinson, F. p.207 *Photoinduced Electron Transfer, Part A, Conceptual Basis* Fox, M. A, Chanon, M., Eds; Elsevier: Amsterdam, 1988
19. (a) Gould, I. R.; Ege, D.; Mattes, S.L.; Farid, S. *J. Am. Chem. Soc.* **1987**, *109*, 3794. (b) Gould, I. R.; Moser, J. E.; Ege, D.; Farid, S. *J. Am. Chem. Soc.* **1988**, *110*, 1991. (c) Gould, I. R.; Moody, R.; Farid, S. *J. Am. Chem. Soc.* **1988**, *110*, 7242. (d) Gould, I. R.; Moser, J. E.; Armitage, B.; Farid, S. Goodman, J. L.; Herman, M. S. *J. Am. Chem. Soc.* **1989**, *111*, 1917. (e) Gould, I. R.; Ege, D.; Moser, J. E.; Farid, S. *J. Am. Chem. Soc.* **1990**, *112*, 4290-4301.
20. (a) Ohno, T.; Yoshimura, A.; Mataga, N. *J. Phys. Chem.* **1990**, *94*, 4871. (b) Kikuchi, K.; Takahashi, Y.; Koike, K.; Wakamatsu, K.; Ikeda, H.; Miyashi, T. *Z. Phys. Chem. (Munich)* **1990**, *167*, 27. (c) Vauthey, E.; Suppan, P.; Haselbach, E. *Helv. Chim. Acta* **1988**, *71*, 93.
21. Marcus, R.A. *J. Chem. Phys.* **1956**, *24*, 966.

22. Could, I. R.; Farid, S.; Young, R. H. unpublished results.
23. Todd, W. P.; Dinnocenzo, J. P.; Farid, S.; Goodman, J. L.; Gould, I. R. *J. Am. Chem. Soc.* **1991**, *113*, 3601.
24. (a) Kalyanasundaram, K. *Photochemistry in microheterogeneous systems* **1987**, Academic Press, London. (b) Fendler, J. H. *J. Phys. Chem.* **1985**, *89*, 2730.
25. (a) Brown-Wensley, K. A.; Mattes, S. L.; Farid, S. *J. Am. Chem. Soc.* **1978**, *100*, 4162. (b) Mattay, J. *Tetrahedron* **1985**, *41*, 2393.
26. Arnold, D. R.; Maroulis, A. J. *J. Am. Chem. Soc.* **1976** *98*, 5931.
27. (a) Okamoto, A.; Snow, M. S.; Arnold, D. R. *Tetrahedron* **1986**, *42*, 6175. (b) Okamoto, A.; Arnold, D. R. *Can. J. Chem.* **1985**, *63*, 2340.
28. (a) Arnold, D. R.; Lamont, L. J. *Can. J. Chem.* **1989**, *67*, 2119. (b) Arnold, D. R.; Fahie, B. J.; Lamont, L. J.; Wierzchowski, J.; Young, K. M. *Can. J. Chem.* **1987**, *65*, 2734.
29. (a) Sankararaman, S.; Perrier, S.; Kochi, J. K. *J. Am. Chem. Soc.* **1989**, *111*, 6448. (b) Ci, X.; Whitten, D. G. *J. Am. Chem. Soc.* **1989**, *111*, 3459. (c) Albin, A.; Mella, M. *Tetrahedron* **1986**, *42*, 6219. (d) Camaioni, D. M.; Franz, J. A. *J. Org. Chem.* **1984**, *49*, 1607. (e) Eaton, D. F. *Pure Appl. Chem.* **1984**, *56*, 1191. (f) Reichel, L. W.; Griffin, G. W.; Muller, A. J.; Das, P. K.; Ege, S. N. *Can. J. Chem.* **1984**, *62*, 424. (g) Davis, H. F.; Das P. K.; Reichel, L. W.; Griffin, G. W. *J. Am. Chem. Soc.* **1984**, *106*, 6968. (h) Gotoh, T.; Kato, M.; Yamamoto, M.; Nishijima, Y. *J. Chem. Soc., Chem. Commun.* **1981**, 90.
30. Arnold, D.R.; Du, X.; Henseleit, K. M. *Can. J. Chem.* **1991**, *69*, 839-852.
31. Popielarz, R.; Arnold, D. R. *J. Am. Chem. Soc.* **1990**, *112*, 3068.
32. (a) Perrott, A. L.; Arnold, D. R. *Can. J. Chem.* **1992**, *70*, 272. (b) Arnold, D. R.; Lamont, L. J.; Perrott, A. L. *Can. J. Chem.* **1991**, *69*, 225.
33. Yates, B. F.; Bouma, W. J.; Radom, L. *Tetrahedron* **1986**, *42*, 6225.
34. (a) Gassman, P. G.; Olson, K. D.; Walter, L.; Yamaguchi, R. *J. Am. Chem. Soc.* **1981**, *103*, 4977. (b) Gassman, P.G.; Olson, K. D. *J. Am. Chem. Soc.* **1982**, *104*, 3740. (c) Roth, H. D.; Schilling, M. L. M.; Gassman, P.G.; Smith, J. L. *J. Am. Chem. Soc.* **1984**, *106*, 2711. (d) Gassman, P. G.; Hay,

- B.A. *J. Am. Chem. Soc.* **1986**, *108*, 4227. (e) Roth, H. D. *Acc. Chem. Res.* **1987**, *20*, 343.
35. Gassman, P. G.; Carroll, G. T. *Tetrahedron* **1986**, *42*, 6201.
36. (a) Hammerich, O.; Parker, V. D. *Adv. Phys. Org. Chem.* **1984**, *20*, 50-187. (b) Bordwell, F. G.; Cheng, J.-P. *J. Am. Chem. Soc.* **1989**, *111*, 1792-1795.
37. Breslow, R.; Grant, J. *J. Am. Chem. Soc.* **1977**, *99*, 7745.
38. Nicholas, A. M. de P.; Arnold, D. R. *Can. J. Chem.* **1982**, *60*, 2165.
39. Yoshino, A.; Ohahsi, M.; Yonezawa, T. *J. Chem. Soc., Chem. Commun.* **1971**, 97.
40. (a) Guttenplan, J. B.; Cohen, S. G. *J. Am. Chem. Soc.* **1972**, *94*, 4040. (b) Lee, L. Y. C.; Ci, X.; Giannotti, C.; Whitten, D. G. *J. Am. Chem. Soc.* **1986**, *108*, 175.
41. Saeva, F. D. *Topics in Current Chemistry* **1990**, *156*, p59. Springer-Verlag Berlin Heidelberg 1990.
42. Kim, J. K.; Bunnett, J. F. *J. Am. Chem. Soc.* **1970**, *92*, 7643.
43. Rossi, R. A.; Bunnett, J. F. *J. Org. Chem.* **1973**, *38*, 1407.
44. Rossi, R. A.; Rossi, R. H. de *Aromatic substitution by the S_{RN}1 mechanism*, *ACS Monograph* **1983**, 178.
45. (a) Kornblum, N. *Angew. Chem. Int. Ed. Engl.* **1975**, *14*, 734. (b) Bunnett, J. F. *Acc. Chem. Res.* **1978**, *11*, 413.
46. (a) Kornblum, N.; Michel, R. E.; Kerber, R. C. *J. Am. Chem. Soc.* **1966**, *88*, 5662. (b) Russell, G.A.; Danen, W. C. *J. Am. Chem. Soc.* **1966**, *88*, 5663.
47. Yasuda, M.; Pac, C.; Sakurai, H. *Bull. Chem. Soc. Jpn.* **1980**, *53*, 502.
48. Majima, T.; Pac, C.; Nakasone, A.; Sakurai, H. *J. Am. Chem. Soc.* **1981**, *103*, 4499.
49. Farid, S.; Shealer, S. E. *J. Chem. Soc., Chem. Commun.* **1973**, 677.
50. Mattes, S. L.; Farid, S. *J. Am. Chem. Soc.* **1986**, *108*, 7356.

51. Mattes, S. L.; Farid, S. *J. Chem. Soc., Chem. Commun.* **1980**, 126.
52. Calhoun, G. C.; Schuster, G. B. *J. Am. Chem. Soc.* **1984**, *106*, 6870.
53. Farid, S.; Hartman, S. E.; Evans, T. R. In "The Exciplex"; Gordon, M.; Ware, W. R., Eds.; Academic Press: New York, 1975; p.327.
54. Neunteufel, R. A.; Arnold, D. R. *J. Am. Chem. Soc.* **1973**, *95*, 4080.
55. Gassman, P. G.; Saliya, A. D. S. *J. Am. Chem. Soc.* **1991**, *113*, 9870.
56. Mizuno, K.; Yoshioka, K.; Otsuji, Y. *Chem. Lett.* **1983**, 941.
57. Yamada, S.; Kimura, Y.; Ohashi, M. *J. Chem. Soc., Chem. Commun.* **1977**, 667.
58. Pac, C.; Nakasone, A.; Sakurai, H. *J. Am. Chem. Soc.* **1977**, *99*, 5806.
59. (a) Mareano, P. S.; Stavinoha, J. L.; Pepe, G.; Meyer, E. F. *J. Am. Chem. Soc.* **1978**, *100*, 7114. (b) Stavinoha, J. L.; Mareano, P. S. *J. Am. Chem. Soc.* **1981**, *103*, 3136.
60. (a) Kubo, Y.; Suto, M.; Araki, T.; Mazzocchi, P. H.; Klingler, L.; Shook, D.; Somich, C. *J. Org. Chem.* **1986**, *51*, 4404. (b) Maruyama, K.; Kubo, Y. *J. Org. Chem.* **1985**, *50*, 1426. (c) Mazzocchi, P. H.; Minamikawa, S.; Wilson, P. *J. Org. Chem.* **1985**, *50*, 2681.
61. (a) Mattay, J.; Runsink, J.; Rumbach, T.; Ly, C.; Gersdorf, J. *J. Am. Chem. Soc.* **1985**, *107*, 2557. (b) Mattay, J. *Tetrahedron* **1985**, *41*, 2393.
62. Borg, R. M.; Arnold, D. R.; Cameron, T. S. *Can. J. Chem.* **1984**, *62*, 1785.
63. (a) Arnold, D. R.; Snow, M. S. *Can. J. Chem.* **1988**, *66*, 3012-3026. (b) Arnold, D. R.; Du, X. *J. Am. Chem. Soc.* **1989**, *111*, 7666.
64. Arnold, D. R.; McMahon, K. unpublished results.
65. (a) Mattes, S. L.; Farid, S. *J. Chem. Soc., Chem. Commun.* **1980**, 126. (b) Mattes, S. L.; Farid, S. *J. Am. Chem. Soc.* **1983**, *105*, 1386. (c) Mattes, S. L.; Farid, S. *J. Am. Chem. Soc.* **1986**, *108*, 7356.
66. Weller, A. Z. *Phys. Chem. (Munich)* **1970**, *69*, 183.
67. Mattes, S. L.; Farid, S. *J. Am. Chem. Soc.* **1982**, *104*, 1454.

68. Andrieux, C. P.; Gallardo, I.; Saveant, J.-M. *J. Am. Chem. Soc.* **1989**, *111*, 1620.
69. (a) Lan, J. Y.; Schuster, G.B. *Tetrahedron Lett.* **1986**, *27*, 4261. (b) Fischer, H. *J. Am. Chem. Soc.* **1986**, *108*, 3925.
70. Arnold, D. R.; Wong, P. C.; Maroulis, A. J.; Cameron, T. S. *Pure Appl. Chem.* **1980**, *52*, 2609.
71. Majima, J.; Pac, C.; Nakasone, A.; Sakurai, H. *Chem. Lett.* **1979**, 1133.
72. Almenningen, A.; Bastiansen, O.; Fernholt, L.; Cyvin, B. N.; Samdal, S. *J. Mol. Struct. (Theochem.)* **1985**, *128*, 59, and 115.
73. For the recent papers, see: (a) Akiyama, M.; Watanabe, T.; Kakihana, M. *J. Phys. Chem.* **1986**, *90*, 1752. (b) Roberts, R. M. G. *Magn. Reson. Chem.* **1985**, *23*, 52.
74. Tsuzuki, S.; Tanabe, K. *J. Phys. Chem.* **1991**, *95*, 139 and references therein.
75. Courtneidge, J. L.; Davies, A. G.; Clark, T.; Wilhelm, D. *J. Chem. Soc. Perkin Trans. II* **1984**, 1197.
76. (a) Shim, S. C.; Lee, H. G. *Photochem. Photobio.* **1989**, *46*, 59-75. (b) Mizuno, K.; Ichinose, N.; Tamai, T.; Otsuji, Y. *Tetrahedron Lett.* **1985**, *26*, 5823. (c) Goodman, B. F.; Schuster, G. B. *J. Am. Chem. Soc.* **1984**, *106*, 7254. (d) Masnovi, J. M.; Levine, A.; Kochi, J. K. *J. Am. Chem. Soc.* **1985**, *107*, 4356. (e) Simon, J. D.; Peters, K. S. *Acc. Chem. Res.* **1984**, *17*, 277. (f) *J. Am. Chem. Soc.* **1983**, *105*, 4875. (g) *J. Am. Chem. Soc.* **1982**, *104*, 6142. (h) McCullough, J. J.; Yeroushakmi, S. *J. Chem. Soc.* **1983**, *55*, 254. (j) Goodman, J. I.; Peters, K. S. *J. Am. Chem. Soc.* **1985**, *107*, 6459.
77. Goodson, B. E.; Schuster, G. B. *Tetrahedron Lett.* **1986**, *27*, 3123.
78. (a) Bates, T. H.; Best, J. V. F.; Williams, T. F. *J. Chem. Soc.* **1962**, 1521. (b) Mayer, R.; Bochov, K.; Zieger, W. *Z. Chem.* **1964**, *4*, 348.
79. Frank, G. *J. Chem. Soc. (B)* **1968**, 130.
80. The reduction potential of benzophenone is -2.16 V (SCE), hence the reduction potential of acetophenone must be more negative than this number. Gersdorf, J.; Mattay, J.; Gorner, H. *J. Am. Chem. Soc.* **1987**, *109*, 1203.

81. Zheng, B.-w.; Ming, Y.-f.; Cao, Y. *Photochem. Photobio.* **1984**, *40*, 581.
82. (a) Fang, J.-M.; Chen, M.-Y.; Cheng, M.-C.; Lee, G.-H.; Wang, Y.; Peng, S.-M. *J. Chem. Research (S)* **1989**, 272. (b) Claisse, J. A.; Davies, D. I.; Parfitt, L. T. *J. Chem. Soc.* **1970**, *112*, 258. C.
83. Mattes, S. L.; Farid, S. *Organic Photochemistry* Padwa, A., Ed.; Marcel Dekker: New York, **1983**, V. 6, p. 233.
84. (a) Delpech, B.; Khuong-Huu, Q. *J. Org. Chem.* **1978**, *43*, 4898. (b) Pancrazi, A.; Kabore, I.; Delpech, B.; Khuong-Huu, Q. *Tetrahedron Lett.* **1979**, 3729. (c) Mirand, C.; Massiot, G.; Levy, L. *J. Org. Chem.* **1982**, *47*, 4169.
85. Frisch, M. J.; Binkley, J. S.; Schlegel, H. B.; Raghavachari, K.; Melius, C. F.; Martin, R. L.; Stewart, J. J. P.; Bobrowicz, F. W.; Rohlfing, C. M.; Kahn, L. R.; DeFrees, D. J.; Seeger, R.; Whiteside, R. A.; Fox, D. J.; Fleuder, E. M.; Pople, J. A. *Gaussian86. Release H*; Carnegie Mellon University: Pittsburgh, PA, 1984.
86. *Gaussian 90, revision H*, M.J. Frisch, M.Head-Gordon, G.W.Trucks, J. B.Foresman, H.B.Schlegel, K.Raghavachari, M.Robb, J.S.Binkley, C.Gonzalez, D.J. DeFrees, D.J.Fox, R.A.Whiteside, R. Seeger, C.F.Melius, J.Baker, R.L.Martin, L.R. Kahn, J.J. P. Stewart, S.Topiol, and J,A.Pople, Gaussian, Inc., Pittsburgh PA, 1990.
87. Mulliken, R. S. *J. Chem. Phys.* **1955**, *23*, 1833.
88. Hehre, W. J.; Radim, L.; Schkeyer, P. v. R.; Pople, J. A. *Ab initio Molecular Orbital Theory*; Wiley: New York, 1986.
89. Shim, S. C.; Lee, H. G. *Photochem. Photobio.* **1989**, *46*, 59-75.
90. Okamoto, A.; Snow, M. S.; Arnold, D.R. *Tetrahedron*, **1986**, *42*, 6175.
91. Wayner, D. D. M.; McPhee, D. J.; Griller, D. *J. Am. Chem. Soc.* **1988**, *110*, 132.
92. Jaun, B.; Schwarz, J.; Breslow, R. *J. Am. Chem. Soc.* **1980**, *102*, 5741.
93. Bruno, J.W.; Marks, T. J.; Lewis, F. D. *J. Am. Chem. Soc.* **1982**, *104*, 5580.
94. Ohashi, M.; Kud, H.; Yamada, S. *J. Am. Chem. Soc.* **1979**, *101*, 2201.

95. Harwood, L. H. *Aldrichimica Acta* **1985**, *18*, 25.
96. Nicholson, R. S.; Shain, I. *Anal. Chem.* **1964**, *36*, 706; **1965**, *37*, 178.
97. Sheldon, R. A.; Kochi, J. K. *J. Am. Chem. Soc.* **1970**, *92*, 4395.
98. Shelton, J. R.; Liang, C. K.; Kovacic, P. *J. Am. Chem. Soc.* **1968**, *90*, 354.
99. Gassman, P. G.; Carroll, G. T. *Tetrahedron* **1986**, *42*, 6201.
100. Gassman, P. G.; Olson, K. D. *J. Am. Chem. Soc.* **1982**, *104*, 3740.
101. (a) Rao, V. R.; Hixson, S. S. *J. Am. Chem. Soc.* **1979**, *101*, 6458.
(b) Mizuno, K.; Ogawa, J.; Kagano, H.; Otsuji, Y. *Chem. Lett.* **1981**, 437.
(c) Mazzocchi, P. H.; Somich, C. *Tetrahedron Lett.* **1988**, *29*, 513.
102. Dinnocenzo, J. P.; Todd, W. P.; Simpson, T. R.; Gould, I. R. *J. Am. Chem. Soc.* **1990**, *112*, 2462.
103. Gassman, P. G.; Mlinaric-Majerski, K. *J. Org. Chem.* **1986**, *51*, 2397.
104. Wayner, D. D. M.; Boyd, R. J.; Arnold, D. R.; *Can. J. Chem.* **1983**, *61*, 2310-2315.
105. Qin, X.; Snow, L.D.; Williams, F. *J. Am. Chem. Soc.* **1984**, *106*, 7640.
106. Roth, H. D.; Schilling, M. L. M. *J. Am. Chem. Soc.* **1983**, *105*, 6805.
107. $\Delta G = 23.06(2.31+1.66)-1.29-97.6 = -7.34$ kcal/mol.
108. D.G. Patil, J.S. Yadav, H.P.S Chawla, and Sukh Dev. *Indian J. Chem.* **1983**, *22B*, 189.
109. (a) Dinnocenzo, J. P.; Todd, W. P.; Simpson, T. R.; Gould, I. R. *J. Am. Chem. Soc.* **1990**, *112*, 2462. (b) Maslak, P.; Narvaez, J. N. *Angew. Chem. Int. Ed. Engl.* **1990**, *29*, 283 (1990). (d) X. Ci, X.; Whitten, D. G. *J. Am. Chem. Soc.* **1989**, *111*, 3459.
110. (a) Bauld, N. L. *Tetrahedron* **1989**, *45*, 5307. (b) Dinnocenzo, J. P.; Conlon, D. A. *J. Am. Chem. Soc.* **1988**, *110*, 2324. (c) Roth, H. P. *Acc. Chem. Res.* **1987**, *20*, 343. (d) McLafferty, F. W.; Barbalas, M. P.; Turecek, F. *J. Am. Chem. Soc.* **1983**, *105*, 1. (e) Padwa, A.; Chou, C. S.; Rieker, W. F. *J. Org. Chem.* **1980**, *45*, 4555.

111. (a) Feng, R.; Wesdemiotis, C.; Zhang, M.-Y.; Marchetti, M.; McLafferty, F. W. *J. Am. Chem. Soc.* **1989**, *111*, 1986. (b) T. Hsieh, J.P. Gillman, M.J. Weiss, and G.G. Meisels. *J. Phys. Chem.* **1981**, *85*, 2722.
112. (a) Fujisawa, J.; Sato, S.; Shimokoshi, K. *Chem. Phys. Lett.* **1986**, *124*, 391. (b) Toriyama, K.; Nunome, K.; Iwasaki, M.; Shida, T.; Ushida, K. *Chem. Phys. Lett.* **1985**, *122*, 118. (c) Fujisawa, J.; Sato, S.; Shimokoshi, K.; Shida, T. *J. Phys. Chem.* **1985**, *89*, 5481. (d) Iwasaki, M.; Toriyama, K.; Nunome, K. *Faraday Disc. Chem. Soc.* **1984**, *78*, 19. (e) Ushida, K.; Shida, T.; Iwasaki, M.; Toriyama, K.; Nunome, K. *J. Am. Chem. Soc.* **1983**, *105*, 5496. (f) Shida, T.; Egawa, Y.; Kubodera, H. *J. Chem. Phys.* **1980**, *73*, 5963.
113. Clark, T.; Nelson, S. F. *J. Am. Chem. Soc.* **1988**, *110*, 868.
114. Wiberg, K. B.; Martin, E. *J. Am. Chem. Soc.* **1985**, *107*, 5035.
115. (a) Clark, T. *J. Am. Chem. Soc.* **1987**, *109*, 6838. (b) Hoppilliard, Y.; Bouchoux, G. *Org. Mass Spectrom.* **1982**, *17*, 534.
An *ab initio* (UHF/6-31G*) study of the 1,3-hydrogen migration of the radical cation of 1-propene has identified a similar structure to $46^{+\bullet}$ b shown in Figure 5.4) as a transition state (a). An earlier calculation using semi-empirical methods (MINDO/3) indicated the same structure was an intermediate; however, no energy minimum was found for the 1,3-methyl migration of the radical cation of 1-butene ($46^{+\bullet}$) (b).
116. Ushida, K.; Shida, T.; Walton, J. C. *J. Am. Chem. Soc.* **1986**, *108*, 2805.
117. Bothner-By, A. A.; Naar-Colin, C.; Bunther, H. *J. Am. Chem. Soc.* **1962**, *84*, 2748.
118. (a) Rosenstock, H. M.; Draxl, K.; Steiner, B. W.; Herron, J. T. *J. Phys. Ref. Data* **1977**, *6*, Suppl. 1. (b) Lossing, F. P. *Can. J. Chem.* **1972**, *50*, 3973-3981. (c) Wang, D.P.; Lee, L. C.; Srivastava, S. K. *Chem. Phys. Lett.* **1988**, *152*, 513-18. (d) Holmes, J. L.; Lossing, F. P. *Int. Mass Spectrosc. Ion Proc.* **1984**, *58*, 113. (e) Weidner, U.; Schweig, A. *THEOCHEM.* **1988**, *40*, 125-31. (f) Masclet, P.; Grosjean, D.; Mouvier, G. *J. Electr. Spectrosc. Relat. Phenomena* **1973**, *2*, 225-257. (g) Tsang, W. *J. Am. Chem. Soc.* **1985**, *107*, 2872.
119. Reed, R. B.; Weinstock, R. B.; Weinhold, F. *J. Chem. Phys.* **1985**, *83*, 735
120. Stenhagen, E.; Abrahamsson, S.; McLafferty, F. W. "Registry of mass spectral data" John Wiley and Sons, Toronto, 1974, p9 and 76.

121. Mitchell, A. L.; Terlder, J. M. *J. Chem. Soc. Perkin Trans.* **1986**, *2*, 1197.
122. Bauld, N. L. *J. Computational Chem.* **1990**, *11*, 896.
123. (a) Lias, S. G.; Ausloos, P. *Int. J. Mass Spectrom. Ion Proc.* **1987**, *81*, 165.
(b) Lossing, F. P.; Traeger, J. C. *Int. J. Mass Spectrom Phys.* **1976**, *19*, 9.
124. Turecek, F.; Hanus, U. *Tetrahedron* **1983**, *39*, i499.
125. Moon, S.; Waxman, B. H. *J. Org. Chem.* **1969**, *34*, 288.
126. It is known that vicinal carbon-hydrogen coupling ($^3J_{C-H}$) follows a Karplus relationship similar to that pertaining to vicinal hydrogen-hydrogen coupling ($^3J_{H-H}$), dependent on the dihedral angle of the coupled nuclei. In general, the magnitude of $^3J_{C-H}$ is about 0.6 that of the analogous $^3J_{H-H}$.
Marshall, J. L. "Carbon-carbon and carbon-proton NMR coupling: Application to organic stereochemistry and conformational analysis." Verlag Chemie International, Deerfield Beach, FL. 1983.
127. (a) Wong, P. C.; Arnold, D. R. *Tetrahedron Lett.* **1979**, 2101. (b) Roth, H. D.; Schilling, M. L. M. *J. Am. Chem. Soc.* **1980**, *102*, 7956.
128. Roth, H. D.; Schilling, M. L. M. *J. Am. Chem. Soc.* **1981**, *103*, 7210.
129. Maroulis, Y.; Shigemitsu, Y.; Arnold, D. R. *J. Am. Chem. Soc.* **1978**, *100*, 538.
130. Mizuno, K.; Yoshioka, K.; Otsuji, Y. *J. Chem. Soc., Chem. Commun.* **1984**, 1665.
131. (a) Wilhelm, D; Backvall, J.-E.; Nordberg, R.E.; Norin T. *Organometallics* **1985**, *4*, 1296-1302. (b) Larock, R.C.; Song, H.; Kim, S.; Jacobsin, R.A. *J. Chem. Soc., Chem. Commun.* **1987**, 834.
132. Belleau, B.; Gulini, U.; Gour-Salin, B. *Can. J. Chem.* **1985**, *63*, 1268.
133. Busing, W. R.; Martin, K. O.; Levy, H. A. *ORFLS*. A FORTRAN crystallographic least squares program, Report ORNL-TM-305, Oak Ridge National Laboratory, Oak Ridge, Tennessee (1962).
134. *TEXSAN* - *TEXRAY* Single Crystal Structure Analysis Package, Version 5.0. Molecular structure Corporation, The Woodlands, Texas (1989).